



**Synthesis and characterization of (cyclopentadienone)iron
tricarbonyl complexes and their application to stereoselective
catalytic transformations**

PhD in Chemical and Environmental Sciences – XXIX Cycle

Dipartimento di Scienza e Alta Tecnologia

Università degli Studi dell'Insubria

PhD dissertation:

Sofia VAILATI FACCHINI

Supervisor: Prof. Umberto PIARULLI

Co-Supervisor: Prof. Albrecht BERKESSEL

2015/2016

Acknowledgement

I would like to thank my family and my friends for all their effort, motivation and support not only spiritually throughout writing this thesis, but also for my life in general. Their encouragement and unconditional love was essential to never give up.

“Never give up on what you really want to do. The person with big dreams is more powerful than one with all the facts.” A. Einstein

And all the people involved in this project:



Prof. Umberto Piarulli for giving me the opportunity to start my PhD, for his support and for his contribution to my scientific education.



Prof. Albrecht Berkessel for giving me precious advice on my research and of course the opportunity to spend 11 months in Köln, where I met all the people of the AKB group; I will never forget all the amazing moments that we spent all together.

Dr. Jörg Martin Neudörfl for the X-ray crystal structure.



Prof. Cesare Gennari

Dr. Luca Pignataro

Dr. Alessandra Forni for the X-ray crystal structure.

Piotr Gajewski

Marc Renom Carrasco

Dr. Raffaella Ferraccioli



Dr. Laurent Lefort



Prof. Johannes G. de Vries

Prof. Emma Gallo (Università degli Studi di Milano)

Dr. Wacharee Harnying (Universität zu Köln)

Prof. Gianluigi Broggin (Univeristà degli Studi dell'Insubria)

for correcting my thesis and as members of my examination committee.

Index

Index	4
1. Preface	10
2. Introduction: iron	14
2.1. Electronic configuration, oxidation states, coordination geometries of iron	14
2.2. General difficulties related to the development of new iron catalysts	15
2.3. Fundamental reactions that play a key role in iron catalysis	15
2.4. Importance of the ligands	16
3. Iron-catalyzed hydrogenation and asymmetric hydrogenation	19
3.1. Fe-H complexes	20
3.2. Hydrogenation of alkenes and alkynes	21
3.2.1. Homoleptic ironcarbonyl complexes	21
3.2.2. Biomimetic complexes: iron porphyrins	22
3.2.3. Multidentate P ligand iron complexes	24
3.2.4. <i>P,N,P</i> - and tetradentate <i>N</i> -ligand complexes	27
3.2.5. Bis(imino)pyridine complex	28
3.2.6. (Cyclopentadienyl)iron complex	32
3.2.7. Iron nanoparticles	33
3.3. Hydrogenation of carbonyl compounds	35
3.3.1. Iron carbonyl	35
3.3.1.1 Diaminophosphine ligand and terpyridine ligand	35
3.3.1.2 Iron porphyrines and macrocyclic complexes	37
3.3.2. <i>P,N,N,P</i> -complexes	39
3.3.3. <i>P,N,P</i> -pincer ligand	44
3.3.4. Isonitrile complex	47
3.3.5. (Cyclopentadienone)iron complexes	48

3.3.5.1 Modification of the Knölker-Casey complex	51
3.3.5.2 Asymmetric reductions	54
3.3.5.3 Reductive amination of aldehydes, ketones and alcohols	56
3.4. Hydrogenation of sodium carbonate and carbon dioxide	58
3.5. Summary of iron catalyzed reduction	61
4. Results and Discussion.....	63
4.1. Aim of the thesis	64
4.2. Towards a (<i>R</i>)-BINOL derived complexes	65
4.2.1. Replacement of a CO ligand with a chiral phosphoramidite ligand	69
4.3. Towards the synthesis of a library of 3,3'-substituted chiral (cyclopentadienone) iron tricarbonyl complex	73
4.3.1. Screening condition and optimization	77
4.3.2. Synthesis of the library of new chiral pre-catalyst	80
4.3.3. Catalytic tests with new chiral (cyclopentadienone)iron complexes	88
4.3.4. Substrate screening with the best chiral (cyclopentadienone)iron complex	85 89
4.3.5. Variation of the 2,5-substituents of the cyclopentadienone ring	90
4.4. Towards planar chirality	93
4.4.1. Catalytic test with the new [bis(hexamethylene)cyclopentadienone]iron tricarbonyl complex	96
4.5. Synthesis of a planar chiral (cyclopentadienone)iron tricarbonyl complex	102
5. Conclusion and Outlook.....	108
6. Experimental Part.....	111
6.1. General Conditions	111
6.1.1. Materials	112
6.2. Synthesis of complex (<i>R</i>)-58	113
6.2.1. (<i>R</i>)-2,2'-bis(trifluoromethanesulfonyloxy)-1,1'-binaphthyl [60]	113
6.2.2. (<i>R</i>)-2,2'-dimethyl-1,1'-binaphthyl [61]	114

6.2.3. (<i>R</i>)-2,2'-Bis(bromomethyl)-1,1'-binaphthyl [62]	114
6.2.4. (<i>R</i>)-2,2'-Bis(iodomethyl)-1,1'-binaphthyl [63]	115
6.2.5. (<i>R</i>)-2,2'-Bis(3-(trimethylsilyl)prop-2-ynyl)-1,1'-binaphthyl [64]	116
6.2.6. Complex (<i>R</i>)-58	116
6.3. Replacement of one CO ligand with phosphoramidite ligand	117
6.3.1. Synthesis of a phosphoramidite ligand: Monophos [65]	117
6.3.2. General procedure for replacing one CO ligand with a phosphoramidite	118
6.3.3. Complex 71 [(<i>S</i>)-Monophos]	118
6.3.4. Complex 72 [(<i>S</i>)-Monophos] and 73 [(<i>R</i>)-Monophos]	119
6.3.5. Complex 70	119
6.3.6. Complex 74 [(<i>S</i>)-Monophos]	120
6.3.7. Complex 66 [(<i>S</i>)-Monophos] and 67 [(<i>R</i>)-Monophos]	120
6.4. Synthesis of complex (<i>R</i>)-85	122
6.4.1. (<i>R</i>)-2,2'-bis(methoxymethoxy)-1,1'-binaphthyl [87]	122
6.4.2. (<i>R</i>)-3,3'-dihydroxy-2,2'-bis(methoxymethoxy)-1,1'-binaphthyl [89]	123
6.4.3. (<i>R</i>)-3,3'-Dimethoxy-1,1'-bi-2-naphthol [90]	124
6.4.4. (<i>R</i>)-3,3'-dimethoxy-1,1'-bi-2-naphthol [91]	124
6.4.5. (<i>R</i>)-3,3'-Dimethoxy-2,2'-bis(trifluoromethanesulfonyloxy)-1,1'-binaphthyl [92]	125
6.4.6. (<i>R</i>)-3,3'-Dimethoxy-2,2'-dimethyl-1,1'-binaphthyl [93]	126
6.4.7. (<i>R</i>)-3,3'-Dimethoxy-2,2'-bis(bromomethyl)-1,1'-binaphthyl [94]	126
6.4.8. (<i>R</i>)-2,2'-Bis(iodomethyl)-3,3'-dimethoxy-1,1'-binaphthyl [95]	127
6.4.9. (<i>R</i>)-(3,3'-dimethoxy-1,1'-binaphthyl-2,2'-diyl)bis(prop-1-yne-3,1-diyl)) bis(trimethylsilane) [96]	128
6.4.10. Complex (<i>R</i>)-85	129
6.5. Modification of the chiral Knölker complex	129
6.5.1. Complex (<i>R</i>)-86	129
6.5.2. Complex (<i>R</i>)-97	133
6.5.3. Complex (<i>R</i>)-98	133

6.5.4. Complex (<i>R</i>)-99	134
6.5.5. Complex (<i>R</i>)-100	135
6.5.6. Complex (<i>R</i>)-101	136
6.5.7. Complex (<i>R</i>)-102	136
6.5.8. Complex (<i>R</i>)-103	137
6.5.9. Complex (<i>R</i>)-104	138
6.5.10. Conditions adopted for the attempted synthesis of complex 105	139
6.5.11. Free ligand 106	140
6.5.12. Free ligand 107	140
6.5.13. Free ligand 108	141
6.6. Synthesis of (cyclopentadienone)iron tricarbonyl complexes using an intermolecular cyclative carbonylation/complexation	143
6.6.1. Cyclooctyne [122]	143
6.6.2. [Bis(hexamethylene)cyclopentadienone]iron tricarbonyl complex 123	144
6.6.3. Cyclododecyne [128]	148
6.6.4. [Bis(decamethylene)cyclopentadienone]iron tricarbonyl complex [129]	149
6.7. Towards a planar chirality	150
6.7.1. 2,3-diphenyl-4,5-dipropylcyclopenta-2,4-dien-1-one [152]	150
6.7.2. Complex 155	150
6.7.3. 2,3,5-triphenyl-4-(1-hydroxy-1ethyl)-cyclopenta-2,4-dien-1-one [154]	151
6.7.4. Complex 156	152
6.7.5. Racemic resolution of 4-phenyl-but-3-yn-2-ol	152
6.8. General procedure for hydrogenation	154
6.8.1. General procedure for hydrogenation reactions with Me ₃ NO as activator	154
6.8.2. General procedure for photolytically induced hydrogenation	154
6.8.3. General procedure for the transfer hydrogenation	155
6.8.4. Conditions for conversion and <i>ee</i> determination by GC for products in Table 9	155
6.8.5. NMR conversion and conditions for conversion by GC for products in Table 12	157

6.8.6 Determination of the hydrogenation kinetics of acetophenone	159
7. Literature	162
Appendix	171
7.1. NMR Spectra	171
7.1.1. Complex (R)-58	171
7.1.2. Complex 66	172
7.1.3. Complex 67	173
7.1.4. Complex (R)-85	174
7.1.5. Complex (R)-86	175
7.1.6. Complex (R)-97	176
7.1.7. Complex (R)-98	177
7.1.8. Complex (R)-99	178
7.1.9. Complex (R)-100	179
7.1.10. Complex (R)-101	180
7.1.11. Complex (R)-102	181
7.1.12. Complex (R)-103	182
7.1.13. Free ligand 106	184
7.1.14. Free ligand 107	184
7.1.15. Free ligand 108	186
7.1.16. Complex 123	187
7.1.17. Complex 155	188

1. Preface

In the past 20 years, sustainability emerged as one of the keywords in the fields of society, politics and science. The key challenge nowadays is the need to produce high-quality products with minimum energy and waste. Especially in chemistry, one of the fundamental research goals is to develop sustainable, efficient and selective synthesis. In particular, the concept of sustainability is clearly defined by the use of low waste chemical transformations plus the use of catalysts in order to decrease the amount of energy required by a process; in fact catalysis leads to more efficient reactions in terms of energy consumption and waste production. The catalytically active species form reactive intermediates by coordination of the organic substrates, thus decreasing the activation energy required for the transformation. Formation of product should occur with regeneration of the catalyst and it can be described by its turnover-number (TON) providing a measure of how many catalytic cycles are executed by one molecule of catalyst.

Catalysis is an important field in both academic and industrial research, approximately 80% of all chemical and pharmaceutical products on industrial scale are obtained using catalyst. During the last 50 years various catalysts based on transition metals were developed, in particular, catalytic systems based on noble metals like palladium, iridium, ruthenium and rhodium turned out to be very effective for a broad range of chemical transformations.

Unfortunately, especially in the field of the asymmetric reactions, the number of the implemented processes is limited, and despite all advances in the technology, most of chiral pharmaceutical intermediates are still prepared via traditional resolution of diastereomeric salts.

This lack of applied catalytic processes can be explained by various reasons:

- a) time-to-market pressure does not give enough time to optimize or to develop new catalytic methods;
- b) high cost of the catalysts (both the choice of the central metal and the design of the ligands) coupled with the relatively low turnover numbers that can be achieved in most cases makes this technology too expensive;
- c) limited availability of noble metals, as long-term supply for the chemical process could exceed their occurrence in nature;
- d) toxicity problems, since even trace amounts of toxic metals are often not allowed to occur in the final products, and they are usually difficult to recycle;

e) technology works fine on a limited number of benchmark substrates; however the catalyst is often too slow on real pharmaceutical intermediates (this is often caused by the presence of nitrogen-containing substituents that can bind to the catalyst).

These limitations concern not only pharmaceutical companies but also other industrial sectors (like agro-chemistry, food industry or cosmetic sector) which require the use of enantiopure compounds.

For these reasons, most catalytic reactions satisfy the criteria to reach a sustainable transformation only on a microscopic scale, in fact cheap catalysts, readily accessible and non-toxic are needed for these purposes. Replacing precious metals with cheap first-row transition metals would be a major breakthrough, with an enormous scientific and industrial impact. In Table 1 and Figure 1, a comparison of prices of noble metals (expressed in price per gram) with base metals (price per kilogram) is reported, showing that the latter are at least 1000 times cheaper.^{[1][2]} For this reason, catalysis with inexpensive transition metals is an area undergoing rapid growth.^[3]

Metal	Price		Abundance (ppm)
Ru	1.22	€/g	1.0×10^{-3}
Rh	18.56	€/g	1.0×10^{-3}
Ir	16.24	€/g	1.0×10^{-3}
Pd	20.23	€/g	1.5×10^{-2}
Pt	32.86	€/g	5.0×10^{-3}
Au	38.68	€/g	4.0×10^{-3}
Fe	0.4996	€/Kg	5.63×10^4
Co	23.65	€/Kg	2.5×10^1
Ni	9.34	€/Kg	8.4×10^1
Cu	4.4	€/Kg	6.0×10^1

Table 1. Prices of noble and base metals

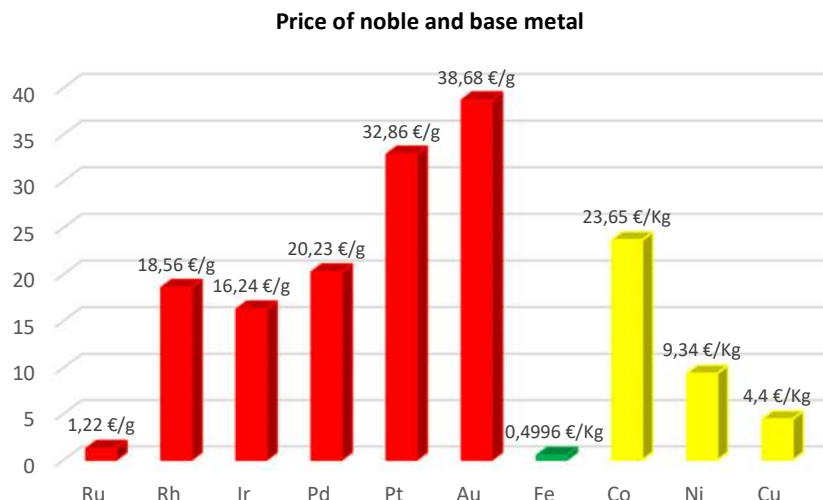


Figure 1. Prices of noble and base metals (July 2016)^[3]

Global efforts in sustainability, coupled with high prices of noble metals, have recently attracted considerable attention in developing iron catalysis, because iron is an abundant, inexpensive, and environmentally non-toxic metal.^[4] Iron is a fundamental element of our planet, the second most common metal after aluminium and it is accountable for one third of the Earth's mass.

People have known and used iron since nearly 3200 years and it always played a crucial role in humans' world. Iron is essential in biology, we can find iron-based-proteins in all living organisms, from bacteria to human. The red color of our blood is caused by iron-containing proteins – hemoglobin and myoglobin – thanks to these complexes, blood is able to transport oxygen in our bodies. In many other processes, iron is the acting metal in the active site of many important redox enzymes: e.g. cellular respiration and oxidation and reduction in plants and animals. In addition to that over 80% of nitrogen is originated from the Haber-Bosch process of synthesizing ammonia using a heterogeneous iron catalyst. Iron can be considered as one of the least toxic transition metals,^[5] and its use implicates less toxicity problems since limits for residual iron traces are hundreds times greater when compared to noble metals.^[6] Iron is relatively cheap and tolerant to a number of functional groups, making it an interesting alternative to other transition metals typically applied in catalysis, especially for applications in pharmaceutical industry.

These features are in line with the principles of Green Chemistry, which promoted the increasing research activity in the iron field starting about 15 years ago, as demonstrated by an increasing number of research articles published in the area (Figure 2 showed a Scopus® search from 1970 till December 2015 for journal articles containing the phrase “iron catalysis”).

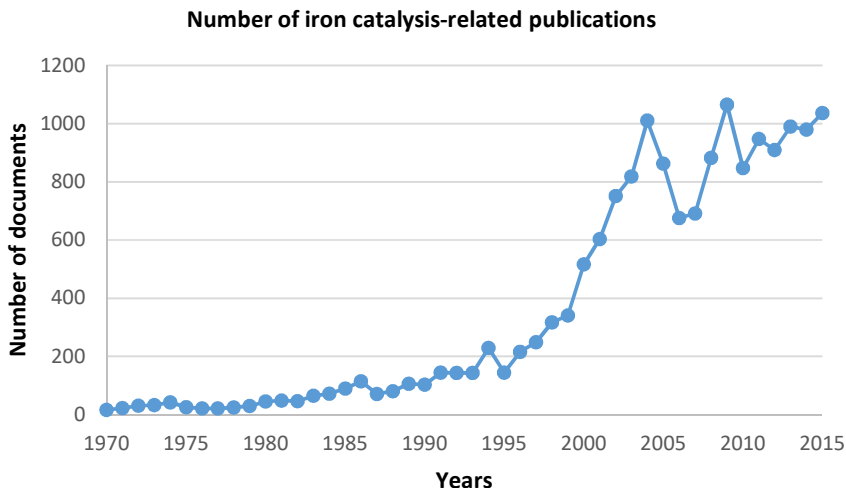


Figure 2. Number of iron catalysis-related publications over the last 50 years

Rudyard Kipling, winner of the Nobel Prize in Literature in 1907, started his poem “Cold iron” with these lines:

“Gold is for the mistress — silver for the maid —

Copper for the craftsman cunning at his trade.

“Good!” said the Baron, sitting in his hall,

“But Iron — Cold Iron — is master of them all”..,

Nowadays, Beller reported in 2008^[7] and Carsten Bolm in 2009^[8] that a new iron age has begun, “from Rust to a Rising Star”.

On the other hand, the Fe-based catalytic reductions reported so far suffer from serious limitations, such as difficult synthesis/lack of robustness of the catalyst, moderate activity/(enantio)selectivity, high cost/poor atom economy of the catalyzed process. These limitations need to be overcome, in order for Fe-catalysis to become of practical utility for the industrial production of fine chemicals.

2. Introduction: iron

2.1. Electronic configuration, oxidation states, coordination geometries of iron

Iron is the second most abundant element in the earth's crust, it belongs to group VIII and period IV, with an electronic configuration of $[\text{Ar}]3d^64s^2$. It is difficult to find iron as a pure metal in nature due to its tendency to be oxidized in the presence of oxygen and moisture. The most common oxidation states of iron are +2 and +3, as is showcased by its halides: iron(II) chloride known as ferrous chloride and iron(III) chloride, ferric chloride. In air, most of iron(II) complexes are readily oxidized to the corresponding iron(III), which is the most stable and widespread iron species. Other observed oxidation states are +6, 0, -1, -2, but compared to other elements of the VIII group, iron never reaches its full oxidation state of +8.

In its low oxidation states, it may act as an iron-centered nucleophile and catalyze reactions such as nucleophilic substitutions, additions to carboxylic substrates, cycloisomerization and others.^[9] Iron(II) complexes (d^6), show a coordination number of six with an octahedral ligand sphere, while iron(III) (d^5), can coordinate from three to eight ligands but also often exhibits an octahedral coordination. In its most common oxidation states (+2 and +3), iron has a tendency to engage in single electron transfer reactions, and for this reason it has found widespread application as a catalyst for redox processes.^[10]

In 1963 Pearson introduced the hard and soft acids and bases (HSAB) principle, assigning Fe^{3+} as a hard acid and Fe^{2+} as borderline acid,^[11] and for the quantification Parr and Pearson introduced the so called η values as an absolute measure for hardness. These values are determined relative to Al^{3+} (the metal with the highest η value of 45.8).^[12] As expected, the hardness increases with the oxidation state: Fe^0 ($\eta = 3.9$), Fe^{2+} ($\eta = 7.2$), Fe^{3+} ($\eta = 13.1$). Iron(0) is a soft Lewis acid, it coordinates five or six ligands in a trigonal bipyramidal and octahedral geometry. It should be noted that if the transition-metal atoms act as Lewis acid, it is in an excited valence state, so iron atoms are $3d^8$ and not $3d^64s^2$. Despite these general studies, the observed Lewis acidity strongly depends on the type of the reaction that is promoted or catalyzed.

Iron(0) and iron(II) complexes are the main oxidation states used in iron catalysis. Iron carbonyl complexes are of special interest due to their high stability, containing an iron(0) center capable of coordinating complex organic ligands.

By contrast, many Fe-complexes have little propensity to participate in two-electron processes, which are typical of many reactions catalyzed by precious metals for example hydrogenations. Due to this reason, until recent years, iron has been scarcely exploited for classical transition metal reactions (oxidative addition/reductive elimination).

2.2. General difficulties related to the development of new iron catalysts

First-row transition metal catalysts possess unique features, which usually are not found with classical precious metal compounds. In particular, in order to mimic noble metals, iron must suppress one-electron redox reactions and facilitate the two-electron redox interplay (e.g. Fe(0)/Fe(II)). Other potential obstacles resulting from the propensity to undergo one-electron processes are related to radical chemistry and multiple oxidation states.^[13] Furthermore, most of Fe(II)-complexes are paramagnetic due to the small energy gap (Δ_0) between the t_{2g} and the e_g orbitals (Figure 3), and therefore NMR spectroscopy is scarcely useful for their characterization, which mostly relies on mass spectrometry and X-ray diffraction.

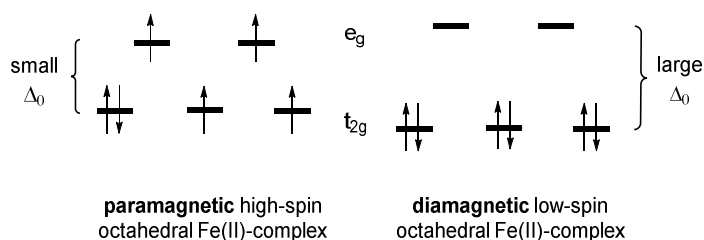
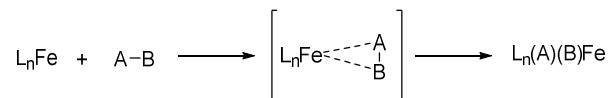


Figure 3. MO diagrams for octahedral crystal field: distribution of six valence electrons in high-spin and low-spin Fe(II)-complexes

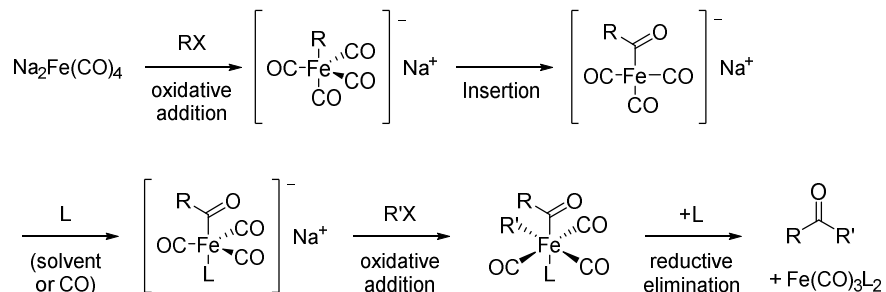
2.3. Fundamental reactions that play a key role in iron catalysis

Halogen-metal exchange, ligand exchange, insertion, haptotropic migration, transmetallation, oxidative addition, reductive elimination, β -hydride elimination and demetallation are fundamental reactions that play a key role in transition metal catalysis.

Oxidative addition (Scheme 1) is generally observed in d^8 systems such as Pd(II), Ni(II), Ir(I), Rh(I), Co(I), Os(0), and also for iron it is possible that the oxidation state increases from (0) to (II). The reactivity for this elemental reaction step increases from right to left in the periodic table and from top to bottom within the respective triad. It is furthermore influenced by the ligand sphere: strong σ -donor ligands and poor π -acceptor ligands favor the oxidative addition due to increased electron density at the metal.

**Scheme 1. Oxidative addition**

Another important reaction is the insertion; hydroformylation^[14] and alkene polymerization are well-known industrial processes. Scheme 2 shows how carbon monoxide is used to obtain aldehydes and ketones from the carbonylation of alkyl groups.

**Scheme 2. Example of insertion of carbon monoxide**

The reductive elimination (last step in Scheme 2) releases the organic product in a concerted mechanism, in which the electron count of the metal is reduced by two. A potential limiting aspect for iron catalysis is the tendency for coordinative saturation; in diene-iron complexes, for example, the dissociation of a ligand or the reductive elimination is not favored, and the free ligand can be obtained after the removal of the iron by demetallation. This usually requires harsh oxidative conditions, which oftentimes led to the decomposition of the complex by giving inert iron oxides, while at the same time, such strong conditions might also destroy sensitive organic ligands. Consequentially, milder conditions are needed to obtain the desired product. For example, in iron-mediated [2+2+1] cycloadditions, the demetallation of the (η^4 -cyclopentadienone)iron tricarbonyl complexes is achieved by using a different method [see paragraph 3.3.5, Scheme 48].^[15]

2.4. Importance of the ligands

Homogeneous transition metal based catalysis has seen a rapid growth in recent years, mainly thanks to the selectivity (chemo, regio, stereo) requirements, which is highly desirable for new processes and products, but also because of an environmental advantage related to the minimization of side products according to "green chemistry".^[16]

A ligand is the keystone of a catalytic system and allows to tune the reactivity and selectivity by modifying its steric and/or electronic properties, in order to improve the catalytic properties of

the complex.^[17] For these reasons, the properties of a complex are defined by the interaction between the ligands and the metal center. The metal complex can be stabilized by tri- and tetradentate ligands which can bear phosphorus and/or nitrogen donors such as porphyrins or diiminodiphosphine.

Ligands can be also modified for specific needs and stability,^[18] and in many cases their structures are not affected during the reaction, acting as “spectators”.

The main drawback for base metals is their electronic structure, which is prone to one-electron redox changes, different from noble metals, that, as already mentioned, easily undergo two-electron redox changes, (e.g. Rh(I)/Rh(III), Ir(I)/Ir(III), Pd(0)/Pd(II)), which can be used to promote bond breaking or making. Overcoming this one-electron transfer tendency is a challenge, both for reactivity control as well as for stabilizing and maintaining the catalytic functions of the complexes. Recent advances in transition metal catalysis brought new types of “reactive” ligands, endowed with the characteristic property of synergistic cooperating with the metal to mimic the bond-making and bond-breaking processes.^[19] These ligands can be divided into two categories: redox non-innocent or cooperative ligands.

In 1966 Jørgensen introduced the term “non-innocent”: “ligands are innocent when they allow oxidation states of the central atom to be defined”.^[20] Since it is ambiguous to determine the oxidation state, usually set of spectroscopic studies have to be performed, like: Raman or electron paramagnetic resonance (EPR), X-ray absorption (XAS), UV-vis or Mössbauer spectroscopy. These ligands have the ability to delocalize part of the electronic density of the complexes. In this way they become a kind of “electronic reservoir” during the reaction and catalytic process, and allow multi-electron transformations for base metals. Radical-type transformation can also be initiated and controlled, and redox processes can also occur. As a result, new “redox isomers” can form, which should not be confused with resonance structures, and can exhibit a variety of different properties and reactivities.

Cooperative (or chemically non-innocent) ligands are “participating directly in bond-activation and undergo reversible chemical transformations”.^[21]

The metal part of the complex acts as a binding site and brings reactants together, in that way, the metal and the ligand act cooperatively in a synergistic way and their interactions trigger a chemical transformation, but at the same time can show also an intrinsic reactivity.

“Non-innocent” does not identify a particular group of ligands, it is rather a state, which can be attributed to any ligand under the right conditions. Observed “non-innocent” behavior of a ligand in a metal complex does not guarantee that it will act in the same way with a different metal or

under different conditions. Only detailed spectroscopic investigations can confirm the “non-innocent” nature of the ligand in the specific transformation.

3. Iron-catalyzed hydrogenation and asymmetric hydrogenation

It has been often overlooked, that the first catalytic homogenous hydrogenation was not based on a noble metal but on copper.^[22] In any case the most commonly accepted date for the birth of homogenous reduction is 1966, when Wilkinson found $\text{RhCl}(\text{PPh}_3)_3$ as an effective catalyst for the hydrogenation of alkenes.^[23] Replacement of the triphenylphosphine ligands from this catalyst with a chiral phosphine led to the first examples of asymmetric hydrogenation (AH). Subsequently research on rhodium complexes bearing different ligands spread, and a huge variety of ligands were developed (e.g. monodentate phosphines,^[24] chiral bidentate or monodentate phosphorus ligands,^[25] BINAP^[26]). It was clear, as already mentioned, that the choice of proper ligands for a given metal center is essential to obtain a high level of catalytic activity and selectivity for the desired transformation.

It is well known that stereochemistry plays a crucial role in synthesis of new drugs or agrochemicals. Compounds have to precisely fit into the active sites of enzymes and it is also common that two enantiomers of the same molecule can show completely different properties. In the case of fragrances or flavor additives, they can just smell or taste differently. In the case of drugs, one enantiomer can have a therapeutic use, while second can be highly toxic or even possess strong teratogenic properties (e.g. Thalidomide). For these reasons, enantiopure chiral molecules, especially in the field of pharmaceutical intermediates, are regulated by the US's Food and Drug Administration (FDA).^[27]

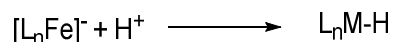
Enantioselective catalysis is in principle the most efficient strategy for the synthesis of enantiopure molecules and in particular asymmetric hydrogenation is a suitable method for large-scale applications due to its operational simplicity, atom economy, high conversions (and enantiomeric excesses) which can be obtained without harsh, dangerous and energy-consuming conditions. Enantioselective transfer hydrogenation for the reduction of ketones, imines and conjugated C=C double bonds, using isopropanol and formic acid/trimethylamine instead of H_2 , also gained a prominent position in recent years, even if the most used sources of hydrogen remains molecular hydrogen.^[28]

As already mentioned in the last 15 years there was a development of iron catalysis, where some iron complexes demonstrated to have catalytic activity for the reduction of unsaturated substrates (alkenes, ketones, aldehydes, imines) by molecular hydrogen or different hydride sources, in which the Fe-H is involved as a key intermediate.

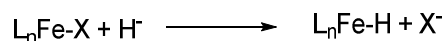
3.1. Fe-H complexes

The synthesis of iron hydride complexes can be done *via* different routes:

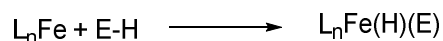
- 1) Protonation of an anionic iron complexes:



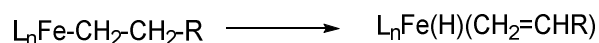
- 2) Substitution of halides (one electron donor ligand) with a hydride, using NaBH₄ or LiAlH₄ as hydrogen source:



- 3) Oxidative addition of H₂ or E-H to a low valent and unsaturated iron complex:

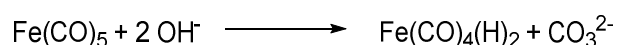


- 4) β -elimination of an alkyl iron complex to obtain the hydride complex coordinated to the olefin:



Fe-H plays an important role in homogenous catalysis; hydride complexes usually act as important intermediates in the catalytic cycle for hydrometalation such as e.g., hydrosilylation or hydrogenation reactions.^[29]

The first iron hydride complex, Fe(CO)₄(H)₂, was reported in 1931 by Hieber and Leutert,^[30] the complex was synthesized and isolated at low temperature from Fe(CO)₅ and OH⁻:



but it decomposed at room temperature into Fe(CO)₅, Fe(CO)₃ and H₂.

In Figure 4 three iron hydride complexes are presented, which were prepared, isolated and characterized spectroscopically and in some cases also X-ray crystal structures were obtained. The first structurally characterized iron complex contained a μ -H ligand, [NEt₃H][HFe₃(CO)₁₁] (Structure a, Figure 4),^[31] was reported in 1965. In 1970, the first terminal hydride iron complex was characterized by X-ray analysis, CpFeH(CO)(SiCl₃)₂.^[32] In 1972, the first X-ray structure of a dihydride iron complex, *cis*-[Fe(H)₂{PPh(OEt)₂}]₄, was reported.^[33]

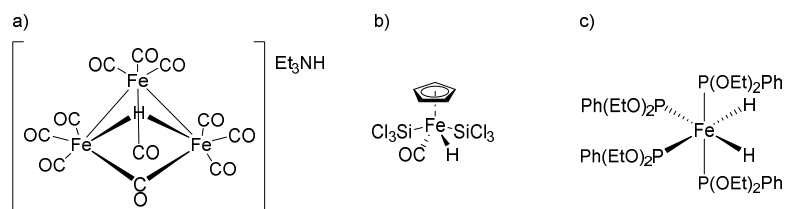


Figure 4. Lewis representations of the first X-ray crystal structures of three types of iron hydride complexes a, b and c

The spectroscopic characterization of this class of compounds can be problematic, but still it is possible to find characteristic signals in different spectroscopic methods.

The $^1\text{H-NMR}$ spectra for diamagnetic iron hydride complexes show diagnostic signals in high field. IR spectra are also helpful because the Fe-H stretching frequencies are observed in the range of $1500 - 2200\text{ cm}^{-1}$, even though sometimes the intensities are weak and thus the method is not reliable. Crystallography methods are helpful to prove the structure of the complex, but in many cases the hydrides themselves are not detected, due to poor scattering of X-rays of the hydride and the estimation of Fe-H bond should be carefully evaluated.

3.2. Hydrogenation of alkenes and alkynes

3.2.1. Homoleptic ironcarbonyl complexes

In the presence of carbon monoxide iron can form three stable homoleptic complexes: ironpentacarbonyl $\text{Fe}(\text{CO})_5$,^[34] diironnonacarbonyl $\text{Fe}_2(\text{CO})_9$ and triirondodecacarbonyl $\text{Fe}_3(\text{CO})_{12}$ (Figure 5). These compounds represent the source of iron for most artificial complexes.

The first iron complex, $\text{Fe}(\text{CO})_5$, was discovered in 1891 by Berthelot^[35] and Mond,^[36] it is a stable 18-electron complex and show a trigonal-bipyramidal geometry, where the carbon monoxide ligands are strong ligands capable of stabilizing low spin electronic structures of iron(0).

$\text{Fe}(\text{CO})_5$ was used in the early attempts for iron-catalyzed hydrogenations.^[37] In 1964 Frankle *et al.* hydrogenated methyl linoleate and methyl linolenate to get monoenoic fatty esters.^[38] Unfortunately, the reaction had to be performed at high hydrogen pressure (250 – 300 atm) and high temperature (200 °C). Due to these harsh conditions, there was very low chemoselectivity, making this method unacceptable also for industrial purposes.

Also Noyori and co-workers used iron pentacarbonyl to obtain saturated ketones from α,β -unsaturated ketones with very good yields.^[39] Subsequently Wrighton discovered that the reactivity of $\text{Fe}(\text{CO})_5$ was improved under UV irradiation at room temperature, but unfortunately only poor yields and limited substrate scope were obtained.^[40]

The mechanism of the hydrogenation was studied by Grant and co-workers,^[41] where the active species in the hydrogenation was formed upon heating (>150 °C) or upon constant UV-irradiation of $\text{Fe}(\text{CO})_5$ to obtain $\text{Fe}(\text{CO})_3$, containing a vacant site for the coordination.

$\text{Fe}_2(\text{CO})_9$ is prepared *via* photolytic reaction from $\text{Fe}(\text{CO})_5$,^[42] while $\text{Fe}_3(\text{CO})_{12}$ can be obtained from $\text{Fe}_2(\text{CO})_9$ by a thermal reaction. Due to slowly degradation, leading to pyrophoric iron, the last two complexes, which contain direct metal-metal bonds must be carefully handled under inert atmosphere.

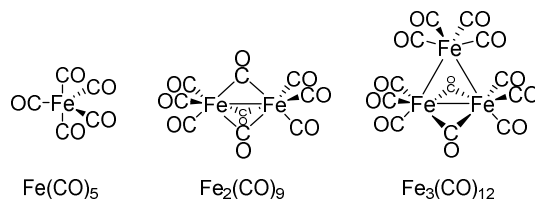
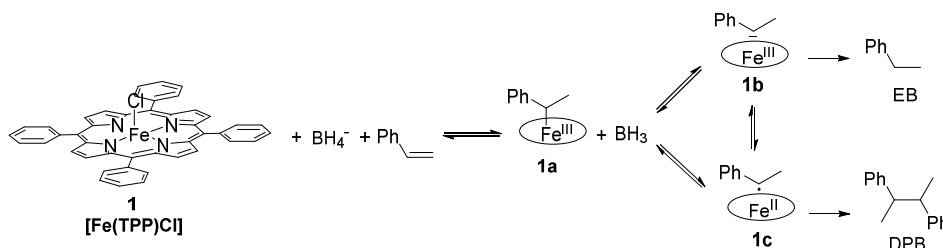


Figure 5. Homoleptic iron carbonyl complexes

3.2.2. Biomimetic complexes: iron porphyrins

Porphyrins are a group of heterocyclic macrocycles, composed of four modified pyrrole subunits interconnected at their α -carbon atoms via methine bridges ($=\text{CH}-$). Several biomimetic catalysts took inspiration from natural iron-porphyrin complexes, in particular from the “heme”, a cofactor of the protein hemoglobin. Kano and co-workers used Fe-porphyrins together with NaBH_4 as a hydride source to radically hydrogenate styrene, obtaining TOFs up to 81 h^{-1} .^[43] The key in this mechanism is the formation of the σ -alkyliron(III) complex **1a** (Scheme 3), through the coordination of styrene to complex **1**. Intermediate **1a**, in the presence of a polar protic solvent, seems to be stabilized by extensive solvation, and rapidly transfers a proton from the solvent to styrene to afford the final product, ethylbenzene (EB).

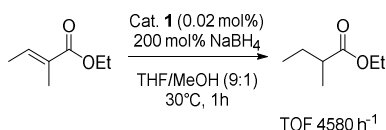


Scheme 3. Mechanism of the reduction of styrene using [Fe(TPP)Cl] **1** in the presence of NaBH_4

In fact, the role of the solvent is crucial to favor the equilibria between **1a** and **1b**, respect to **1b** and **1c**; in particular polar solvents are able to separate 1-phenylethyl radicals, which may couple

with each other to give the by-product, 2,3-diphenylbutane (DPB). In addition, isotope labeling experiments revealed that hydrogen atoms on the α - and β -position of the ethylbenzene come from the hydroxy proton of ethanol (C_2H_5OD) and the hydride of $NaBD_4$.

Sakaki *et al.* reported a similar approach with porphyrin $[Fe(TPP)Cl]$ **1** to hydrogenate α,β -unsaturated esters with high turnover frequencies (TOFs) up to 4850 h^{-1} (Scheme 4).^[44] Again, deuterium labeling studies revealed that besides a hydride from $NaBH_4$, a proton from methanol was transferred during the hydrogenation to the β - and α -carbons of the double bond. Unfortunately, in some cases isomerization was observed (e.g. from oct-1-ene to oct-2-ene).



Scheme 4. Hydrogenation of α,β -unsaturated esters using $[Fe(TPP)Cl]$ **1**

Several other complexes containing iron were found in the active site of natural proteins, e.g. a diiron complex in $[Fe-Fe]$ -hydrogenases, a binuclear $[Fe-Ni]$ -hydrogenase complex and a monoiron complex in $[Fe]$ -hydrogenase (Figure 6). In $[Fe-Fe]$ -hydrogenases (**a**), two Fe centers are bridged by a CO ligand and a small organic moiety, even though it is not clear if the moiety is a dithiolate.^[45] On the other hand, $[Ni-Fe]$ -hydrogenase (**b**) contains a large subunit with the Ni-Fe cluster^[46] and a small one, an iron-sulfur cluster ($[4Fe-4S]$).

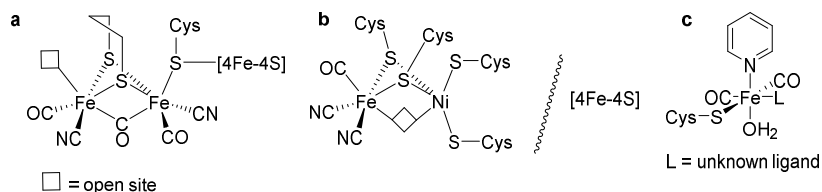
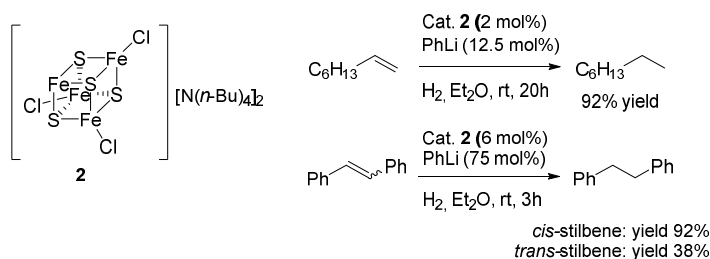


Figure 6. Models for the active site of $[Fe-Fe]$, $[Ni-Fe]$, and $[Fe]$ -hydrogenases

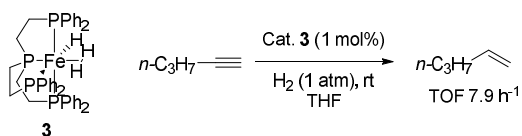
Inoue *et al.*, inspired by iron-sulfur clusters present in the active sites of hydrogenase enzymes, proposed a biomimetic approach.^[47] The Fe_4S_4 cluster showed catalytic activity, in the presence of PhLi and hydrogen gas, in the hydrogenation of 1-octene and *cis*- and *trans*-stilbene with very good yields, although the iron cluster was more active with (*Z*)-alkenes (Scheme 5) and the selectivity favored terminal vs. internal double bonds when hexamethylphosphoric triamide (HMPT) was used as a cosolvent.



Scheme 5. Reduction of olefins using bio-inspired iron-sulfur clusters catalyst

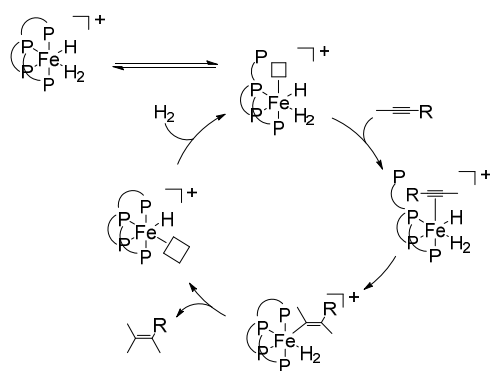
3.2.3. Multidentate P ligand iron complexes

Bianchini and co-workers developed the first catalyst able to hydrogenate alkyne bond bearing a multidentate *P* ligand **3** in 1992.^[48] This catalyst was able to promote the reduction of terminal alkynes to corresponding alkenes at room temperature, under atmospheric pressure of H_2 (Scheme 6).



Scheme 6. Selective hydrogenation of 1-pentyne using multidentate P complex

The proposed catalytic cycle shows a cooperative involvement of the ligand during the transformation, as it can leave a free coordination site for the incoming substrate by releasing one terminal phosphine arm (Scheme 7).

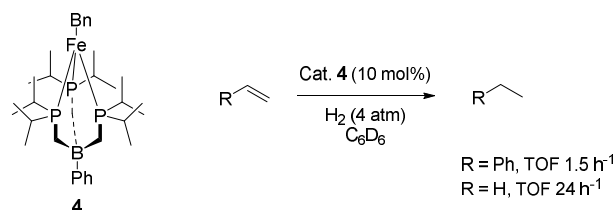


Scheme 7. Catalytic cycle of the reduction of alkynes by a multidentate P-Fe complex

Subsequently a substrate scope was performed, and it was observed that bulkier substituents on terminal alkynes $\text{RC}\equiv\text{CH}$ ($\text{R} = \text{Ph}, \text{SiMe}_3, n\text{-Pr}, n\text{-Pent}, \text{CH}=\text{CH}(\text{OMe})$) gave lower conversions, and at the same time the rate of the conversion slowed down.^[49] Luckily the reaction always

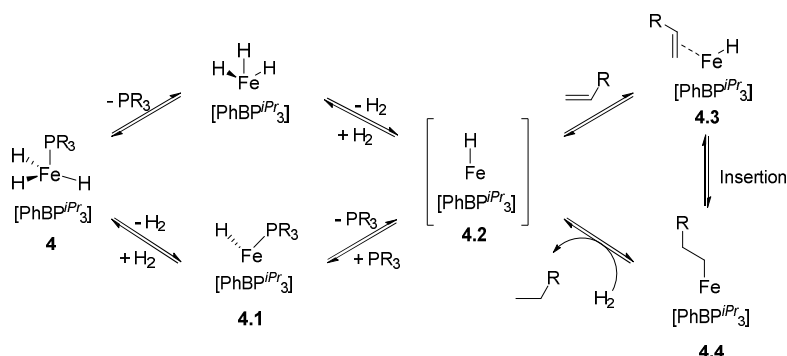
proceeded with a full selectivity of reducing alkynes to alkenes over alkanes, and it was postulated that the iron hydride disfavored the insertion of the olefins, in fact in the case of ethylene, a coordination to the metal center was observed, though it did not proceed further to insertion, even under different harsh conditions.

In 2004 Peters and Daida reported the hydrogenation of olefins catalyzed by a polydentate phosphine complex **4** (Scheme 8).^[50] The hydrogenation of alkenes required a high catalyst loading (10 mol%), but mild reaction conditions (rt, low pressure), while alkynes were undergoing undesired side reactions, such as reductive dimerization or polymerization.



Scheme 8. Hydrogenation of olefins catalyzed by a polydentate phosphine complex

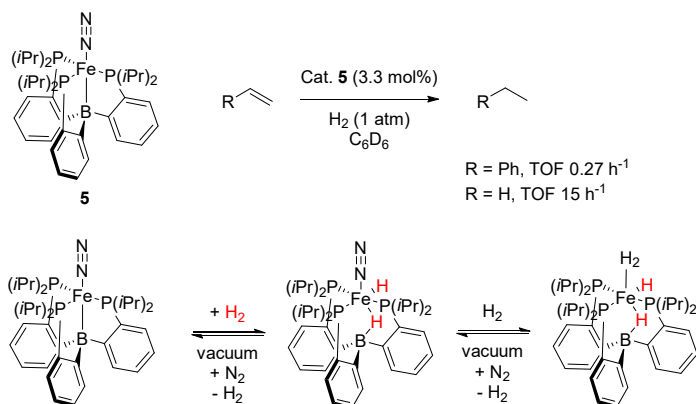
Peters proposed a plausible mechanism (Scheme 9), involving an unusual Fe(II)/Fe(IV) catalytic cycle, with reversible dissociation of the ligand from the iron center in a similar way described by Bianchini.^[51] In this mechanism, the iron(IV) trihydride phosphine complex **4** undergoes hydrogen loss to give the coordinatively unsaturated monohydride complex **4.1** (detected by NMR), followed by olefin coordination (**4.2**) and its insertion into the Fe-hydride complex to give the stable alkyl complex (**4.3**), which reacts with H₂ to release the alkane and regenerate the active species (**4.2**).



Scheme 9. Proposed mechanism for the reduction of alkenes by polydentate phosphine complex

Furthermore, Peters developed a new ferraboratrane complex **5** (Scheme 10) for the hydrogenation of ethene and styrene, albeit with low TOFs (up 15 h⁻¹).^[51] Despite these

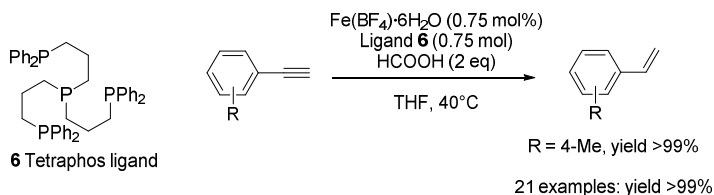
synthetically not promising results, mechanistic studies about the transformation were performed, which revealed a reversible iron-boron bond cleavage, where the boron atom can act as a shuttle for hydride transfer to substrate.



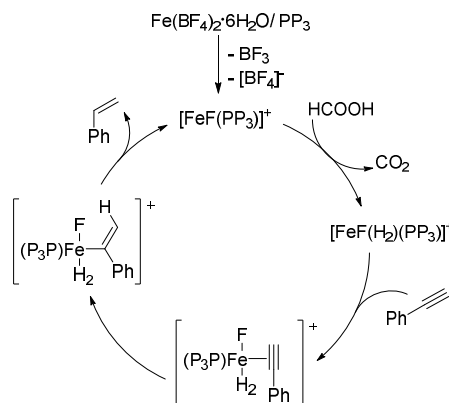
Scheme 10. Hydrogenation of olefins using a ferraboratrane complex 5

In 2012 Beller and co-workers reported a selective hydrogenation of alkynes to alkenes; the active catalyst was formed *in situ*, starting from $\text{Fe}(\text{BF}_4)_2 \cdot 6\text{H}_2\text{O}$ and a tetraphos ligand **6**, using formic acid as a hydrogen donor. In this way, quantitative yields for a broad range of aromatic and aliphatic terminal alkynes were observed. These were reduced under mild and base-free conditions, and several functional groups were tolerated (Scheme 11).^[52]

The catalytically active species is formed *in situ* by adding the tetraphos ligand (PP_3) to the iron precursor, which splits the formic acid under concomitant carbon dioxide release to form $[\text{FeF}(\text{H}_2)(\text{PP}_3)]^+$. Finally, phenylacetylene after coordination to the iron center, is reduced and the catalyst releases styrene to regenerate the active catalyst (Scheme 12).^[52]



Scheme 11. Selective semihydrogenation of (hetero)aromatic and aliphatic alkynes

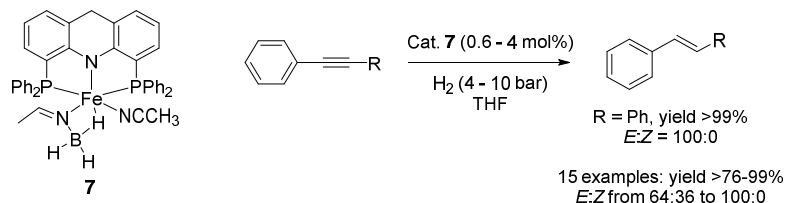


Scheme 12. Proposed mechanism for the reduction of alkynes using $\text{Fe}(\text{BF}_4)_2 \cdot 6\text{H}_2\text{O}$ in the presence of a tetraphos ligand (PP_3)

3.2.4. *P,N,P*- and tetradentate *N*-ligand complexes

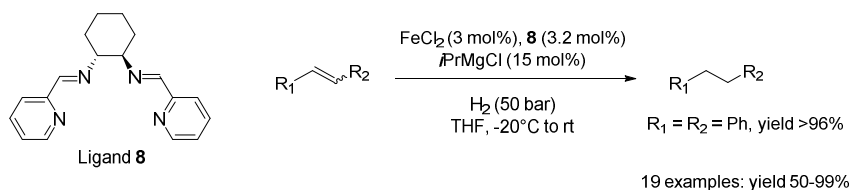
In 2013 Milstein and co-workers reported an acridine-based *P,N,P*-iron pincer complex **7** for the hydrogenation of alkynes to alkenes with high yields and excellent *E*-selectivity (Scheme 13).^[53]

This reaction was carried out under mild conditions (4-10 bar H_2) and did not require the addition of an external base. Furthermore, the presence of many functional groups like carbonyl, nitrile or halogen substituents was tolerated by this catalytic system.



Scheme 13. Hydrogenation of alkynes using an acridine-based *P,N,P*-iron pincer complex

Thomas and co-workers formed an iron complex *in situ* from a tetradentate iminopyridine ligand **8** and FeCl_2 (Scheme 14), which was subsequently reduced with an organometallic coupling reagent (*i*PrMgCl) to form active, low valent catalyst, thus avoiding the isolation of the highly air- and moisture sensitive low valent iron species. In this way, a broad range of mono-substituted, 1,1- and 1,2-substituted aryl- and alkyl-substituted alkenes were hydrogenated.^[54]



Scheme 14. Reduction of olefins using an iron complex from a tetradentate iminopyridine ligand

3.2.5. Bis(imino)pyridine complex

Bis(imino)pyridine iron complexes are a very important group of iron catalysts as highly efficient catalysts for the hydrogenation of alkenes, presented by Chirik and co-workers in 2004.^[56]

The design of this catalyst took inspiration from the observation of previously reported active iron carbonyl compounds **10** in the hydrogenation of alkenes, in which it was proven that $\text{Fe}(\text{CO})_3$ with a vacant site was the active species,^[41] plus a polymerization catalyst reported by Gibson and Brookhart **11** (Figure 7).^[57]

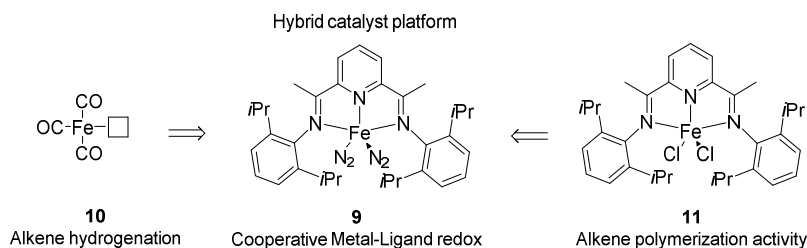
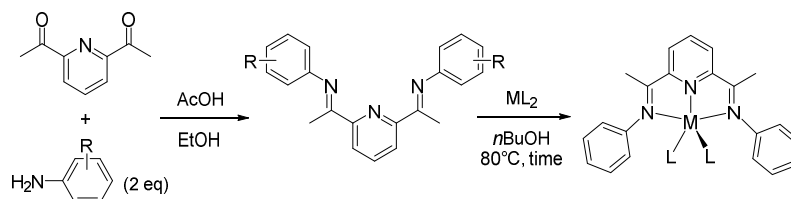


Figure 7. Bisiminopyridine iron complex

Diiminopyridine (PDI) ligands are pyridine derivative with imine sidearms attached to the 2,6-positions, where the three nitrogen centers can bind metals forming a so called pincer complex. These ligands are “non-innocent”, which means that they can change their oxidation state during the course of the catalytic cycle.



Scheme 15. Synthesis of bis(imino)pyridine iron complexes

Chirik chose DIP ligands because they are easily synthesized and easy-to-tune structurally in order to obtain a library of new catalysts.^[58] The ligand, as shown in Scheme 15, can be synthesized by

Schiff base condensation of commercially available 2,6-diacetylpyridine with two equivalents of substituted anilines (e.g. 2,4,6-trimethylaniline and 2,6-diisopropylaniline).

Unsymmetric variations have been developed subsequently by successive condensation of different anilines. The dicarbonyl portion of the backbone can be further modified (e.g 2,6-dipyridylcarboxaldehyde and 2,6-dibenzoylpyridine), even though the most commonly modification was achieved changing the anilines (Figure 8).

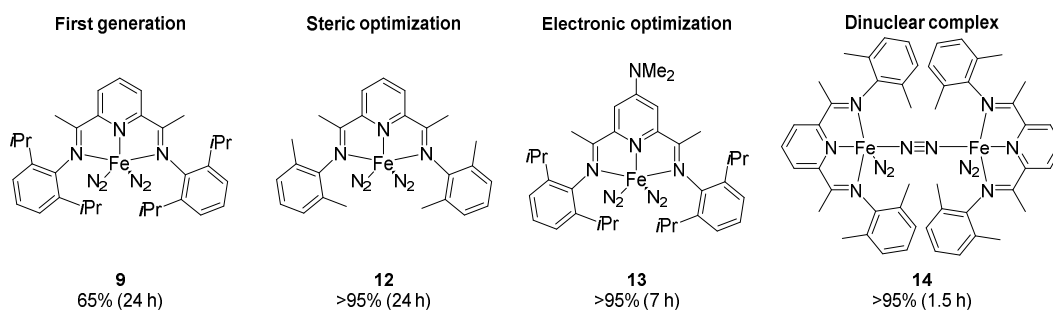


Figure 8. Different types of bis(imino)pyridine iron complexes

The highly conjugated ligand framework of bis(imino)pyridine stabilizes metals in an unusual oxidation state, in fact the ability of the neutral complex to accept up to three electrons leads to ambiguity about the oxidation states of the metal center. The complex $\text{Fe}(\text{PDI})(\text{N}_2)_2$ **9**, obtained by reduction of the ferrous dihalide complex **11** with sodium amalgam, seemed to be an 18-electron complex, consisting of Fe(0) centre with five 2-electron ligands in a formal $\text{Fe}(0)(\text{PDI})$ complex (Figure 9). Despite this, a combination of spectroscopic techniques and density functional theory (DFT) calculations indicated, that this complex is better described as a high spin Fe(II) (d^6) derivative of $[\text{PDI}]^{2-}$, so the metal center transferred two electrons to the ligand.^[59]

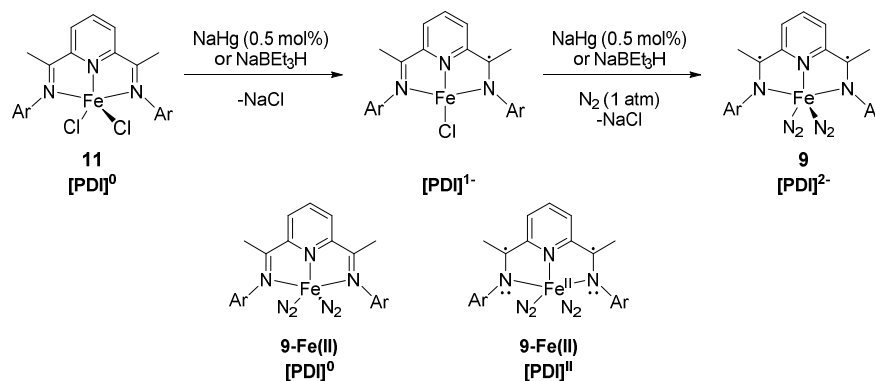
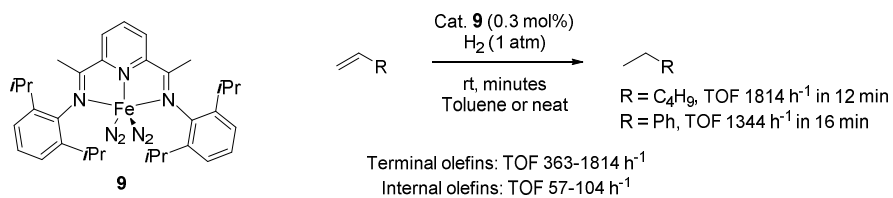


Figure 9. Redox activity of bis(imino)pyridine ligands in iron coordination compounds

This non-innocent behavior allows iron-PDI complexes to participate in two-electrons redox reactions, in which the oxidation state at the metal remains unaltered throughout the catalytic cycle, and the two electrons stored in the ligand are shuttled from the ligand to the substrate.

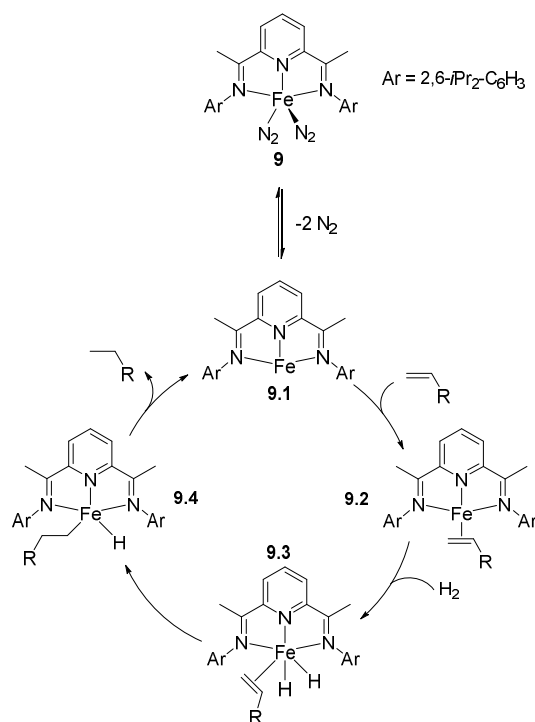
Complex **9** showed an excellent activity in the hydrogenation of olefins, particularly for a base metal, with TOF of 1814 h^{-1} for the reduction of 1-hexene at room temperature in 12 minutes and under 1 atm of H_2 (Scheme 16). This result was comparable to the efficiency of many classical noble metal catalysts like Pd/C, Wilkinson's $(\text{Ph}_3\text{P})_3\text{RhCl}$ and Crabtree's $[(\text{COD})\text{Ir}(\text{PCy}_3)\text{Py}]\text{PF}_6$, under identical conditions. Internal alkenes required longer reaction times in comparison to terminal olefins and the system was not affected by different functional groups like amines, ketones, esters or ethers.^[59] In the case of α,β -unsaturated ketones, a decomposition of the catalyst was noted and only TOFs up to 240 h^{-1} were obtained in the hydrogenation of α,β -unsaturated esters to the corresponding saturated esters. Another advantage of catalyst **9** was the possibility to conduct the reaction without solvent.



Scheme 16. Hydrogenation of olefins using a bis(imino)pyridine iron complex 9

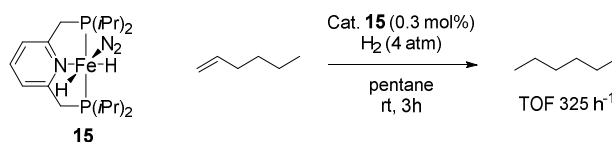
The steric optimization of the ligand led to the development of complex **12** (Figure 8), which improved the activity of the catalyst, but a more remarkable effect was obtained upon introduction of electron-donating substituents, e.g. NMe_2 at the 4-position of the pyridine ring (complex **13**). Also, the dinuclear catalyst **14** revealed excellent catalytic activity.

The proposed catalytic cycle, in Scheme 17, shows that loss of N_2 forms the active species **9.1**; and subsequent coordination of the olefin gives **9.2**. This path is preferred over an oxidative addition of H_2 . Then oxidative addition occurs to provide the olefin dihydride intermediate **9.3**, and finally, olefin insertion leads to **9.4**. Reductive elimination yields the corresponding alkane and regenerates the active species.



Scheme 17. Proposed catalytic cycle of the hydrogenation catalyzed by a bis(imino)pyridine iron complex **9**

Chirik and co-workers also evaluated the possibility to replace the imino functionalities with phosphino groups (Scheme 18).^[61] Complex **15** had a different coordination model, where one nitrogen ligand was replaced by a hydride. Unfortunately, the efforts did not lead to an increased activity. During the hydrogenation of 1-hexene a lower TOF (325 h⁻¹) was achieved respect to the one obtained with complex **9**.

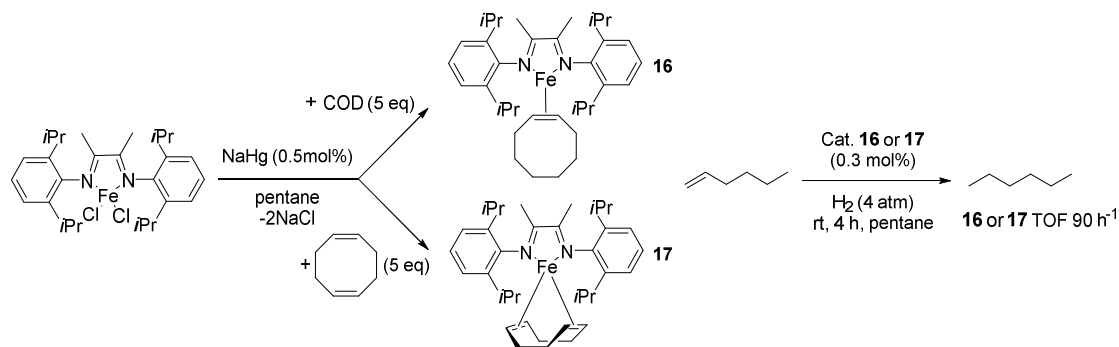


Scheme 18. Hydrogenation of 1-hexene using a bis(diisopropylphosphino)pyridine iron complex

Later on complexes with different imino functionalities were developed and new iron α -diimine complexes were developed (Scheme 19).^[62] Since the dinitrogen-substituted complexes were comparably unstable, ligands like alkynes, alkenes (**16**) or dialkenes (**17**) were introduced to stabilize the structure. Despite these efforts relatively low TOFs of 90 h⁻¹ were achieved in the hydrogenation of 1-hexene.

Despite the significant achievements made by Chirik's group, their catalysts are highly air-sensitive, so synthesis and manipulation must take place under rigorously dry conditions and

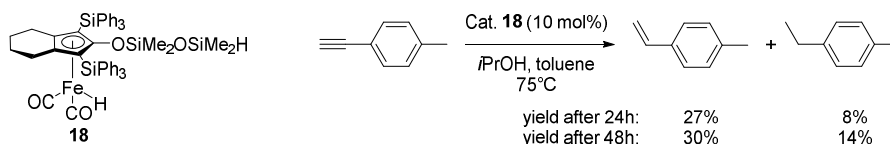
argon atmosphere, inside a glovebox. This makes an industrial application of this process nearly impossible.



Scheme 19. Synthesis and hydrogenation activity of α -diimine iron alkyne complexes **16 and **17****

3.2.6. (Cyclopentadienyl)iron complex

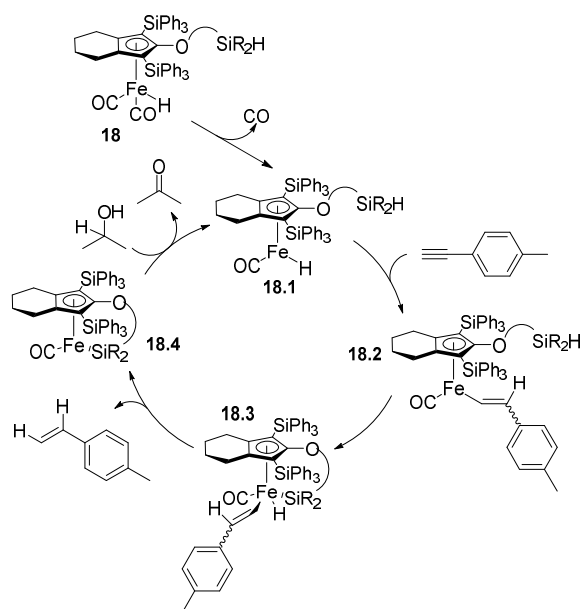
In 2014, Nakazawa and co-workers reported a very interesting example of transfer hydrogenation of alkynes with isopropanol, using a (hydrido)iron complex **18** with a Si-H functionalized cyclopentadienyl ligand. Unfortunately, the reaction is not very chemoselective, oftentimes leading to mixtures of the corresponding alkenes and alkanes (Scheme 20).^[55]



Scheme 20. Transfer hydrogenation of alkynes with isopropanol, using complex **18**

Even though the obtained results were not so impressive, it was the first reported example of iron complex involved in a transfer hydrogenation from isopropanol to be able to reduce an alkyne or an alkene. This complex did not hydrogenate polar unsaturated bonds like in ketones or aldehydes.

Mechanistic studies revealed that hydrogen atoms were transferred first by hydrometalation (Scheme 21, 18.2), followed by reductive elimination (18.3 to 18.4).



Scheme 21. Proposed mechanism of the transfer hydrogenation of alkynes with isopropanol, using complex 18

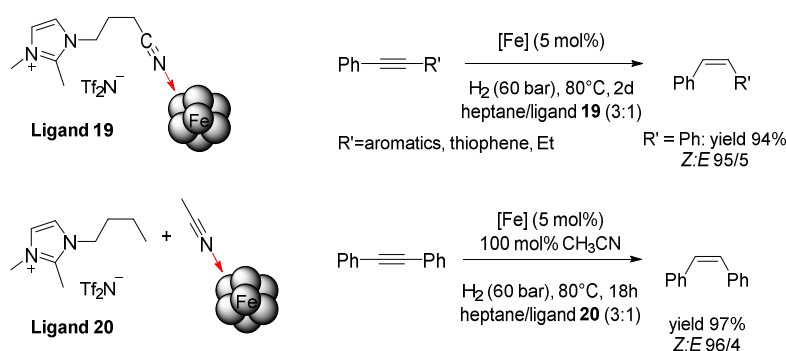
3.2.7. Iron nanoparticles

De Vries and co-workers reported a non-ligand approach using iron nanoparticles (NPs) for the homogenous reduction of alkenes and alkynes.^[63] Based on a methodology described by Bedford, Fe-NPs were prepared by reducing FeCl₃ with EtMgCl in THF.^[64] The hydrogenation was conducted using 5 mol% of Fe-NPs under mild reaction conditions (10-20 bar of H₂, THF and 25 °C). *Cis*-1,2 and 1,1-disubstituted alkenes gave a fast and quantitative conversion, while 1,2-*trans*-disubstituted and cyclic *cis*-alkenes were reduced slower. 1-octyne was hydrogenated with a TOF of 118 h⁻¹. Unfortunately the hydrogenation of tri- and tetrasubstituted alkenes with Fe-NPs was unsuccessful. In addition to this limitation, the presence of OH groups in the substrate slowed down the rate of the reaction. Fe-NPs obtained by the described method were found to be moderately stable, and were successfully applied in the continuous hydrogenation of norbornene, an important intermediate in the synthesis of pharmaceutical drugs.

Another development in this field was the use of iron nanoparticles supported on graphene, which were found to be catalytically active in hydrogenation reactions with various cyclic and terminal olefins.^[65] The main advantage was the efficient removal of the nanoparticles by simple magnetic decantation, and the so re-obtained NPs were shown to still be comparably catalytically active. The iron(0) particles obtained as products of the reaction of iron(III) chloride with ethylmagnesium chloride were found to contain about eight iron atoms as determined by X-ray absorption

spectroscopy. These small nanoclusters are most likely stabilized by the coordination of THF molecules.^[66]

Wangelin and co-workers induced a high Z-selectivity in alkene hydrogenation, using Fe-NPs in a biphasic heptane/ionic liquid system.^[67] The presence of a nitrile function was essential for achieving high Z-selectivity, and the location of the nitrile group was not relevant: it could be introduced either as a substituent in the ionic liquid or as an acetonitrile additive (Scheme 22). The iron nanoparticles were easily removed thanks to the ionic liquid, which prevented aggregation and allowed to decant them. Furthermore, the layer could be reused six times without any loss in catalytic activity. Starting from different alkyl and aryl alkynes, the products were obtained in high yields and in most cases with almost complete Z-selectivity.



Scheme 22. Fe-NPs in a biphasic heptane/ionic liquid system

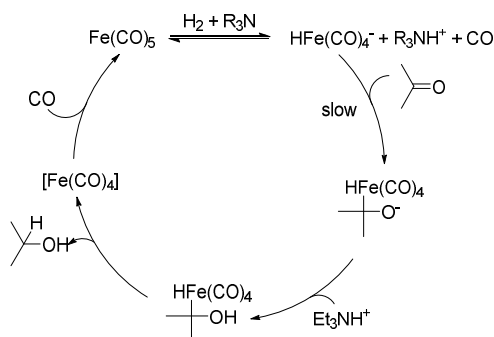
Beller's group was able to obtain ultrasmall monodisperse Fe-NPs, about 2 nm in diameter, from the decomposition of $\{\text{Fe}[\text{N}(\text{SiMe}_3)_2]\}_2$ under a hydrogen atmosphere.^[68] These ultrasmall NPs are good models for the determination of the intrinsic reactivity of iron because they are well-defined and are not oxidized at their surface. The ultrasmall Fe-NPs were tested in hydrogenation under mild reaction conditions, 2.4 mol% of catalyst, 10 bar of H_2 , in mesitylene at room temperature. The iron nanoparticles were found to be active in the hydrogenation of terminal alkenes and alkynes, as well as cyclic alkenes, but were ineffective for non-cyclic internal alkenes and internal alkynes.

3.3. Hydrogenation of carbonyl compounds

The hydrogenation of carbonyl compounds has long been dominated by rhodium, ruthenium, and iridium catalysts. Even though iron catalysts have also been studied for this purpose for decades, it was only recently that their efficiency was brought to levels that allow them to compete with noble metal catalysts for specific applications.^[69]

3.3.1. Iron carbonyl

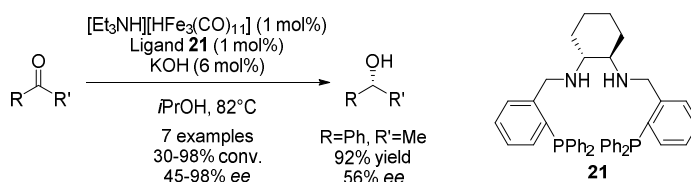
The only option for the catalytic hydrogenation of carbonyl compounds was the use of noble metals, until the 1980s. This changed when Markó and co-workers reported the use of $\text{Fe}(\text{CO})_5$ together with triethylamine to hydrogenate various ketones (moderate conversion) and aldehydes (quantitative conversion) to the corresponding alcohols (Scheme 23). Markó and co-workers were forced to use quite harsh conditions, 100 bar of total pressure (98.5% H_2 + 1.5% CO) at 20 °C for aldehydes and 150 °C for ketones.^[70]



Scheme 23. Proposed mechanism for the hydrogenation of ketones using $\text{Fe}(\text{CO})_5$

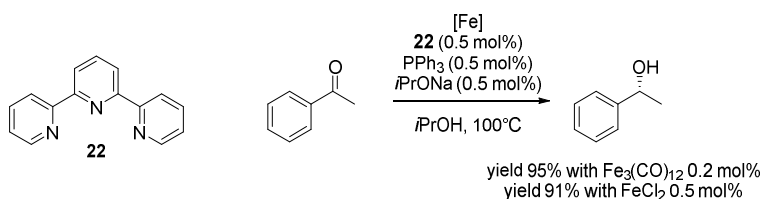
3.3.1.1. Diaminophosphine ligand and terpyridine ligand

In 2004, Gao and co-workers took inspiration from Markó's catalytic system by adding a chiral diaminophosphine ligand **21**. The iron catalyst was formed in situ from the carbonyl(hydrido)iron cluster $[\text{Et}_3\text{NH}][\text{HFe}_3(\text{CO})_{11}]$ and the corresponding ligand. This system was tested in the asymmetric transfer hydrogenation, using isopropanol as a hydrogen source, and revealed good to very high conversions with moderate to good enantiomeric excesses. The highest *ee* values (up to 98% *ee*) were obtained for sterically crowded ketones (Scheme 24).^[71]



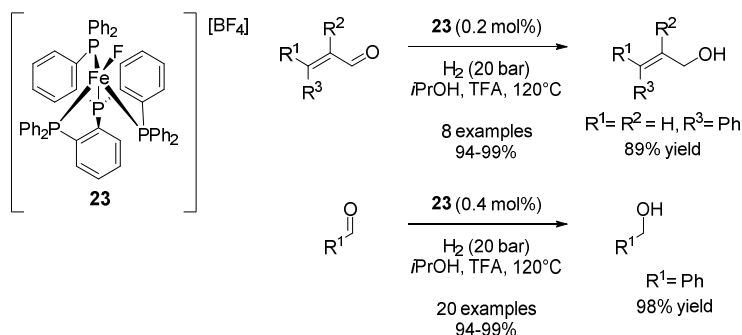
Scheme 24. Transfer hydrogenation in the presence of a chiral diaminophosphine ligand **21**

Beller and co-workers introduced a three-component catalytic system consisting of: $Fe_3(CO)_{12}$ or $FeCl_2$, a terpyridine ligand **22** and triphenylphosphine, in isopropanol as solvent and hydrogen donor in the presence of a base (Scheme 25). The system worked in the transfer hydrogenation for aliphatic and aromatic ketones.^[72] The corresponding alcohols were obtained in good to excellent yields without a significant difference between the two iron catalysts, but the reaction outcome was strongly dependent on the choice of the base, but when $iPrONa$ or $tBuONa$ were used, the corresponding alcohols were obtained with high yields.



Scheme 25. Three component catalytic system for transfer hydrogenation

Beller's group additionally developed a well-defined iron(II) tetradentate phosphine complex **23** for the selective hydrogenation of α,β -unsaturated aldehydes.^[73] Excellent yields of allylic alcohols were obtained from the corresponding allylic aldehydes, as well as alcohols from aromatic, heteroaromatic or alkyl aldehydes (Scheme 26).

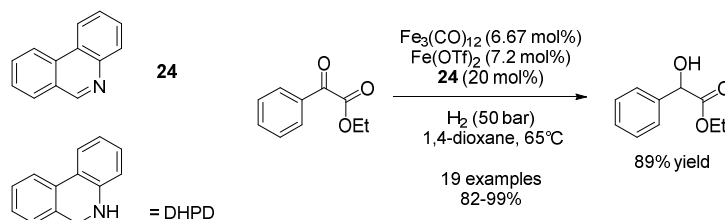


Scheme 26. Catalytic hydrogenation of aldehydes and α,β -unsaturated aldehydes by complex **23** $[FeF(L)][BF_4]$

This complex is believed to easily provide a free coordination site for the incoming substrate by temporarily releasing one terminal phosphine arm, as proposed by Bianchini and co-workers, for the related iron-catalyzed hydrogenation of alkynes.^[48]

Beller and co-workers also developed a dual iron-catalyzed process for the hydrogenation of α -keto and α -imino esters (Scheme 27).^[74]

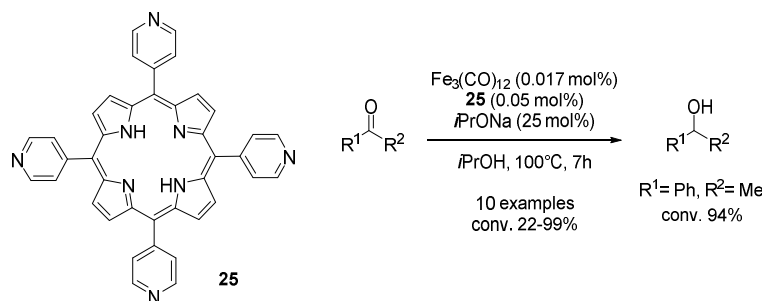
The hydrogen transferring agent is the NAD(P)H model dihydrophenanthridine (DHPD). A combination of $\text{Fe}_3(\text{CO})_{12}$ and iron(II) triflate was employed as iron sources. The former is the catalyst of the hydrogenation of the DHPD and the transfer hydrogenation is catalyzed by Lewis acids, which can be the iron carbonyl, a derived species or the iron(II) salt.



Scheme 27. Iron-catalyzed biomimetic reduction of ethyl phenylglyoxylate using DHPD

3.3.1.2. Iron porphyrins and macrocyclic complexes

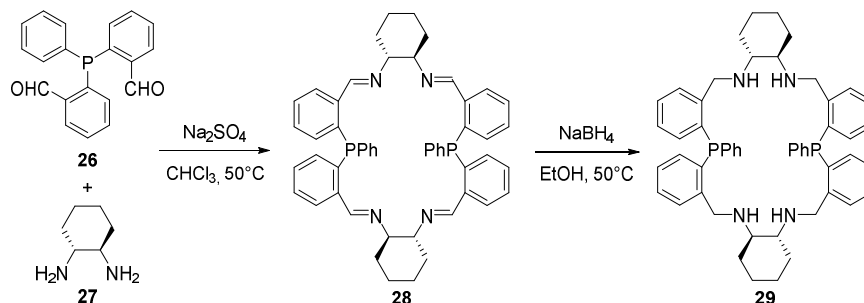
Beller's group also followed a biomimetic approach, using *in situ* generated iron porphyrins instead of iron triphenylphosphine systems (Scheme 28).^[75] This system was less base-dependent and allowed to obtain excellent conversions in the transfer hydrogenation of ketones with isopropanol, again independently from the applied iron source. Conversions up to 99% and TOFs up to 642 h^{-1} were reported for this biomimetic transformation. The method could also be applied to different 2-aryloxy- or 2-alkyloxy-substituted ketones with TOF up to 2500 h^{-1} .^[76]



Scheme 28. Iron porphyrin applied in transfer hydrogenation

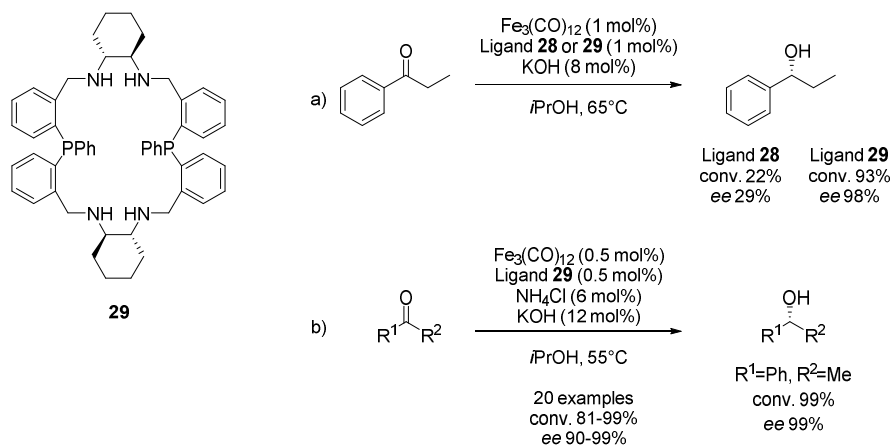
Gao synthesized macrocyclic structures by a condensation of bis(*o*-formylphenyl)-phenylphosphane **26** and (*R,R*)-cyclohexane-1,2-diamine **27** which led to the formation of a 22-

membered diiminodiphosphine macrocycle **28** (Scheme 29).^[77] Ligand **28** was then reduced with NaBH₄, to obtain the corresponding diaminodiphosphine ligand **29**.



Scheme 29. Synthesis of the macrocyclic structures **28** and **29**

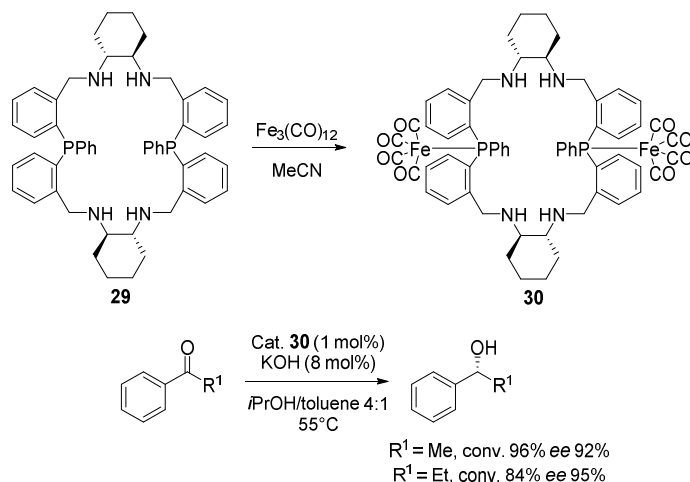
The new macrocycles **28** and **29**, together with Fe₃(CO)₁₂, were compared in asymmetric transfer hydrogenation (ATH) of propiophenone (Scheme 30a). The diaminodiphosphine ligand **29** appeared to be much more active than diiminodiphosphine macrocycle **28**. By contrast with the previously reported catalyst **25**/Fe₃(CO)₁₂ the use of different iron sources (like iron(0) Fe₂(CO)₉, iron(II) FeCl₂ or iron(III) FeCl₃) gave almost no activity in the reaction with both ligands.



Scheme 30. Asymmetric transfer hydrogenation of ketones catalyzed by iron complexes formed from chiral macrocycle **28** or **29**

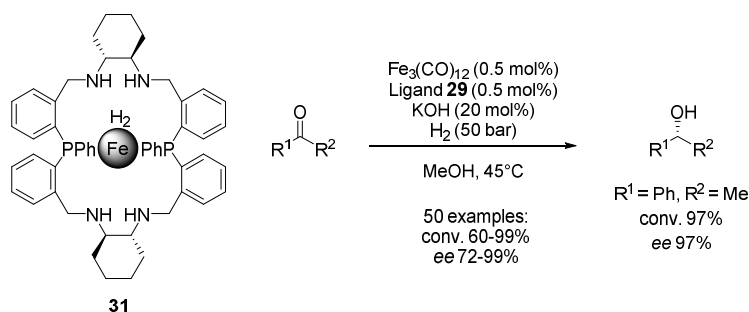
Gao and co-workers discovered that the use of ammonium salts as additives is promoting the reaction, even though their role remains unknown. The substrate screening revealed high activity of the catalytic system for a broad range of aromatic and heteroaromatic ketones (Scheme 30b).^[77] To obtain more details about the interactions between the iron and the macrocycle, Gao and co-workers synthesized iron complex **30**, which was postulated to be a possible reactive intermediate. Gao and co-workers managed to isolate complex **30** from the corresponding ligand **29** (Scheme 31). Since this complex was insoluble in *i*PrOH, the transfer hydrogenation reaction

was carried out in a mixture of toluene and *i*PrOH, but its catalytic activity was far inferior to the catalytic system formed *in situ*, shown in Scheme 30, this suggested that complex **30** is not the active species in the ATH of ketones.^[78]



Scheme 31. Synthesis of chiral $\text{P}_2\text{N}_4\text{-Fe(0)}$ complex **30 and its catalytic activity**

Ligand **29** has also recently been applied in the asymmetric hydrogenation of aromatic and heteroaromatic ketones (Scheme 32), to the corresponding chiral alcohols in high yields and excellent *ee* values.^[79] Further studies on the hydrogenation's mechanism revealed the formation of chiral macrocycle-modified iron nanoparticles, which is believed to be the active species.



Scheme 32. Asymmetric hydrogenation using macrocyclic ligand **29**

3.3.2. *P,N,N,P*-complexes

In 2008, taking inspiration by Gao, Morris and co-workers synthesized the well-defined iron diiminophosphine complexes **32a-b**.^[80] Complexes **32a-b** were prepared by condensation of commercially available diamines and phosphinealdehyde (Figure 10) and it was expected that due to the hydrogenation reaction course, the imine donors in the synthesized complexes would be reduced to amines.^[81]

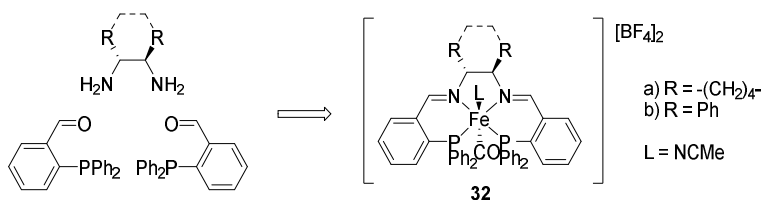
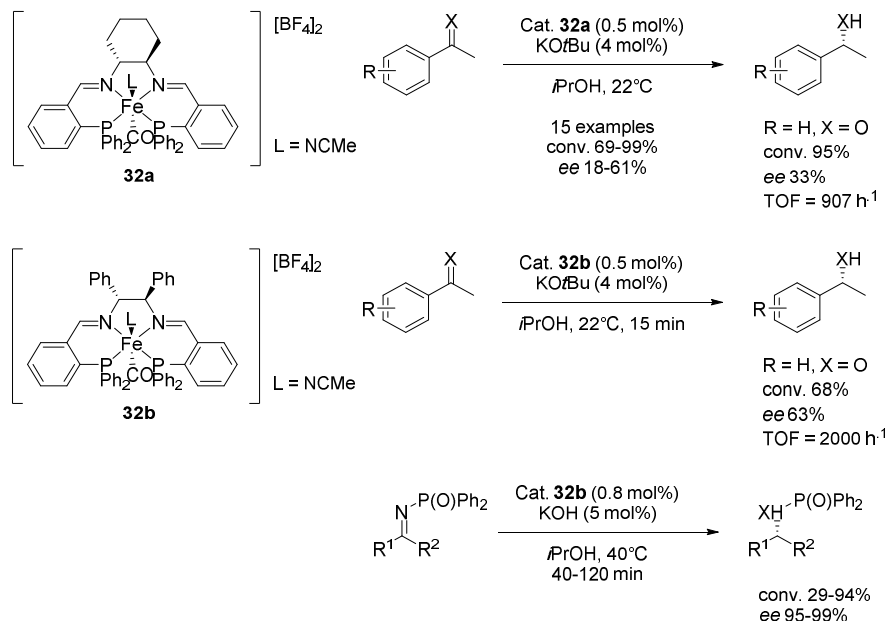


Figure 10. Synthesis of *P,N,N,P*-complexes

Complex **32a** was tested in the asymmetric transfer hydrogenation of different ketones and imines using isopropanol and led to high conversions and TOFs up to 907 h^{-1} (comparable to the TOF's reported for an analogue ruthenium catalyst), but only modest enantioselectivities were achieved (Scheme 33). The transfer hydrogenation of α,β -unsaturated ketones was complicated by some reduction of the C=C bond.

Several modifications of the ligands have been studied in terms of their influence on the catalytic activity of the iron complex. Changing the starting diamine, complex **32b** was obtained and compared to complex **32a** showing higher activity and selectivity (Scheme 33).^[82]



Scheme 33. Transfer hydrogenation of ketones and imines using iron diiminophosphine complex **32a-b**

In subsequent studies Morris discovered that the active species in the reaction were actually iron nanoparticles formed from complexes **32a-b**. In fact, electron microscopy imaging showed that iron nanoparticles were forming during the reaction.^[83] Support to this proposition derived not only from scanning transmission electron microscopy (STEM), but also from superconducting quantum interference device (SQUID), and X-ray photoelectron spectroscopy (XPS) analysis.

According to Morris, the flexible six-membered chelate rings were responsible for the occurring of the formation of Fe-NPs, in fact under reducing conditions, they allowed ligand dissociation to form active Fe-NPs. This was the first reported example of use of Fe-NPs to promote enantioselective transformations. To avoid this phenomenon, Morris and co-workers developed a second generation diiminophosphine complexes **33a-e**, containing five-membered rings, synthesized from the condensation of an enantiopure diamine and dialkyl- or diarylphosphinoacetaldehydes (Figure 11).^{[84][85]}

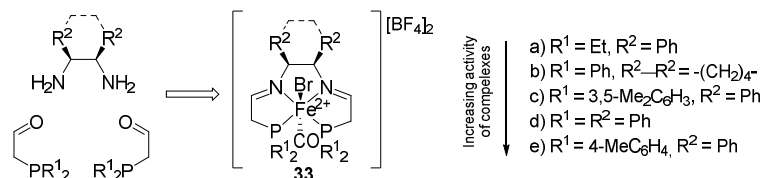
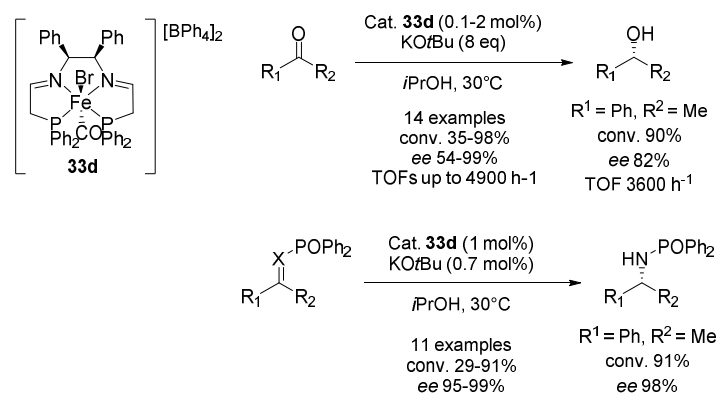


Figure 11. Second generation diiminophosphine complexes

Using the second generation catalyst, the maximum TOF obtained was 30000 h^{-1} with high enantiomeric excesses (up to 90%) for complex **33e**. The substituents on phosphorus were crucial for the activity; moderate size and moderate donor ability were required, otherwise complexes were catalytically inactive.^[86]

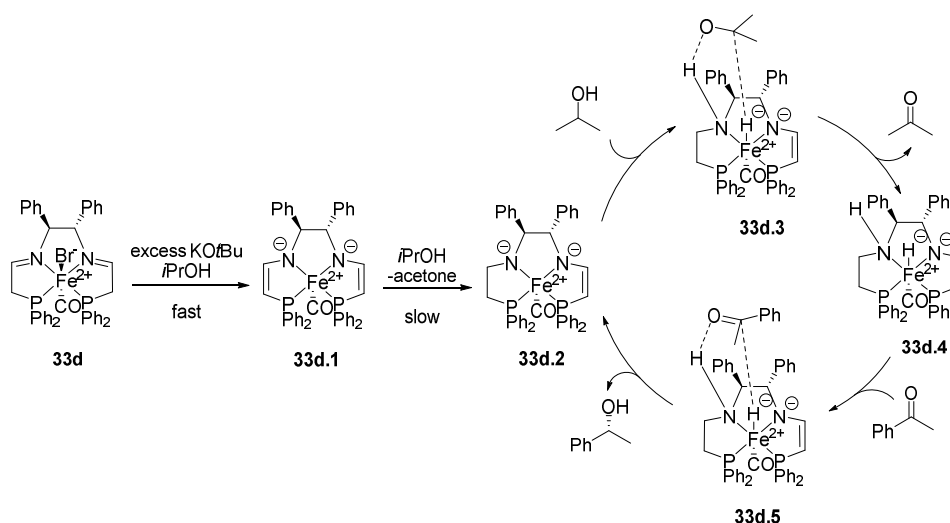
Complex **33d** was an efficient catalyst for the reduction of functionalized acetophenones containing alkyl groups, cyclic alkanes, halogens and aromatic rings (Scheme 34). Furthermore, it was also active for the ATH of a variety of prochiral ketimines bearing diphenylphosphino group at the nitrogen, which showed high conversions (up to 91%) with excellent *ee* (95-99%).



Scheme 34. Transfer hydrogenation of ketones and ketimines using a second generation iron diiminophosphine complex 33d

Further mechanistic studies revealed that the ligand is modified twice (Scheme 35).^[87] The first step to activate the catalyst is a deprotonation of **33d** using a base in order to form bis-anionic

biseneamide **33d.1**. In the second activation step, a slow addition of a proton and a hydride from the isopropanol to one of the enamide groups occurs, in order to form the intermediate **33d.2**. This hydrogenated side “monoanionic amido-enamido complex” is the active iron complex. If both side were hydrogenated, the complex would be non-active.^[88] During the catalytic cycle the *P,N,N,P*-ligand **33d.2** takes a proton and a hydride from isopropanol to form first **33d.3** and then **33d.4**, which then delivers them to the substrate to form **33d.5**. The hydride transfer from iron to the carbonyl group of acetophenone proceeds according to an outer-sphere pathway, where the substrate is not coordinated to the metal, and the proton is transferred from the amino group of the ligand to the carbonyl oxygen (similar to the mechanism reported by Noyori for Ru(II)^[89]). This is an example of redox non-innocent ligand, as the diiminodiphosphino ligand actively participates in the mechanism of C=O reduction by mediating the proton transfer.



Scheme 35. Proposed mechanism of the second generation catalyst complex **33d**

The third generation catalysts presented by Morris are shown in Figure 12, complexes **34a-e** contain unsymmetrical ligands, obtained by condensation of enantiopure *P-NH-NH₂* diamine and dialkyl- or diaryl-phosphinoacetaldehydes.^[88]

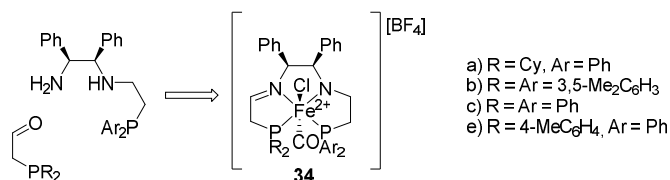
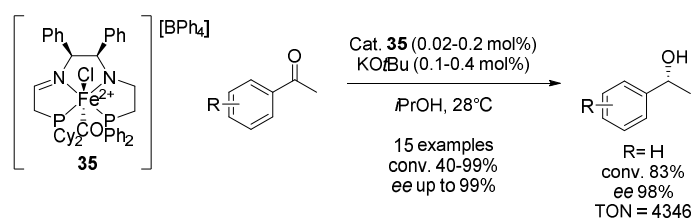


Figure 12. Third generation diiminophosphine complexes

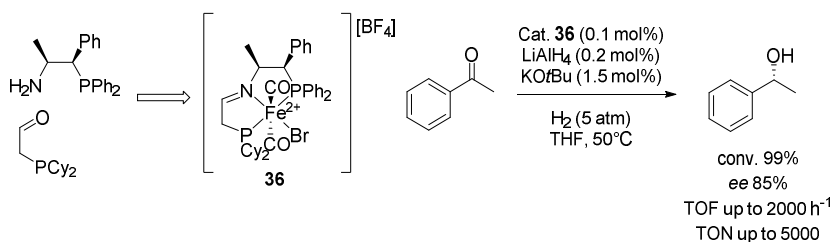
Treatment of new complexes with base, allowed to directly convert them to catalytically active unsymmetrical amide-enamide catalysts, as already previously explained. These catalysts were tested in the asymmetric transfer hydrogenation and they were found to be very active for a huge variety of ketones and ketoimines, with TOF up to 200 s^{-1} (at 50% of conversion), TONs up to 6100 and 99% *ee* (Scheme 36).^[88]

Recently a new unsymmetrical tetradentate *P-NH-N-P'* ligand has been synthesized, the new precatalyst **35** was tested in the ATH of ketones and gave a TONs up to 4300 and enantiomeric excesses up to 99%. The enantioselectivity of the system increased at the expense of the catalytic activity. The flexibility of the synthesis of these third generation catalysts offers the possibility of tuning their structure for the optimum reduction of a given substrate.



Scheme 36. Catalytic activity of the new iron(II) $\text{Ph}_2\text{P-NH-N-PCy}_2$ complex **35**

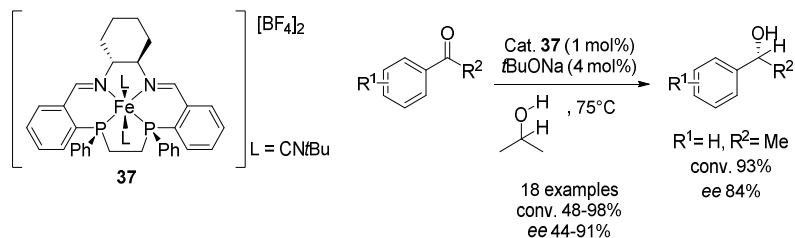
Morris' group, besides transfer hydrogenation with isopropanol, expanded their research also towards new catalysts for the asymmetric hydrogenation using molecular hydrogen.^[90] The new complex **36** was obtained by the condensation of enantiopure *P-NH₂* amine and dicyclohexylphosphinoacetaldehyde (Scheme 37). The activation of the catalyst was performed using LiAlH_4 to obtain the active *P-NH-P* catalyst for reducing ketones and imines. Complex **36** showed TOFs up to 1980 h^{-1} with *ee* up to 85%, but the structure of the active catalyst is still under investigation.



Scheme 37. Fourth generation pre-catalyst **36** applied in transfer hydrogenation

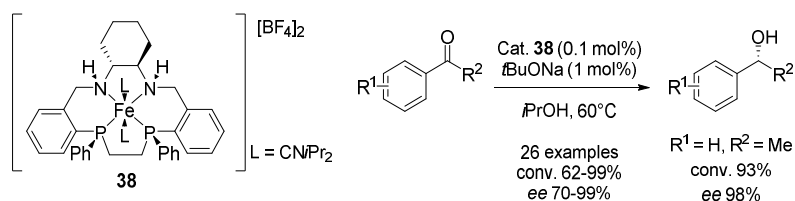
Recently Mezzetti and co-workers reported the first example of enantiomerically pure C2-symmetric macrocyclic ligands and the corresponding isolated iron(II) complexes.^{[91][92]}

Chiral P_2N_2 -Iron(II) complex **37** revealed very good activity in ATH, both in terms of conversion and enantioselectivity (Scheme 38).^[93]



Scheme 38. Catalytic activity of a diimino-macrocycle **37**

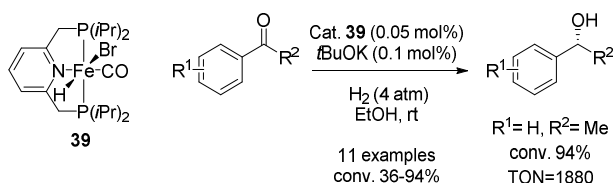
Replacing the diimino macrocycle, with a diamino analogue, led to even higher activity in ATH of ketones (Scheme 39). Using 0.1 mol% of the catalyst, excellent results in terms of yields (up to 98%) and enantioselectivities (up to 91% *ee*) were obtained with ketones, enones and imines.^[94] In both the presented classes of complexes, iron's isonitrile ligands, turned out to affect both the enantioselectivity and the activity of the catalyst.



Scheme 39. Asymmetric transfer hydrogenation using catalyst **38**

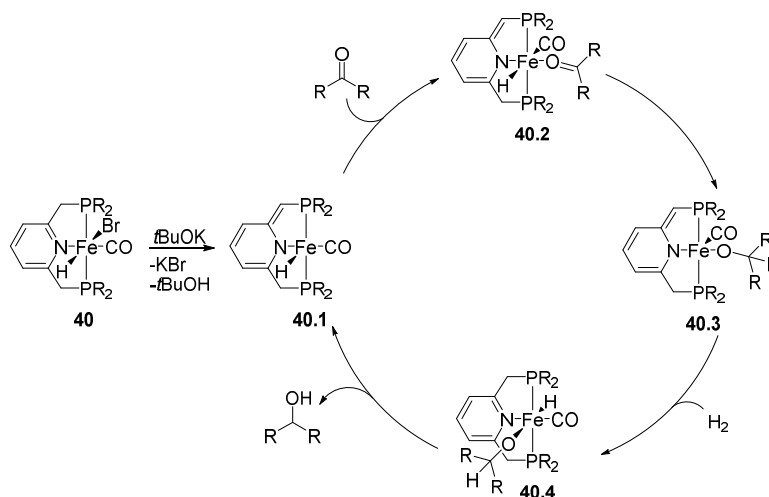
3.3.3. P,N,P -pincer ligand

In 2011 Milstein and co-workers synthesized a (hydrido)iron(II) pincer P,N,P -complex **39** for the ATH of ketones, achieving high turnover numbers up to 1880.^[95] The reaction proceeded under mild condition, 4 atm of H_2 using only 0.05 mol% catalyst loading, in ethanol at room temperature (Scheme 40).



Scheme 40. Catalytic activity of the (hydrido)iron(II) pincer P,N,P -complex **39**

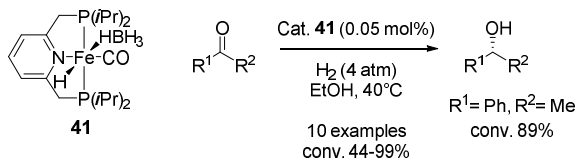
The proposed mechanism is represented in Scheme 41, the active species is a reactive dearomatized complex **40.1**, which is stabilized by reversible addition of ethanol to generate the aromatic complex **40**. The coordination of the ketone to **40.1**, followed by isomerization to intermediate **40.2**, makes the insertion of the substrate into the Fe-H bond possible. The alkoxy-carbonyl complex **40.3** gives the aromatic hydrido-alkoxy complex **40.4**, when it reacts with hydrogen. Finally, elimination of the corresponding alcohol regenerates the active species. Remarkably, in this mechanism the pyridine ring of the tridentate ligand plays a key role flipping between the aromatic (**40.4**) and the dearomatized form (**40.1**), thus acting as a redox non-innocent ligand.



Scheme 41. Possible reaction mechanism for ketones hydrogenation using complex **40**

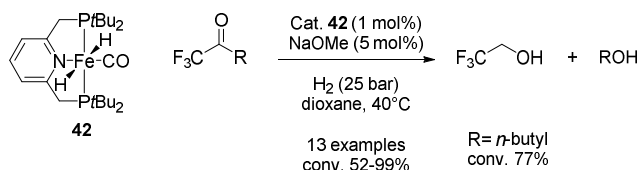
Subsequently Milstein developed a second-generation iron pincer catalyst **41** containing a borohydride ligand. The reaction was performed under similar conditions used for catalyst **40**, but no additional base was required and TONs up to 1980 were achieved (Scheme 42).^[96]

Different substrates could be converted to the corresponding alcohols in good to high yields (44-99%). Unfortunately benzaldehyde gave only low yields of benzylic alcohol, and α,β -unsaturated ketones led to mixtures of hydrogenated products.



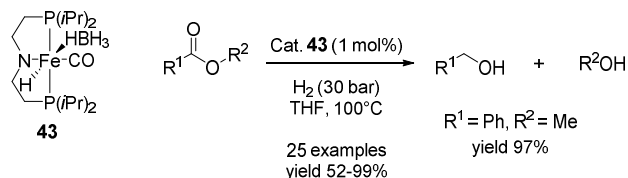
Scheme 42. Catalytic activity of the second-generation iron pincer catalyst

In 2014 Milstein observed that the *P,N,P*-ligand complex **41** (from the first generation of iron pincer catalyst), was also active in the hydrogenation of esters, in combination with a base (Scheme 43).^[97] This was the first example of iron catalyst being able to catalyze this transformation, even though only activated trifluoroacetic esters were hydrogenated to trifluoroethanol. For this reason, there is not a real practical application.



Scheme 43. Hydrogenation of trifluoroacetic esters with cat 42

The iron catalyzed hydrogenation of non-activated esters was described subsequently by Beller^[98] and Guan/Fairweather.^[99] Both groups, inspired by osmium-catalysts for hydrogenation of esters,^[100] discovered independently the catalytic activity of the hydrido borohydride *P,N,P*-pincer iron complex towards esters. The reaction was performed by Beller's group at 30 bar of H₂, in THF at 100-120 °C under base-free conditions with excellent yield (Scheme 44), while Guan/Fairweather used toluene or THF at 115 °C and 10-16 bar of H₂. Fully saturated alcohols were obtained from corresponding α,β -unsaturated esters. This catalyst was also active with fatty esters under neat conditions.



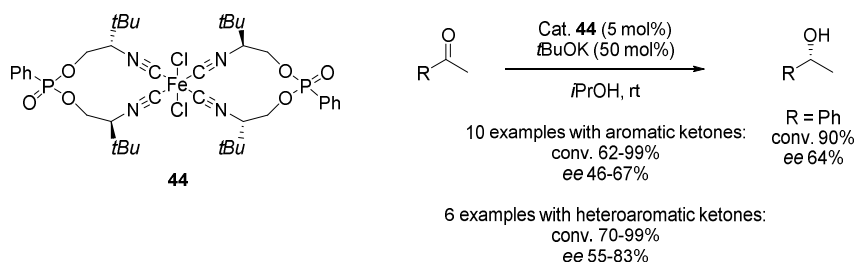
Scheme 44. Hydrogenation of activated esters using catalyst 43

Complexes **42** and **43** opened a new chapter in the ester hydrogenation, proving that it can be done using complexes with a cheap and abundant metal such as iron. But in order to be suitable for a real industrial application, their catalytic activity has to be improved, and the complex pincer ligands should be ideally replaced with less expensive and easy-to-handle ones.

In addition, Beller using the hydrido borohydride *P,N,P*-pincer iron complex described the selective hydrogenation of aliphatic and aromatic nitriles under mild conditions, and in particular adiponitrile to 1,6-hexamethylenediamine, an important building block for the polymer industry.^[101]

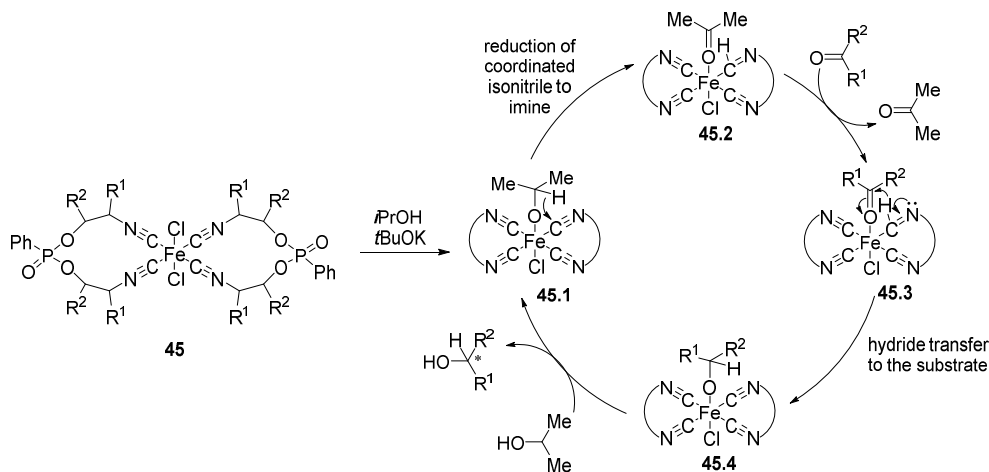
3.3.4. Isonitrile complex

In 2010 Reiser and co-workers reported a chiral bis(isonitrile)iron(II) complex **44** for the ATH of aromatic and heteroaromatic ketones.^[102] The asymmetric transfer hydrogenation was performed under mild conditions, at room temperature in isopropanol as solvent and hydrogen source in the presence of a base (Scheme 45). Very good conversions were obtained but only modest enantioselectivities could be achieved (up to 67% *ee*).



Scheme 45. Catalytic activity of the iron(II)-bis(isonitrile) complex **44**

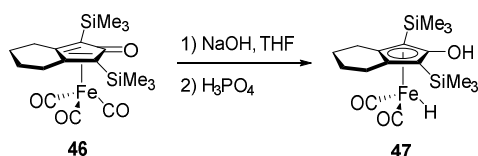
A Meerwein-Ponndorf-Verley-type mechanism was proposed for this transfer hydrogenation (Scheme 46). After activation of **45** with *t*BuOK, and coordination of the isopropanol to the iron (**45.1**), a reduction of the coordinated isonitrile ligand to an imine can be observed (**45.2**). In this way, acetone is formed and removed, so the reaction follows an inner-sphere pathway, with substrate coordination at the Fe(II) center (**45.3**). It can be also underlined that the formation of an iron hydride species does not take place in the catalytic cycle. Finally the imine with a hydride absorbed from isopropanol, transfers it to the substrate (**45.4**) with subsequent release of the product. In this case the ligand showed a clearly non-innocent behavior.



Scheme 46. Proposed mechanism for a general iron(II)-bis(isonitrile) complex **45**

3.3.5. (Cyclopentadienone)iron complexes

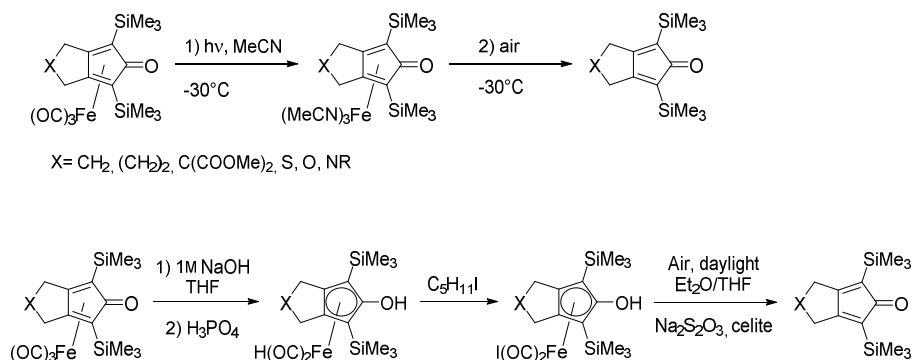
(Cyclopentadienone)iron tricarbonyl complexes were firstly reported by Reppe and Vetter in 1953,^[103] with the particularity of being easily synthesized and purified, due to their stability to air, moisture and column chromatography on silica gel. Unfortunately, it took 40 years until they were studied with more attention by Knölker^[104] and Pearson.^[105] In 1999, Knölker and co-workers synthesized and isolated the first (hydroxycyclopentadienyl)iron dicarbonyl complex **47** from the active stable (cyclopentadienone)iron tricarbonyl complex **46** using a Hieber-base reaction (Scheme 47) when the main focus was to obtain the free ligand.^[106]



Scheme 47. (Hydroxycyclopentadienyl)iron dicarbonyl complex 47 obtained by Hieber-base reaction from (cyclopentadienone)iron tricarbonyl complex 46

Demetallation could be achieved using UV irradiation (Scheme 48), which induced ligand exchange of carbon monoxide by acetonitrile, leading to a labile tri(acetonitrile)iron complex, and subsequent bubbling of air through the solution at low temperature to obtain the free ligands in high yields.^[15]

A different method for demetallation is the Hieber-type reaction (Scheme 48), using sodium hydroxide to obtain the corresponding hydride complex followed by ligand exchange with iodopentane to afford the iodoiron intermediate, which is easily demetallated in the presence of air and daylight at room temperature.^[106]



Scheme 48. Two different method of demetallation (a) UV irradiation and (b) Hieber-type reaction

The potential use of the active hydride **46** remained concealed until 2007, when Casey and Guan reported its highly efficient catalytic activity for the chemoselective hydrogenation of aldehydes, ketones and imines under mild conditions.^[107]

Complex **47** showed similar properties to the structurally related Shvo catalyst **48**, which was known since 1985 (Figure 13), a dimeric structure of a dinuclear ruthenium hydride complex, in which the hydride ligand bridges the two ruthenium metal center.^[108]

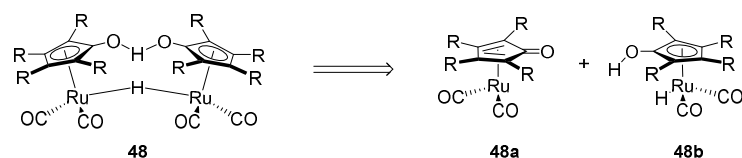
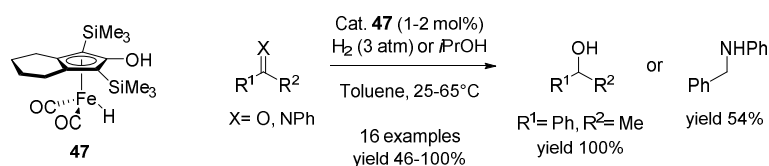


Figure 13. Dinuclear ruthenium hydride complex, known as Shvo catalyst

The dissociation of the dimeric species **48** in solution led to the formation of the monomeric ruthenium complex which is the catalytic active species. In particular the 16e⁻ complex **48a** provides **48b** by activation of H₂. Catalyst **48b** was used in the hydrogenation of aldehydes, ketones,^[108] imines^[110] and alkenes, with the obstacle for the latter to be bound by the complex, forming a stable complex that gradually poisons the catalyst.^[109] Catalyst **48b** was also used in transfer hydrogenation by Bäckvall and co-workers.^[110]

Casey and Guan demonstrated that hydride **47** is a highly efficient catalyst for the chemoselective hydrogenation of aldehydes, ketones and imines under mild conditions (3 atm of hydrogen, at room temperature in toluene) (Scheme 49). A large number of functional groups were tolerated under these reaction conditions, such as isolated carbon-carbon double or triple bonds, halides, nitro groups or epoxides and esters. Hydride **47** has been successfully applied also in transfer hydrogenation conditions, using isopropanol.^{[7][107][111]} Sun and coworkers performed computational studies to confirm that catalyst **47** is not able to hydrogenate olefins and alkynes under relatively low temperatures.^[112]



Scheme 49. Hydrogenation and transfer hydrogenation using (hydroxycyclopentadienyl)iron complex **47**

The main drawback of the active hydride **47**, was its sensitivity to air, moisture and light. For this reason, it was necessary to prepare it and handle it in a glove-box. Later contributions

demonstrated that it is possible to use bench-stable (cyclopentadienone)iron pre-catalyst **46** and to activate it *in situ* (Figure 14).

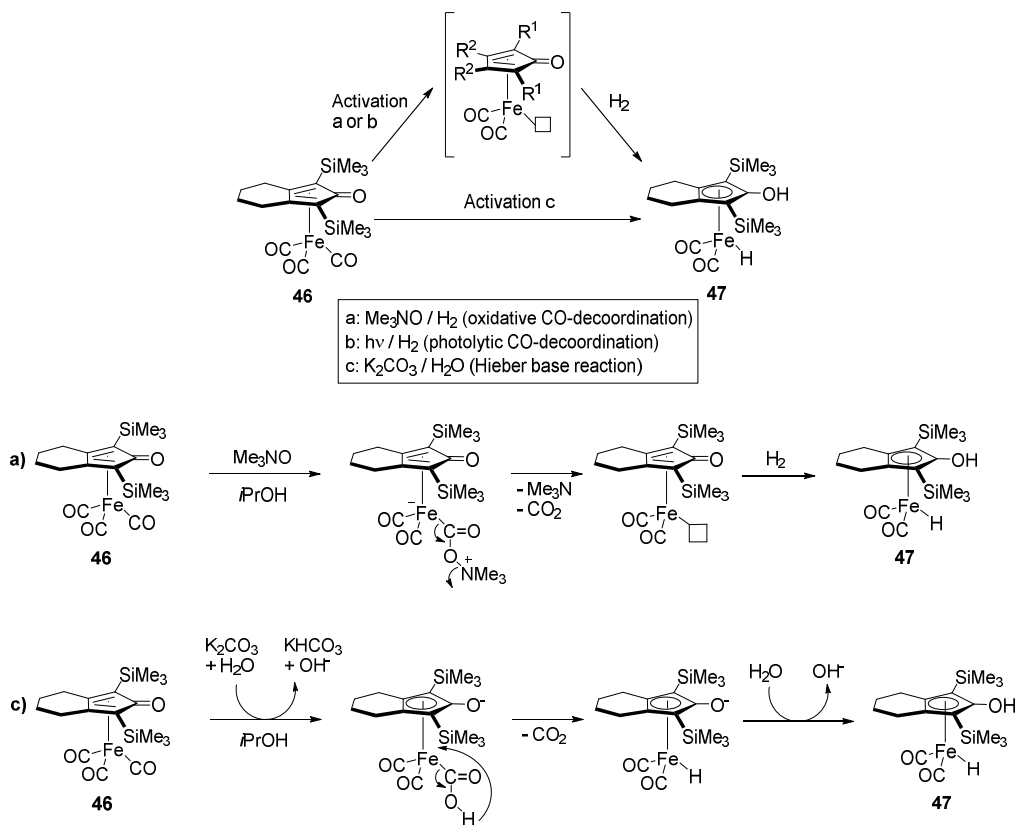
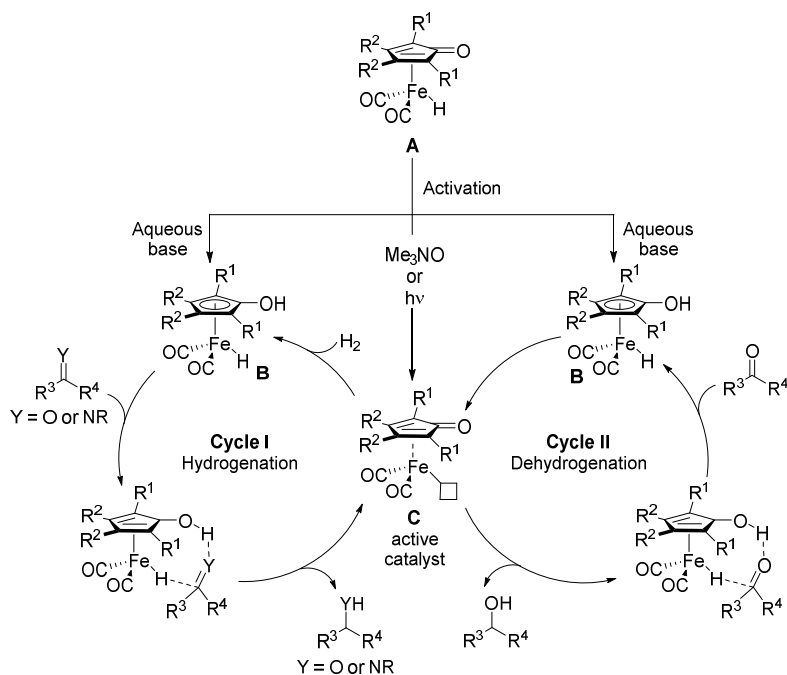


Figure 14. Activation of (cyclopentadienone)iron tricarbonyl pre-catalyst **46 to form the active hydride species **47****

The first method is based on the mono-decoordination of one of the CO ligands with oxidative cleavage using Me_3NO .^[113] The same effect can be also obtained by UV irradiation.^[117] The active complex **C** can be considered as a frustrated Lewis pair, so in presence of hydrogen it can split H_2 to form the active hydride **B**. The hydride itself, as previously reported, can be also obtained by *in situ* Hieber reaction of (cyclopentadienone)iron **A** with aqueous bases (e.g.: K_2CO_3).^{[114][115]}

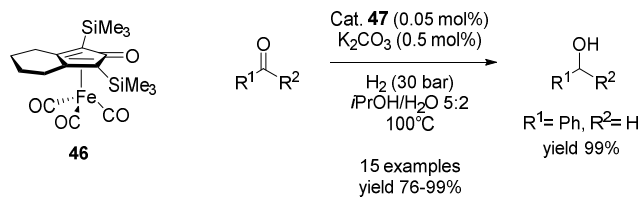
The mechanism of the transformation of this non-innocent ligand has been carefully investigated.^[116] The ligand is able to interconvert between cyclopentadienone **C** and hydroxycyclopentadienyl **B** form, allowing an unusual catalytic cycle involving Fe(0) and Fe(II) (Scheme 50, Cycle I). The active species **C** splits hydrogen and then catalyzes the reduction of carbonyl compounds according to a concerted outer-sphere mechanism, in which the substrate is not directly connected to the iron, but there is an interaction between the OH group of the ligand, which allows transient substrate's activation by hydrogen-bonding and the hydride delivery by the iron. Additionally, hydride **B** (Scheme 50, Cycle II) is also able to catalyze the dehydrogenation of

alcohols to carbonyl compounds in an Oppenauer-type oxidation and "hydrogen-borrowing" reactions (like amination of alcohols).



Scheme 50. Catalytic pathways: hydrogenation of C=O and C=N double bonds (Cycle I) and Oppenauer-type alcohol oxidation (Cycle II) catalyzed by (cyclopentadienone)iron complexes.

Beller optimized the reaction conditions for ketones hydrogenation, obtaining TON up to 3800 using pre-catalyst **46** (Scheme 51).^[114]



Scheme 51. Hydrogenation of ketones using bench-stable **46**

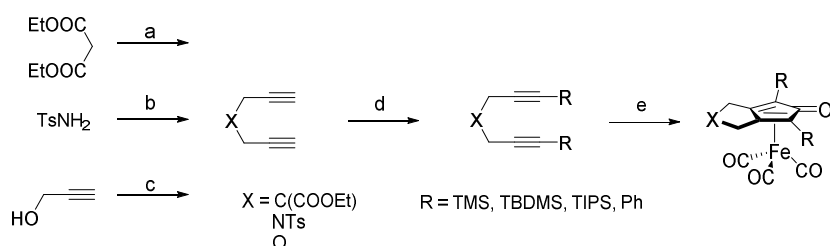
3.3.5.1. Modification of the Knölker-Casey complex

From the point of view of ligand design, two main strategies for the modification of the framework of the Knölker-type complexes have been followed, in order to improve the catalytic activities or achieve novel reactivity.

The first strategy is the modification of the substitution pattern of the cyclopentadienone ring, by tuning the steric and electronic properties of the complexes:

- changing the nature of the cycle fused to the cyclopentadienone ring, replacing the original six-membered ring of the Knölker-Casey complex or the modification of the nature of the substituents at the 2- and 5-positions.

A five-membered ring was obtained in two step synthesis, starting from the silylation of the commercially available 1,6-heptadiyne followed by a [2+2+1] cycloaddition. Other alkylation presented in Figure 15 allowed to obtain alkyl chains or heteroatoms (O, S,^[104b] N^[113a]) in the backbone. While the TMS groups were replaced with different silyl groups (TBDMS or TIPS), or phenyl groups.^{[113a][114]}



a) NaH (2.2 eq), propargylic bromide (2.2 eq), THF, 3 h, reflux; b) K₂CO₃, propargylic bromide (2.2 eq), acetone, rt, 24 h; c) NaOH, propargylic bromide (1 eq), triethylbenzyl ammonium chloride, H₂O, 60 °C, 3 h; d) *n*BuLi, trialkylsilyl chloride, THF, -78 °C, 3 h; v) Fe₂(CO)₉, toluene, 110 °C, 18 h - 3 days.

Figure 15. Modification of the substitution pattern of the cyclopentadienone

The catalytic activity of these complexes was tested and it was observed that catalysts which bear phenyl substituent on the cyclopentadienone, led to the lowest yields. This behavior was explained either by the electronic properties of the aromatic substituent compared to a silyl group or the lack of steric hindrance around the iron center, which led to a possible dimerization of the complex, as shown in the X-ray analysis, and in a decreased stability, since the complex become thermally labile. The second hypothesis could also be confirmed evaluating the increase steric bulk of the silyl substituent, which resulted in an improvement of the catalytic activity (TBDMS = TIPS > TMS).

Concerning the backbone, there is not clear explanation for the behavior of the complexes, even though DFT calculations, demonstrate that the presence of a heteroatom, stabilized the transient 16-electron species and have less propensity to dimerize.

- Finally, also the carbonyl moiety has been recently silylated (see paragraph 3.2.6).^[55]
- Chiral versions were also synthesized, but they will be discussed in the next paragraph.^[118]

[117]

The second strategy to modulate the structure of these complexes relies on the substitution of one of the carbonyls with other ligands. The exchange of the ligand was performed in oxidative

conditions using Me_3NO , in the presence of the new ligand such as nitriles (acetonitrile^{[15][119]} or benzonitrile^[135]), pyridines,^[135] phosphines (triphenylphosphine),^[105] and more recently *N*-heterocyclic carbenes (NHC),^[136] (Figure 16).

A chiral version using a phosphoramidite ligand was presented by Berkessel^[117] in order to induce enantioselectivity, but this will be discussed in the next paragraph.

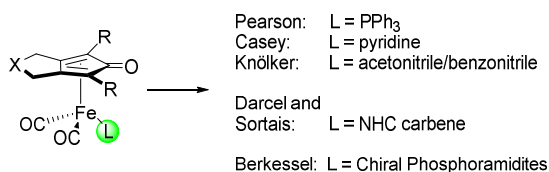
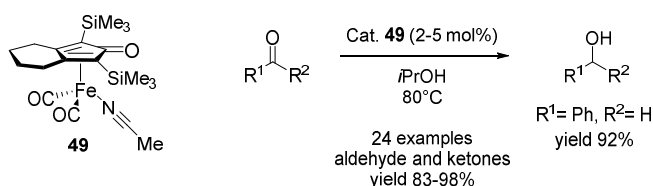


Figure 16. General modifications of Knölker-type complexes: replacement of one CO ligand

On a different approach, in order to obtain a labile ligand easily to remove to form the active hydride complex, Funk and co-workers employed the air-stable nitrile-ligated (cyclopentadienone)iron complex **49**, originally synthesized by Knölker^[15] as catalysts for the transfer hydrogenation of aldehydes and ketones using isopropanol as hydrogen source (Scheme 52).^[119] Excellent yields for a large number of primary and secondary alcohols were obtained.



Scheme 52. Example of air-stable nitrile-ligated (cyclopentadienone)iron complex

In the case of the NHC carbenes, the complexes were prepared using a photolytic method, under UV irradiation for 20 h in toluene. These catalysts were then tested in the dehydration of primary benzamides into benzonitrile derivatives, under hydrosilylation conditions, using the inexpensive PMHS (polymethylhydrosiloxane) as dehydrating reagent.

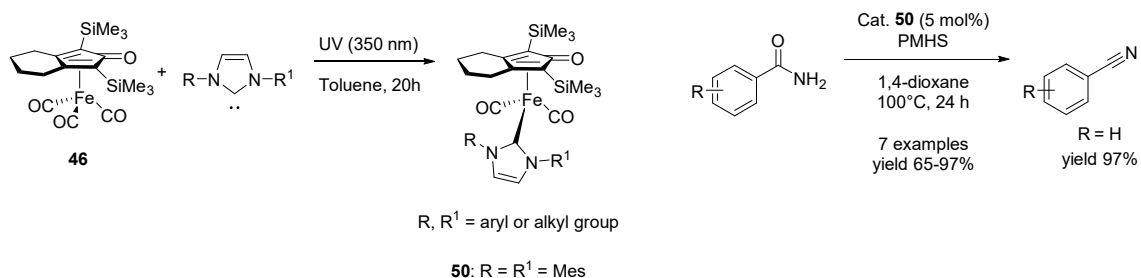
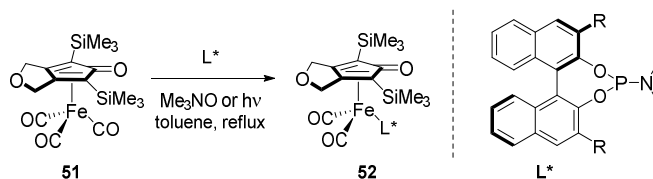


Figure 17. NHC-carbenes derived iron complexes and their application to the dehydration of primary benzamides into benzonitrile

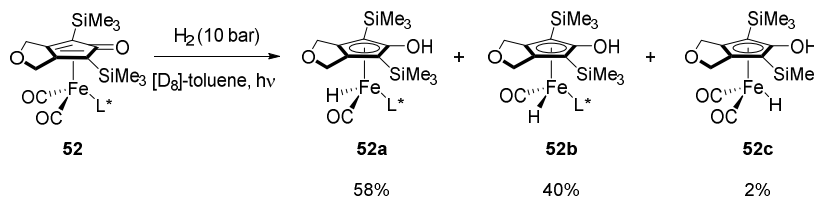
3.3.5.2. Asymmetric reductions

The groups of Berkessel^[117] in 2011 and Wills^[118] in 2012 made the first attempts to perform enantioselective reductions using Knölker-type complexes. Berkessel replaced one of the CO ligands starting from **51** with a chiral phosphoramidite ligand **L*** by a photolytic method (under UV irradiation) or an oxidative one (Me₃NO) (Scheme 53).



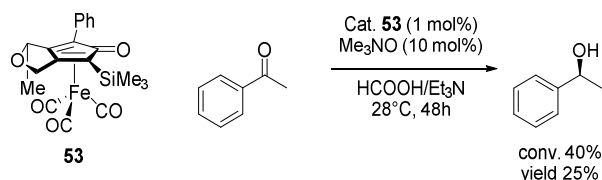
Scheme 53. (Cyclopentadienone)iron complex containing a chiral phosphoramidite ligand 52

Pre-catalyst **52** hydrogenated acetophenone with only 31% *ee*, in addition the reaction required constant UV irradiation to remove the second CO ligand and form the active hydride species. Berkessel performed NMR studies to investigate the reason for this low enantioselectivity, and found out that under hydrogen, two iron hydride diastereoisomers **52a** and **52b** were formed at the newly generated iron-stereocenter in a ratio 1:0.69 (Scheme 54), due to the non-selective dissociation of CO from pre-catalyst **52**, this also explained why the enantioselectivity of the reaction is low. Moreover, upon hydrogenation, also a partial removal of the chiral ligand was observed, giving 2% of the achiral active hydride complex **52c**.



Scheme 54. Formation of diastereoisomers upon hydrogenation of 52

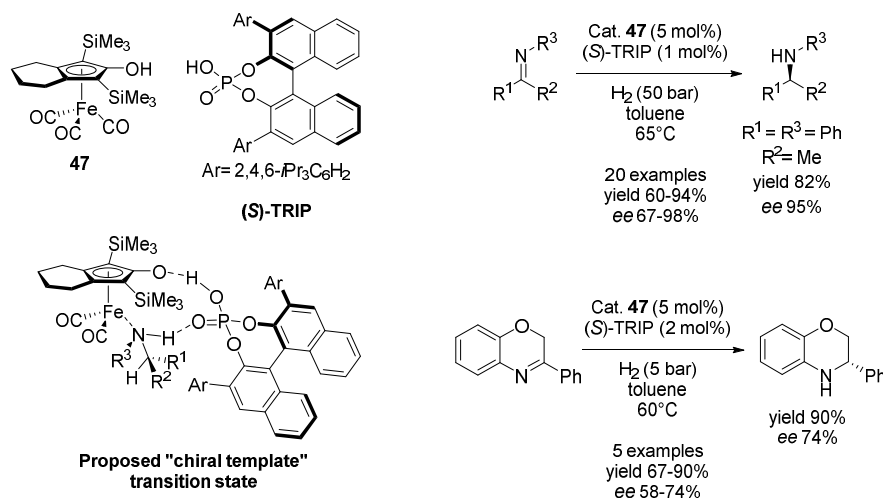
Wills presented a different approach to solve the chirality problem. The new chiral cyclopentadienone pre-catalyst **53** was obtained by insertion of a remote chiral center in addition to the planar symmetry of a (cyclopentadienone)iron complex (Scheme 55).^[118] Complex **53** was tested in the ATH of acetophenone in the presence of formic acid/triethylamine as a hydrogen source, but only *ee* up to 25% was achieved. This poor enantiocontrol was independent on the metal employed, as the corresponding ruthenium chiral catalyst was able to achieve only 21% *ee*.



Scheme 55. Asymmetric transfer hydrogenation using a chiral (cyclopentadienone)iron complex

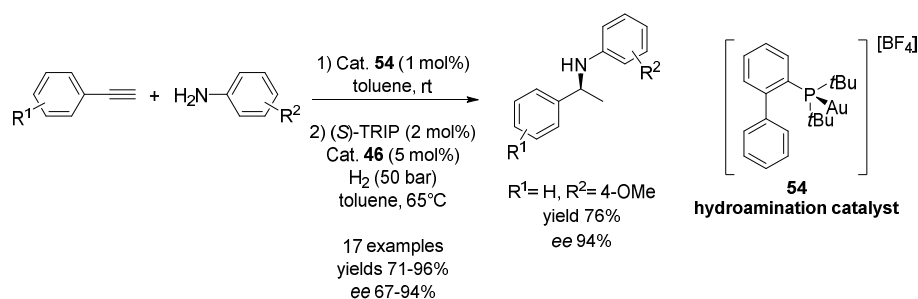
Beller and co-workers developed a procedure for the asymmetric hydrogenation of *N*-aryl ketoimines using an achiral pre-catalyst **47** in combination with a chiral phosphoric acid, (*S*)-TRIP.^[120] The proposed mechanism is displayed in Scheme 56, where the Brønsted acid acts as a “chiral template” forming hydrogen bonds simultaneously with the catalyst and with the substrate. A wide variety of different *N*-aryl ketoimines were hydrogenated with high yields and excellent *ee*.

Employing the same system it was also possible to hydrogenate quinoxalines to tetrahydroquinoxalines and 2H-1,4-benzoxazines to dihydro-2H-benzoxazines, with high yields and excellent *ee*.^[121] Furthermore, Beller and co-workers applied this methodology also for the asymmetric reductive amination of ketones with anilines, once more with high yields and excellent *ee*.^[123]



Scheme 56. “Chiral template system” using iron pre-catalyst **47 and (*S*)-TRIP**

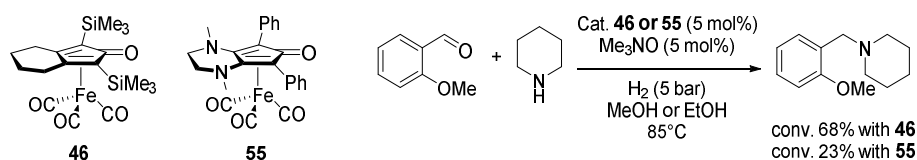
The above-mentioned methodology was employed in a combinatorial multi step, one-pot hydroamination of alkynes followed by enantioselective hydrogenation (Scheme 57).^[124] The first step was catalyzed by a gold(I) complex **54**, followed by hydrogenation carried out using **46** with a chiral Brønsted acid, to afford high yields and high enantioselectivities.



Scheme 57. One-pot enantioselective reductive hydroamination using **52**, **46** and (*S*)-TRIP

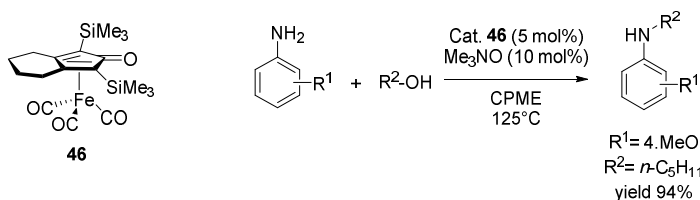
3.3.5.3. Reductive amination of aldehydes, ketones and alcohols

Cyclopentadienone complex **46** was also applied to reductive amination by Renaud and co-workers.^[125] The reaction was applied to primary or secondary amines and also ketones and aldehydes. Subsequently, Renaud discovered that more electron-rich (cyclopentadienone)iron complex **55** was more effective for the reductive amination of aromatic aldehydes (Scheme 58).^[126]



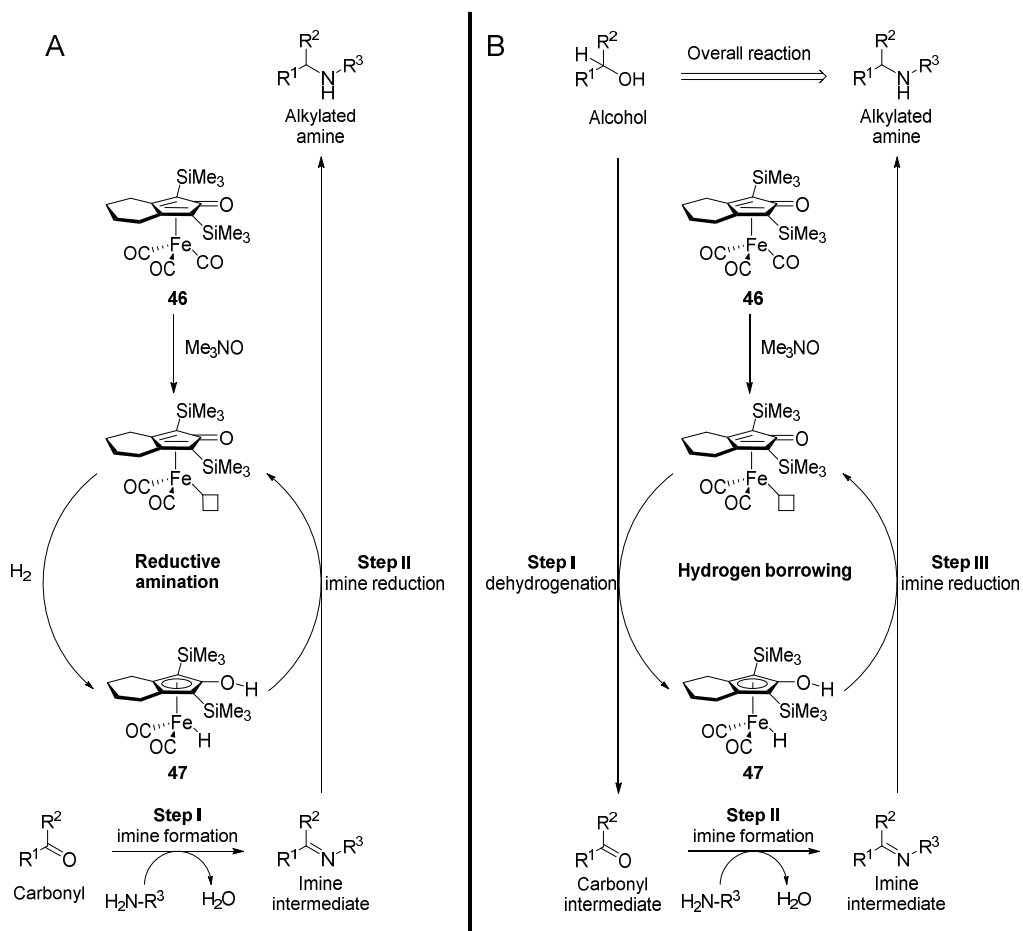
Scheme 58. Reductive amination using complexes **46** and **55**

Further amine functionalization was exploited by Feringa and Barta using (cyclopentadienone)iron complex **46**. Simple and direct *N*-alkylation of amines with alcohols using a hydrogen-borrowing process was performed.^[127] Different primary alcohols and amines were coupled with good yields.



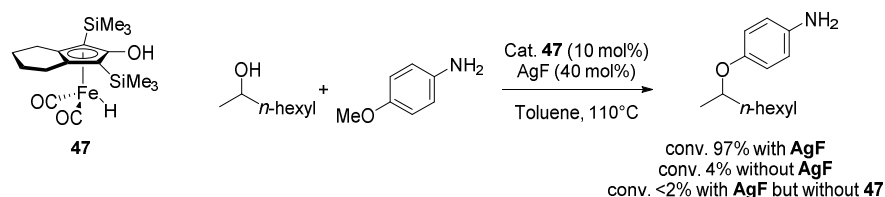
Scheme 59. *N*-alkylation of amines with alcohols using complex **46**

In comparison to the reductive amination by Renaud (Scheme 58 and Scheme 60A), alcohol substrates were acting as a hydrogen source in the process in Scheme 60B, easier to perform. The only drawback of this hydrogen borrowing process, was its ineffectiveness with different substrate than primary alcohols.



Scheme 60. A) reductive amination and B) hydrogen borrowing methodologies to obtain alkylated amines

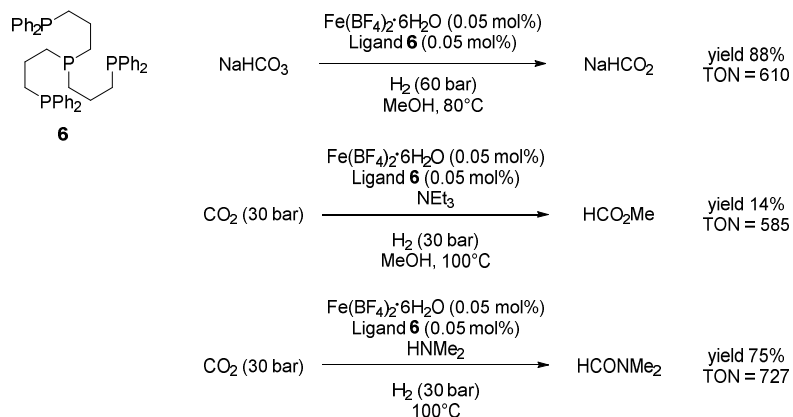
Recently, Zhao and co-workers improved significantly the hydrogen borrowing strategy.^[128] Using iron hydride **47** together with a Lewis acid, such as AgF, they managed to perform amination not only of primary alcohols, but also secondary (Scheme 61). The mechanism of this transformation proceeded via hydrogen borrowing from alcohol (as so, use of an enantiopure alcohol leads to racemate product). Unfortunately the role of the Lewis acid is not clear, but it can be assumed that AgF can assist the imine formation step and activate it towards reduction by iron hydride **47**.



Scheme 61. Amination of secondary alcohol supported by Lewis acid using catalyst 47

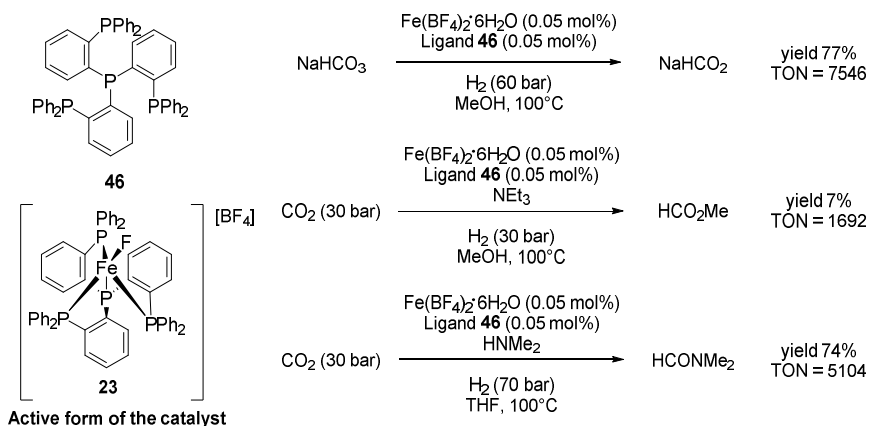
3.4. Hydrogenation of sodium carbonate and carbon dioxide

The first hydrogenation of carbon dioxide and sodium bicarbonate was described by Beller in 2010, using an iron catalyst (Scheme 62).^[129] The catalyst was formed *in situ* from $\text{Fe}(\text{BF}_4)_2 \cdot 6\text{H}_2\text{O}$ and the tetraphos ligand **6**. The obtained results were very promising for the application of an iron catalyst in this new field.

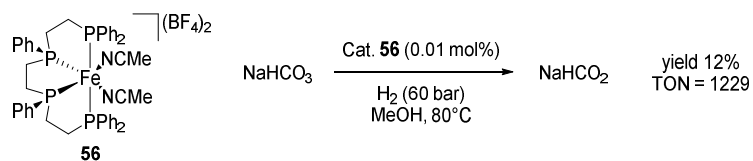


Scheme 62. Sodium bicarbonate and carbon dioxide hydrogenation using an iron catalyst and tetraphos ligand **6**

Subsequently Beller exploited an analogous *in situ* formed catalytic system with ligand **46**. A huge improvement in the catalyst activity was observed (Scheme 63).^[130] Sodium bicarbonate was hydrogenated reaching excellent TONs up to 7500. Carbon dioxide was reduced to methyl formate using methanol, as a solvent, and trimethylamine, as a base, with TONs up to 1700. When the hydrogenation was carried out in the presence of a secondary amine and DMF in THF, TONs up to 5100 were obtained.



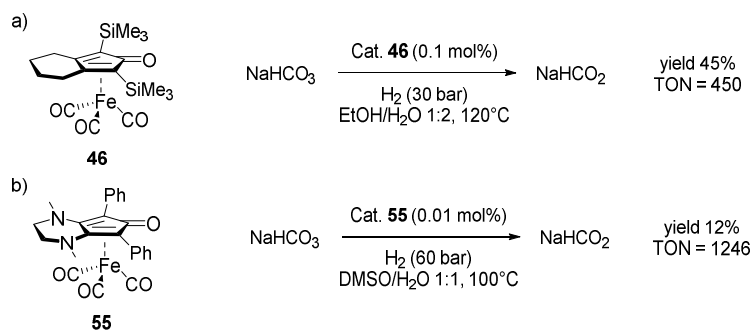
Scheme 63. Hydrogenation of sodium bicarbonate and carbon dioxide using tetraphos ligand **46**



Scheme 66. Hydrogenation of sodium bicarbonate using catalyst 56

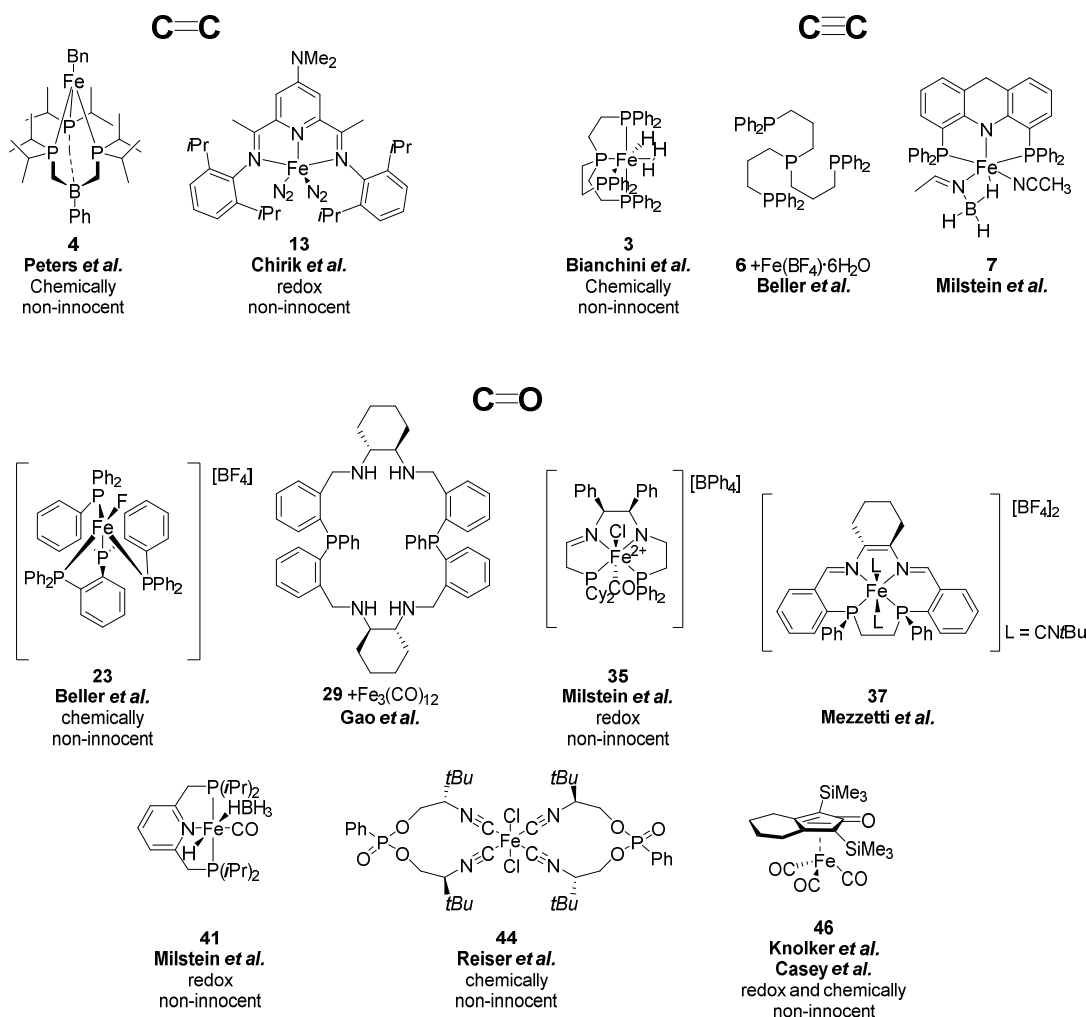
Recently Zhou proved that the (cyclopentadienone)iron complex **46** can work also in the hydrogenation of sodium bicarbonate with a good TON up to 450 (Scheme 67a).^[133] Unfortunately attempts to hydrogenate carbon dioxide were unsuccessful.

Renaud described a diamino-cyclopentadienone iron complex **55** for hydrogenating sodium bicarbonate with TONs up to 1246 (Scheme 67b).^[134]



Scheme 67. Hydrogenation of sodium bicarbonate using iron complex 46(a) and 55(b)

3.5. Summary of iron catalyzed reduction



In the last 20 years, iron catalyzed reductions progressed really fast. Definitely Chirik and co-workers reported the biggest contribution to the olefin reduction (complex **13**) and up to now no examples of more active catalysts for carbon-carbon double bond reduction were reported. In addition, no asymmetric hydrogenation was reported with any olefin. The best results in alkyne reduction were reported by Beller and co-workers (Fe(BF₄)·6H₂O with ligand **6**) and Milstein and co-workers (complex **7**), both systems providing good activity and selectivity, but a good catalyst for reduction of alkynes to fully unsaturated alkanes is still missing.

A lot of structurally different catalyst for the reductions of C=O bond were developed and proved to be efficient: *P,N,N,P*-ligands (**35**), macrocyclic *P₂N₄*- (**29**) or *P₂N₂*-ligands (**37**), pincer *P,N,P*-ligands (**41**), *P,P,P,P*-ligands (**23**), isonitrile (**44**) or cyclopentadienyl (**46**). Approximately all of the

reported ligands act as chemically or redox non-innocent, demonstrating that this is the best option to stabilize low valent iron species.

Most of the catalysts described, suffer at least one of these serious limitations: difficult synthesis, lack of robustness and moderate activity/enantioselectivity. These catalysts are often difficult to handle due to air- and moisture-sensitivity, therefore a glovebox is required for synthesis and manipulation, and in some cases even for the setup of hydrogenation tests.^[121] These drawbacks need to be overcome in order for iron catalysis to become of practical utility for the industrial manufacturing of fine chemicals.

4. Results and Discussion

(Cyclopentadienone)iron tricarbonyl complexes, as already described in paragraph 3.3.5, are robust pre-catalyst which are particularly attractive due to their versatile applications in redox catalysis: they have been successfully applied in hydrogenations, hydrogen transfer, including asymmetric versions, as well as oxidation, reductive amination and more recently in hydrogen-borrowing reactions.

One of the main advantages, compared to other iron complexes, is their stability to air and moisture. Additionally, they are easily synthesized and purified by simple silica gel chromatography. These characteristics prompted many groups to investigate structural modifications to optimize the reactivity of these complexes.

A major challenge remaining so far unmet is the development of chiral complexes to be used as enantioselective pre-catalyst in the hydrogenation reactions. In fact, both the replacement of one CO ligand with a chiral phosphoramidite by Berkessel and co-workers^[117] and the insertion of a stereocenter in the ring fused to the cyclopentadienone,^[118] only led to marginal enantiomeric excesses. The only somewhat successfully approach was developed by Beller and co-workers, using a chiral phosphoric acid additive as a sort of “chiral template” between catalyst **47** and the substrate. In this way, ketimines could be hydrogenated with excellent conversions and enantiomeric excesses (up to 98%), but this methodology was not applied for ketones (Figure 18).^{[120][121][122][124]}

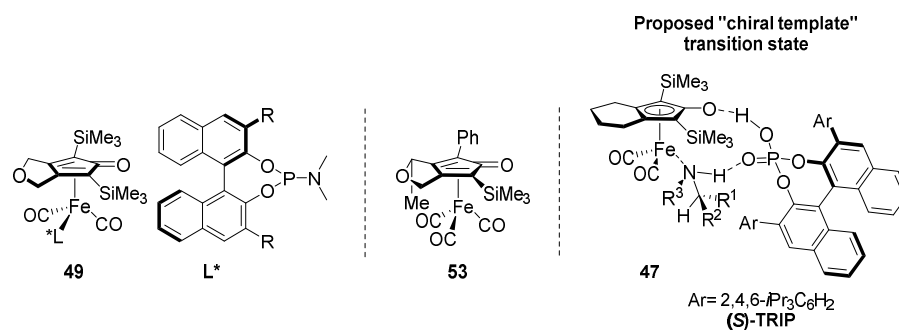


Figure 18. Reported cyclopentadienone iron complexes for enantioselective transformations

4.1. Aim of the thesis

The aim of the research carried out during my PhD was to develop new iron catalysts for the hydrogenation of carbonyl compounds.

In particular, we investigated the field of (cyclopentadienone)iron tricarbonyl complexes looking for chiral complexes for the asymmetric hydrogenation of ketones and the development of more stable and reactive complexes.

For this reasons we took into consideration three different approaches:

- The first approach was the modification of the 3, 4-positions on the cyclopentadienone ring, where we decided to introduced a chiral backbone, in the form of a binaphthyl moiety, in order to prepare new chiral complexes.^{[137][138]}
- In a second approach we replaced one of the CO ligands in the new chiral (cyclopentadienone)iron tricarbonyl complex with a chiral phosphoramidite ligand, in order to improve the enantiomeric excess of the catalyzed process.

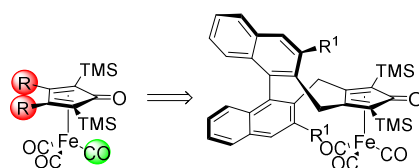


Figure 19. Modifications on the classical (cyclopentadienone)iron tricarbonyl complex

- The third approach involved the modification of the 2,3- and 4,5-positions in two different ways:
 - a) in the first attempts an intermolecular cyclization was applied using two alkynes in the presence of $\text{Fe}(\text{CO})_5$;
 - b) subsequently in order to obtain a complex showing planar chirality, we decided to synthesize the corresponding cyclopentadienone, followed by a complexation using an iron carbonyl source.

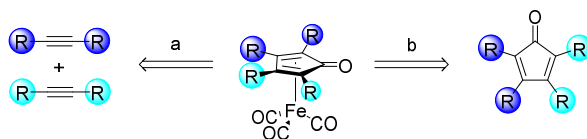


Figure 20. Different approaches to obtain a 2,3- and 4,5-substituted (cyclopentadienone)iron tricarbonyl complexes, showing planar chirality

The catalyst must be prepared in a simple way, including the preparation of the ligands/complexes from commercially available materials, good atom economy and affordable cost of reagents. In

addition, reasonable stability of the catalysts or pre-catalysts to air and moisture should be evaluated in order to avoid the use of a glovebox. Finally the catalytic process should present high efficiency in terms of conversion and enantioselectivity.

4.2. Towards a (*R*)-BINOL derived complexes

As mentioned in section 3.3.5, previous attempts to prepare chiral complexes by the introduction of a stereocenter in the backbone of the cyclopentadienone moiety^[118]; met with relatively low success.

For this reason, we decided to introduce a [(*R*)-1,1'-bi-2-naphthyl] backbone (Figure 21), reasoning that the binaphthyl group with its stable, rigid framework could more efficiently shape the space around the iron atom and induce higher enantiomeric excesses. In addition, (*R*)-BINOL is readily available and relatively cheap chiral starting material (price ~1 €/g).^[140]

A similar approach had recently been proposed by Cramer and co-workers with the synthesis of the chiral Cp rhodium(I) complex **57**.^[139]

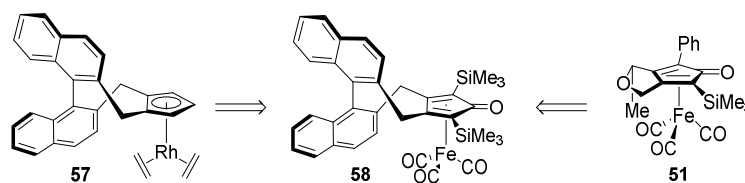
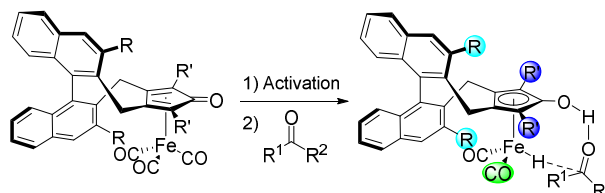


Figure 21. Idea for synthesizing a new chiral iron pre-catalyst **58**

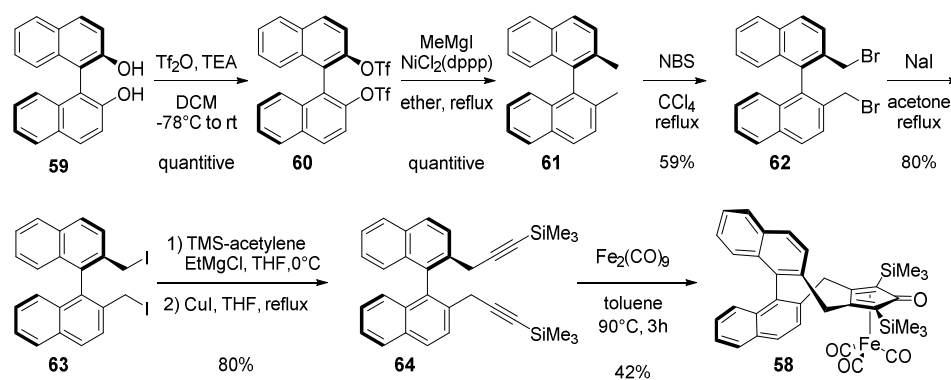
Evaluating the structure of our proposed catalyst we could anticipate that the binaphthyl stereoaxis would be relatively far away from the reaction center. Accordingly, we planned some structural modifications that in principle could improve the transfer of the stereochemical information or act as a directing groups for substrates (Scheme 68), as already reported for others BINOL-derived complexes.^{[139][141]}

On the other hand, another possibility to introduce chirality is to substitute one CO ligand with a chiral ligand (e.g. chiral phosphoramidite).



Scheme 68. General structure of new chiral iron pre-catalysts and possible modifications that could improve the enantioselectivity in the asymmetric hydrogenation

The first attempt was the synthesis of the 3,3'-unsubstituted pre-catalyst **58**, bearing TMS groups in the 2,5-positions of the cyclopentadienone ring (Figure 21). Its synthesis is depicted in Scheme 69, starting from commercially available (*R*)-BINOL **59**. The early steps, up to **62**, are simple chemical transformations, previously reported by Maruoka and co-workers.^[142] (*R*)-BINOL was triflated to **60**, which reacted in a Kumada cross-coupling performed with a methyl-Grignard reagent to obtain the bis-methyl derivative **61**, without loss of enantiopurity (confirmed by optical rotation measurements). The bis-bromide **62** (also commercially available but expensive) was then prepared by radical bromination using NBS.^[143] Unfortunately, using a known procedure for the addition of (TMS-ethynyl)magnesium bromide to benzyl bromide in the presence of CuI,^[144] led to no conversion when the bis-bromide **62** was exposed to these conditions. However, the synthesis of the bis-alkyne **64** could be achieved under similar conditions when the bis-iodide **63** was used, which could be easily obtained through a Finkelstein reaction starting from the bis-bromide **62**. Cyclization of **64** in the presence of Fe₂(CO)₉ under the conditions reported by Renaud and co-workers^[113a] afforded a new pre-catalyst **58**. Complex **58** is stable to air, moisture and can be purified by silica column chromatography. The cyclization step was also performed using the cheaper and more stable Fe(CO)₅, but in this case overnight heating was necessary. The optical rotation of the complex obtained using Fe₂(CO)₉ [α]_D (c=0.43 in CH₂Cl₂) = -32.11, was comparable with the catalyst obtained using Fe(CO)₅ [α]_D (c=0.09 in CH₂Cl₂) = -32.24. It is reasonable to assume that no racemization occurred, but nevertheless experiments to verify this assumptions were conducted.



Scheme 69. Synthesis of new chiral iron complex **58**

To test the enantiomeric purity of **58**, we also prepared the other enantiomer of the complex following the same synthetic path but starting from (*S*)-BINOL, [α]_D (c=0.24 in CH₂Cl₂) = 32.18. Further investigations were performed to verify the enantiomeric purity using chiral HPLC. In this case several chiral columns were used (OD-H, OB-H, AD-H, CELLULOSE2, CELLULOSE3,

CELLULOSE4, AMYLOSE2) injecting the two enantiomers separately (Figure 22, Figure 23) and a racemic mixture prepared by adding equal amounts of the two enantiomers (Figure 24). Unfortunately, despite every attempt in changing the chiral column, flow rate and solvent mixture, it was impossible to obtain a perfect separation of the two peaks when we injected a mixture of the two enantiomers (Figure 24). Nevertheless the presence of the other enantiomer in the samples of either *R* or *S*, complex **58** was never observed.

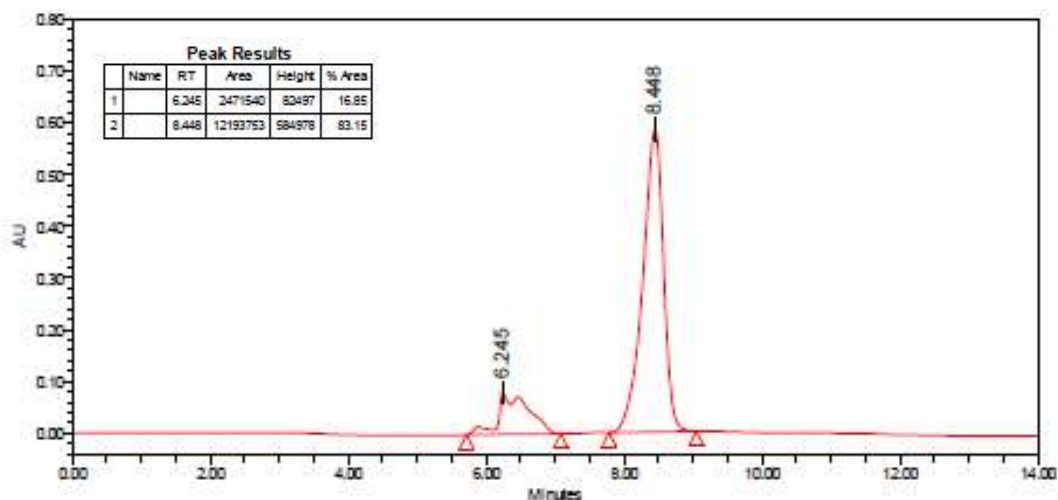


Figure 22. HPLC chromatogram of the (*R*)-enantiomer of complex **58** using CELLULOSE2 as a chiral column, in hexane:*i*PrOH 95:5, 0.5 mL/min

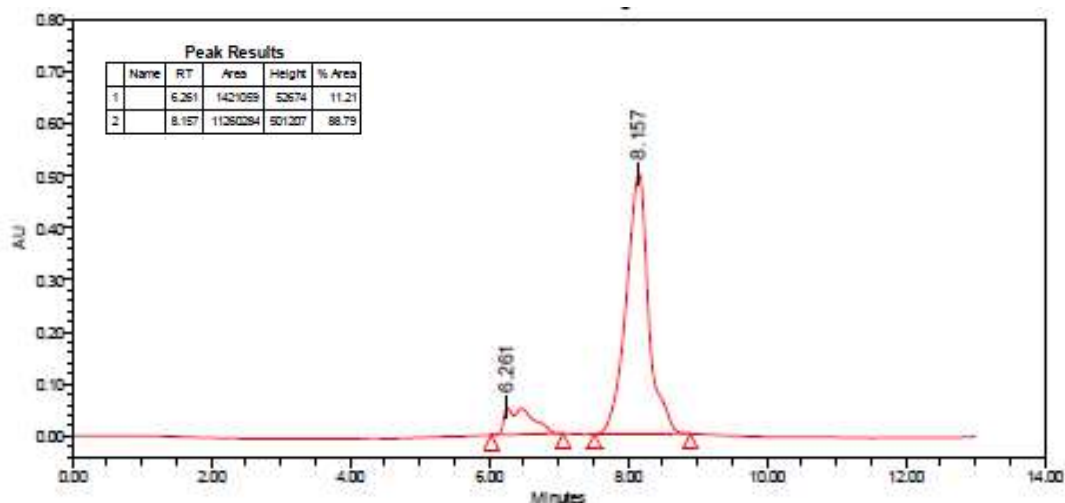


Figure 23. HPLC chromatogram of the (*S*)-enantiomer of complex **58** using CELLULOSE2, as a chiral column, in hexane:*i*PrOH 95:5, 0.5 mL/min

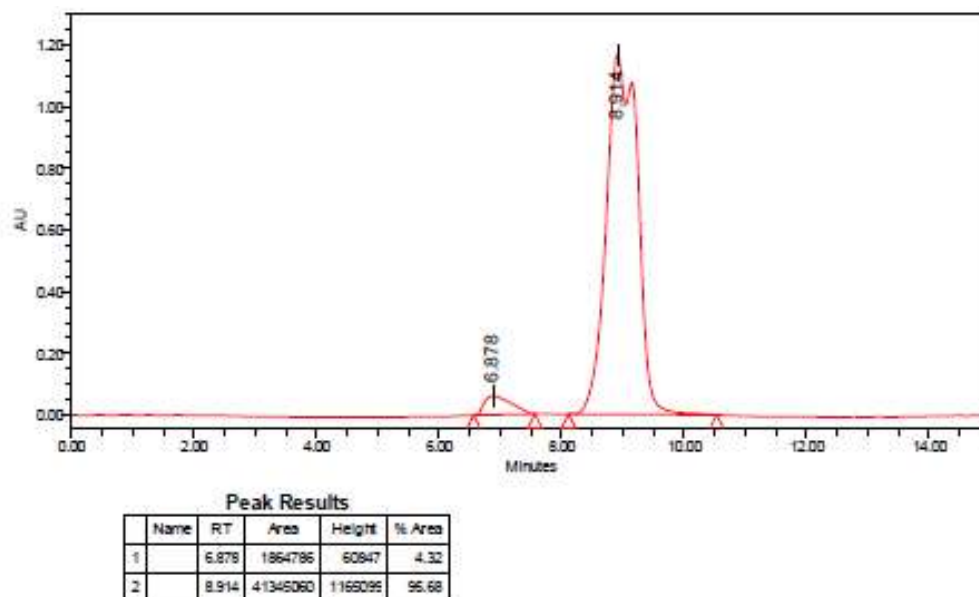
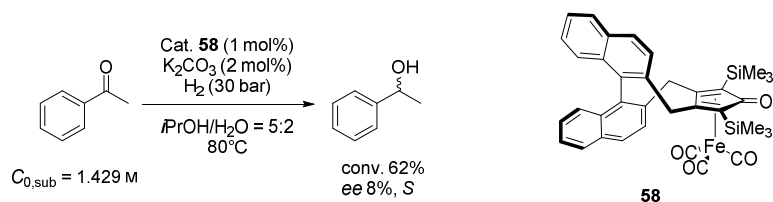


Figure 24. HPLC chromatogram of a mixture of the (*S*)- and (*R*)-enantiomer of complex **58** using CELLULOSE2 as a chiral column, in hexane:*i*PrOH 95:5, 0.5 mL/min

Complex **58** was tested in the hydrogenation of acetophenone giving 62% conversion and a disappointing 8% *ee* (Scheme 70), using previously reported reaction conditions:^[115] employing K_2CO_3 as an activator, 30 bar of hydrogen pressure at 70 °C in a mixture of *i*PrOH/ H_2O . We expected moderate conversion, since the newly synthesized catalyst required optimization of the hydrogenation's condition, while the low enantiomeric excess confirmed our hypothesis that the binaphthyl stereoaxis is relatively far from the reaction center, leading to an inefficient transfer of stereochemical information from the stereogenic element to the reaction center.



Scheme 70. Asymmetric hydrogenation of acetophenone using chiral complex **58**

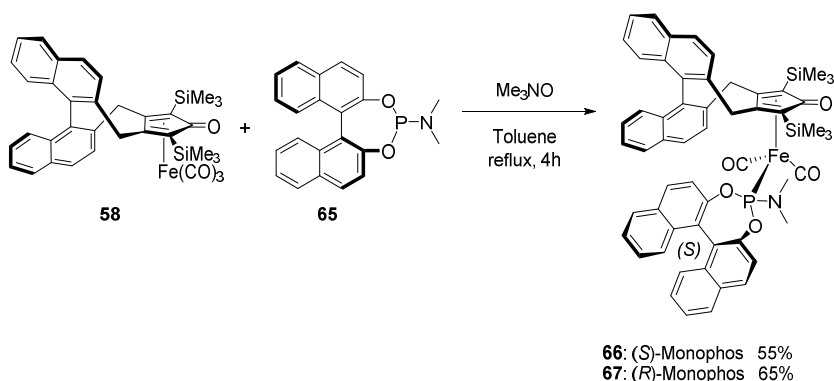
To obviate this problem we devise two solutions: the synthesis of new chiral complexes derivatives with substituents at the 3,3'-positions, and the replacements of a CO ligand with a bigger, maybe chiral ligand, such as the phosphoramidite described by Berkessel (see paragraph 3.3.5.2).^[117]

4.2.1. Replacement of a CO ligand with a chiral phosphoramidite ligand

(*S*)-Monophos **65** was prepared reacting (*S*)-BINOL, with $P(NMe_2)_3$ in toluene following the simple synthetic procedure reported by De-Vries and Feringa.^[145]

Complex **58** was subjected to oxidative removal of one CO using Me_3NO in the presence of the (*S*)-Monophos, yielding the air-stable complex **66** (Scheme 71), which was isolated in good yields and thoroughly characterized.

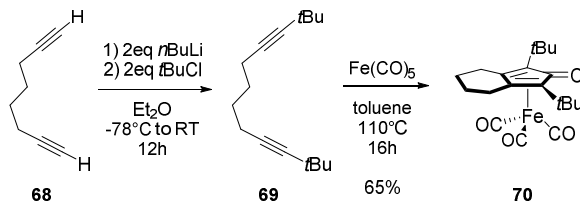
The same reaction was also performed using (*R*)-Monophos, to synthesize complex **67**, in order to evaluate possible match and mismatch combinations in the hydrogenation reaction.



Scheme 71. Replacement of one CO ligand with a chiral phosphoramidite ligand in complex 58

In order to evaluate the reactivity of complexes containing a phosphoramidite ligand, we decided to synthesize complexes **71**, **72**, **73** and **74** by decarbonylation with trimethylamine-*N*-oxide in the same way described in Scheme 71 starting from **46**,^[105b]^[104] **51**^[104] and **70** respectively.

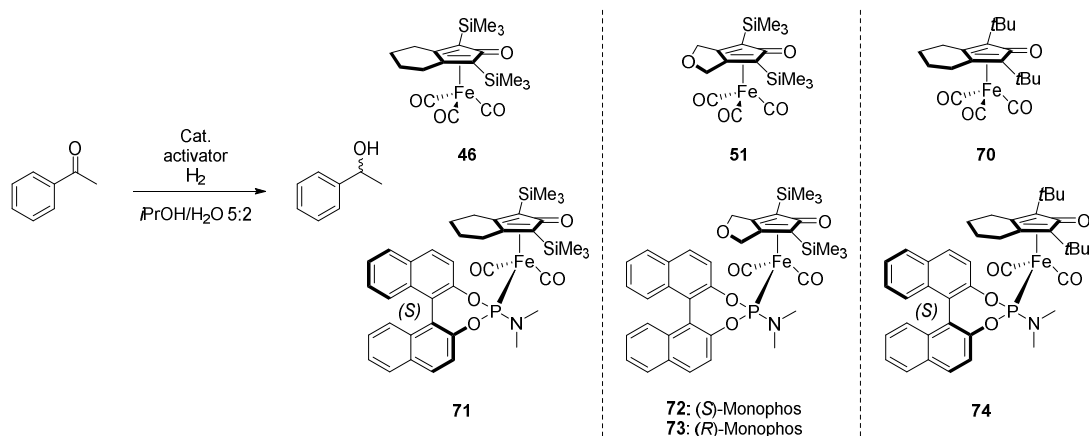
Complex **70** was synthesized (Scheme 72) in a similar way of **46** and **51**, starting from the commercially available 1,7-octadiyne **68**, which was treated with *n*BuLi and *t*BuCl to afford **69**, and then cyclized using $Fe(CO)_5$ to isolate **70** in 65% yield.



Scheme 72. Tethered synthesis of complex 70

The resulting complexes were then employed as pre-catalysts in the hydrogenation of acetophenone, screening different methods for their activation. The results are summarized in Table 2.

Table 2. Screening of different activators using iron tricarbonyl complexes (46, 51, 70) and the corresponding substituted phosphoramidite complexes (71, 72, 74)



Entry	Pre-cat.	Activator	$P H_2$ (bar)	Temperature (°C)	Time (h)	Yield (%) ^[c]	<i>ee</i> (%) ^[c,d]
1	46	K_2CO_3 ^[a]	30	80	16	93	-
		Me_3NO ^[a]	30	70	16	> 99	-
		$h\nu$ ^[b]	10	40	6	78	-
2	71	K_2CO_3 ^[a]	30	80	16	< 5	nd
		Me_3NO ^[a]	30	70	16	< 5	nd
		$h\nu$ ^[b]	10	40	7	92	35, <i>S</i>
3	51	K_2CO_3 ^[a]	30	80	16	66	-
		Me_3NO ^[a]	30	70	16	66	-
		$h\nu$ ^[b]	10	40	6	58	-
4	72	K_2CO_3 ^[a]	30	80	16	< 5	nd
		Me_3NO ^[a]	30	70	16	< 5	nd
		$h\nu$ ^[b]	10	40	6	92	35, <i>S</i>
5	70	K_2CO_3 ^[a]	30	80	16	93	-
		Me_3NO ^[a]	30	70	16	98	-
		$h\nu$ ^[b]	10	40	6	97	-
6	74	K_2CO_3 ^[a]	30	80	16	< 5	nd
		Me_3NO ^[a]	30	70	16	< 5	nd
		$h\nu$ ^[b]	10	40	6	97	31, <i>S</i>

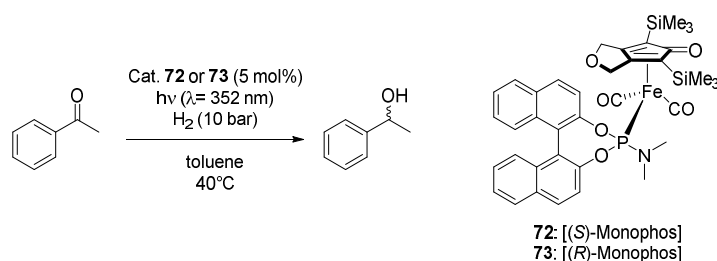
[a] Reaction conditions: acetophenone/Fe/activator = 100:1:2, solvent: 5:2 *i*PrOH/H₂O, $CO_{substrate} = 1.43$ M [b] Reaction vessel irradiated at $\lambda_{max} = 352$ nm and 8 W; Reaction conditions: acetophenone/Fe= 20:1 solvent: toluene, $CO_{substrate} = 0.047$ M. [c] Determined by GC equipped with a chiral capillary column (MEGADEX DACTBS β , diacetyl-*t*-butylsilyl- β -cyclodextrin) and dodecane as internal standard. [d] Absolute configuration is *S* (assigned by comparison of the optical rotation sign with literature data)^[147]

Table 2 shows that tricarbonyl iron complexes (**46**, **51** and **70**) can be activated to form the corresponding active hydride complexes *in situ*, employing K_2CO_3 , Me_3NO or UV irradiation as activator. Good conversions of 1-phenylethanol were obtained. In contrast, the use of phosphoramidite complexes **71**, **72** and **74** led to very low conversions using either K_2CO_3 and

Me₃NO. In fact, UV irradiation is required to remove a second CO ligand to activate the complex and obtain the active hydride catalyst. In all cases just moderate enantiomeric excesses were observed.

Subsequently, a screening of solvents using pre-catalyst **72** was performed (Table 3).

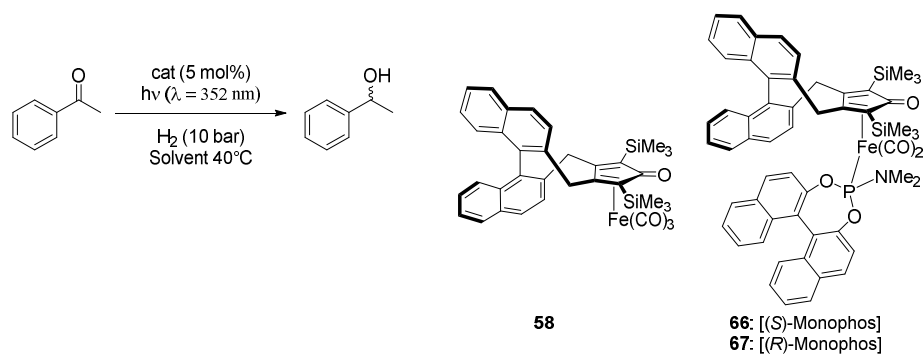
Table 3. Screening of different solvents using complexes **72 and **73**^[a]**



Entry	Pre-catalyst	Solvent	Time - UV irradiation (h)	Yield (%) ^[b]	<i>ee</i> (%) ^[b,c]
1	73 [(<i>R</i>)-Monophos]	Toluene	6	92	31, <i>R</i>
2	72 [(<i>S</i>)-Monophos]	Toluene	6	92	35, <i>S</i>
3	72	Toluene	18 ^[d]	92	13, <i>S</i>
4	72	<i>i</i> PrOH	6	55	30, <i>S</i>
5	72	<i>i</i> PrOH/H ₂ O 5:2	16	11	55, <i>S</i>
6	72	<i>n</i> -butylacetate	3	35	47, <i>S</i>
7	72	EtOAc	6	28	60, <i>S</i>

[a] Reaction vessel irradiated at $\lambda_{\text{max}} = 352$ nm and 8 W; Reaction conditions: acetophenone/Fe= 20:1, $\text{CO}_{\text{substrate}} = 0.047$ M. [b] Determined by GC equipped with a chiral capillary column (MEGADEX DACTBS β , diacetyl-*t*-butylsilyl- β -cyclodextrin) and dodecane as internal standard. [c] Absolute configuration is *S* (assigned by comparison of the optical rotation sign with literature data).^[147] [d] Xenon lamp emits white light over a wide range of wavelengths (from 380 to 950 nm) from 7.5 J/cm² to 12.5 J/cm².

The iron phosphoramidite complex **72**, catalyzed the asymmetric hydrogenation of acetophenone only when subjected to UV irradiation under hydrogen pressure, yielding up to 92% of (*S*)-1-phenylethanol and 35% of *ee* (Table 3, Entry 2). As expected, the catalyst containing (*R*)-Monophos **73**, (Entry 1) gave the opposite selectivity (31% *ee*; major enantiomer: (*R*)-1-phenylethanol). The irradiation under white light (Entry 3) gave very low conversion and loss of *ee* comparing to the UV irradiation. Change of the solvent (Entry 4-7) gave similar or better *ee* but with low conversion.

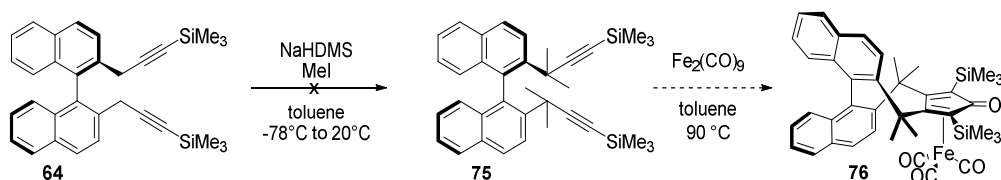
Table 4. Test of pre-catalysts **66** and **67** in the asymmetric hydrogenation of acetophenone^[a]

Entry	Pre-catalyst	Solvent	Time - UV irradiation (h)	Yield (%) ^[b]	ee (%) ^[b,c]
1	58	Toluene	4	35	17, <i>R</i>
2	67 [(<i>R</i>)-Monophos]	Toluene	6	82	39, <i>R</i>
3	66 [(<i>S</i>)-Monophos]	Toluene	7	97	29, <i>S</i>
4	66	<i>i</i> PrOH /H ₂ O 5:2	6	<2	50, <i>S</i>
5	66	<i>i</i> PrOH /H ₂ O 5:2	16	8	52, <i>S</i>
6	66	EtOAc	16	20	43, <i>S</i>

[a] Reaction vessel irradiated at $\lambda_{\text{max}} = 352 \text{ nm}$ and 8 W; Reaction conditions: acetophenone/Fe = 20:1, $\text{CO}_{\text{substrate}} = 0.047 \text{ M}$. [b] Determined by GC equipped with a chiral capillary column (MEGADEX DACTBS β , diacetyl-*t*-butylsilyl- β -cyclodextrin) and dodecane as internal standard. [c] Absolute configuration is *S* (assigned by comparison of the optical rotation sign with literature data)^[147]

The binaphthyl-derived complexes **58**, **66** and **67** were then tested (Table 4) in the hydrogenation of acetophenone under UV irradiation, where **58** yielded up to 35% of 1-phenylethanol and 17% of *ee* (Table 4, Entry 1), while **66** and **67**, containing Monophos, showed an increase of enantiomeric excesses and very good conversions (Entry 2-3). In addition, complex **67** represents the matched combination of **58** and (*R*)-Monophos giving 39% *ee* of (*R*)-1-Phenylethanol, whereas **66** is the mismatched combination with (*S*)-Monophos, which affords (*S*)-1-Phenylethanol in 29% *ee*. Change of the solvent (Entry 4-6) increased the *ee* in the hydrogenation reaction, but with reduced conversion.

Since the results were not so promising, we decided to avoid other trials using different phosphoramidite ligand, but we reasoned that an increased steric bulk next to the cyclopentadienone ring could enhance the transmission of stereochemical information. We planned the synthesis of pre-catalyst **76**, installing four methyl groups directly next to the cyclopentadienone ring. Unfortunately, the methylation of compound **64**, led to a decomposition of the starting material (Scheme 73).



Scheme 73. Attempt to increase the steric bulk next to the cyclopentadienone ring

After this trial, we decided to focus our attention on the 3,3'-position of the binaphthyl moiety, and in particular to install bulky substituents. A simple inspection of molecular models suggested that bulky 3,3'-substituents on the binaphthyl moiety would enhance the enantiofacial discrimination (Figure 25).

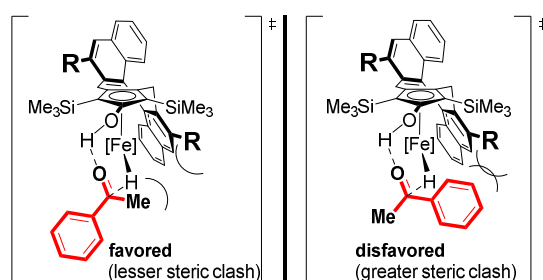


Figure 25. Suggested transition state for the ketone hydrogenation reaction, highlighting the assumed importance of bulky 3,3'-substituents

4.3. Towards the synthesis of a library of 3,3'-substituted chiral (cyclopentadienone)iron tricarbonyl complex

In a first instance, we speculated that the flat and rigid β -naphthyl groups might efficiently play the role of bulky 3-3' substituents (Figure 26).

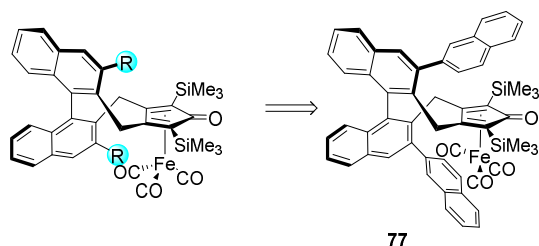
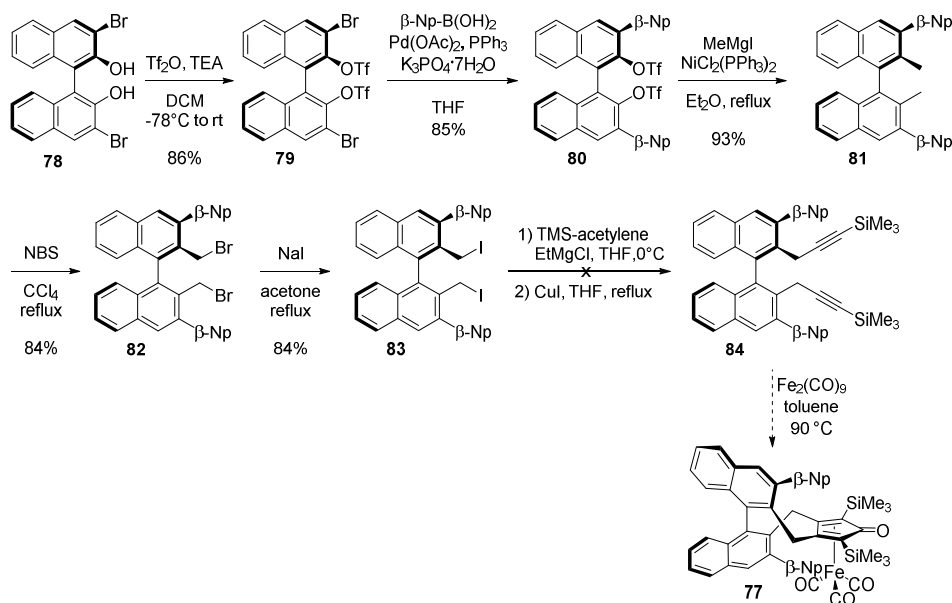


Figure 26. Idea to insert β -naphthyl on the 3-3'-positions of the binaphthyl moiety.

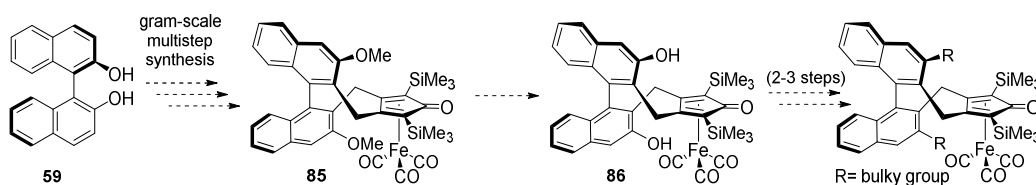
Scheme 74 presents the synthesis starting from the commercially available (*R*)-3,3'-dibromo-[1,1'-binaphthalene]-2,2'-diol, **78**, which was triflated to yield **79**. The arylated product **80** was obtained by a Suzuki-Miyaura cross coupling employing β -naphthyl boronic acid. This reaction proceeded

very slowly, probably due to the bulkiness of the β -naphthyl substituents. A subsequent Kumada coupling with MeMgI afforded **81**, which was brominated under radical conditions to yield the bis-bromide **82**, which was subsequently transformed into the bis-iodide by a Finkelstein reaction with NaI. To our surprise this reaction did not proceed as easily as in the case of the unsubstituted bis-bromide **62**. A mixture of compounds was observed in the crude reaction mixture and it was impossible to separate them. In addition, compound **82** was revealed to be very unstable and underwent rapid degradation. Furthermore, the reaction with the (TMS-ethynyl)magnesium bromide on the crude reaction mixture of **83** did not give the corresponding compound **84**.



Scheme 74. Attempts to synthesize β -naphthyl complex **77**

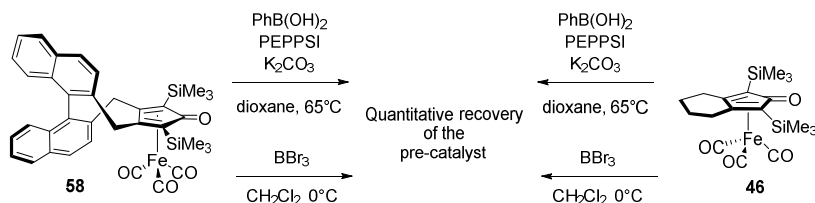
After the unsuccessful synthesis represented in Scheme 74, we decided that it was necessary to introduce the bulky 3,3'-substituents in a late step of the synthetic pathway, since their presence hampered the functionalization of the 2,2'-positions of the binaphthyl system. Additionally, we evaluated the possibility to prepare a small library of 3,3'-substituted complexes to figure out the role of the 3,3'-substituents. In order to facilitate the synthesis, a common precursor easily synthesized on gram scale and easily modifiable in one or two synthetic steps, was necessary (Scheme 75).



Scheme 75. New approach to synthesize new family of chiral iron complexes

It was necessary to evaluate that the cyclopentadienone(iron) tricyarbonyl complex was stable to harsh conditions needed for subsequent modifications, including the use of BBr_3 as a demethylating agent and the formation of HBr , as a side product during the transformation. In addition, the typical experimental conditions of the Suzuki-Miyaura coupling might have caused an *in situ* Hieber reaction, which would have formed the sensitive active hydride complex and eventually lead to decomposition of the complex.

A series of test reactions are represented in Scheme 76, using two pre-catalysts **58** and **46**, and luckily, a quantitative recovery of the iron complexes was accomplished in every case. This proved the stability of our chiral complex and made us confident to proceed with the new synthetic strategy.

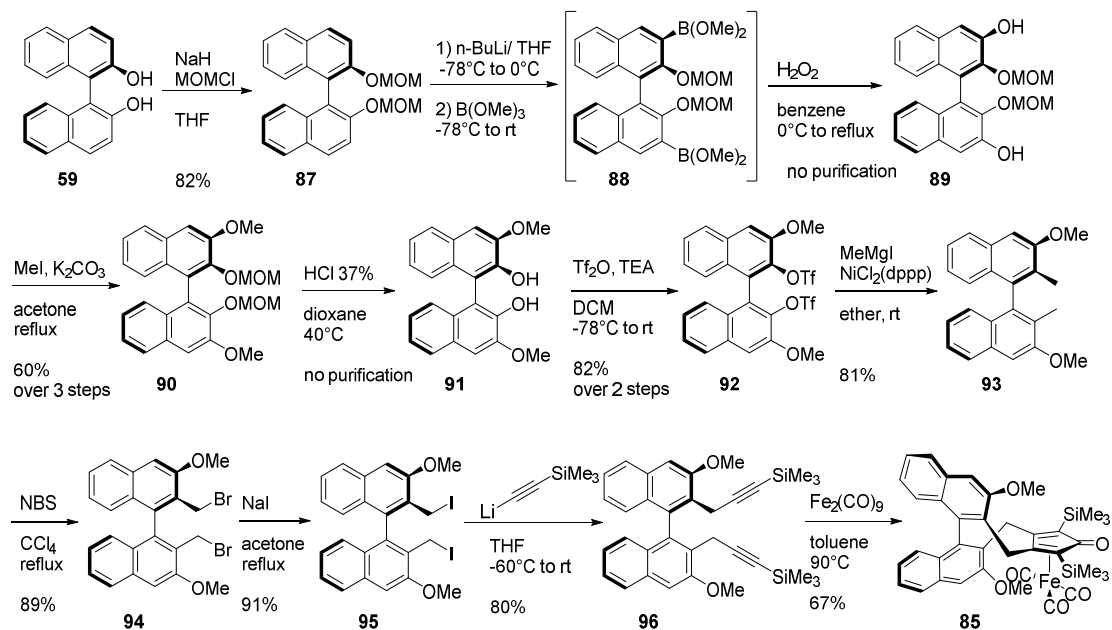


Scheme 76. Testing the stability of cyclopentadienone iron tricyarbonyl complexes

The new synthetic path to insert a 3,3'-dimethoxy-substituents takes inspiration from the synthesis made by Maruoka and co-workers (up to **94**, Scheme 77)^[143] for related binaphthyl-derivatives. We expected that the relatively small methoxy group would result in less sterical hindrance than the bulky β -naphthyl group used in the previous synthetic attempts (Scheme 74). The synthesis starts from (*R*)-BINOL **59**, which is protected using methyl chloromethyl ether (MOMCl), to obtain compound **87**, which was subjected to an *ortho*-lithiation, followed by treatment with trimethyl borate to obtain **88**, which was directly oxidized to **89**. The methylation of the hydroxy group of **89** was performed using MeI in the presence of K_2CO_3 to yield **90**. Acidic hydrolysis removed the MOM protecting group to give 3,3'-dimethoxy-2,2'-binaphthyl derivative **91**. Compound **91** was converted into the bis-triflate **92**, methylated in the presence of MeMgI and $[\text{Ni}(\text{dppp})\text{Cl}_2]$ by Kumada coupling to yield the known compound **93**. Subsequent radical bromination was carried out to yield the bis-bromide **94**,^[139] which was converted into the bis-

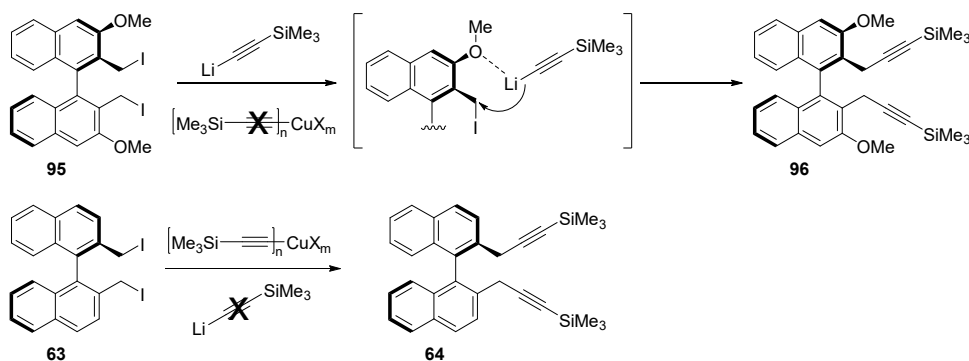
iodide **95**. Surprisingly, the formation of the bis-diyne using the (TMS-ethynyl)magnesium bromide in the presence of CuI, did not work with compound **95**. Different reaction conditions were screened in order to synthesize compound **96**, but without success for the formation of the desired product: 1) additional use of Pd(PPh₃)₄ to CuI; reaction of **95** with Gilman's cuprate (TMS-ethynyl)₂CuLi; 2) Kumada cross coupling using **95** and (TMS-ethynyl)magnesium bromide.

To our delight, substitution of **95** with (TMS-ethynyl)lithium allowed to produce the diyne **96** in high yields, which was cyclized in the presence of Fe₂(CO)₉ to obtain **85** in 67% yield.



Scheme 77. Synthesis of chiral (cyclopentadienone)iron tricarbonyl complex **85**

We suppose that the alkylation of **95** in the presence of (TMS-ethynyl)lithium is assisted by the electron pairs of the methoxy groups in the adjacent 3,3'-position of the binaphthyl moiety (Scheme 78). Additional evidence corroborating this hypothesis was given by the fact that the 3,3'-unsubstituted bis-iodide **63** did not react with (TMS-ethynyl)lithium.



Scheme 78. 3,3'-dimethoxy groups directed the nucleophilic substitution to form the diyne

The synthetic protocol in Scheme 77 was optimized to allow us to simplify our work and proceed on a multi-gram step synthesis (starting from up to 20 g of (*R*)-BINOL) of complex **85**. Eleven steps are required, but no purification had to be used until the synthesis of compound **90** which was purified by column chromatography with a total yield of 55% from (*R*)-BINOL. Only three other chromatographic purifications were used for **92**, **93** and the final complex **85**. Crystallization was used in the purification of the bis-bromide **94** with similar yield obtained with flash column chromatography (84% vs. 89%) and the bis-iodide **95** was purified by simple filtration. Purification of the diyne **96** can be also avoided, to afford the final complex **85** in the same yield (54% for two steps).

4.3.1. Screening conditions and optimization

(Cyclopentadienone)iron tricarbonyl complex **85** was tested in the asymmetric hydrogenation of acetophenone, and similar conversions previously observed in the presence of **58** were obtained, but the enantiomeric excess increased up to 48%, 6 times higher respective to that of the **58** (Table 5, entry 1 and 2). This early result demonstrated the importance of 3,3'-substituents, and we decided to optimize the experimental conditions for this reaction, performing a screening of different activators in order to improve the catalytic results. In particular, several bases of different strength were employed, to optimize the Hieber conditions for the activation of the Fe(0) pre-catalyst, as well as trimethylamine-*N*-oxide to evaluate the efficacy of an oxidative method for the pre-catalyst activation. The reactions were performed under otherwise identical conditions, apart from the nature of the activator. The reaction outcome was evaluated by analysis of the NMR spectra of reactions crudes and injection in GC. In this way it was possible to confirm that no other by products were formed during the reactions thus assuring the selectivity of the reactions. In addition, the isolated yield of 1-phenylethanol, as product of the hydrogenation of acetophenone using complex **85** was determined, thus proving that the

conversions obtained by GC and NMR evaluations are comparable to the isolated yields. This procedure was followed for the screening of activators (Table 5), solvent screening (Table 6) and different pre-catalysts (Table 8).

Table 5. Screening of the activators for new (cyclopentadienone)iron tricarbonyl complex **85^[a]**

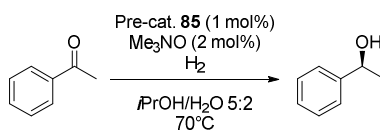
Pre-cat. **85** (1 mol%)
Activator (2 mol%)
H₂ (30 bar)
iPrOH/H₂O 5:2
70°C

Entry	Pre-cat.	Activator	Conv. (%) ^[b]	ee (%) ^[b,c]
1	58	K ₂ CO ₃	62	8
2	85	K ₂ CO ₃	54	49
3	85	Li ₂ CO ₃	9	52
4	85	Na ₂ CO ₃	25	53
5	85	Cs ₂ CO ₃	29	51
6	85	LiOH	49	51
7	85	NaOH	35	50
8	85	KOH	30	52
9	85	K ₃ PO ₄	23	53
10	85	Me ₃ NO	84	50

[a] Reaction conditions: Substrate/Pre-cat./Activator = 100:1:2, $P(\text{H}_2) = 30$ bar, solvent = 5:2 *i*PrOH/H₂O, $\text{CO}_{2,\text{substrate}} = 1.43$ M, $T = 70$ °C, time = 18 h. [b] Determined by GC equipped with a chiral capillary column (MEGADEX DACTBS β , diacetyl-*t*-butylsilyl- β -cyclodextrin). [c] Absolute configuration is *S* (assigned by comparison of the optical rotation sign with literature data)^[147]

This screening showed that the enantiomeric excess is almost independent on the applied activator (entries 2-10). In terms of conversion, initially the most efficient inorganic activator appeared to be K₂CO₃ (entry 2), but the best results were obtained with trimethylamine-*N*-oxide (entry 10). Renaud and co-workers reported the use of Me₃NO to remove one CO ligand from **85**, in this way a vacant site is formed, and filled with H₂ after splitting.^[113]

After finding the optimal activation pathway for the pre-catalyst **85**, optimization studies continued to assess the effects of hydrogen pressure, temperature and solvent (Table 6).

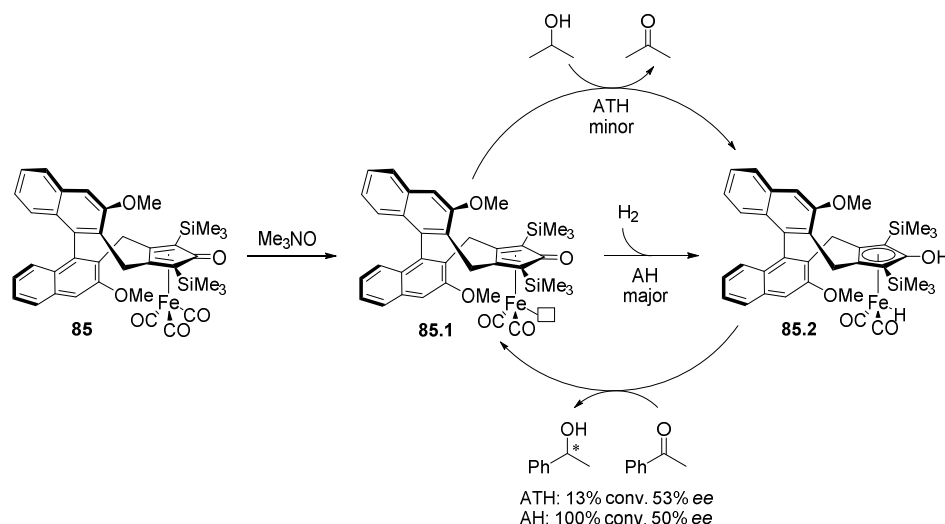
Table 6. Optimization of the reaction parameters of the asymmetric hydrogenation of acetophenone promoted by pre-cat **85^[a]**

Entry	Solvent	<i>P</i> H ₂ (bar)	<i>T</i> (°C)	Conv. (%)	<i>ee</i> (%)
1	<i>i</i> PrOH/H ₂ O 5:2	30	70	84	50
2	<i>i</i> PrOH/H ₂ O 5:2	50	70	85	51
3	<i>i</i> PrOH/H ₂ O 5:2	30	80	59	50
4	<i>i</i> PrOH/H ₂ O 5:2	30	50	33	55
5 ^[d]	<i>i</i> PrOH/H ₂ O 5:2	30	70	100 ^[e]	50
6 ^[f]	<i>i</i> PrOH/H ₂ O 5:2	30	70	58	51
7 ^[g]	<i>i</i> PrOH/H ₂ O 5:2	--	70	13	53
8	<i>i</i> PrOH	30	70	15	54
9	EtOH/H ₂ O 5:2	30	70	21	49
10	CF ₃ CH ₂ OH/H ₂ O 5:2	30	70	74	42
11	DME/H ₂ O 5:2	30	70	56	52
12	Dioxane/H ₂ O 5:2	30	70	56	52
13	CH ₃ CN/H ₂ O 5:2	30	70	3	53
14	DMF/H ₂ O 5:2	30	70	26	54
15	DCE/H ₂ O 5:2	30	70	34	54
16	Toluene/H ₂ O 5:2	30	70	8	53

[a] Reaction conditions: Substrate/Pre-cat. **85**/Me₃NO = 100:1:2, *P*(H₂) = 30 bar, *c*_{0,substrate} = 1.43 M. [b] Determined by GC equipped with a chiral capillary column (MEGADEX DACTBSβ, diacetyl-*t*-butylsilyl-β-cyclodextrin). [c] Absolute configuration is *S* (assigned by comparison of the optical rotation sign with literature data)^[147] [d] 2 mol% **85** (4 mol% Me₃NO) employed. [e] Yield of the isolated product 94%. [f] *c*_{0,substrate} = 0.72 M. [g] no hydrogen was applied to perform only asymmetric transfer hydrogenation

To obtain full conversion, 2 mol% of **85** had to be used (Table 5, entry 5), in fact, increasing the pressure (entry 2) or temperature (entry 3) did not lead to full conversion. A slight increase of enantiomeric excess was observed at lower temperature (entry 4), but with a concomitant decrease of conversion. Additional solvent mixtures were tested (entries 9-16), but none of them led to better results than the 5:2 isopropanol/H₂O mixture. The presence of water appeared to be crucial for the conversion (entry 8), maybe due to the poor solubility of Me₃NO in isopropanol. Substrate concentration was also very important, because when the reaction was diluted twice (entry 6 vs. 1), a remarkable decrease of conversion was observed. Pre-catalyst **85** was also tested in the asymmetric transfer hydrogenation (entry 7), but low conversions were obtained. This underlines that the main catalytic activity is coming from the hydrogenation pathway. Still, a

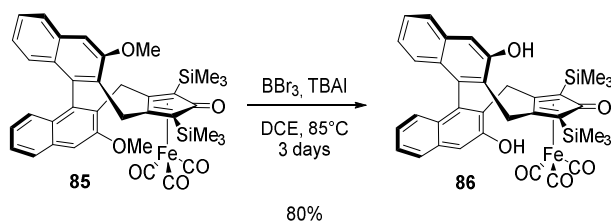
background consisting of transfer hydrogenation with isopropanol is also occurring (TOP, ATH, Scheme 79), luckily this had no negative effect on overall results, since the obtained enantiomeric excess was almost the same.



Scheme 79. Comparison of asymmetric transfer hydrogenation and asymmetric hydrogenation with complex **85**

4.3.2. Synthesis of the library of new chiral pre-catalyst

After the promising enantiomeric excess obtained with **85**, we decided to chase the initial plan to synthesize complexes bearing different 3,3'-substituents from the common precursor **85**. The first attempt to demethylate complex **85**, employing BBr_3 and typical conditions for the demethylation of aryl methyl ethers (0°C , CH_2Cl_2), gave no conversion, but the unreacted substrate gave no sign of decomposition and turned out to be very stable to BBr_3 (as expected after initial experiments with similar complexes presented in Scheme 76). However, using tetra-*n*-butylammonium iodide (TBAI) as an additive^[148] and increasing the reaction temperature (in DCE), the bis-OH derivative **86** was obtained in 80% yield (Scheme 80). Employing these harsh conditions, we proved again the great stability of (cyclopentadienone)iron tricarbonyl complexes.



Scheme 80. Demethylation of complex **86**

Luckily, we were able to grow a crystal of **86** suitable for single-crystal X-ray diffraction analysis by slow diffusion of hexane into a CH_2Cl_2 solution of complex **86** (Figure 27).

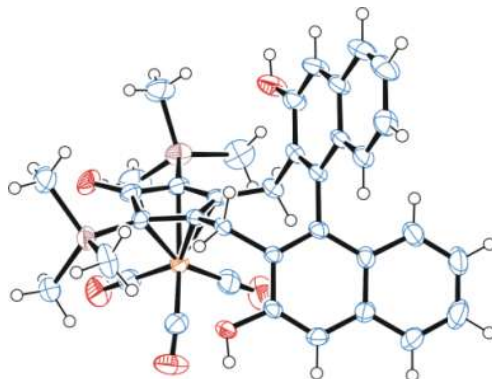
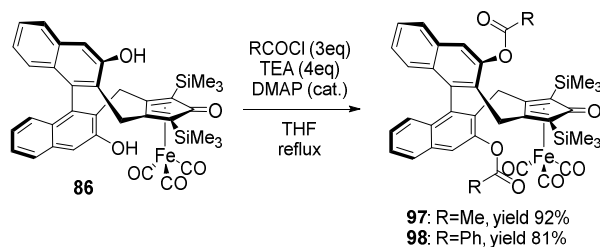


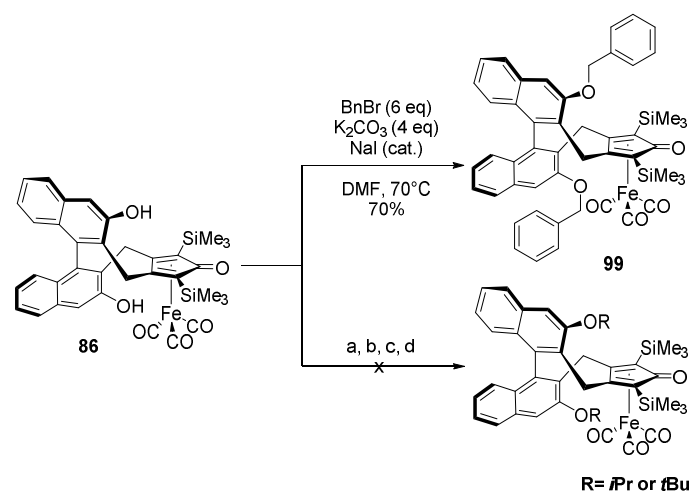
Figure 27. ORTEP diagram (CCDC 1037376) of the molecular structure of **86** (thermal ellipsoids set at the 50% probability level)

Starting from **86**, we planned our strategy of using simple transformation in order to prepare complexes with bulkier 3,3'-substituents. We started with a simple esterification and we were able to obtain two new pre-catalysts in good yields: the bis-acetate **97** and bis-benzoate **98** (Scheme 81).



Scheme 81. Synthesis of ester-derived complexes **97** and **98**

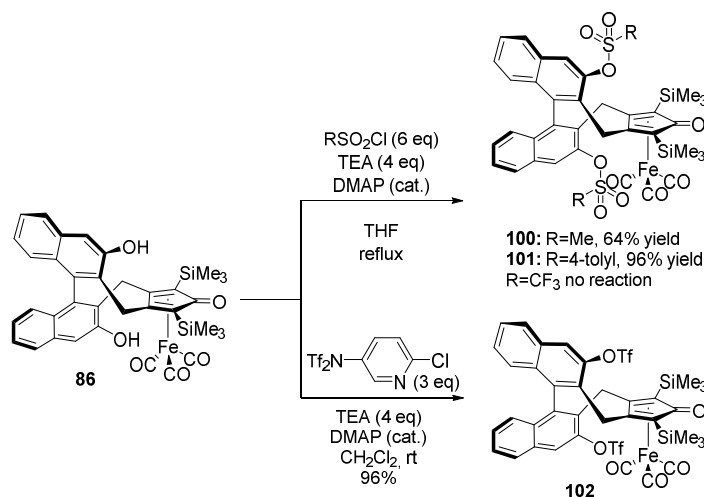
The next goal was to form bis-ether derivatives. Unfortunately, the etherification did not proceed as easily as in the case of esterification. Even though we managed to obtain only the bis(benzyl)ether complex **99** with 70% yield (Scheme 82), attempts to synthesize the bis(isopropyl)ether, or the bis(*tert*-butyl)ether employing isobutene or $(t\text{BuO})_2\text{CHNMe}_2$ were not successful.



R = *i*Pr: a) 2-iodopropane, K₂CO₃, acetone, reflux; b) 2-iodopropane, K₂CO₃, DMF, 100 °C; c) 2-iodopropane, NaH, neat, 75 °C; R = *t*Bu: d) (tBuO)₂CHNMe₂, toluene, 100 °C

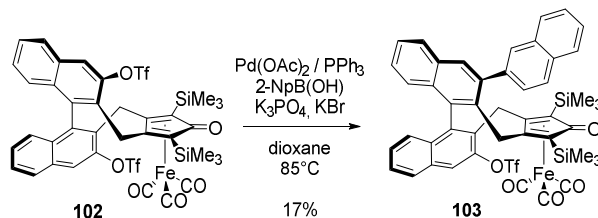
Scheme 82. Synthesis of 3,3'-bis(benzylether) 99 and attempts of preparation of other ether-derived complexes

Sulfonylation of **86** with methanesulfonyl chloride (MsCl) or *p*-toluenesulfonyl chloride (TsCl) occurred in high yields in the presence of triethylamine (TEA) and catalytic amounts of 4-dimethylaminopyridine (DMAP), yielding complexes **100** and **101** (Scheme 83). The bis-triflate derivative **102** was obtained employing the Comins' reagent [*N*-(5-chloro-2-pyridyl)bis(trifluoromethanesulfonylimide)].^[149] On the contrary, the reaction with trifluoromethanesulfonyl chloride (TfCl) or trifluoromethanesulfonic anhydride (Tf₂O) under similar conditions did not afford complex **102**.



Scheme 83. Synthesis of sulfonyl esters-derived complexes 100, 101 and 102

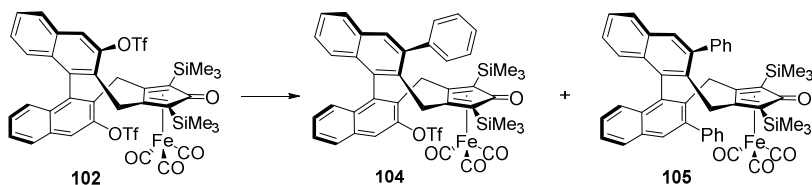
Since the final aim was to insert aryl substituents on the 3,3'-positions of the binaphthyl moiety, we decided to use the bis-triflate **102** in the Suzuki-Miyaura cross-coupling. Unfortunately, under typical conditions for this cross-coupling,^[150] using β -naphthyl boronic acid, only a mono-substituted complex **103** was obtained in 17% yield (Scheme 84). Since the triflate group placed nearby the $\text{Fe}(\text{CO})_3$ group is sterically less accessible, we supposed that the structure of the obtained monosubstitution product **103** is the one represented in Scheme 84, where the bulky aryl group is located far from the Fe center.



Scheme 84. Suzuki-Miyaura coupling with **102**

We attributed the low conversion to the steric bulkiness of the β -naphthyl group and we decided to carry out further attempts using the less demanding phenylboronic acid. We started employing the same reaction conditions used in Scheme 84, but again we were able to obtain just a mono-substituted complex **104** (Table 7, entry 6), albeit in a nearly quantitative way. Slightly modified conditions (Entry 3: $\text{Pd}(\text{OAc})_2/(\text{S})\text{-Phos}$ or entry 4-5: $\text{Pd}(\text{OAc})_2/\text{PPh}_3$ instead of $[\text{Pd}(\text{PPh}_3)_4]$) gave almost the same result. While using PCy_3 (entry 1-2), instead of PPh_3 or $(\text{S})\text{-Phos}$, no reaction or degradation were observed.^{[151][152]} Degradation of the iron complex was also observed, when relatively strong bases and/or water were used, probably caused by a side Hieber-base reaction, in which the unstable (hydroxycyclopentadienyl)iron complex was produced.

Table 7. Screening of different methods for arylation of bis-triflate Fe18 by Suzuki-Miyaura cross-coupling
[a]



Entry	Catalyst	PhB(OH) ₂ [eq]	Base [eq]	Additive [eq]	T (°C)	Solvent	NMR ratio (%)		
							102	104	105
1 ^[151]	15% $\text{Pd}(\text{OAc})_2$ 18% PCy_3	2.5	KF [3.3]		60	THF	97	3	-
2 ^[151]	15% $\text{Pd}(\text{OAc})_2$	2.5	KF [3.3]	KBr [2.2]	60	THF	97	3	-

18% PCy ₃								
3 ^[153]	25% Pd(OAc) ₂ 50% (S)-Phos	3	K ₃ PO ₄ [4]		85	toluene	100	-
4	20% Pd(OAc) ₂ 40% PPh ₃	2.5	K ₃ PO ₄ [3]		85	dioxane	80*	-
5	20% Pd(OAc) ₂ 40% PPh ₃	2.5	KBr [3]	KBr [2.2]	85	dioxane	2	80* -
6 ^[150]	10% Pd(PPh ₃) ₄	2.5	K ₃ PO ₄ [3]	KBr [2.2]	85	dioxane	5	74* -
7 ^[154]	[5%+5%] Pd(PPh ₃) ₄	2.5	K ₃ PO ₄ [3]	KBr [2.2]	85	dioxane		74* -
8	10% Pd(PPh ₃) ₄	2.5	K ₃ PO ₄ [3]	KBr [2.2] H ₂ O [6]	85	dioxane		100 -
9	5% Pd(PPh ₃) ₄	2.5	K ₃ PO ₄ [3]	KBr [5.6]	110	dioxane		100 -
10	5% Pd(PPh ₃) ₄	2.5	K ₃ PO ₄ [5]		100	DMF		<i>degradation</i>
11	5% Pd(PPh ₃) ₄	2.5	K ₃ PO ₄ [3]	TBAB [2.2]	85	dioxane	100	-
12	10% Pd(PPh ₃) ₄	5	K ₃ PO ₄ [6]	KBr [2.2]	85	dioxane/ H ₂ O		<i>degradation</i>
13	10% Pd(PPh ₃) ₄	5	K ₃ PO ₄ [6]	KBr [2.2]	85	dioxane		100 -
14	5% Pd(PPh ₃) ₄	2.5	Ba(OH) ₂ · 8 H ₂ O [3]	KBr [2.2]	85	dioxane		100 -
15 ^[152]	10% Pd(PPh ₃) ₄	5	Ba(OH) ₂ · 8 H ₂ O [6]		85	DME/ H ₂ O		<i>degradation</i>
16 ^[152]	10% Pd(PPh ₃) ₄	5	Ba(OH) ₂ · 8 H ₂ O [3]		85	DME/ H ₂ O		<i>degradation</i>
17	10% Pd(PPh ₃) ₄	2.5	Ba(OH) ₂ [3]	KBr [2.2]	85	dioxane	65	35 -
18	5% Pd(PPh ₃) ₄	2.5	<i>t</i> BuOK [3]	KBr [2.2]	85	dioxane		<i>degradation</i>
19 ^[155]	4% PEPPSI- <i>i</i> Pr	2.5	K ₂ CO ₃ [6]		60	dioxane		100
20	5% PEPPSI- <i>i</i> Pr	2.5	K ₃ PO ₄ [3]		85	dioxane		100
21	5% PEPPSI- <i>i</i> Pr	2.5	<i>t</i> BuOK [2.6]		60	<i>i</i> PrOH		<i>degradation</i>
22 ^[156]	5% Pd(IPr*) (cinnamyl)Cl	3	K ₂ CO ₃ [4]		40	EtOH		<i>degradation</i>
23 ^[157]	5% NiCl ₂ (dppp)	4	K ₃ PO ₄ [8]		100	dioxane		<i>degradation</i>
24	10% PdCl ₂ (dppp)	2.5	K ₃ PO ₄ [3]	KBr [2.2]	85	dioxane	50	50 -
25	10% PdCl ₂ (dppp)	2.5	Ba(OH) ₂ · 8 H ₂ O [3]	KBr [2.2]	85	dioxane	50	50 -

[a] Conversion determined by NMR

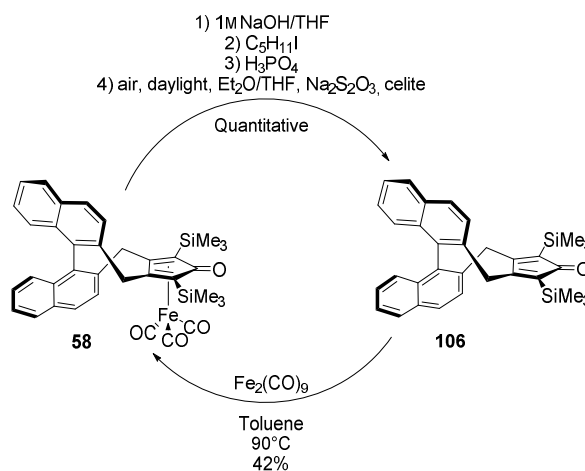
*isolated yield

In total, 25 different palladium and nickel catalyzed cross coupling conditions were tested. Different ligands, bases, solvents and temperatures were evaluated, but unfortunately we were not able to obtain the desired bis-coupled complex **105**.

NMR studies on complex **104** confirmed that mono cross-coupling was taking place only on one side of the molecule. In particular, we supposed that the cross-coupling occurs only on the triflate

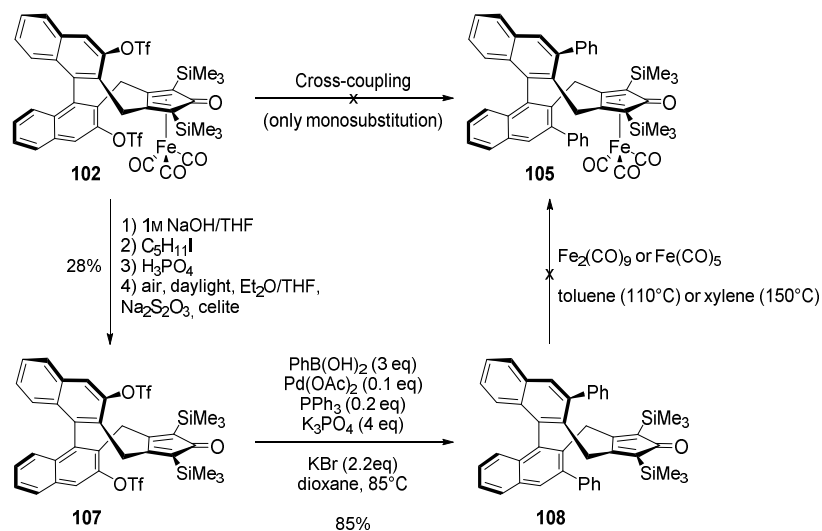
group placed on the opposite side to $\text{Fe}(\text{CO})_3$, since it is sterically less hindered and thus allows an easier access for the cross-coupling.

We decided to explore a different approach to obtain the bis-phenyl derivative **105**. Assuming that $\text{Fe}(\text{CO})_3$ was interfering with the Suzuki-Miyaura cross-coupling, we planned to remove that obstacle by demetallation, perform the cross-coupling on a 3,3'-substituted cyclopentadienone ligand and again form the iron complex. We believed that a subsequent insertion of the iron on the 3,3'-bisphenyl ligand with $\text{Fe}_2(\text{CO})_9$ would have been easier than the cross-coupling with the metal complex. To assess this plan, using the methodology developed by Knölker,^[106] **58** was decomplexed to yield the free ligand **106** quantitatively, and could be successfully re-complexed into **58** (Scheme 85).



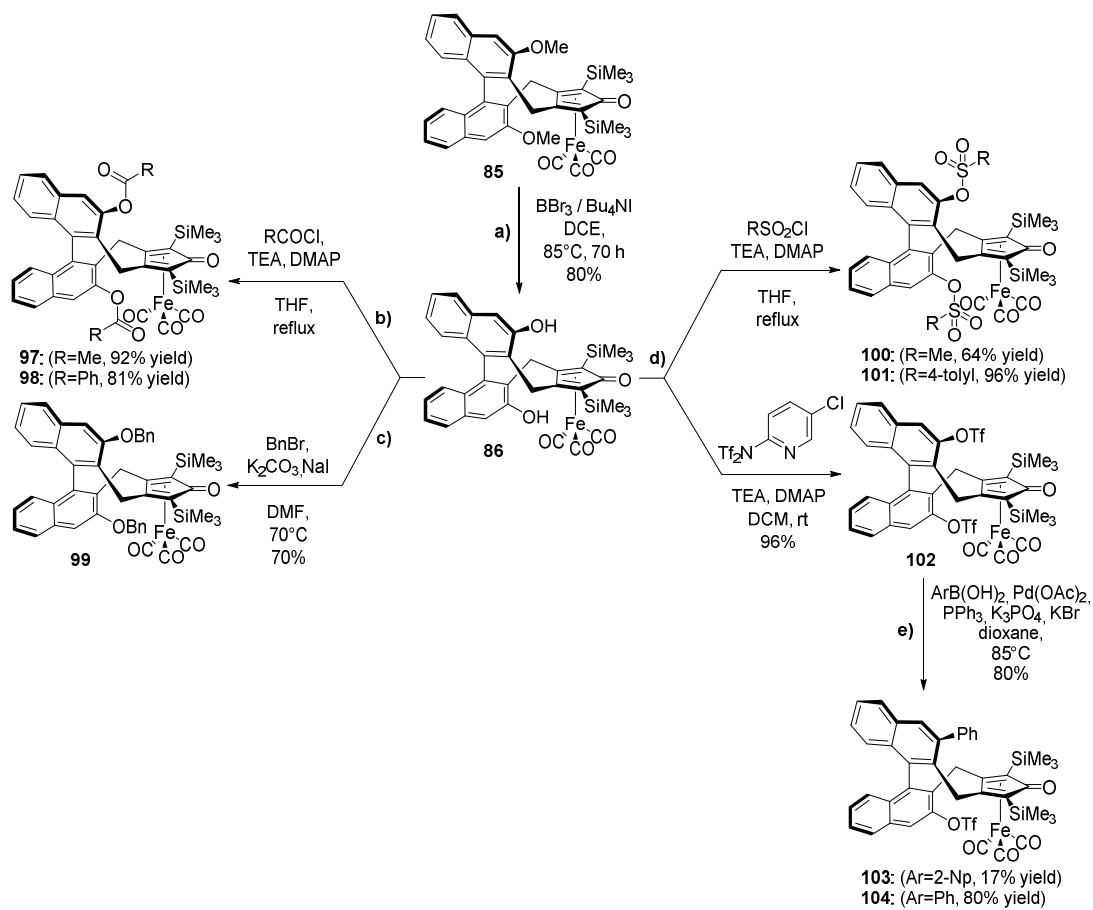
Scheme 85. Reversible decomplexation of 58

After these promising results, we performed the decomplexation directly on the bis-triflate derived complex **102**, as it would give us direct access to the Suzuki-Miyaura coupling with the obtained ligand **107** (Scheme 86). The decomplexation worked, even though just in 28% yield, and as expected, the cross coupling of compound **107** with phenylboronic acid easily gave ligand **108**, bearing two phenyl groups in 3,3'-positions. Meanwhile, this was another indirect proof that the mono-substitution products **103** and **104**, the unreacted triflate group is the one near to the $\text{Fe}(\text{CO})_3$ residue. Unfortunately, despite using different iron sources, higher temperatures, solvents or prolonged reaction times, the re-complexation of ligand **107** failed and no sign of desired iron complex **105** was observed.



Scheme 86. Attempted synthesis of complex 105 from 102 by decomplexation, cross-coupling and re-complexation

In summary, our synthetic efforts allowed us to build a small library of chiral iron complexes, starting from complex **85**. An unprecedented synthetic pathway based on the high chemical and thermal stability of (cyclopentadienone)iron complexes and their direct modifications, using relatively simple transformations (Scheme 87). The strategy involved (a) deprotection of **86** followed by: (b) esterification, (c) etherification, (d) sulfonylation or (e) cross-coupling with the triflate derivative. In this way, we were able to synthesize nine new pre-catalysts in few synthetic steps, avoiding time-consuming for parallel synthesis of each new complex and possible synthetic problems during multi-step synthesis.

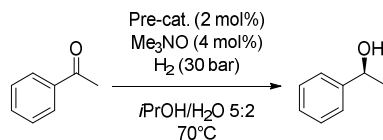


Scheme 87. Scheme of synthetic routes starting from 85 to obtain 9 new different pre-catalysts

4.3.3. Catalytic tests with new chiral (cyclopentadienone)iron complexes

Finally, we decided to test our library of chiral (cyclopentadienone)iron complexes, depicted in Scheme 87, in the asymmetric hydrogenation of acetophenone (Table 8) using the optimized conditions.

Table 8. Screening of pre-catalyst **85**, **86**, **97-104** in the asymmetric hydrogenation of acetophenone ^[a]



Entry	Pre-cat.	Substituents	Conv. (%) ^[b]	ee (%) ^[b,c]
1	85	OMe	100	50
2	86	OH	63	46
3	97	OAc	3	46
4	98	OBz	16	38
5	99	OBn	38	39
6	100	OMs	14	39
7	101	OTs	20	37
8	102	OTf	7	35
9	103	Mono 2-Np	12	47
10	104	Mono Ph	22	52

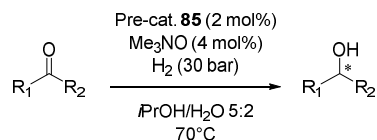
[a] Reaction conditions: substrate/Pre-cat./Me₃NO = 100:2:4, *P*(H₂)=30 bar, solvent=5:2 *i*PrOH/H₂O, *c*_{0,substrate}=1.43 M, T = 70 °C, reaction time = 18 h. [b] Determined by GC equipped with a chiral capillary column (MEGADEX DACTBSβ, diacetyl-*t*-butylsilyl-β-cyclodextrin). [c] Absolute configuration is *S* (assigned by comparison of the optical rotation sign with literature data)^[147]

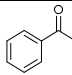
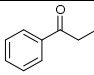
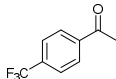
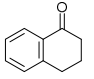
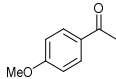
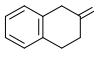
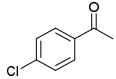
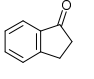
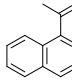
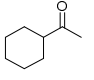
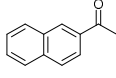
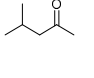
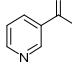
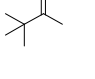
All newly synthesized pre-catalysts showed significantly lower catalytic activities and lower stereoselectivity compared to pre-catalyst **85**. Full conversion of the acetophenone was never reached, and the best result in terms of catalytic activity was achieved with the dihydroxy-substituted pre-catalyst **86** (Table 8, entry 2), derived from **85**. The lesser steric bulk of the 3,3'-substituents can explain the slightly decreased enantiomeric excess of **86** compared to **85**. The low stereoselectivity of the other complexes is not simple to explain, since they bear bigger 3,3'-substituents. Perhaps, esters **97-98** presented low conversion due to the possible carbonyl oxygen coordination to the iron center and its subsequent deactivation.^[113a] In the case of ethers and esters, the bulky substituents are possibly able to move away from the zone of approach of the substrate because of free rotation of the C-O bond. In terms of stereoselectivity, only **103** and **104** pre-catalysts (Entry 9-10) showed a comparable enantiomeric excess to **85**, whereas the other complexes showed significantly lower values (Entries 3-8).

4.3.4. Substrate screening with the best chiral (cyclopentadienone)iron complex **85**

Since the best catalyst for the AH of acetophenone remained the 3,3'-bis-methoxy pre-catalyst **85**, a substrate screening was performed using this complex (Table 9).

Table 9. Substrate screening for pre-catalyst **85**^[a]



Entry	Substrate	Conv. (%) ^[b]	<i>ee</i> (%) ^[c] abs. conf. ^[d]	Entry	Substrate	Conv. (%) ^[b]	<i>ee</i> (%) ^[c] abs. conf. ^[d]
1		100	50, <i>S</i>	8		97	57, <i>S</i>
2		100	46, <i>S</i>	9 ^[e]		25	77, <i>S</i>
3		64	50, <i>S</i>	10		100	13, <i>R</i>
4		100	51, <i>S</i>	11		78	59, <i>R</i>
5		43	68, <i>S</i>	12		89	61, <i>S</i>
6		99	51, <i>S</i>	13		76	0
7		35	50, <i>S</i>	14		22	77, <i>S</i>

[a] Reaction conditions: substrate/Pre-cat. **85**/Me₃NO = 100:2:4, *P*(H₂) = 30 bar, solvent = 5:2 *i*PrOH/H₂O, *c*_{0,substrate} = 1.43 M, *T* = 70 °C, reaction time = 18 h. [b] Determined by GC equipped with a chiral capillary column (see the Experimental part), conversions obtained by GC were confirmed by ¹H-NMR of the reaction crudes, confirming that no other by-products were formed. [c] Determined by GC or HPLC equipped with a chiral capillary column (see the Experimental part). [d] Assigned by comparison of the sign of optical rotation with literature data (see the Experimental part). [e] Substrate/Pre-cat. **85**/Me₃NO = 100:5:10.

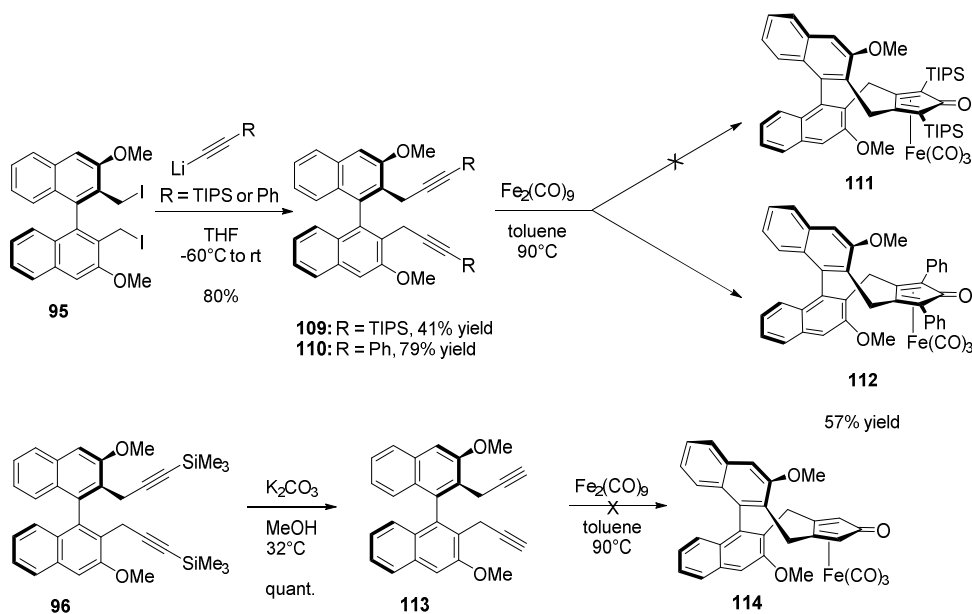
Pre-catalyst **85** was screened with a range of acetophenone derivatives (entries 1-6, 9, 11, 14), as well with heteroaromatic (entries 7, 8, 12) and aliphatic ketones (entries 10, 13). A general trend can be observed; if the substituents next to the carbonyl group were bulkier, higher enantiomeric excesses were observed (up to 77% entry 9 and 14), but along with a decreased conversion as well. With a low steric hindrance, low (13% *ee* for entry 10) or no enantioselectivity (0% *ee* for entry 13) was observed, along with good to full conversion (entries 8-10).

4.3.5. Variation of the 2,5-substituents of the cyclopentadienone ring

In agreement with our initial plan, 2,5-substituents of the cyclopentadienone ring might also influence the transmission of stereochemical information and affect the catalytic performance of the iron complex. For this reason, the modification of pre-catalyst **85** was taken into consideration by replacing the TMS groups in the 2,5-positions with other groups, such as:

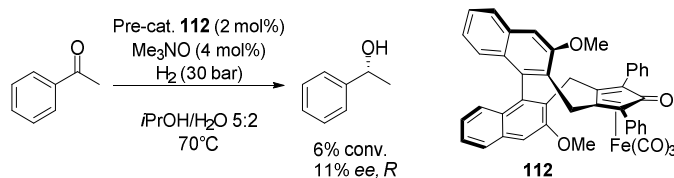
- TIPS (triisopropylsilyl ether) groups: increased steric bulk compared to TMS;
- flat phenyl groups, which in principle could allow to install bulky 3,3''-substituents by cross-coupling reaction;
- the removal of any substituents from the 2,5-positions.

To realize these modifications the synthesis of the cyclative carbonylation precursors was realized starting from the previously synthesized bis-iodide **95**, which was reacted with different ethynyl-lithium compounds in an analogous way described before (Scheme 88). Upon treatment of **95** with [(TIPS)ethynyl]lithium and [(phenyl)ethynyl]lithium, the new diyne compounds **109** and **110** were isolated in good yield. Unfortunately, the subsequent cyclization of the TIPS derivative **111** using $\text{Fe}_2(\text{CO})_9$ led to no conversion, probably due to the excessive steric bulk of the TIPS groups. In contrast, the 2,5-bis-phenyl-substituted derivative **110** was complexed in good yield to obtain **112**. The 2,5-unsubstituted complex, was obtained by removing the TMS groups from diyne **96**, using sodium carbonate in methanol, obtaining quantitative conversion to diyne **113**, which unfortunately underwent degradation during the cyclization conditions.



Scheme 88. Synthesis of complex **85** analogs modified at the 2,5-positions of the cyclopentadienone ring

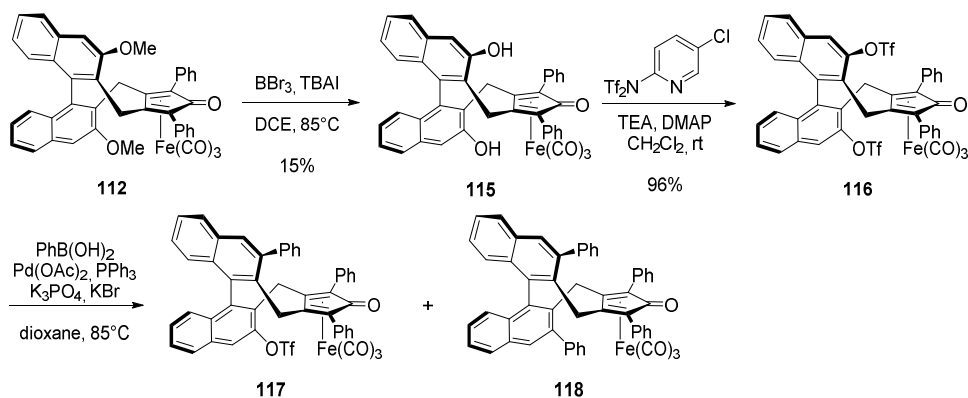
The new complex **112** was tested in the AH of acetophenone, applying our optimized conditions for **85** (Scheme 89).



Scheme 89. Test of pre-catalyst **112 in the asymmetric hydrogenation of acetophenone**

To our surprise, the new pre-catalyst **112** showed very low catalytic activity. Only 6% of the substrate was converted to (*R*)-phenylethanol, with only 11% *ee*. A possible explanation might be that the phenyl groups are not bulky enough to prevent dimerization of the activated hydride of **112**, which could lead to a decomposition as reported by Guan and co-workers for a related iron complex.^[159] Additionally, computational studies on a related achiral (cyclopentadienone)iron complex with 2,5-phenyl groups, confirmed that phenyl groups lead to an increase of the activation energy of the hydrogenation process.^{[117b][160]}

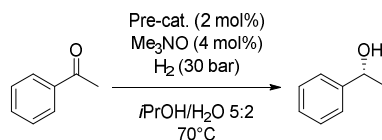
Even after these negative result, we still decided to try to install 3,3'-phenyl substituents and to verify if bulky 2,5-TMS groups were really interfering with the Suzuki-Miyaura cross-coupling or not. The deprotection of complex **112** at room temperature in the presence of BBr_3 proceed slowly and after 3 days of reflux, only a small amount of the desired product was obtained (15% yield), thus suggesting that, the TMS groups exert also some stabilizing effect on the cyclopentadienone ring, contrary to the phenyl groups. Complex **115** was converted to the corresponding triflate **116** using the Comin's reagent, and subjected to the cross-coupling with phenylboronic acid under the best conditions previously reported, reaching a mixture of mono and bis-substituted products **117** and **118**. This result proved that, together with the $\text{Fe}(\text{CO})_3$, also the bulky TMS substituents interfered with the Suzuki-Miyaura coupling because the cross-coupling occur in both side of the molecule in the presence of flat phenyl groups, even though the reaction was very sluggish.



Scheme 90. Synthesis of 3,3'-bis(phenyl)cyclopentadienone iron complex 118

The catalytic activity of complexes **112**, **117** and **118** in the AH of acetophenone was studied (Table 10).

Table 10. Screening of pre-catalyst 112, 117 and 118 in the asymmetric hydrogenation of acetophenone^[a]



Entry	Pre-cat.	Substituents	Conv. (%) ^[b]	ee (%) ^[c,d]
1	112	OMe	6	11, <i>R</i>
2	117	Mono-Ph	10	16, <i>R</i>
3	118	Bis-Ph	20	24, <i>R</i>

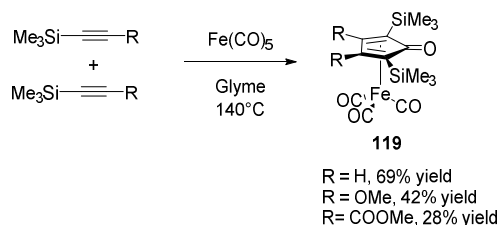
[a] Reaction conditions: substrate/Pre-cat./Me₃NO = 100:2:4, *P*(H₂) = 30 bar, solvent = 5:2 *i*PrOH/H₂O, *C*_{0,substrate} = 1.43 M, *T* = 70 °C, reaction time = 18 h. [b] Determined by GC equipped with a chiral capillary column (MEGADEX DACTBSβ, diacetyl-*t*-butylsilyl-β-cyclodextrin). [c] Absolute configuration is *S* (assigned by comparison of the optical rotation sign with literature data)^[147]

In comparison to the bis-methoxy pre-catalyst bearing two phenyl groups at the 2,5-positions of the cyclopentadienone (complex **112**), both new catalysts **117** and **118** revealed increased catalytic activity. The best result was obtained with **118**, with 20% conversion and 24% *ee*, while **117**, showed lower conversion (10%) and 16% *ee*. Interestingly, complexes with 2,5-TMS substituents (**85**, **86**, **97-104**) produce the (*S*)-phenylethanol, while 2,5-phenyl substituted pre-catalyst (**112**, **117**, **118**) led to the (*R*)-enantiomer. The inversion in the stereochemical preference demonstrated that 2,5-substituents on the cyclopentadienone play an important role in the transmission of the stereochemical information to the substrate.

4.4. Towards planar chirality

As already mentioned, the family of (cyclopentadienone)iron tricarbonyl complexes has gained increasing interest in the last few years. It should be underlined that (cyclopentadienone)iron complexes are usually synthesized by one-pot tethered cyclative carbonylation of diynes with large excesses of iron pentacarbonyl, $\text{Fe}(\text{CO})_5$ or diiron nonacarbonyl $\text{Fe}_2(\text{CO})_9$, which results in concomitant complexation of the iron tricarbonyl moiety (Figure 15, paragraph 17). This approach requires a significant synthetic effort to obtain the diyne precursor with the proper functionalization, thus somehow limiting the possibility to tune the substitution pattern at the cyclopentadienone ring that allowed only for the same substituents at the 2,5- and 3,4-positions respectively.

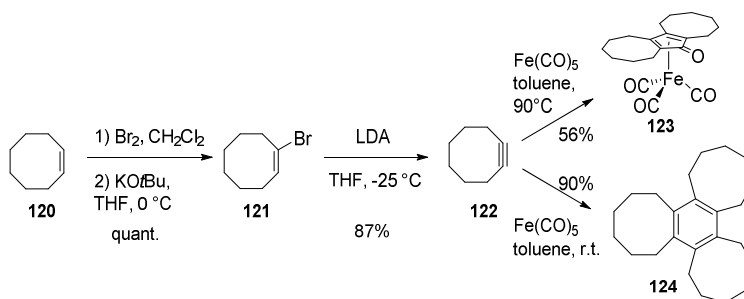
In principle, an intermolecular cyclative carbonylation/complexation could also be envisioned, starting from two discrete alkynes in the presence of the iron carbonyl reagent [$\text{Fe}(\text{CO})_5$ or $\text{Fe}_2(\text{CO})_9$]. However, this approach has a limited scope, as it has been reported to occur in good yields only when very specific types of substituents on the alkyne, such as silyl groups^[104a] or some substituents (e.g., Cl, *Ot*Bu and CF_3) were employed.^[161] Additionally it is important to report that the reaction of trimethylsilylacetylene with an iron source at 140 °C provides just the 2,5-bistrimethylsilylsubstituted(cyclopentadienone)iron tricarbonyl complex (Scheme 91). Very low yields (< 15%) were reported for the cyclization of more common alkynes such as, phenylacetylene and diphenylacetylene.^[162]



Scheme 91. Intermolecular cyclative carbonylation/complexation

Cyclooctyne, the smallest isolated cyclic alkyne, is known to be very reactive, undergoing degradation upon prolonged standing. The compound is not commercially available, but can be easily synthesized in very good yields starting from cyclooctene (Scheme 92):^[163] first the alkene is brominated with Br_2 to form the corresponding 1,2-dibromoalkane. This compound is not isolated but directly treated with *KOt*Bu to yield 1-bromocyclooctene **121** by the elimination of HBr. This vinylbromide is isolated and purified by distillation. Then, a second elimination in the presence of LDA allows to obtain the desired alkyne **123**. According to the literature, when cyclooctyne **123** was reacted with Ni, W, Co and Fe carbonyl complexes,^{[164][165][166]} several

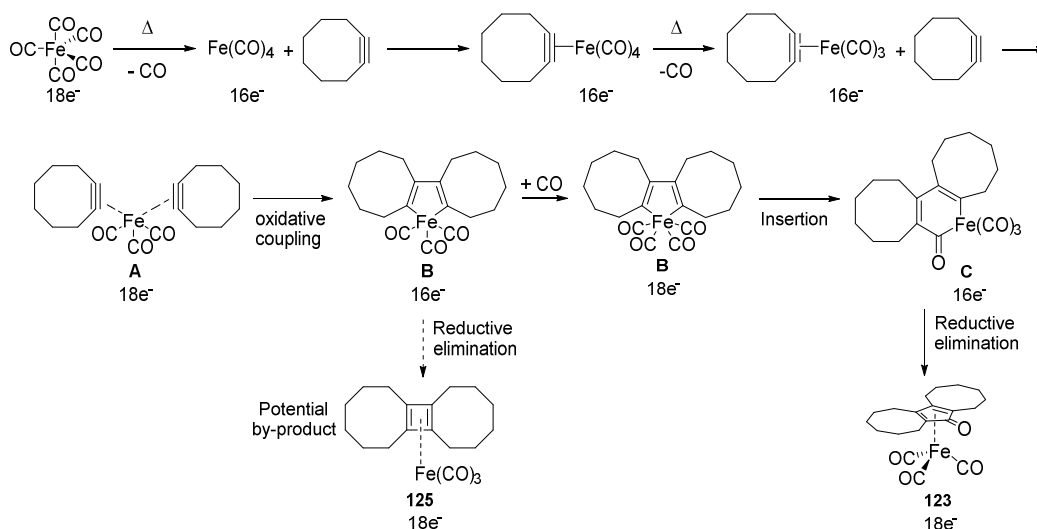
products were isolated, among which, in the case of iron, substantial amounts of tris(hexamethylene)benzene **124** (derived from the cyclotrimerization of the alkyne), and minor quantities of the [bis(hexamethylene)cyclopentadienone]iron complex **123** (Scheme 92). This peculiar behavior raised our attention, and induced us to investigate the reaction, in order to optimize the formation of complex **123**. The cyclative carbonylation of cyclooctyne was then performed in toluene using $\text{Fe}(\text{CO})_5$ under careful control of the temperature. Much to our delight, the reaction at 90 °C afforded complex **123** in a respectable 56% yield. This temperature proved to be optimal and crucial in order to minimize the formation of the trimerization product **124**, and 90 °C seems to be the optimal value. Indeed, when the reaction was performed at r.t., **124** was the only product observed, but also increasing temperature to 110 °C led to an increased formation of trimer at the expense of the desired complex **123**, which was obtained in only 45% yield.



Scheme 92. Synthesis of the [bis(hexamethylene)cyclopentadienone]iron tricarbonyl complex **123**

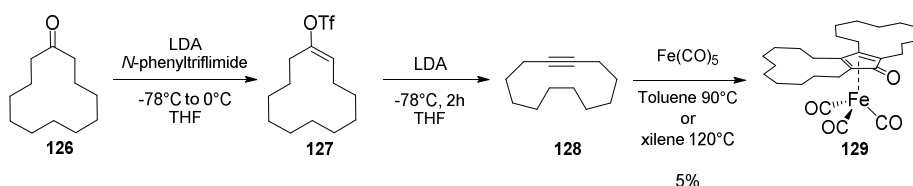
The proposed mechanism for the formation of **123** (Scheme 93) consists of a stepwise iron mediated [2+2+1] cycloaddition,^{[104][105][167][168][169]} which is initiated by the sequential replacement of two carbon monoxides ligands by the two alkyne molecules thus generating the (bis- η^2 -alkyne)iron tricarbonyl complex **A**. At this stage, iron(0) promotes the oxidative coupling of the two bound alkynes to form the intermediate ferrocyclopentadiene structure **B**. Insertion of a molecule of carbon monoxide into the iron-carbon bond followed by a subsequent rearrangement of the ferrohexasdienone structure **C** affords the tricarbonyliron-complexed cyclopentadienone **123**.

On the other hand the iron cyclobutadiene complex **125**, which is a known side-product as reported by Wittig during the use of NiBr_2 ^[166] was never observed in our case.



Scheme 93. Proposed mechanism for the formation of complex **123** in a [2+2+1]cycloaddition

Release of the ring strain of cyclooctyne probably plays an important role in facilitating the intermolecular cyclative carbonylation/complexation process. To confirm this hypothesis, we subjected cyclododecyne **128**, prepared starting from the cyclododecanone **120**,^[170] which mainly differs from cyclooctyne for lesser ring strain, to the same reaction conditions adopted for the synthesis of **123** (Scheme 94). As expected, the reaction of compound **128** in the presence of Fe(CO)_5 afforded the desired complex **129** only in very poor yield (5%), and no improvement could be obtained by changing the solvent (toluene, xylene) or increasing the reaction temperature. In this case, no trimerization product was observed and it was possible to recover the cyclododecyne.



Scheme 94. The low-yielding synthesis of [bis(decamethylene)cyclopentadienone]iron tricarbonyl complex **129**

Complex **123** was thoroughly characterized spectroscopically, and crystals suitable for X-ray diffraction analysis could be grown by cooling a saturated solution of the [bis(hexamethylene)-cyclopentadienone]iron complex **123** in *n*hexane/ CH_2Cl_2 . The X-ray structure reveals the usual piano-stool geometry with a certain degree of flexibility (Figure 28).

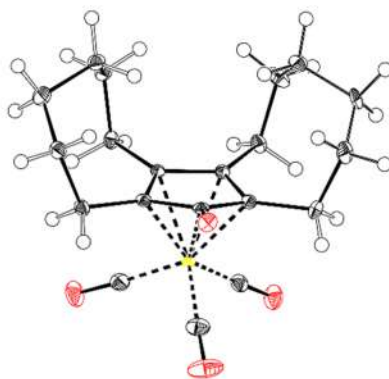
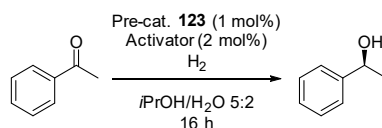


Figure 28. ORTEP diagram (CCDC 1511079) of the molecular structure of the [bis(hexamethylene)cyclopentadienone]iron complex **123**

4.4.1. Catalytic test with the new [bis(hexamethylene)cyclopentadienone]iron tricarbonyl complex

The [bis(hexamethylene)cyclopentadienone]iron tricarbonyl **123** was tested in the reduction of ketones by hydrogenation and transfer hydrogenation.

Table 11. Test of pre-catalyst **123** in the hydrogenation of acetophenone and screening of different activators^[a]



Entry	Activator	P (H_2) [bar]	T [$^{\circ}C$]	Conv. [%] ^[b]
1	K_2CO_3	10	70	< 5
2	$h\nu$ ^[c]	10	40	> 99
3	Me_3NO	10	70	52
4	K_2CO_3	30	70	51
5	Me_3NO	30	70	> 99

[a] Reaction conditions: Substrate/Pre-cat. **123**/activator = 100:1:2, solvent: 5:2 *i*PrOH/ H_2O , $C_{0,substrate}$ = 1.43 M, reaction time = 16 h. [b] Determined by GC equipped with a chiral capillary column (MEGADEX DACTBS β , diacetyl-*t*-butylsilyl- β -cyclodextrin). [c] Reaction vessel irradiated at λ_{max} = 352 nm and 8 W; solvent = toluene, Substrate/Pre-cat. **123** = 20:1, $C_{0,substrate}$ = 0.047 M.

We firstly screened the known methodologies for the *in situ* activation of the pre-catalyst (Table 11). Use of K_2CO_3 (in situ Hieber reaction) only led to a moderate conversion (Table 11, entry 1), while the other activation strategies (entries 2-3) were more successful: photolysis of a CO ligand by UV irradiation yielded full conversion, and oxidative cleavage with Me_3NO gave 52% conversion.

Increasing the hydrogen pressure to 30 bar, the conversion grew to 51% in the presence of K_2CO_3 (entry 4) and to completeness in the presence of Me_3NO (entry 5).

A substrate scope screening of pre-catalyst **123** was then performed adopting the activation protocol with Me_3NO , which is compatible with standard hydrogenation equipment as it does not require UV irradiation.

Table 12. Substrate screening for the hydrogenation of ketones in the presence of pre-catalyst **123^[a]**

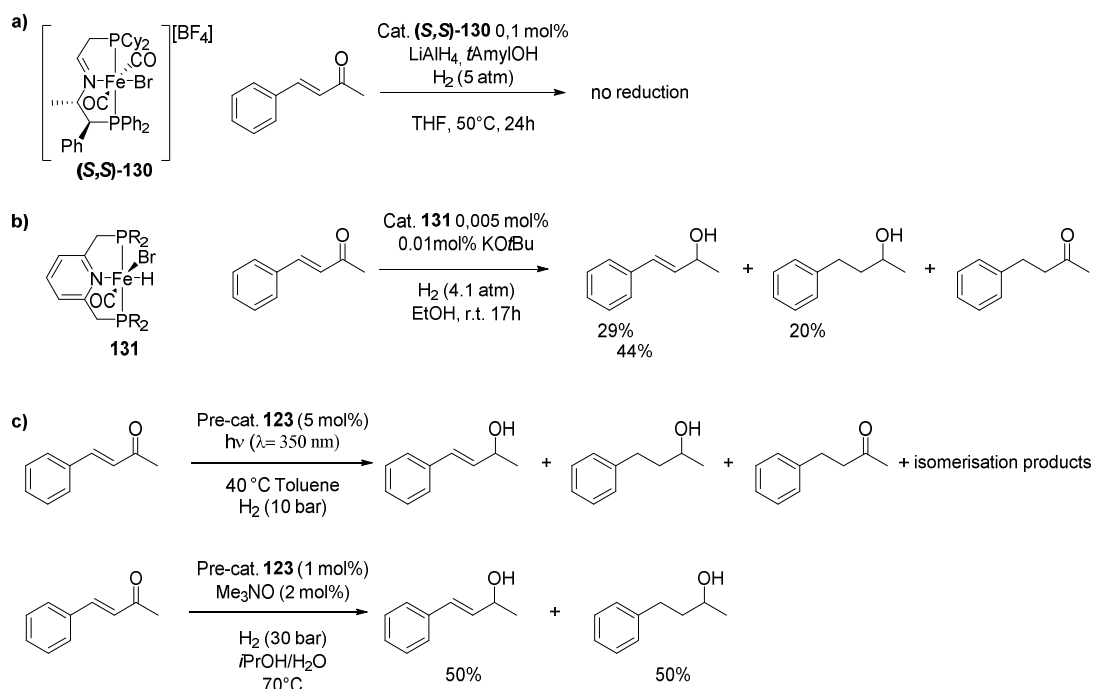
Entry	Substrate	Conv. [%] ^[b]	Entry	Substrate	Conv. [%] ^[b]
1		> 99 (98) ^[c]	10		> 99
2		> 99	11		15
3		> 99 (98) ^[c]	12		> 99 <i>cis</i> : <i>trans</i> = 60:40
4		> 99 (98) ^[c]	13		> 99 (94) ^[c]
5		> 99	14		> 99 (86) ^[c]
6		> 99	15	$C_{10}H_{21}CHO$	> 99
7		> 99	16		> 99 ^[d]
8		80	17		99
9		> 99	18		No reduction
			19	$Ph-C\equiv C-Ph$	No reduction

[a] Reaction conditions: substrate/Pre-cat. **123**/ Me_3NO = 100:1:2, $P(H_2)$ = 30 bar, solvent: 5:2 *i*PrOH/ H_2O , $C_{0,substrate}$ = 1.43 M, T = 70 °C, reaction time = 16 h. [b] Determined by 1H -NMR of the crude reaction mixture. [c] isolated yield; the reactions were carried out on a 2 mmol scale following the General Procedure (paragraph 6.8.1).

Several 4-, 3- and 2-substituted acetophenones were fully hydrogenated (Table 2, entries 2-6), regardless of the electron withdrawing or electron donating nature of the substituent. Notably, reducible groups such as carbon-halogen bonds (entries 4 and 6) or nitro group (entry 2) were not affected under the reaction conditions. 2-Acetylpyridine (entry 7) was also hydrogenated with full conversion, despite the presence of a coordinating nitrogen atom that - in principle - could poison the catalyst. α -Tetralone (entry 8) was the only aryl ketone to be hydrogenated with less than quantitative yield. Aliphatic ketones (entries 9-12) showed quantitative conversion with the exception of isophorone (entry 11). An α,β -unsaturated ketone was hydrogenated with only 15% yield. Despite the low conversion, it should be remarked that there was full selectivity for the C=O bond. No competing reduction of the conjugated C=C double bond was observed. Quite expectedly, the aldehyde substrates (entries 13-16) were smoothly hydrogenated to the corresponding alcohols. In the case of cinnamaldehyde (entry 16), some 3-phenyl-1-propanol (from reduction of both C=O and C=C) was also obtained, together with the expected cinnamyl alcohol. An activated ester (entry 17) was also hydrogenated to the corresponding alcohol with full conversion. As a limitation, alkynes (entry 19) and amides (entry 18) appear not to be suitable substrates, consistent with what was reported for the other Knölker-Casey-type complexes.^[116]

In addition, we tried to reduce benzalacetone in a selective way. The use of UV irradiation led to a mixture of hydrogenated product and isomerization products, while the use of Me₃NO produced a 1:1 mixture of 4-phenyl-3-buten-2-ol (from C=O reduction) and 4-phenylbutan-2-ol (from reduction of both C=O and C=C). Even though this reduction is not chemoselective, it can be considered a good result when compared to the data reported by Morris and co-workers^[90] employing a iron-pincer complex (**S,S**)-**130**, where no conversion was observed after 24 h, or the one reported by Milstein,^[171] **131** where a mixture of hydrogenated products were shown. For the (cyclopentadienone)iron tricarbonyl complexes, Beller reported just the hydrogenation of α,β -unsaturated aldehydes with very high efficiency for the selective reduction of the carbonyl moiety.^[114] As – in a control experiment – 4-phenyl-3-buten-2-ol itself did not react at all under the same experimental conditions, we assume that 4-phenylbutan-2-ol was formed by 1,4-reduction of benzalacetone followed by hydrogenation of the C=O double bond.

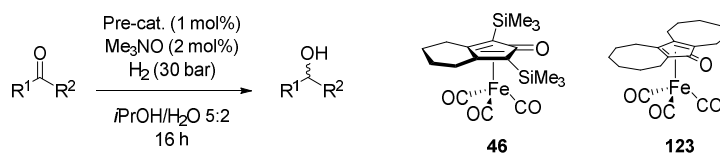
The amount of over-reduction product (5%) was much lower in the case of the corresponding α,β -unsaturated aldehyde (entry 16) respective to the benzalacetone (Scheme 95). This difference is explained by the fact that – in the case of entry 16 – 1,2-reduction of C=O competes more efficiently with the 1,4-reduction pathway due to the higher reactivity of the aldehyde compared to the keto group.



Scheme 95. Reduction of benzalacetone using: (a) Morris catalyst (S,S)-130; b) Milstein catalyst 131 and c) pre-catalyst 123 under UV irradiation or Me₃NO as activators.

After these results we decided to compare the catalytic activity of the [bis(hexamethylene)cyclopentadienone]iron tricarbonyl complex **123** to the “classical” (cyclopentadienone)iron complex **46** in the hydrogenation of acetophenone at low catalyst loading (0.1 mol%). As can be seen in Table 13, higher turnover numbers (TON) and turnover frequencies (TOF) were observed for complex **123** compared to **46**.

Table 13. Comparison between complexes **46** and **123** in the hydrogenation of acetophenone^[a]



Entry	Pre-cat.	Conv. [%]	TON	TOF [h ⁻¹]
1	46	13	130	7.5
2	123	62	620	35.9

[a] C₀, substrate = 1.429 M, substrate/Pre-cat./Me₃NO = 100:0.1:0.2, P(H₂) = 30 bar, T = 70 °C, 17 h, solvent = 5:2 iPrOH/H₂O.

Such a remarkable difference in terms of activity prompted us to evaluate the kinetics of the acetophenone hydrogenation in the presence of pre-catalysts **46** and **123** (activated with Me₃NO).

The conversions were calculated from the hydrogen uptake, measured with a computer-controlled Parr autoclave system, shown in Figure 29.

As can be seen in Figure 29, in the initial part of the two experiments ($t < 20$ min) the *in situ* formed complexes **46** and **123** showed similar activity, with typical pseudo-first order kinetic profiles. However, after about 20 min the two catalysts started behaving very differently: while the **123**-derived catalyst went on following pseudo-first order kinetics (Figure 29, blue diamonds \blacklozenge), the **46**-catalyzed reaction slowed down (Figure 29, red squares \blacksquare) and then proceeded until completion at reduced rate. These findings seem to suggest that the “classical” **46**-derived catalyst undergoes rather fast decomposition,^[159] so that most of it is transformed into a less active or inactive species before the hydrogenation of the acetophenone is complete. On the contrary, the catalyst derived from the new [bis(hexamethylene)cyclopentadienone]iron complex **123** seems to be more robust and does not undergo substantial decomposition before the hydrogenation is finished. The lower stability of catalyst **46** would also explain the lower TON, TOF and conversion obtained with the former at 0.1 mol% catalytic loading (Table 13).

Table 14. Kinetic parameters of the hydrogenation of acetophenone in the presence of pre-catalysts **46** and **123** after short reaction time ($t < 20$ min)^[a]

Entry	Pre-cat.	k_{app} [min^{-1}] ^[b]	$t_{1/2}$ [min]	k [$\text{L mol}^{-1} \text{min}^{-1}$] ^[b]
1	46	0.040	17.5	7.9
2	123	0.036	19.3	7.2

[a] Substrate/pre-cat./ Me_3NO = 100:1:2; solvent: 5:2 *i*PrOH/ H_2O ; $C_{0, \text{substrate}}$ = 0.501 M; $P(\text{H}_2)$ = 30 bar; $C_{\text{cat.}}$ = 5 mM. [b] $k_{app} = k \cdot C_{\text{cat.}}$

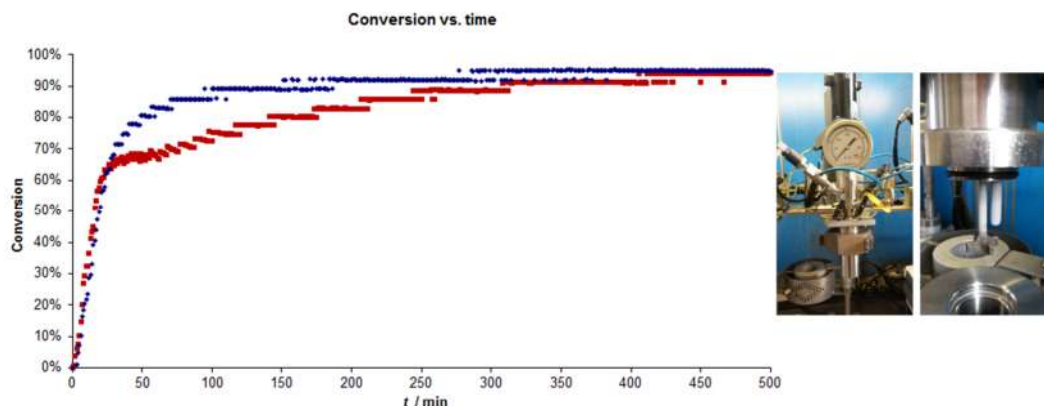
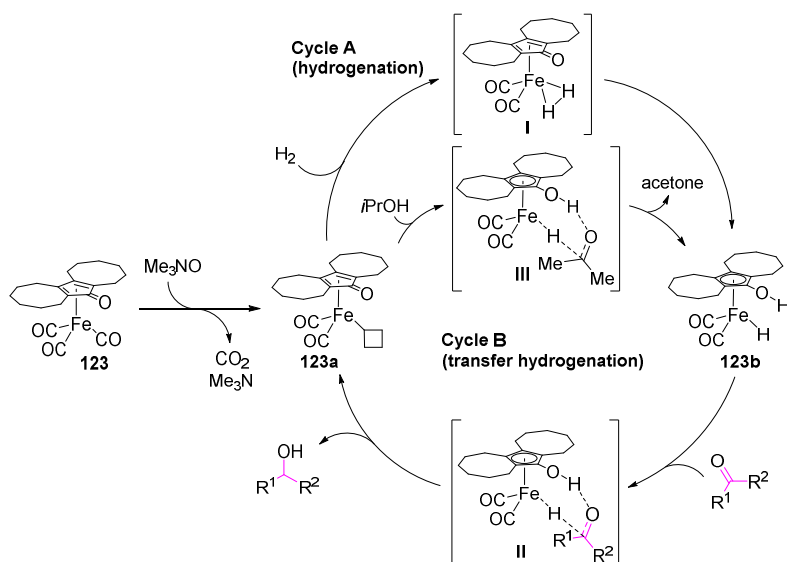


Figure 29. Kinetics of acetophenone hydrogenation promoted by pre-catalyst **46** (\blacksquare) and **123** (\blacklozenge) activated with Me_3NO . Reaction conditions: Substrate/Pre-cat./ Me_3NO = 100:1:2; solvent: 5:2 *i*PrOH/ H_2O ; $C_{0, \text{substrate}}$ = 0.501 M; P_{H_2} = 30 bar; T = 70 °C; $C_{\text{cat.}}$ = 5 mM

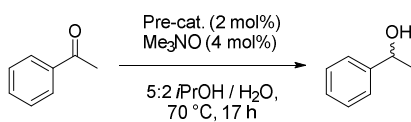
The proposed mechanism for the hydrogenation of acetophenone, shown in Scheme 96 (Cycle A), is the one commonly accepted for Knölker-Casey catalysts:^{[107][135]} after the activation of pre-catalyst **123** by de-coordination of one CO ligand, the active species **123a** splits H₂ generating the (hydroxycyclopentadienyl)iron complex **123b**. The latter reacts with the substrate through a concerted pericyclic transition state (II), forming complex **123a** together with the reaction product.



Scheme 96. Proposed mechanism for ketones hydrogenation (Cycle A) and transfer hydrogenation (Cycle B) promoted by complex **123** activated with Me₃NO

Casey and Guan reported that the isolated (hydroxycyclopentadienyl)iron complex **47** is also able to catalyze the transfer hydrogenation of acetophenone with *i*PrOH.^[107] We thus tested the (cyclopentadienone)iron complex **46** and our new [bis(hexamethylene)cyclopentadienone]iron complex **123**, activated in situ with Me₃NO, in this reaction (Table 15).

Table 15. Transfer hydrogenation of acetophenone with *i*PrOH of pre-catalysts **123** and **46**^[a]



Entry	Pre-cat.	Conv. [%] ^[b]
1	46	34
2	123	90

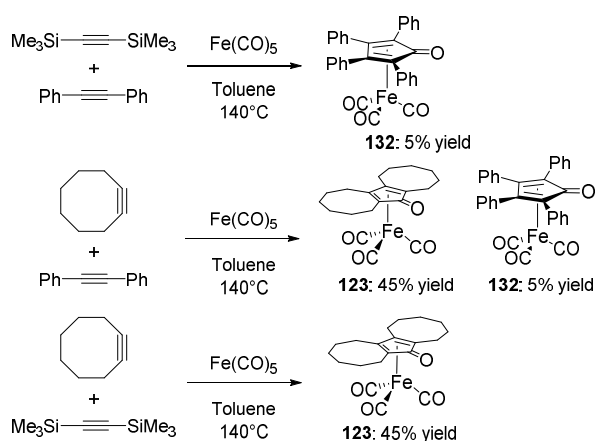
[a] Substrate/Pre-cat./Me₃NO = 100:2:4, *c*_{0, substrate} = 0.7 M, 70 °C, 17 h, solvent: 5:2 *i*PrOH/H₂O. [b] Determined by GC equipped with a chiral capillary column (MEGADEX DACTBSβ, diacetyl-*t*-butylsilyl-β-cyclodextrin).

Just as observed in the classical hydrogenation, pre-catalyst **123** was found more active than the “Knölker complex” **46**: while only moderate conversion was obtained in the presence of the latter complex (Table 15, entry 1), use of pre-catalyst **123** allowed to obtain almost full conversion (Table 15, entry 2).

This finding is in agreement with the hypothesis that mechanism and active catalytic species are similar to those of the hydrogenation: as shown in Scheme 96 (Cycle B), first the active complex **123a** dehydrogenates *i*PrOH (through the pericyclic transition state III) forming the hydride **123b**, then the latter reduces the substrate (through transition state II).

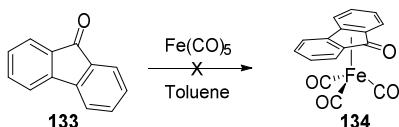
4.5. Synthesis of a planar chiral (cyclopentadienone)iron tricarbonyl complex

Having shown that complexes bearing different substituents than silylated groups at positions 2,5 can indeed yield active catalysts for the hydrogenation of ketones by choosing an appropriate substituent pattern, we decided to explore intermolecular cyclizations using combinations of different alkynes in the presence of $\text{Fe}(\text{CO})_5$ to obtain complexes devoid of planar symmetry, and therefore chiral, as a different approach to enantioselective Knölker-Casey catalysts (Scheme 97). Different combinations were investigated combining diphenylacetylene, bis-trimethylsilylacetylene and cyclooctyne, but unfortunately none of them afforded the mixed complex (with two different substituents at positions 2 and 5): the combinations of cyclooctyne afforded mainly complex **123**, the [bis(hexamethylene)cyclopentadienone]iron tricarbonyl previously described, and in the case of diphenylacetylene minute amounts of the (tetraphenyl)cyclopentadienone iron complex **132**, already known in literature were also formed.



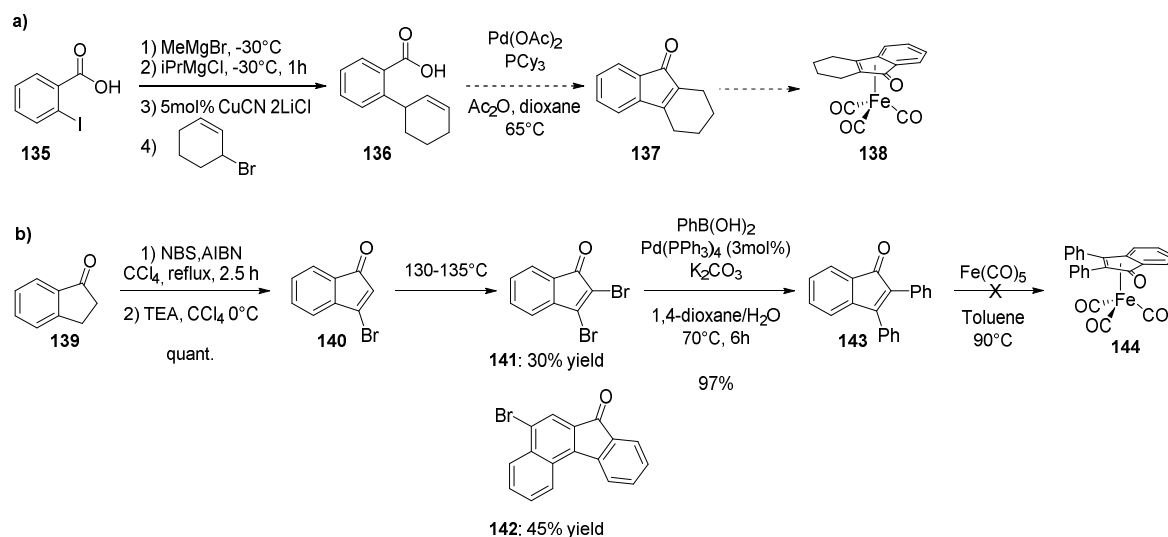
Scheme 97. Attempts of intermolecular cyclative/carbonylation using different alkynes

An alternative way to obtain cyclopentadienone complexes is the complexation of a cyclopentadienone with an iron source. For this reason, we thought that using fluorenone as a starting point might be a reasonable idea: it is commercially available and it can be easily brominated in the 2,7-positions using $\text{Br}_2/\text{H}_2\text{O}$ at 90°C ,^[172] in this way various substituents could have been installed. Unfortunately, when we tried to complex fluorenone with $\text{Fe}(\text{CO})_5$, we just recovered the starting material (Scheme 98), probably due to the presence of two aromatic rings, which delocalize the charge.



Scheme 98. Attempts directed towards the complexation of fluorenone

After this trial, we decided to focus our attention on different ligands: **137** and **143**. In the first case (Scheme 99a) the synthesis starts from the 2-iodobenzoic acid **135**, which reacts in an acyl Heck-Heck reaction with allylbromide to give 3-bromo-cyclohex-1-ene (**136**). Unfortunately, we were not able to isolate the desired ligand in the following step, 3,4-dihydro-1H-fluoren-9(2H)-one **137**, even after changing the Pd source or working under anhydrous conditions.^[173]



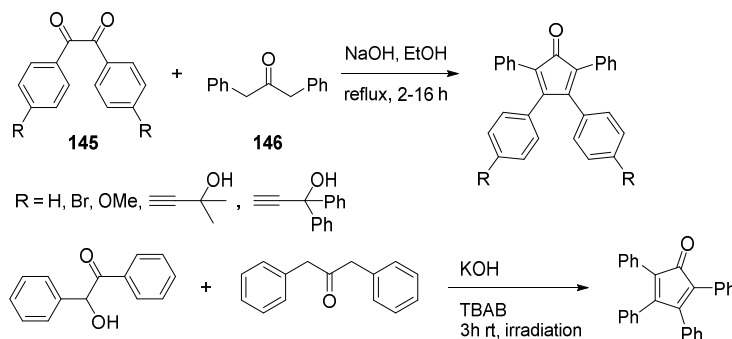
Scheme 99. Attempts directed towards the synthesis of complexes 138 and 144 starting from ligands 137 and 143

In the second synthesis in Scheme 99b, 1-indanone (**139**) was brominated to 3-bromoindenone **140**, which was subjected to a thermal decomposition to give the desired product **141**, 2,3-dibromoindenone, and a side product **142**, identified as 5-bromo-7-benzo-fluorenone.^[175]

Compound **141**, was subjected to a Suzuki-Miyaura cross-coupling to afford the 2,3-diphenylindenone **143** in 97% yield.^[176] Fatefully, when we tried to form the iron complex, we recovered just the starting material. After these attempts we concluded that even one aromatic ring on the cyclopentadienone was enough to avoid the complexation using $\text{Fe}(\text{CO})_5$.

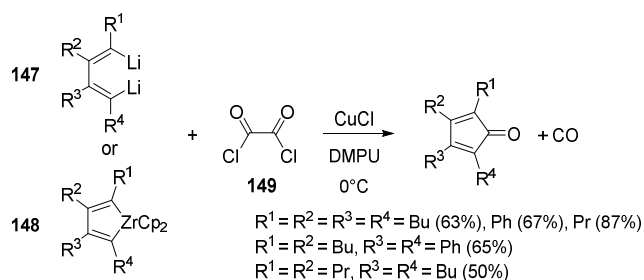
It should be noted that only few methods for the synthesis of cyclopentadienones are known in the literature. The most common synthetic route to tetraarylcyclopentadienones involves the reaction of diaryl- α -diketones **145** (obtained by benzoin condensation of benzaldehydes followed by oxidation), with diphenylacetone **146** in the presence of KOH or NaOH, in refluxing EtOH for variable reaction times depending on the substituents (2-16 h).^[177]

Recently, a microwave-assisted condensation was developed, with consequent reduction of solvent and reaction time which goes from 2-16 h to 25 min under microwave heating.^[178]

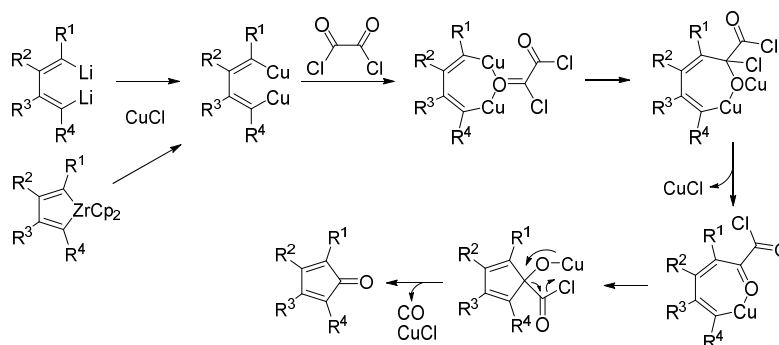


Scheme 100. Synthesis of tetraarylcyclopentadienones starting from diaryl- α -diketones and diphenylacetone

Another approach (Scheme 101) is the 1,1-cycloaddition of oxalyl chloride (**149**) with 1,4-dilithio-1,3-dienes (**147**) or zirconcyclopentadienes (**148**), which forms the cyclopentadienone derivatives in the presence of CuCl (2 eq.). During the nucleophilic addition step the C-C bond of 1,2-dicarbonyl is cleaved. The mechanism of the reaction is shown in Scheme 102, which suggests the formation of a chelated intermediate.^[179]

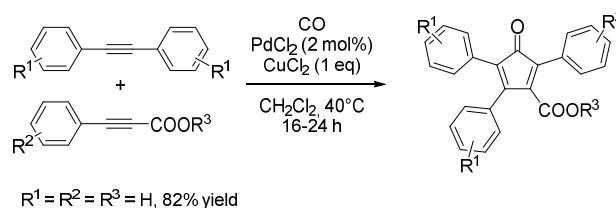


Scheme 101. 1,1-cycloaddition of oxalyl chloride with 1,4-dilithio-1,3-dienes or zirconcyclopentadienes



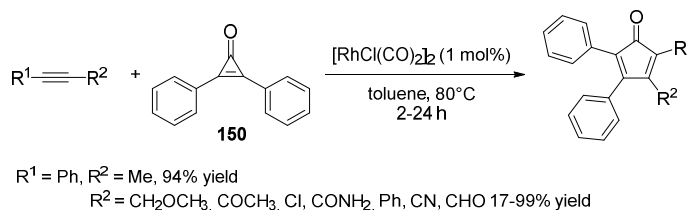
Scheme 102. Proposed mechanism for the 1,1-cycloaddition

A palladium-catalyzed [2+2+1] cyclocarbonylation of alkynes, under atmospheric pressure of carbon monoxide is reported in Scheme 103. The transformation is carried out under mild conditions and ligand-free conditions.^[180]



Scheme 103. A palladium-catalyzed [2+2+1] cyclocarbonylation of alkynes

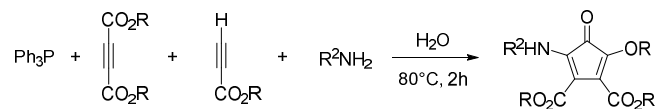
A different approach, reported in literature and shown in Scheme 104, involves the use of cyclopropenones, as excellent 3-carbon components in Rh(I)-catalyzed [3 + 2] cycloadditions with a wide range of alkynes, providing cyclopentadienones in a selectively way and high yield.^[181] This Rh(I)-catalyzed [3 + 2] cycloaddition tolerates a broad range of aryl alkyne substituents: methyl-, methoxymethyl-, methyl ketone-, chloride-, and amide-functionalized phenylacetylenes. All react efficiently and regioselectively. Free alcohol, nitrile, aldehyde, and even 1,3-diyne moieties also react to provide cyclopentadienones with high regioselectivity.



Scheme 104. Rh(I)-catalyzed [3 + 2] cycloadditions between cyclopropenones and alkynes

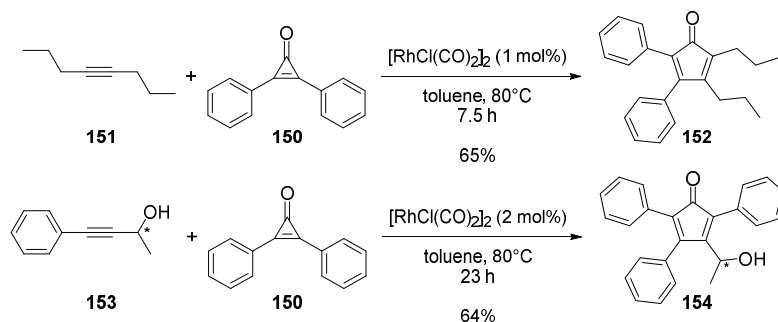
More recently a water-accelerated multicomponent synthesis has been used as a key method for the preparation of cyclopentadienone derivatives, the three component condensation reactions

of primary amines with alkyl propiolates in the presence of triphenylphosphine in water at 80 °C formed the 4-oxo-2,5-cyclopentadiene-1,2-dicarboxylate derivatives (Scheme 105).^[182]



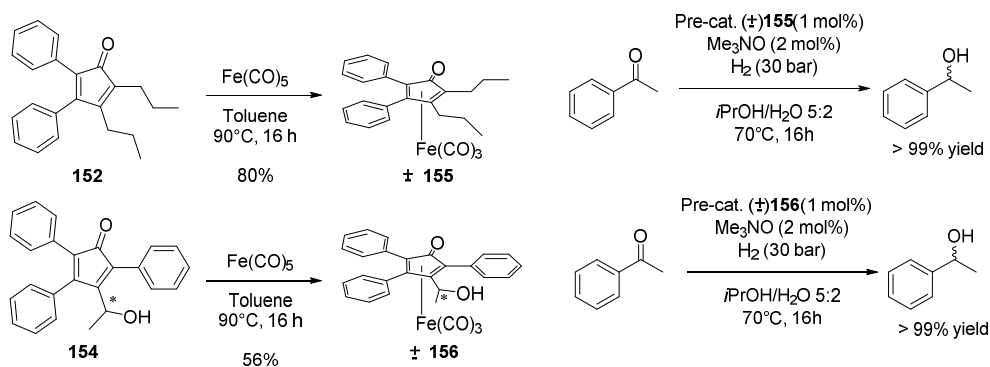
Scheme 105. Water-accelerated multicomponent synthesis

Following the synthesis reported by Wender and co-workers (Scheme 104),^[181] we were able to synthesize two new different cyclopentadienone ligands using $[\text{RhCl}(\text{CO})_2]_2$ in the presence of diphenylcyclopropanone **150** and an alkyne (Scheme 106). In particular, we decided to employ 4-octyne **151** to yield **152** in 65% yield and a propargylic alcohol, 4-phenyl-3-butyn-2-ol, **153** to afford **154** in similar yield (Scheme 106).



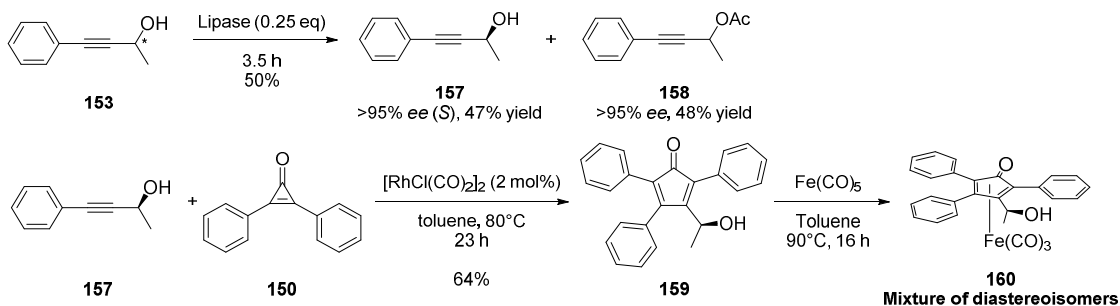
Scheme 106. Synthesis of cyclopentadienone 152 and 154

Complex **155** and **156** were synthesized in the presence of $\text{Fe}(\text{CO})_5$ in toluene at 90 °C (Scheme 107). These are the first examples of cyclopentadienone iron complexes with planar chirality. The early results in the hydrogenation reactions showed full conversion under the standard conditions, using Me_3NO as an activator.



Scheme 107. Synthesis and catalytic activity of two new planar chiral catalysts 155 and 156 (racemic mixtures)

Since compound **156** was reactive in the hydrogenation of acetophenone, we decided to proceed with the resolution of the alkynol, using an enantioselective esterification of a propargylic alcohol employing a lipase from *Pseudomonas* sp. (AK),^[183] in this way we obtained the final complex as a diastereoisomeric mixture (Scheme 108).



Scheme 108. Synthesis of a new planar chiral catalysts 160 (mixture of diastereoisomers)

Work is in progress to separate the racemates of **155** and **156**, and to establish a procedure to obtain a single diastereoisomer of **160**.

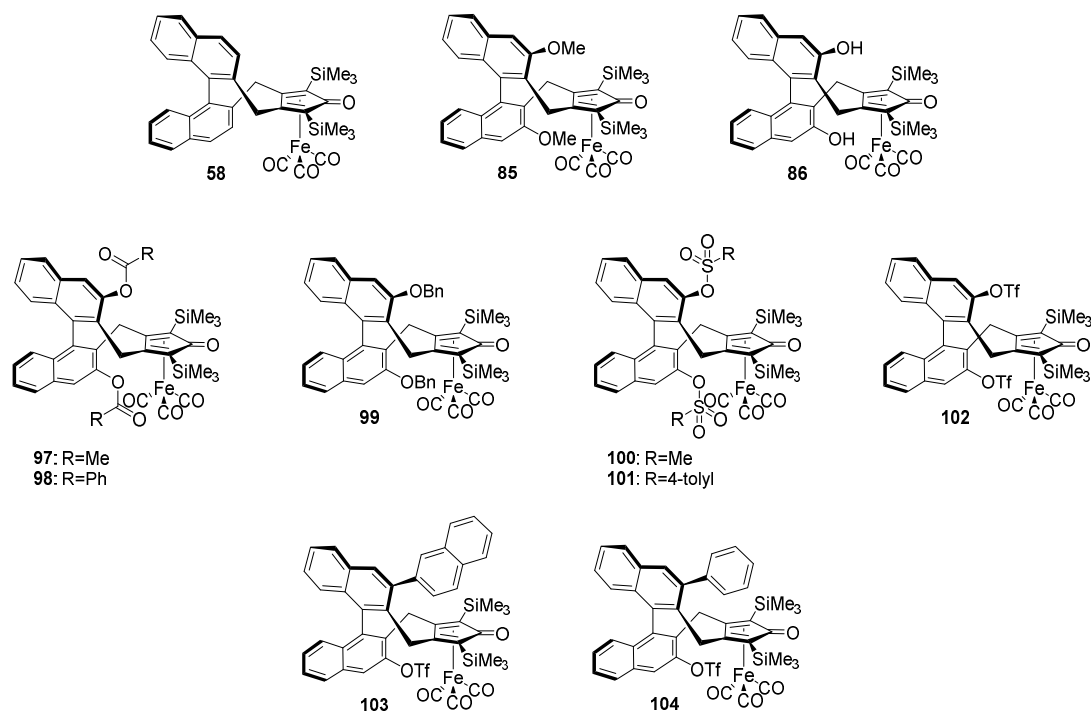
5. Conclusion and Outlook

My thesis was focused on finding new catalysts based on the most abundant transition metal – iron. In the last 20 years, this cheap and non-toxic metal has become the object of increasing interest in the scientific community, and remarkable progresses have been made in the development of iron catalyzed reactions. Despite these efforts there is still a lot of work to do to improve iron catalysts in order to become competitive with respect to the noble metal complexes. In fact, many of these iron catalysts are highly air- and/or moisture-sensitive, and their synthesis can be very difficult. In order for the homogeneous iron catalysts to become industrially relevant, more easy-to-prepare and stable catalysts have to be developed.

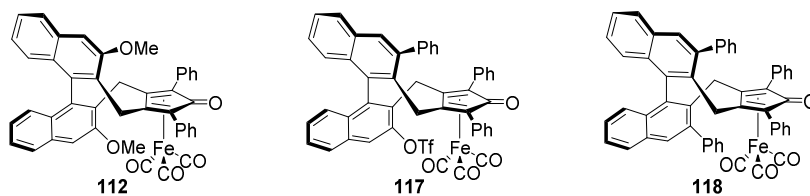
During my PhD work, I focused my attention on the synthesis and characterization of (cyclopentadienone)iron tricarbonyl complexes and their application to stereoselective catalytic transformations. We chose (cyclopentadienone)iron complexes, because these complexes have the advantage of being easily synthesized and stable to air, water and light, in contrast to other iron complexes used for homogenous asymmetric hydrogenation. These catalysts can be activated *in situ* by reaction with bases, Me₃NO or UV irradiation and converted into the active catalysts used for hydrogenation reaction, and this allowed to avoid the use of a glovebox.

My research started with the development of a new binaphthyl-derived chiral (cyclopentadienone)iron tricarbonyl complexes, which displayed high stability to air, moisture and chromatography. We started from the unsubstituted chiral complex, which was obtained in 6 steps from the (*R*)-BINOL, with an overall yield of 23%. The new complex **58** was tested in the hydrogenation of acetophenone, under the standard conditions reported by Beller, employing K₂CO₃, but very low enantiomeric excess was observed. We attribute this low *ee* to the remote position of the stereoaxis respective to the active center, and simple molecular models suggest that the presence of bulky 3,3'-substituents on the binaphthyl moiety can improve the level of the stereocontrol. We proceeded with the synthesis of a 3,3'-substituted version of the complex, and in particular, we decided to introduce a methoxy substituents. The synthesis, starting from the (*R*)-BINOL, required 11 steps but only 4 flash chromatography columns were necessary to achieve the pure complex **85** with an overall yield of 15%. The new methoxy-substituted complex catalyzes the asymmetric hydrogenation of ketones with better enantioselectivity (up to 77% *ee*) compared to any other reported chiral (cyclopentadienone)iron tricarbonyl complexes reported in literature.^{[117][118]} In fact this result was nearly three times higher than previously reported enantiomeric excess in the literature for chiral (cyclopentadienone)iron complexes.

As the obtained enantioselectivity increases with the steric bulk of the binaphthyl 3,3'-substituents, we focused our attention on the synthesis of new complexes with various 3,3'-substituents starting from the 3,3'-dihydroxy-substituted complex, which was prepared by demethylation of the methoxy substituted pre-cat. Using rather simple transformation, e.g. esterification, etherification, sulfonylation and triflation reactions, we prepared six complexes with different substituents at the 3,3'-positions on the binaphthyl moiety from the common hydroxy derived precursor. In this way, a library of chiral (cyclopentadienone)iron pre-catalysts was developed. In addition, a Suzuki-Miyaura cross-coupling on the bis-triflate derived complex to install bulky aryl group was performed, but unfortunately just the mono-coupling derived complexes were obtained. Substitution at the 3,3'-positions of the binaphthyl system affected both the activity and the enantioselectivity in an unclear manner, and the methoxy-substituted complex remained the best pre-catalyst.

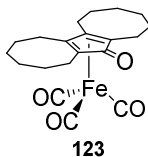


The synthesis of analogs of methoxy substituted compound featuring different substituents at the 2,5-positions of the cyclopentadienone ring was then undertaken, and the 2,5-bis(phenyl)-substituted compound was prepared. Compared to the methoxy substituted complex, the latter showed low catalytic activity and the opposite stereochemical preference in the asymmetric hydrogenation of acetophenone. This finding suggests that both the binaphthyl 3,3'-substituents and the cyclopentadienone 2,5-substituents of the new catalysts play a role in the transmission of the stereochemical information.

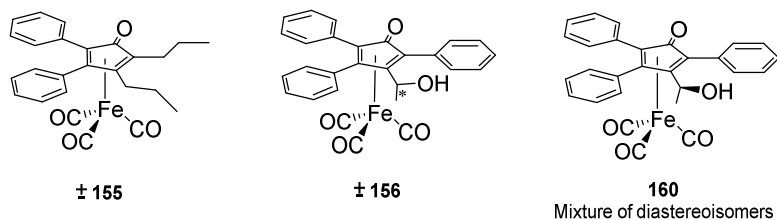


In addition we also synthesized and fully characterized a new [bis(hexamethylene)cyclopentadienone]iron tricarbonyl complex **123**. This new compound has been obtained in a preparatively useful yield (56%) by reaction of cyclooctyne with $\text{Fe}(\text{CO})_5$. The obtained yield is remarkable for this kind of intermolecular cyclative carbonylation/complexation, which usually gives good results only with a few, properly substituted alkynes.^{[104][161][162]}

The observed reactivity of cyclooctyne, the smallest cyclic alkyne, is probably due to ring strain, as suggested by the lack of reactivity of its unstrained higher homolog cyclododecyne during the cyclative carbonylation. The cyclooctyne-derived complex has been tested as pre-catalyst in the hydrogenation of ketones, in which, after activation with Me_3NO , it displayed a catalytic activity superior (in terms of TON and TOF) to that of the well-known Knölker-Casey complex. The same trend was also observed in the transfer hydrogenation of acetophenone, which allowed to obtain a higher conversion compared to the Knölker-Casey complex. Kinetic studies on the hydrogenation of acetophenone of the two catalysts were also performed. This suggests that the difference between the two (cyclopentadienone)iron pre-catalysts is due to the higher stability of cyclooctyne-derived complex.



Finally, we also started to explore the field of (cyclopentadienone)iron tricarbonyl complexes which contain planar chirality, performing the cyclopentadienone ligand and subsequently inserting iron to form the desired complex. We evaluated the catalytic activity of the obtained planar chiral pre-catalyst, the results are promising, but the research to separate the two enantiomers (**155**, **156**) or the two diastereoisomers (**160**) is still under investigation.



6. Experimental Part

6.1. General Conditions

All reactions were carried out in anhydrous conditions in flame-dried glassware with magnetic stirring under nitrogen or argon atmosphere, unless otherwise stated.

The solvents for reactions were distilled over the following drying agents and transferred under nitrogen: CH_2Cl_2 (CaH_2), MeOH (CaH_2), THF (Na), dioxane (Na), Et_3N (CaH_2). Dry Et_2O , acetone, toluene and CHCl_3 (over molecular sieves in bottles with crown cap) were purchased from Sigma Aldrich and stored under nitrogen.

The reactions were monitored by analytical thin-layer chromatography (TLC) using silica gel 60 F254 pre-coated glass plates (0.25 mm thickness). Visualization was accomplished by irradiation with a UV lamp and/or staining with a potassium permanganate alkaline solution. Flash column chromatography was performed using silica gel (60 Å, particle size 40-64 μm) as stationary phase, following the procedure by Still and co-workers.^[184]

Proton NMR spectra were recorded on a Bruker spectrometer operating at 400.13 MHz. Proton chemical shifts are reported in ppm (δ) with the solvent reference relative to tetramethylsilane (TMS) employed as the internal standard (CDCl_3 δ = 7.26 ppm; CD_2Cl_2 , δ = 5.32 ppm; $[\text{D}]_6$ acetone, δ = 2.05 ppm; $[\text{D}]_6$ DMSO, δ = 2.50 ppm; CD_3OD , δ = 3.33 ppm). The following abbreviations are used to describe spin multiplicity: s = singlet, d = doublet, t = triplet, q = quartet, m = multiplet, br = broad signal, dd = doublet-doublet, td = triplet-doublet. ^{13}C -NMR spectra were recorded on a 400 MHz spectrometer operating at 100.56 MHz, with complete proton decoupling. Carbon chemical shifts are reported in ppm (δ) relative to TMS with the respective solvent resonance as the internal standard (CDCl_3 , δ = 77.16 ppm; CD_2Cl_2 , δ = 54.00 ppm; $[\text{D}]_6$ acetone, δ = 29.84 ppm, 206.26 ppm; $[\text{D}]_6$ DMSO, δ = 39.51 ppm; CD_3OD , δ = 49.05 ppm). The coupling constant values are given in Hz.

Infrared spectra were recorded on a standard FT/IR spectrometer. Optical rotation values were measured on an automatic polarimeter Jasco P1010 with a 1 dm cell at the sodium D line (λ = 589 nm).

Gas chromatography was performed on a GC instrument equipped with a flame ionization detector, using a chiral capillary column.

High resolution mass spectra (HRMS) were performed on a Fourier Transform Ion Cyclotron Resonance (FT-ICR) Mass Spectrometer APEX II & Xmass software (Bruker Daltonics) – 4.7 T

Magnet (Magnex) equipped with ESI source, available at CIGA (Centro Interdipartimentale Grandi Apparecchiature) c/o Università degli Studi di Milano.

Low resolution mass spectra (MS) were acquired either on a Thermo-Finnigan LCQ Advantage mass spectrometer (ESI ion source) or on a VG Autospec M246 spectrometer (FAB ion source).

Elemental analyses were performed on a Perkin Elmer Series II CHNS/O Analyzer 2000. X-ray intensity data were collected with a Bruker Apex II CCD area detector by using graphite monochromated Mo-K α radiation.

Melting point were determined on a Büchi B-540 instrument.

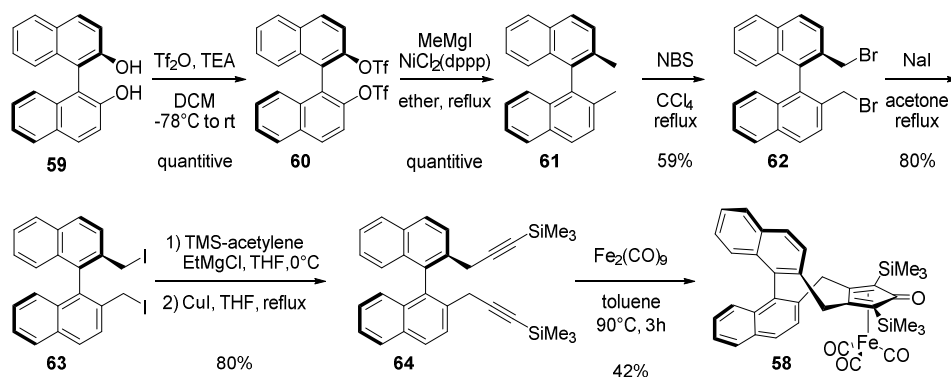
Chiral HPLC analysis were performed on a Shimadzu instrument equipped with a Diode Array detector.

6.1.1. Materials

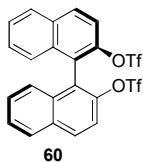
Commercially available reagents were used as received: trifluoromethanesulfonic anhydride, triethylamine, methylmagnesium bromide (3 M in Et₂O), *N*-Bromosuccinimide, benzoyl peroxide, ethynyltrimethylsilane, ethylmagnesium bromide (1 M in THF), *n*-BuLi (1.6 M in hexanes), BBr₃ (1 M in CH₂Cl₂), Bu₄NI, NaI, MeI, CuI, Fe₂(CO)₉, DMAP, acetyl chloride, benzoyl chloride, benzyl bromide, chloromethyl methyl ether, methanesulfonyl chloride, *p*-toluenesulfonyl chloride, *N*-(5-chloro-2-pyridyl)bis(trifluoromethane-sulfonimide), Pd(OAc)₂, K₃PO₄, PPh₃, KBr, phenylboronic acid, PCy₃, (*S*)-Phos, Pd(cinnamyl)(IPr)Cl, PdCl₂(dppp), NiCl₂(dppp), Ba(OH)₂·H₂O, Ba(OH)₂ anhydrous, Bu₄NBr, KF, K₂CO₃, *t*BuOK, Me₃NO, 1-iodopentane, ethynyltriisopropylsilane, ethynylbenzene and also compounds (ketones, aldehydes and esters) used in the substrate screening were purchased from commercial suppliers (TCI Chemicals, ACROS, Sigma Aldrich) and used as received.

(*R*)-(+)-1,1'-bi(2-naphthol), (*S*)-(-)-1,1'-Bi(2-naphthol) (BINOL) and (*R*)-3,3'-dibromo-[1,1'-binaphthalene]-2,2'-diol **78** are commercially available. Also (*R*)-2,2'-bis(bromomethyl)-1,1'-binaphthyl **62** is commercially available, but it can be easily synthesized from BINOL according to the procedure described by Ooi *et al.*^[185], while (*R*)-2,2'-bis(bromomethyl)-3,3'-dimethoxy-1,1'-binaphthyl **94** was synthesized according to the procedure described by Cramer and co-workers.^[139]

6.2. Synthesis of complex (R)-58



6.2.1. (R)-2,2'-bis(trifluoromethanesulfonyloxy)-1,1'-binaphthyl [60]



Trifluoromethanesulfoic anhydride (8.51 mL, 50.6 mmol, 2.2 eq) was added dropwise at $-78\text{ }^{\circ}\text{C}$ to a stirred mixture of (*R*)-BINOL (6.58 g, 23.0 mmol, 1 eq) and triethylamine (9.62 mL, 69.0 mmol, 3 eq) in CH_2Cl_2 (60 mL), under nitrogen in a Schlenk tube fitted with a Teflon screw cap. After the addition, the cooling bath was removed and the reaction mixture was stirred for 2 h at room temperature. The mixture was then poured into ice-cold 1 M HCl (40 mL) and extracted with hexane. The organic extracts were washed with saturated NaHCO_3 , brine and dried over Na_2SO_4 . Evaporation of solvent gave the crude 2,2'-bis(trifluoromethanesulfonyloxy)-1,1'-binaphthyl **60**, which can be either purified by flash column chromatography (9:1 hexane/ CH_2Cl_2) to give a white powder or used in the following step without further purification.^[186]

Yield 12.66 g (quantitative yield); m.p. $83\text{--}89\text{ }^{\circ}\text{C}$; $[\alpha]_{\text{D}}^{24} = -147.7^{\circ}$ ($c = 1.01$ in CHCl_3).

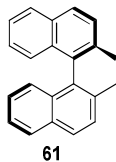
^1H NMR (400 MHz, CDCl_3): δ 8.16 (d, $^3J = 9.1$ Hz, 2H), 8.02 (d, $^3J = 8.3$ Hz, 2H), 7.64 (d, $^3J = 9.1$ Hz, 2H), 7.60 (ddd, $^3J = 8.3$ Hz, $^3J = 6.9$ Hz, $^4J = 1.1$ Hz, 2H), 7.43 (ddd, $^3J = 8.3$ Hz, $^3J = 6.9$ Hz, $^4J = 1.1$ Hz, 2H), 7.28 (d, $^3J = 8.4$ Hz, 2H).

^{13}C NMR (100 MHz, CDCl_3): 119.3, 123.5, 126.8, 127.3, 128.0, 128.4, 132.0, 132.3, 133.1, 145.4.

IR (KBr): $\nu = 3062, 1508, 1424, 1246, 1140, 1065, 963, 865\text{ cm}^{-1}$.

HRMS (ESI+): m/z 549.9878 $[\text{M}]^+$ (calcd. for $\text{C}_{22}\text{H}_{12}\text{F}_6\text{O}_6\text{S}_2$ 549.9979).

6.2.2. (*R*)-2,2'-dimethyl-1,1'-binaphthyl [61]



2,2'-Bis(trifluoromethanesulfonyloxy)-1,1'-binaphthyl **60** (12.66 g, 23.0 mmol, 1 eq) and NiCl₂(dppp) (0.374 g, 0.69 mmol, 3 mol%) were dissolved in Et₂O (30 mL), in a Schlenk tube fitted with a Teflon screw cap, under nitrogen. A 3 M ethereal solution of methylmagnesium iodide (30.7 mL, 92.0 mmol, 4 eq) was added dropwise at 0 °C. Then, the reaction mixture was heated to reflux and stirred overnight. The mixture was poured into ice-cold 1 M HCl and the obtained mixture was filtered over celite to remove the catalyst. The filtrate was extracted with Et₂O and the organic extracts were washed with brine and dried over Na₂SO₄. Evaporation of the solvent and purification of the residue by column chromatography on silica gel (100:1 hexane/ether) gave (*R*)-2,2'-dimethyl-1,1'-binaphthyl **61**, as a white powder. ^[187]

Yield 6.36 g (98%); m.p. = 74-78 °C; [α]_D²⁴ = -39° (*c* = 1.12 in CHCl₃).

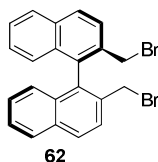
¹H NMR (400 MHz, CDCl₃): δ 7.92 (d, ³*J* = 8.4 Hz, 4H), 7.54 (d, ³*J* = 8.4 Hz, 2H), 7.42 (ddd, ³*J* = 8.4, ³*J* = 6.9, ⁴*J* = 1.2 Hz, 2H), 7.24 (ddd, ³*J* = 8.4, ³*J* = 6.9, ⁴*J* = 1.2 Hz, 2H), 7.08 (d, ³*J* = 8.4 Hz, 2H), 2.07 (s, 6H).

¹³C (100MHz, CDCl₃): δ 135.2, 134.3, 132.8, 132.2, 128.8, 127.8, 127.3, 126.1, 125.7, 124.9, 20.1.

IR (KBr): ν = 3049, 2918, 1506, 1352, 1026, 814, 746 cm⁻¹.

HRMS (ESI+): *m/z* 282.1400 [M]⁺ (calcd. for C₂₂H₁₈ 282.1409).

6.2.3. (*R*)-2,2'-Bis(bromomethyl)-1,1'-binaphthyl [62]



A mixture of (*R*)-2,2'-dimethyl-1,1'-binaphthyl **61** (6.36 g, 22.52 mmol, 1 eq), *N*-bromosuccinimide (NBS) (8.42 g, 47.3 mmol, 2.1 eq), and benzoyl peroxide (82 mg, 0.338 mmol, 1.5 mol%) in CCl₄ (40 mL) was heated and refluxed overnight. In addition, during the first 4 h the reaction mixture was irradiated using a 100 W lamp. The resulting mixture was cooled to room temperature and then poured into water and extracted with EtOAc. The organic extracts were dried over Na₂SO₄ and

concentrated. The residue was purified by crystallization from CH_2Cl_2 /hexane to give (*R*)-2,2'-bis(bromomethyl)-1,1'-binaphthyl **62**.^[188]

Yield 7.55 g (77%); m.p. = 180-183 °C; $[\alpha]_{\text{D}}^{24} = +148^\circ$ ($c = 1.70$ in benzene).

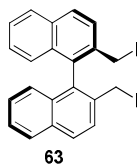
^1H NMR (400 MHz, CDCl_3): δ 8.03 (d, $^3J = 8.7$ Hz, 2H), 7.94 (d, $^3J = 8.1$ Hz, 2H), 7.77 (d, $^3J = 8.4$ Hz, 2H), 7.51 (ddd, $^3J = 8.1$ Hz, $^3J = 6.9$, $^4J = 1.2$ Hz, 2H), 7.28 (ddd, $^3J = 8.4$, $^3J = 6.9$, $^4J = 1.2$ Hz, 2H), 7.09 (d, $^3J = 8.7$ Hz, 2H), 4.28 (s, 4H).

^{13}C (100 MHz, CDCl_3): δ 134.2, 134.1, 133.3, 132.5, 129.9, 128.2, 127.8, 127.1, 126.88, 126.87, 31.6.

IR (KBr): $\nu = 3047, 1595, 1506, 1433, 1360, 1329, 1211, 1026, 968, 821, 756, 721, 687$ cm^{-1} .

HRMS (ESI+): m/z 437.9612 $[\text{M}]^+$ (calcd. for $\text{C}_{22}\text{H}_{16}\text{Br}_2$ 437.9619).

6.2.4. (*R*)-2,2'-Bis(iodomethyl)-1,1'-binaphthyl [63]



NaI (13.6 g, 91 mmol, 10 eq) was added to a stirred suspension of (*R*)-2,2'-bis(bromomethyl)-1,1'-binaphthyl **62** (4.01 g, 9.1 mmol) in acetone (50 mL), in a Schlenk tube fitted with a Teflon screw cap under nitrogen. The Schlenk was sealed and the mixture was heated to 58 °C and stirred overnight. To prevent possible photodegradation of **63**, the reaction vessel was covered tightly with aluminum foil and the reaction workup was done in the presence of the smallest possible amount of light. After cooling down to 40 °C, acetone was removed in vacuo, and the obtained solid was dried under high vacuum for 30 min. Water (100 mL) was added, and the obtained suspension was stirred for 30 min. The mixture was filtered on a ceramic frit, and the solid product **63** was washed with water (100 mL), sat. aq. $\text{Na}_2\text{S}_2\text{O}_3$ (100 mL), water (100 mL), and ice-cold 2:1 MeOH/hexane mixture (100 mL). Product **63** – a pale yellow powder – was dried on a frit and then under high vacuum.

Yield 3.89 g (80% yield); m.p. = 130-132 °C (dec.); $[\alpha]_{\text{D}}^{24} = +112.81^\circ$ ($c = 0.345$ in CH_2Cl_2).

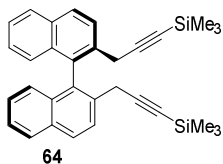
^1H NMR (400 MHz, $[\text{D}_6]$ acetone): δ 7.34 (d, $^3J = 8.6$ Hz, 2H), 7.25 (d, $^3J = 8.2$ Hz, 2H), 7.06 (d, $^3J = 8.6$ Hz, 2H), 6.77 (td, $^3J = 8.2$ Hz, $^4J = 1.1$ Hz, 2H), 6.55 (td, $^3J = 8.2$ Hz, $^4J = 1.2$ Hz, 2H), 6.25 (d, $^3J = 8.6$ Hz, 2H), 3.62 (d, $^2J = 9.5$ Hz, 2H AB system), 3.51 (d, $^2J = 9.5$ Hz, 2H, AB system).

^{13}C NMR (100 MHz, $[\text{D}_6]$ acetone): δ 136.2, 134.1, 133.0, 130.3, 129.2, 129.1, 127.8, 127.5, 127.3, 5.7.

IR (film): $\nu = 2292.2, 1461.9, 1377.3, 1156.6 \text{ cm}^{-1}$.

Elemental analysis (%): C 49.26, H 3.03 (calcd. for $\text{C}_{24}\text{H}_{20}\text{O}_2$: C 49.47, H 3.02).

6.2.5. (R)-2,2'-Bis(3-(trimethylsilyl)prop-2-ynyl)-1,1'-binaphthyl [64]



A solution of ethynyltrimethylsilane (0.565 mL, 4.0 mmol, 4 eq) in THF (5 mL) was added dropwise to a 1 M solution of ethylmagnesium bromide in THF (4.0 mL, 4.0 mmol, 4 eq) kept at 0 °C. The reaction mixture was heated to reflux and stirred for 1 h. After cooling to room temperature, CuI (0.095 g, 0.500 mmol, 0.5 eq) and compound **63** (0.534 g, 1.0 mmol, 1 eq) were added. The mixture was heated to reflux and stirred overnight. The reaction was quenched with saturated aqueous NH_4Cl (5 mL), and the obtained aqueous phase was extracted with EtOAc (3 × 25 mL). The organic layer was washed with H_2O (20 mL) and brine (20 mL), dried over Na_2SO_4 and concentrated *in vacuo*. Purification by column chromatography (95:5 hexane/ CH_2Cl_2) gave the product **64** as a light yellow oil.

Yield 0.38 g (80%); m.p. = 56 °C; $[\alpha]_{\text{D}}^{24} = +134.55^\circ$ ($c = 0.348$ in CH_2Cl_2).

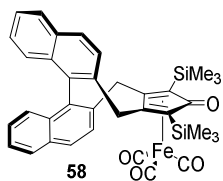
^1H NMR (400 MHz, CD_2Cl_2): δ 8.03 (d, $^3J = 8.5$ Hz, 2H), 7.95 (d, $^3J = 8.2$ Hz, 2H), 7.89 (d, $^3J = 8.5$ Hz, 2H), 7.45 (td, $^3J = 8.2$ Hz, $^4J = 1.1$ Hz, 2H), 7.24 (td, $^3J = 8.2$ Hz, $^4J = 1.3$ Hz, 2H), 6.99 (d, $^3J = 8.5$ Hz, 2H), 3.35 (d, $^2J = 19$ Hz, 2H, AB system), 3.22 (d, $^2J = 19$ Hz, 2H, AB system), 0.12 (s, 18H).

^{13}C NMR (100 MHz, CD_2Cl_2): δ 134.2, 133.7, 133.4, 133.0, 129.1, 128.7, 127.2, 127.2, 126.3, 126.0, 104.5, 87.6, 25.1, 0.3.

IR (film): $\nu = 3059.0, 2959.8, 2174.8, 1484.9, 1265.1, 1249.8 \text{ cm}^{-1}$.

HRMS (ESI+): m/z 497.20980 $[\text{M} + \text{Na}]^+$ (calcd. for $\text{C}_{32}\text{H}_{34}\text{Si}_2\text{Na}$: 497.20913).

6.2.6. Complex (R)-58



Diyne **64** (0.510 g, 1.07 mmol, 1 eq) and $\text{Fe}_2(\text{CO})_9$ (0.781 g, 2.14 mmol, 2 eq) were dissolved in dry toluene (9 mL) and heated to 90 °C for 4 h, under argon. After cooling down to room temperature, the reaction mixture was filtered through a pad of celite. The filtrate was concentrated *in vacuo*, and the residue was purified by flash column chromatography (8:2 hexane/ CH_2Cl_2) to obtain (*R*)-**58** as a pale yellow solid.

Yield 0.320 g (46%); m.p. = 209 °C (dec.); $[\alpha]_{\text{D}}^{19} = -32.24^\circ$ ($c = 0.9$ in CH_2Cl_2).

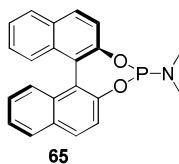
^1H NMR (400 MHz, CD_2Cl_2): δ 8.04 (d, $^3J = 8.5$ Hz, 2H), 7.99 (d, $^3J = 8.8$ Hz, 1H), 7.97 (d, $^3J = 8.8$ Hz, 1H), 7.68 (d, $^3J = 8.5$ Hz, 1H), 7.55 (d, $^3J = 8.5$ Hz, 1H), 7.52-7.45 (m, 2H), 7.30 (td, $^3J = 8.5$ Hz, $^4J = 1.1$ Hz, 1H), 7.25 (td, $^3J = 8.5$ Hz, $^4J = 1.1$ Hz, 1H), 7.20 (d, $^3J = 8.5$ Hz, 1H), 7.09 (d, $^3J = 8.5$ Hz, 1H), 3.76 (d, $^2J = 15.7$ Hz, 1H), 3.67 (d, $^2J = 14.1$ Hz, 1H), 3.45 (d, $^2J = 15.7$ Hz, 1H), 3.38 (d, $^2J = 14.1$ Hz, 1H), 0.41 (s, 9H), 0.26 (s, 9H).

^{13}C NMR (100 MHz, CD_2Cl_2): δ 209.8, 181.4, 137.0, 135.6, 135.0, 134.6, 133.4, 132.5, 130.0, 129.7, 128.9, 128.7, 127.5, 127.3, 127.1, 127.0, 126.9, 126.5, 113.1, 111.5, 76.0, 74.0, 34.8, 32.8, 0.9, 0.5. IR (film): $\nu = 3054.69, 2953.93, 2060.1, 2005.1, 1985.4, 1626.2, 1507.6, 1429.5, 1264.1, 1248.7$ cm^{-1} .

HRMS (ESI+): m/z 643.14164 $[\text{M} + \text{H}]^+$ (calcd. for $\text{C}_{36}\text{H}_{35}\text{O}_4\text{Si}_2\text{Fe}$: 643.14294).

6.3. Replacement of one CO ligand with phosphoramidite ligand

6.3.1. Synthesis of a phosphoramidite ligand: Monophos [65]



A mixture of (*R*)-binaphthol (2.0 g, 6.98 mmol) and hexamethyl phosphorous triamide (1.60 g, 9.77 mmol, 1.4 eq) in 10 mL of dry toluene was refluxed under argon atmosphere for 2 h. After cooling down to room temperature, the precipitate was filtered on a frit and washed with Et_2O to obtain white crystals.

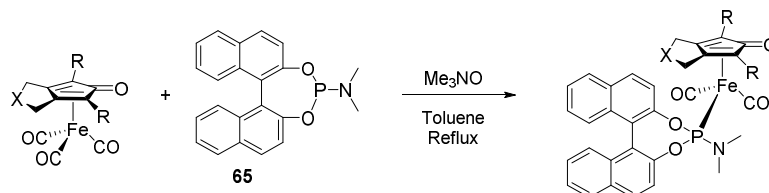
Yield 2.02 g (80%); m.p. 190-192 °C.

^1H NMR (400 MHz, CDCl_3): δ 7.99 (d, $^3J = 8.8$ Hz, 1H), 7.93-7.95 (m, 3H), 7.54 (d, $^3J = 8.8$ Hz, 1H), 7.43-7.45 (m, 3H), 7.42 (d, $^3J = 8.8$ Hz, 1H), 7.38 (d, $^3J = 8.5$ Hz, 1H), 7.26-7.32 (m, 2H), 2.58 (d, $^3J = 9.1$ Hz, 6H).

^{13}C NMR (400 MHz; CDCl_3): δ 150.01, 149.98, 149.07, 132.83, 132.61, 131.39, 130.74, 130.27, 130.02, 128.35, 128.27, 127.01, 126.93, 126.10, 124.79, 124.59, 123.96, 123.93, 122.81, 122.11, 121.98, 121.97, 36.05, 35.91.

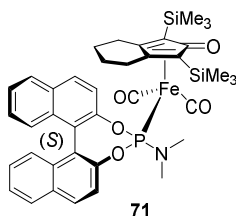
^{13}P -NMR (161.9 MHz; CD_2Cl_2): δ 148.76.

6.3.2. General procedure for replacing one CO ligand with a phosphoramidite



Me_3NO (1.0 eq) was added to a degassed solution of the Fe-complex (1.0 eq) and the corresponding phosphoramidite **65** (1.1 eq) in dry toluene (30 mL) and then the mixture was refluxed for 4 h, under argon. After cooling the mixture to room temperature, the solvent was removed under pressure, and the residue was purified by flash column chromatography (8:2 *n*-hexane/EtOAc) to obtain the final complex.

6.3.3. Complex **71** [(*S*)-Monophos]



Pale yellow solid

Yield 52 mg (42%); m.p. 215 °C (dec.).

^1H NMR (400 MHz, CD_2Cl_2): δ 8.04 (d, $^3J = 9.0$ Hz, 1H), 8.01 (d, $^3J = 9.0$ Hz, 1H), 7.97-7.92 (dd, $^3J = 8.2$ Hz, $^4J = 3.0$ Hz, 2H), 7.75 (d, $^3J = 9.0$ Hz, 1H), 7.42-7.46 (m, 2H), 7.21-7.33 (m, 5H), 2.59 (d, $^2J = 10.5$ Hz, 6H), 2.30-2.80 (br. m, 4H), 1.20-1.80 (br. m, 4H), 0.22 (s, 9H), -0.09 (s, 9H).

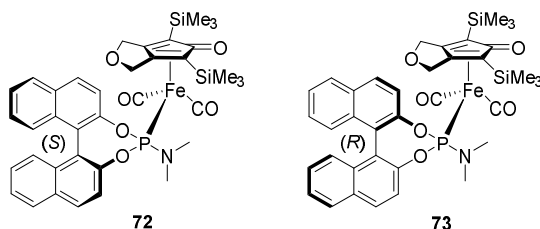
^{13}C NMR (400 MHz, CD_2Cl_2): δ 214.2, 213.8, 179.9, 147.4, 148.3, 133.1, 132.9, 131.5, 131.3, 130.8, 130.6, 128.4, 128.2, 126.9, 126.6, 126.4, 125.5, 125.3, 123.4, 122.4, 122.1, 120.6, 38.1, 31.0, 24.4, 22.4, 22.0, 0.1, -0.2.

^{31}P NMR (161.9 MHz, CD_2Cl_2): δ 193.7.

IR (ATR): $\nu = 2943, 2002, 1944, 1591, 1508, 1464, 1433, 1398, 1370, 1325, 1287, 1242, 1227, 1204, 1175, 1072, 978, 947, 841, 822, 770, 748, 712, 683, 650, 619 \text{ cm}^{-1}$.

HRMS (ESI+): m/z 750,00 $[M + Na]^+$ (calcd. for $C_{39}H_{44}FeNNaO_5PSi_2$: 749,1845).

6.3.4. Complex 72 [(*S*)-Monophos] and 73 [(*R*)-Monophos]



Pale yellow solid

72: Yield 181 mg (66%); m.p. 215 °C (dec.)

73: Yield 176 mg (94%); m.p. 215 °C (dec.)

^1H NMR (300 MHz, CD_2Cl_2): δ 8.06 (d, $^3J = 9.0$ Hz, 1H), 8.02 (d, $^3J = 9.0$ Hz, 1H), 7.94-7.98 (dd, $^3J = 8.2$ Hz, $^4J = 3.0$ Hz, 2H), 7.84 (d, $^3J = 9.0$ Hz, 1H), 7.44-7.49 (m, 2H), 7.19-7.33 (m, 5H), 5.08 (d, $^2J = 12.0$ Hz, 1H), 4.73-4.85 (m, 3H), 2.47 (d, $^2J = 10.5$ Hz, 6H), 0.23 (s, 9H), -0.36 (s, 9H).

^{13}C NMR (300 MHz, CD_2Cl_2): δ 213.1, 213.0, 182.0, 148.9, 148.1, 133.1, 133.0, 131.7, 135.5, 131.1, 131.0, 128.6, 128.4, 127.1, 126.9, 126.8, 126.5, 125.8, 125.4, 123.6, 122.7, 121.9, 120.4, 112.7, 108.5, 71.5, 68.7, 68.1, 62.3, 37.4, 0.6, -1.1.

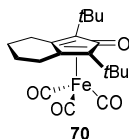
^{31}P NMR (161.9 MHz, CD_2Cl_2): δ 194.6.

IR (ATR): $\nu = 2015, 1958, 1603, 1503, 1460, 1410, 1323, 1245, 1225, 1070, 1026, 976, 947, 840, 750, 713, 693 \text{ cm}^{-1}$.

HRMS (ESI+): m/z 738.157 $[M + H]^+$ (calcd. for $C_{37}H_{40}FeNO_6PSi_2$: 738,1559).

Elemental analysis (%): C 57.49, H 5.38, N 1.76 (calcd. for $C_{37}H_{40}FeNO_6PSi_2$: C 57.73, H 5.30, N 1.80).

6.3.5. Complex 70



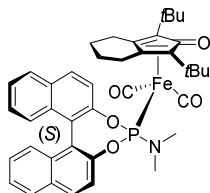
Yield 76 mg (72%); m.p. 152 °C.

^1H NMR (400 MHz; CDCl_3): δ 2.77-2.82 (m, 2H), 2.57-2.62 (m, 2H), 1.77 (br s, 4H), 1.33 (s, 18H).

^{13}C NMR (161.9 MHz, CDCl_3): δ 210.2, 173.4, 100.4, 92.3, 33.3, 29.9, 24.9, 22.1.

IR (ATR): ν = 2949.16, 2862.36, 2048.4, 1980.89, 1950.03, 1620.21, 1454.33, 1435.04, 1388.75, 1361.74, 1355.96, 1300.02, 1205.51, 1089.78, 1074.35, 1016.49, 974.05, 966.34, 852.54, 748.38, 736.38, 736.81, 626.87 cm^{-1} .

6.3.6. Complex 74 [(*S*)-Monophos]



Pale yellow solid

Yield 126 mg, (45%); m.p. = 135.5 °C.

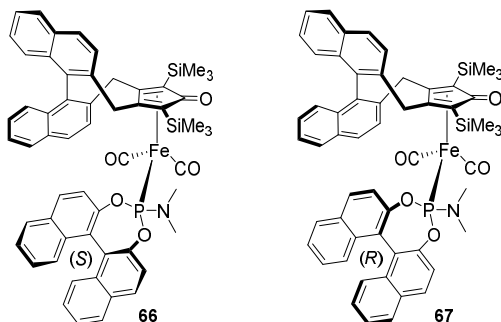
^1H NMR (400 MHz; CD_2Cl_2): δ 8.06 (d, 3J = 8.9 Hz, 1H), 8.03 (d, 3J = 8.9 Hz, 1H), 7.97 (d, 3J = 8.2 Hz, 2H), 7.84 (d, 3J = 8.9 Hz, 1H), 7.43-7.49 (m, 2H), 7.32 (d, 3J = 8.7, 2H), 7.22-7.29 (m, 3H), 2.71-2.82 (m, 4H), 2.64 (d, 2J = 10.3 Hz, 6H), 2.38-2.59 (m, 4H), 1.34 (s, 9H), 1.16 (s, 9H).

^{13}C NMR (400 MHz, CD_2Cl_2): δ 215.96, 131.97, 131.26, 129.01, 128.72, 127.24, 127.05, 126.79, 125.89, 125.73, 122.85, 121.12, 38.42, 38.36, 30.22, 30.12, 25.47, 24.81, 22.43, 21.90.

^{31}P NMR (161.9 MHz, CD_2Cl_2): δ 193.7.

IR (ATR): ν = 2926.01, 2850.79, 1996.32, 1940.39, 1612.49, 1591.27, 1506.41, 1483.26, 1463.97, 1433.11, 1390.68, 1361.74, 1325.1, 1284.59, 1226.73, 1203.58, 1172.72, 1072.42, 975.98, 945.12, 852.54, 823.6, 808.17, 790.81, 771.53, 748.38, 711.73, 680.87, 650.01 cm^{-1} .

6.3.7. Complex 66 [(*S*)-Monophos] and 67 [(*R*)-Monophos]



Complex **66**: pale yellow solid

Yield 90 mg, (55%); m.p. = 225 °C;

^1H NMR (400 MHz, CD_2Cl_2): δ 8.06 (d, $^3J = 8.4$ Hz, 1H), 8.02 (d, $^3J = 8.2$ Hz, 1H), 7.97 (d, $^3J = 8.2$ Hz, 1H), 7.94 (d, $^3J = 8.5$ Hz, 1H), 7.93 (d, $^3J = 8.5$ Hz, 1H), 7.86 (d, $^3J = 8.4$ Hz, 1H), 7.69 (d, $^3J = 8.1$ Hz, 1H), 7.57-7.59 (m, 1H), 7.52 (d, $^3J = 8.5$ Hz, 1H), 7.44-7.49 (m, 2H), 7.38-7.41 (m, 1H), 7.34-7.36 (m, 1H), 7.25-7.28 (m, 1H), 7.21-7.24 (m, 3H), 7.16-7.19 (m, 4H), 7.11 (d, $^3J = 8.5$ Hz, 1H), 7.09 (d, $^3J = 8.5$ Hz, 1H), 7.06 (d, $^3J = 8.5$ Hz, 1H), 3.89 (d, $^2J = 15.8$ Hz, 1H), 3.48 (d, $^2J = 15.8$ Hz, 1H), 3.23-3.33 (m, 2H), 2.22 (d, $^2J = 10.0$ Hz, 6H), 0.49 (s, 9H), 0.24 (s, 9H).

^{13}C NMR 400 MHz, CD_2Cl_2): δ 214.17, 214.02, 213.96, 179.53, 149.39, 149.31, 148.23, 148.18, 136.80, 136.03, 134.66, 134.25, 132.90, 132.81, 132.73, 132.64, 132.45, 132.05, 131.27, 131.08, 130.56, 130.23, 129.91, 129.07, 128.55, 128.31, 128.15, 126.89, 126.83, 126.69, 126.53, 126.37, 126.28, 126.21, 126.19, 125.73, 125.44, 125.34, 125.04, 122.71, 121.74, 121.03, 120.67, 37.45, 34.94, 31.33, 26.91, -1.11, -0.24.

^{31}P NMR (161.9 MHz, CD_2Cl_2): δ 195.22.

IR (ATR): $\nu = 2924.09, 2906.73, 2848.86, 2011.76, 1950.03, 1606.7, 1593.2, 1508.33, 1463.97, 1402.25, 1325.1, 1286.52, 1244.09, 1224.8, 1178.51, 1143.79, 1072.42, 1028.06, 979.84, 947.05, 850.61, 821.68, 765.74, 750.31, 732.95, 713.66, 696.3, 682.3, 682.3, 682.8, 650.01$ cm^{-1} .

Complex **67**: pale yellow solid

Yield 56 mg, (55%); m.p. = 223 °C.

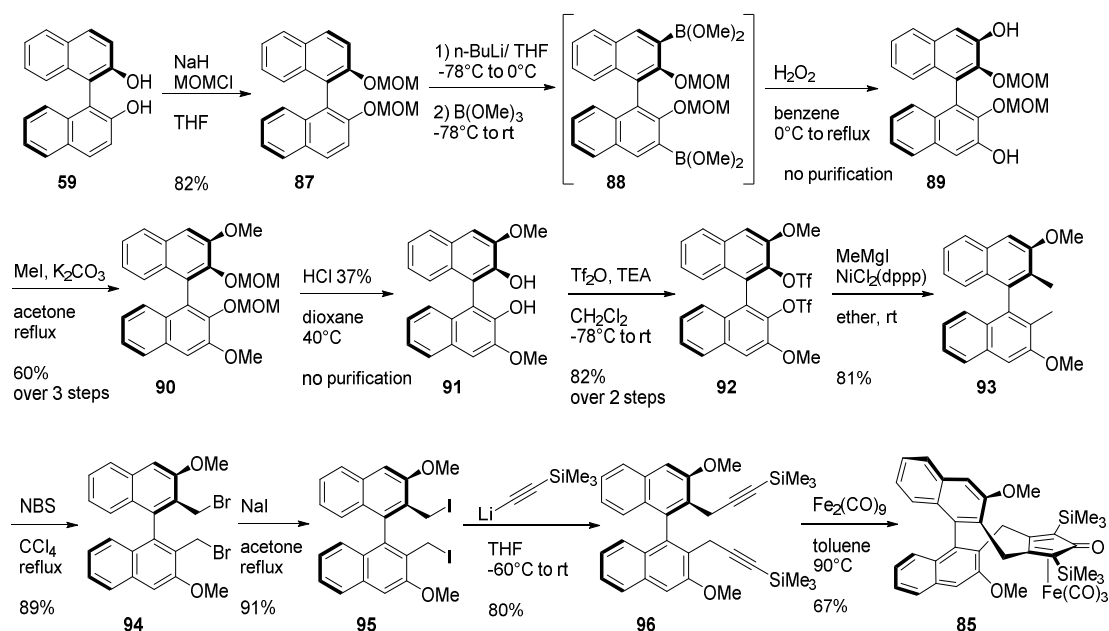
^1H NMR (400 MHz, CD_2Cl_2): δ 8.11-7.95 (m, 6H), 7.84 (ddd, $^3J = 13.0, 8.4, ^4J = 3.5$ Hz, 4H), 7.61-7.15 (m, 12H), 7.09 (d, $^3J = 8.4$ Hz, 1H), 6.92 (d, $^3J = 8.4$ Hz, 1H), 4.05 (d, $^2J = 14.7$ Hz, 2H), 4.02 (dd, $J = 14.8, 5.1$ Hz, 4H), 4.00 (d, $J = 4.0$ Hz, 2H), 3.72 (dd, $^2J = 13.7, ^4J = 3.1$ Hz, 1H), 3.61 (d, $^2J = 18.5$ Hz, 2H), 1.81 (d, $^2J = 15.8$ Hz, 6H), 0.29 (s, 9H), 0.22 (s, 9H).

^{13}C NMR (400 MHz, CD_2Cl_2): δ 214.17, 214.02, 213.96, 179.53, 149.39, 149.31, 148.23, 148.18, 136.80, 136.03, 134.66, 134.25, 132.90, 132.81, 132.73, 132.64, 132.45, 132.05, 131.27, 131.08, 130.56, 130.23, 129.91, 129.07, 128.55, 128.31, 128.15, 126.89, 126.83, 126.69, 126.53, 126.37, 126.28, 126.21, 126.19, 125.73, 125.44, 125.34, 125.04, 122.71, 121.74, 121.03, 120.67, 37.45, 34.94, 31.33, 26.91, -1.11, -0.24.

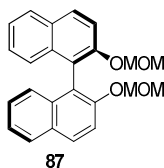
^{31}P NMR (161.9 MHz, CD_2Cl_2): δ 195.52

IR (ATR): $\nu = 2924.09, 2906.73, 2848.86, 2011.76, 1950.03, 1606.7, 1593.2, 1508.33, 1463.97, 1402.25, 1325.1, 1286.52, 1244.09, 1224.8, 1178.51, 1143.79, 1072.42, 1028.06, 979.84, 947.05, 850.61, 821.68, 765.74, 750.31, 732.95, 713.66, 696.3, 682.3, 682.3, 682.8, 650.01$ cm^{-1} .

6.4. Synthesis of complex (R)-85



6.4.1. (R)-2,2'-bis(methoxymethoxy)-1,1'-binaphthyl [87]



A solution of (R)-BINOL (20.2 g, 70.5 mmol, 1 eq) in THF (100 mL) was added dropwise from a dropping funnel to a suspension of NaH (6.50 g, 60% in mineral oil, 162.5 mmol, 2.3 eq) in dry THF (300 ml) at 0 °C under argon atmosphere. After stirring for 1 h at room temperature, chloromethyl methyl ether (MOMCl) (12.5 mL, 162.5 mmol, 2.3 eq) was slowly added at 0 °C. Then the reaction mixture was allowed to warm to room temperature and stirred overnight. The reaction was quenched with saturated aqueous NH₄Cl (100 mL) and extracted with EtOAc. The combined organic layers were washed with brine, dried over Na₂SO₄, and concentrated *in vacuo*. The resultant residue was crystallized from methanol to give the aimed product as a white crystal.

Yield 21.65 g (82%); m.p. = 103–104 °C; [α]_D²⁰ = +94.3° (c = 1.1 in CHCl₃)

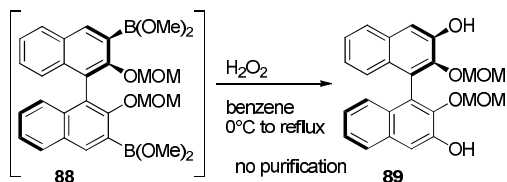
¹H NMR (400 MHz, CDCl₃) δ : 8.01 (d, ³J = 9.2 Hz, 2H), 7.93 (d, ³J = 8.4 Hz, 2H), 7.64 (d, ³J = 8.4 Hz, 2H), 7.39 (t, ³J = 8.0 Hz, 2H), 7.28–7.24 (m, 2H), 7.14 (d, ³J = 8.3 Hz, 2H), 5.12 (d, ²J = 6.2 Hz, 2H), 5.06 (d, ²J = 6.2 Hz, 2H), 3.21 (s, 6H).

^{13}C NMR (100 MHz, CDCl_3): δ 152.6, 134.0, 129.8, 129.4, 127.8, 126.3, 125.5, 124.0, 121.2, 117.2, 95.1, 55.8.

IR (solid): ν = 2904, 1590, 1505, 1236, 1146, 1010, 808 cm^{-1} .

HRMS: m/z 374.1527 $[\text{M}]^+$ (calcd. for $\text{C}_{24}\text{H}_{22}\text{O}_4$: 374.1518).

6.4.2. (*R*)-3,3'-dihydroxy-2,2'-bis(methoxymethoxy)-1,1'-binaphthyl [89]



Under argon atmosphere, to a solution of **87** (18.92 g, 50.5 mmol, 1 eq) in THF (150 mL) was added dropwise a 1.6 M hexane solution of *n*-BuLi (76 mL, 122 mmol, 2.4 eq) at $-78\text{ }^\circ\text{C}$. The colour of the mixture changed from light yellow into brown. This mixture was allowed to warm to $0\text{ }^\circ\text{C}$ and stirred for 1 h, then cooled back to $-78\text{ }^\circ\text{C}$. Trimethoxyborane (17 mL, 152 mmol, 3 eq) was added dropwise and the resulting mixture was allowed to warm to room temperature and stirred overnight. Removal of THF under vacuum afforded the crude borate **88**, which was suspended in benzene (175 mL), and hydrogen peroxide (30% aqueous solution, 15.5 mL) was added dropwise at $0\text{ }^\circ\text{C}$. This mixture was heated and refluxed for 2 h. After cooling to $10\text{ }^\circ\text{C}$, the resulting mixture was poured into ice-cooled saturated Na_2SO_3 and extracted with EtOAc. The organic extracts were washed with brine and dried over Na_2SO_4 . Evaporation of the solvent and purification of the residue by column chromatography on silica gel (2:1 hexane/EtOAc) gave (*R*)-3,3'-dihydroxy-2,2'-bis(methoxymethoxy)-1,1'-binaphthyl **89**.

Yield 18.06 g (88% yield); m.p. $120\text{ }^\circ\text{C}$; $[\alpha]_{\text{D}}^{20} = -70.2^\circ$ ($c = 0.28$ in CHCl_3).

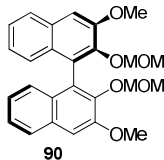
^1H NMR (400 MHz, CDCl_3): δ 7.82 (d, $^3J = 8.4$ Hz, 2H), 7.58 (s, 2H), 7.52 (s, 2H), 7.39 (ddd, $^3J = 8.1$, $^3J = 6.9$, $^4J = 1.2$ Hz, 2H), 7.14 (ddd, $^3J = 8.1$, $^3J = 6.9$, $^4J = 1.2$ Hz, 2H), 7.04 (d, $^3J = 8.4$ Hz, 2H), 4.77 (d, $^2J = 6.3$ Hz, 2H), 4.71 (d, $^2J = 6.3$ Hz, 2H), 3.40 (s, 6H).

^{13}C NMR (100 MHz, CDCl_3): δ 147.9, 144.8, 132.0, 128.2, 126.6, 125.7, 125.5, 125.3, 124.0, 111.8, 99.6, 57.5.

IR (KBr): ν = 3410, 2900, 1597, 1510, 1445, 1344, 1248, 1211, 1159, 1063, 984, 912, 876, 752, 680 cm^{-1} .

HRMS (ESI+): m/z 405.1333 $[\text{M} - \text{H}]^-$ (calcd. for $\text{C}_{24}\text{H}_{21}\text{O}_6$: 405.1351).

Elemental analysis (%): C 70.71, H 5.44, O 23.55 (calcd. for $\text{C}_{24}\text{H}_{22}\text{O}_6$: C 70.92, H 5.46, O 23.62).

6.4.3. (*R*)-3,3'-Dimethoxy-1,1'-bi-2-naphthol [90]

A mixture of compound **89** (18.06 g, 44.4 mmol), K_2CO_3 (27.61 g, 199.8 mmol, 4.5 eq) and methyl iodide (13.8 mL, 222 mmol, 5 eq) in acetone (200 mL) was heated and refluxed overnight. The resulting mixture was poured into water and extracted with EtOAc. The organic extracts were washed with brine and dried over Na_2SO_4 . Evaporation of the solvent gave the crude (*R*)-3,3'-dimethoxy-2,2'-bis(methoxymethoxy)-1,1'-binaphthyl **90**, which can be either purified by flash column chromatography (3:1 hexane/EtOAc) or used in the following step without further purification.

Yield 16.9 g (88% yield); m.p. 129 °C; $[\alpha]_D^{20} = +45.6^\circ$ ($c = 0.59$ in $CHCl_3$).

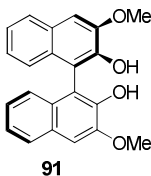
1H NMR (400 MHz, $CDCl_3$): δ 7.83 (d, $^3J = 8.1$ Hz, 2H), 7.38 (ddd, $^3J = 8.1$, $^3J = 6.0$, $^4J = 2.1$ Hz, 2H), 7.32 (s, 2H), 7.09-7.17 (m, 4H), 4.93 (d, $^2J = 5.7$ Hz, 2H), 4.85 (d, $^2J = 5.7$ Hz, 2H), 4.05 (s, 6H), 2.59 (s, 6H).

^{13}C NMR (100 MHz, $CDCl_3$): δ 151.9, 144.3, 131.2, 128.9, 126.7, 126.2, 125.2, 123.9, 107.2, 98.0, 56.0, 55.7.

IR (KBr): $\nu = 3003, 2959, 2895, 1594, 1462, 1429, 1342, 1248, 1201, 1159, 1115, 1074, 1020, 980, 922, 752$ cm^{-1} .

HRMS (ESI+): m/z 457.1612 $[M + Na]^+$ (calcd. for $C_{26}H_{26}NaO_6$: 457.1622).

Elemental analysis (%): C 71.81, H 6.05, O 21.97 (calcd. for $C_{26}H_{26}O_6$: C 71.87, H 6.03, O 22.09).

6.4.4. (*R*)-3,3'-dimethoxy-1,1'-bi-2-naphthol [91]

Compound (*R*)-**90** was dissolved in dioxane (110 mL) and 37% concentrated aqueous HCl (3 mL) was added and the mixture was heated to 45 °C for 3.5 h. After aqueous workup, the organic extracts were washed with brine, dried over Na_2SO_4 , and concentrated to afford (*R*)-3,3'-dimethoxy-1,1'-bi-2-naphthol [**91**], which can be directly used for the following reaction.

An analytical sample of **91** was purified by column chromatography on silica gel (1:1 EtOAc/hexane). M.p. 242 °C; $[\alpha]_D^{20} = +27.6^\circ$ ($c = 0.26$ in CHCl_3).

^1H NMR (400 MHz, CDCl_3): δ 7.83 (d, $^3J = 8.1$ Hz, 2H), 7.37-7.34 (m, 4H), 7.20-7.10 (m, 4H), 6.05 (s, 2H), 4.12 (s, 6H).

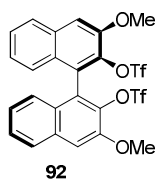
^{13}C NMR (100 MHz, CDCl_3): δ 147.1, 143.6, 129.0, 128.8, 126.8, 124.6, 124.5, 124.0, 114.4, 106.2, 56.0

IR (KBr): $\nu = 3479, 1622, 1464, 1425, 1337, 1313, 1257, 1167, 1117, 1018, 883, 831, 748$ cm^{-1} .

HRMS (ESI+): m/z 345.1126 $[\text{M} - \text{H}]^-$ (calcd. for $\text{C}_{22}\text{H}_{17}\text{O}_4$: 345.1121).

Elemental analysis (%): C 76.14, H 5.23, O 18.21 (calcd. for $\text{C}_{22}\text{H}_{18}\text{O}_4$: C 76.29, H 5.24, O 18.48).

6.4.5. (*R*)-3,3'-Dimethoxy-2,2'-bis(trifluoromethanesulfonyloxy)-1,1'-binaphthyl [92]



Compound **91** was dissolved in dry CH_2Cl_2 (120 mL) and dry TEA (20 mL, 150 mmol, 3 eq) was added to the mixture. After cooling at -78°C , Tf_2O (18.5 mL, 110 mmol, 2.2 eq) was added dropwise and the resulting mixture was allowed to warm to room temperature and stirred for 2 h. The mixture was then poured into ice-cooled 1 M HCl (180 mL) and extracted with CH_2Cl_2 . The organic extracts were washed with saturated NaHCO_3 , brine and dried over Na_2SO_4 . The residual crude product was then purified by column chromatography on silica gel (95:5 hexane/ Et_2O) to give (*R*)-3,3'-dimethoxy-2,2'-bis-(trifluoromethanesulfonyloxy)-1,1'-binaphthyl **92**.

Yield 23.6 g (87% over 2 steps); m.p. 139 °C; $[\alpha]_D^{20} = -118.3^\circ$ ($c = 0.24$ in CHCl_3).

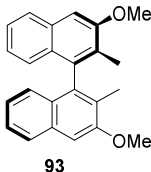
^1H NMR (400 MHz, CDCl_3): δ 7.88 (d, $^3J = 8.4$ Hz, 2H), 7.54 (ddd, $^3J = 8.4$, $^3J = 6.9$, $^4J = 1.2$ Hz, 2H), 7.50 (s, 2H), 7.24 (ddd, $^3J = 7.8$, $^3J = 6.9$, $^4J = 1.2$ Hz, 2H), 7.15 (d, $^3J = 7.8$ Hz, 2H), 4.12 (s, 6H).

^{13}C NMR (100 MHz, CDCl_3): δ 149.1, 137.6, 132.9, 127.7, 127.6, 126.8, 126.6, 125.4, 124.6, 118.0 (q, $J_{\text{C-F}} = 321$ Hz), 109.4, 56.4.

IR (KBr): $\nu = 3466, 1603, 1468, 1425, 1331, 1209, 1132, 1105, 1011, 947, 895, 813, 745$ cm^{-1} .

HRMS (ESI+): m/z 633.0067 $[\text{M} + \text{Na}]^+$ (calcd. for $\text{C}_{24}\text{H}_{16}\text{F}_6\text{NaO}_8\text{S}_2$: 633.0083).

Elemental analysis (%): C 47.06, H 2.81, O 18.43 (calcd. for $\text{C}_{24}\text{H}_{16}\text{F}_6\text{O}_8\text{S}_2$: C 47.22, H 2.64, O 18.67).

6.4.6. (*R*)-3,3'-Dimethoxy-2,2'-dimethyl-1,1'-binaphthyl [93]

Compound **92** (8.56 g, 14.0 mmol, 1 eq) and NiCl₂(dppp) (0.51 g, 0.94 mmol, 6.7 mol%) were dissolved in 55 mL of dry Et₂O, under argon. A 3 M ethereal solution of MeMgI (23.5 ml, 70 mmol, 5 eq) was added dropwise at 0 °C and the reaction mixture was stirred for 3 days at room temperature. The mixture was cooled with an ice bath, and poured slowly into ice-cold 1 M HCl (80 mL). The obtained mixture was filtered on celite to remove the catalyst and then the filtrate was extracted. The combined organic phases were washed with brine and then dried over Na₂SO₄. The residual crude product was then purified by column chromatography on silica gel (86:14 hexane/CH₂Cl₂) to give (*R*)-3,3'-Dimethoxy-2,2'-dimethyl-1,1'-binaphthyl **93**.

Yield 3.88 g (81%); m.p. 197 °C; [α]_D²⁰ = +16.5° (c = 0.50 in CHCl₃).

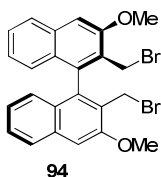
¹H NMR (400 MHz, CDCl₃): δ 7.81 (d, ³J = 8.1 Hz, 2H), 7.37 (ddd, ³J = 8.1, ³J = 6.9, ⁴J = 1.2 Hz, 2H), 7.24 (s, 2H), 7.07 (ddd, ³J = 8.1, ³J = 6.9, ⁴J = 1.2 Hz, 2H), 6.97 (d, ³J = 8.1 Hz, 2H), 4.05 (s, 6H), 1.94 (s, 6H).

¹³C NMR (100 MHz, CDCl₃): δ 156.3, 136.5, 133.1, 128.1, 127.4, 126.5, 125.7, 125.3, 123.5, 104.2, 55.4, 13.5.

IR (KBr): ν = 2953, 1599, 1456, 1421, 1323, 1232, 1194, 1165, 1115, 1022, 748 cm⁻¹.

HRMS (FAB): m/z 342.1620 [M⁺] (calcd. for C₂₄H₂₂O₂: 342.1608).

Elemental analysis (%): C 83.92, H 6.42, O 9.31 (calcd. for C₂₄H₂₂O₂: C 84.18, H 6.48, O 9.34).

6.4.7. (*R*)-3,3'-Dimethoxy-2,2'-bis(bromomethyl)-1,1'-binaphthyl [94]

A mixture of 3,3'-dimethoxy-2,2'-dimethyl-1,1'-binaphthalene **93** (3.77 g, 10.9 mmol, 1 eq), NBS (4.26 g, 23.9 mmol, 2.2 eq) and benzoyl peroxide (0.085 g, 3.2 mol %) in CCl₄ (60 mL) was refluxed for 3 h, while irradiating with a 100 W lamp. After 22 h the reaction was cooled down and filtered

on a frit to remove succinimide and the solvent was removed under reduced pressure to obtain a foamy solid. The residue was purified by recrystallization from Et₂O/hexane to obtain (R)-3,3'-Dimethoxy-2,2'-bis(bromomethyl)-1,1'-binaphthyl **94** as white crystals.

Yield 4.85 g (89%); m.p. 215–217 °C; $[\alpha]_D^{20} = -158.9^\circ$ ($c = 0.30$ in CH₂Cl₂).^[139]

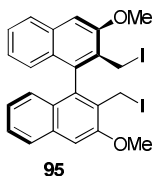
¹H NMR (400 MHz, CDCl₃): δ 7.83 (d, ³J = 8.3 Hz, 2H), 7.45 (ddd, ³J = 8.1, ³J = 6.8, ⁴J = 1.3 Hz, 2H), 7.34 (s, 2H), 7.12 (ddd, ³J = 8.2, ³J = 6.8, ⁴J = 1.3 Hz, 2H), 7.01 (d, ³J = 8.3 Hz, 2H), 4.28 - 4.37 (m, 4H), 4.13 (s, 6H).

¹³CNMR (100 MHz, CDCl₃): δ 155.5, 136.4, 134.6, 127.7, 127.3, 127.2, 126.7, 126.6, 124.2, 106.4, 55.8, 27.8.

IR (ATR): $\nu = 3061, 3004, 2960, 2936, 2830, 1619, 1597, 1568, 1502, 1449, 1422, 1407, 1387, 1361, 1327, 1294, 1265, 1238, 1215, 1195, 1169, 1151, 1131, 1106, 1019, 908, 865, 834, 788, 747, 731, 690$ cm⁻¹.

HRMS (ESI): m/z 419.0645 [M - Br]⁺ (calcd. for C₂₄H₂₀BrO₂: 419.0641).

6.4.8. (R)-2,2'-Bis(iodomethyl)-3,3'-dimethoxy-1,1'-binaphthyl [95]



NaI (16.5 g, 110 mmol, 10 eq) was added to a stirred suspension of **94** (5.50 g, 11.0 mmol) in acetone (55 mL), in a Schlenk tube fitted with a Teflon screw cap, under nitrogen. The mixture was heated to reflux and stirred overnight. To prevent possible photodegradation of **95**, the reaction vessel was covered tightly with aluminium foil and the reaction workup was done in the presence of the smallest possible amount of light. After cooling down to 40 °C, acetone was removed *in vacuo*, and the obtained solid was dried under high vacuum for 30 min. Water (100 mL) was added, and the obtained suspension was stirred for 30 min. The mixture was filtered on a ceramic frit, and the solid product **95** was washed with water (100 mL), saturated aqueous Na₂S₂O₃ (120 mL), water (150 mL), and ice-cold 2:1 MeOH/hexane mixture (100 mL). Product **95**, a pale-yellow powder, was dried on a frit and then under high vacuum.

Yield 5.94 g (91%); m.p. = 169-173 °C (dec.); $[\alpha]_D^{24} = +133.48$ ($c = 0.52$ in acetone).

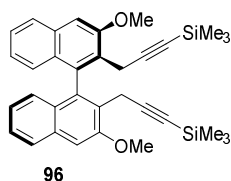
^1H NMR (400 MHz, $[\text{D}_6]$ acetone): δ 7.93 (d, $^3J = 8.2$ Hz, 2H), 7.57 (s, 2H), 7.47 (td, $^3J = 8.1$ Hz, $^4J = 1.1$ Hz, 2H), 7.13 (td, $^3J = 8.1$ Hz, $^4J = 1.2$ Hz, 2H), 6.9 (d, $^3J = 8.1$ Hz, 2H), 4.28 (d, $^2J = 8.9$ Hz, 2H, AB system), 4.20 (d, $^2J = 8.9$ Hz, 2H, AB system), 4.16 (s, 6H).

^{13}C NMR (100 MHz, $[\text{D}_6]$ acetone): δ 156.5, 136.1, 135.7, 128.1, 128.1, 128.0, 127.9, 127.6, 125.1, 107.6, 56.3, 0.1.

IR (film): $\nu = 3060.5, 2959.7, 2935.6, 1618.0, 1597.7, 1570.7, 1445.9, 1422.7, 1327.3, 1158.0$ cm^{-1} .

HRMS (ESI+): m/z 616.94566 $[\text{M} + \text{Na}]^+$ (calcd. for $\text{C}_{24}\text{H}_{20}\text{I}_2\text{O}_2\text{Na}$: 616.94449).

6.4.9. (R)-(3,3'-dimethoxy-1,1'-binaphthyl-2,2'-diyl)bis(prop-1-yne-3,1-diy) bis(trimethylsilane) [96]



n-BuLi (1.6 M hexane solution, 11.6 mL, 18.5 mmol, 3 eq) was added dropwise to a solution of ethynyltrimethylsilane (1.82 g, 2.62 mL, 18.5 mmol, 3 eq) in THF (12 mL) kept at -60 °C. The obtained mixture was allowed to warm to 0 °C and stirred for 30 min at this temperature, then it was cooled down again to -60 °C. A solution of bis-iodide **95** (3.63 g, 6.11 mmol, 1 eq) in THF (45 mL) was added and then the mixture was allowed to warm to room temperature and stirred overnight. The reaction was quenched with saturated aqueous NH_4Cl and extracted three times with Et_2O . The combined organic extracts were dried over Na_2SO_4 and concentrated *in vacuo*. Diyne **96** can be either purified by flash column chromatography (8:2 hexane/ CH_2Cl_2) or used in the following step without further purification.

Yield 2.61 g (80%); m.p. = 75 - 83 °C; $[\alpha]_{\text{D}}^{24} = +55.56$ ($c = 0.555$ in CHCl_3).

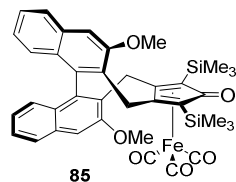
^1H NMR (400 MHz, CDCl_3): δ 7.81 (d, $^3J = 8.2$ Hz, 2H), 7.40 (t, $^3J = 8.2$ Hz, 2H), 7.32 (s, 2H), 7.09-7.02 (m, 4H), 4.08 (s, 6H), 3.40 (d, $^2J = 16.6$ Hz, 2H, AB system), 3.29 (d, $^2J = 16.6$ Hz, 2H, AB system), 0.00 (s, 18H).

^{13}C NMR (100 MHz, CDCl_3): δ 155.9, 136.1, 134.0, 128.3, 126.9, 126.6, 126.6, 126.3, 124.0, 106.0, 104.5, 83.6, 55.8, 19.6, 0.16.

IR (film): $\nu = 3062.9, 2958.3, 2898.0, 2173.9, 1620.4, 1597.7, 1446.8, 1327.3, 1248.7, 1109.8$ cm^{-1} .

HRMS (ESI+): m/z 557.23139 $[M + Na]^+$ (calcd. for $C_{34}H_{38}O_2Si_2Na$: 557.23025).

6.4.10. Complex (R)-85



Diyne **96** (3.27 g, 6.11 mmol, 1 eq) and $Fe_2(CO)_9$ (4.55 g, 12.5 mmol, 2 eq) were dissolved in dry toluene (45 ml) and heated to 90 °C for 4.5 h, under argon. After cooling down to room temperature, the reaction mixture was filtered through a pad of celite (rinsing with CH_2Cl_2). The filtrate was concentrated *in vacuo*, and the residue was purified by flash column chromatography (93:7 hexane/EtOAc) to obtain (R)-**85** as a pale yellow solid.

Yield: 2.88 g (67% yield); m.p. = 233-237 °C (dec.); $[\alpha]_D^{23} = -129.38$ ($c = 0.41$ in CH_2Cl_2).

1H NMR (400 MHz, $CDCl_3$): δ 7.84 (m, 2H), 7.42 (t, $^3J = 7.2$ Hz, 2H), 7.33 (s, 1H), 7.30 (s, 1H), 7.11-7.03 (m, 2H), 6.92 (d, $^3J = 8.4$ Hz, 2H), 4.37 (d, $^2J = 15.5$ Hz, 1H), 4.15 (d, $^2J = 13.7$ Hz, 1H), 4.04 (s, 3H), 3.94 (s, 3H), 3.26 (d, $^2J = 13.7$ Hz, 1H), 3.12 (d, $^2J = 15.5$ Hz, 1H), 0.43 (s, 9H), 0.32 (s, 9H).

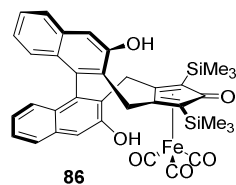
^{13}C NMR (100 MHz, $CDCl_3$): δ 208.7, 181.1, 155.1, 154.8, 138.6, 137.2, 133.9, 133.8, 127.4, 127.2, 127.1, 127.0, 126.9, 126.8, 126.6, 126.5, 126.4, 124.3, 124.1, 115.4, 107.8, 106.3, 105.7, 75.2, 74.9, 55.6, 54.8, 26.3, 26.2, 0.7, 0.2.

IR (film): $\nu = 3059.5, 2960.2, 2169.0, 2059.6, 2004.2, 1987.3, 1620.4, 1598.7, 1454.1, 1246.3, 1111.3$ cm^{-1} .

HRMS (ESI+): m/z 703.16264 $[M + H]^+$ (calcd. for $C_{38}H_{39}O_6Si_2Fe$: 703.16410).

6.5. Modification of the chiral Knölker complex

6.5.1. Complex (R)-86



In a Schlenk tube fitted with a Teflon screw cap, BBr_3 (1M CH_2Cl_2 solution, 14.0 mL, 14.0 mmol, 10 eq) was added dropwise to a stirred solution of (*R*)-**85** (0.99 g, 1.41 mmol, 1 eq) and Bu_4NI (1.30 g, 3.52 mmol, 2.5 eq) in DCE (40 mL) kept at 0 °C. The Schlenk was sealed and the mixture was heated to 84 °C and stirred for 3 days. After this time, the reaction was cooled down to 0 °C and ice-cold H_2O (50 mL) was added. The mixture was extracted with CH_2Cl_2 (3 × 20 mL), washed with brine (30 mL) and then dried over Na_2SO_4 . Filtration of the CH_2Cl_2 solution through a short pad of silica allowed to remove the ammonium salts (which eluted before the product), then complex (*R*)-**86** – a pale yellow solid – was purified by flash column chromatography (83:17 to 77:23 hexane/AcOEt).

Yield 0.762 g (80%); m.p. = 187-195 °C (dec.); $[\alpha]_{\text{D}}^{23} = -115.07$ ($c = 0.515$ in CH_2Cl_2).

^1H NMR (400 MHz, CDCl_3): $\delta = 7.71$ (d, $^3J = 8.2$ Hz, 2H), 7.39-7.35 (m, 3H), 7.31 (s, 1H), 7.06 (t, $^3J = 7.5$ Hz, 2H), 6.98 (dd, $^3J = 8.3$ Hz, $^4J = 2.3$ Hz, 2H), 6.32 (br s, 2H), 4.34 (d, $^2J = 15.6$ Hz, 1H), 4.14 (d, $^2J = 13.8$ Hz, 1H), 3.24 (d, $^2J = 13.8$ Hz, 1H), 3.11 (d, $^2J = 15.5$ Hz, 1H), 0.41 (s, 9H), 0.31 (s, 9H).

^{13}C NMR (100 MHz, CDCl_3): $\delta = 208.4, 180.3, 152.3, 152.2, 138.9, 137.7, 134.0, 133.9, 127.3, 127.3, 127.1, 126.4, 126.1, 125.5, 123.8, 123.6, 114.7, 110.4, 109.5, 76.3, 75.4, 29.8, 26.4, 0.9, 0.5$.

IR (film): $\nu = 3236.0, 2953.4, 2852.7, 2065.9, 2010.4, 1996.9, 1575.1, 1342.2, 1248.2$ cm^{-1} .

HRMS (ESI+): m/z 675.13152 [$\text{M} + \text{H}$] $^+$ (calcd. for $\text{C}_{36}\text{H}_{35}\text{O}_6\text{Si}_2\text{Fe}$: 675.13277).

X-Ray Crystal structure analysis of complex (*R*)-**86**

Crystals suitable for X-ray diffraction analysis have been obtained by slow diffusion of hexane into a CH_2Cl_2 solution of complex (*R*)-**86**. Crystal data and details of data collection and refinement are given in Table 16. Intensity data were collected with a Bruker Apex II CCD area detector by using graphite monochromated Mo- $K\alpha$ radiation. Data reduction was performed with SAINT, and absorption corrections based on multiscan were obtained with SADABS.^[189] The structure was solved by direct methods using SHELXS-97 and refined by SHELXL-2013.^[190] The program ORTEPIII was used for graphics.^[191] Anisotropic thermal parameters were used for all non-hydrogen atoms. The isotropic thermal parameters of H atoms were fixed at 1.2 (1.5 for methyl groups) times those of the atom to which they were attached. All H atoms were placed in calculated positions and refined using a riding model with freely rotating methyl groups.

Table 16. Details of the crystal data and structure refinement for compound (*R*)-86

<i>Crystal Data</i>	
Empirical formula	C ₄₀ H ₄₄ FeO ₈ Si ₂
Moiety formula	C ₃₆ H ₃₄ FeO ₆ Si ₂ ·C ₄ H ₁₀ O·H ₂ O
Formula weight	764.78
Crystal system	Orthorhombic
Space group	<i>P</i> 2 ₁ 2 ₁ 2 ₁
<i>a</i> /Å	11.1452(5)
<i>b</i> /Å	16.4340(7)
<i>c</i> /Å	22.8671(10)
<i>V</i> /Å ³	4188.3(3)Å ³
<i>Z</i>	4
Temperature/K	130(2)
Density (calculated) <i>D_x</i> /Mg m ⁻³	1.213
Absorption coefficient <i>μ</i> /mm ⁻¹	0.464
Color, habit	orange, prism
Dimensions /mm	0.30×0.30×0.20
<i>Data Collection</i>	
radiation, <i>λ</i> /Å	Mo Kα, 0.71073
2 θ_{\max} /°	49.34
<i>h</i> range	-13→13
<i>k</i> range	-19→19
<i>l</i> range	-26→26
Measured reflections	55474
Independent reflections	7102
Reflections with <i>I</i> >2 σ (<i>I</i>)	6162
<i>R</i> _{int}	0.0577
<i>Refinement on F²</i>	
Data, restraints, parameters	7102, 1, 488
<i>S</i>	1.049
Final <i>R</i> , <i>wR</i> [<i>F</i> ² >2 σ (<i>F</i> ²)]	0.0377, 0.0920
Final <i>R</i> , <i>wR</i> (all data)	0.0478, 0.0985
Flack parameter	0.000(7)
(Δ / σ) _{max}	0.001
$\Delta\rho_{\max}$, $\Delta\rho_{\min}$ /eÅ ⁻³	0.359, -0.270

An ORTEP view of the complex is presented in Figure 30 and selected geometrical parameters are collected in Table 17. The structure includes one water molecule, disordered over three positions labelled Ow1, Ow2 and Ow3 with occupancies 0.4, 0.4 and 0.2, respectively (only Ow1 is shown in Figure 30 for clarity) and one Et₂O molecule. The latter, which is strongly hydrogen-bonded to one hydroxyl group (O1–H1) of the complex through its oxygen atom O7 (O1⋯O7, 2.752 Å; O1–H1⋯O7, 164.4°), was probably bonded to the complex during solubilization attempts made before the crystallization.

The crystal structure of (*R*)-86 shows typical geometrical parameters observed in related structures. In particular, the cyclopentadienone ring strongly deviates from planarity, with atom

C24 significantly bent away from the iron atom (see Table 17). The dihedral angle between the l.s. plane through the coordinated butadiene and the plane defined by C23, C24 and C25, $13.9(2)^\circ$, is typical for cyclopentadienone-iron complexes. The dihedral angle between the l.s. planes through the carbon atoms of the naphthyl moieties, $67.9(1)^\circ$, is quite similar to that found in other binaphthyl derivatives where the *ortho* positions are connected through a (diylidmethylene)cyclopentadienyl group. In Table 17 are also reported the relevant distances concerning atom O₂, which remarkably affects the level of enantioselectivity in ketone hydrogenation.

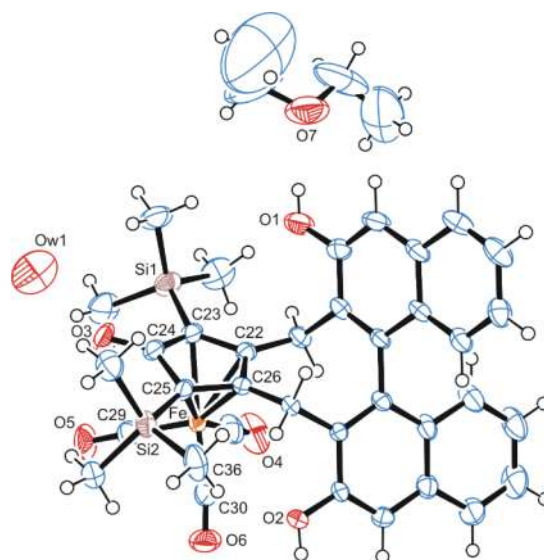
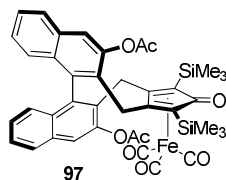


Figure 30. ORTEP view of the asymmetric unit of (*R*)-86·Et₂O·H₂O. Thermal ellipsoids are drawn at the 50% probability level (CCDC 1037376)

Table 17. Selected interatomic distances (Å) for (*R*)-86

Fe–C22	2.095(4)	O2…C29	5.356(3)
Fe–C26	2.115(4)	O2…O5	6.296(3)
Fe–C23	2.139(4)	O2…Fe	4.016(2)
Fe–C25	2.145(4)	O2…O3	6.429(2)
Fe–C24	2.310(4)	O2…Si2	4.408(2)
		O2…C36	3.641(4)

6.5.2. Complex (R)-97



Acetyl chloride (32 μL , 0.44 mmol, 3 eq) was slowly added to a stirred solution of (*R*)-**96** (100 mg, 0.15 mmol, 1 eq), Et_3N (83 μL , 0.59 mmol, 4 eq) and DMAP (1.6 mg, 0.015 mmol, 0.1 eq) in THF (2 mL), then the mixture was refluxed for 3 h. After this time, the mixture was diluted CH_2Cl_2 and washed with 0.5 M HCl (2 \times 5 mL), sat. aq. NaHCO_3 (5 mL) and brine (5 mL). The organic phase was then dried over Na_2SO_4 . Complex (*R*)-**97** – a pale yellow solid – was purified by flash column chromatography (90:10 to 85:15 hexane/ AcOEt).

Yield 103.3 g (92%); m.p. = 162-166 $^\circ\text{C}$; $[\alpha]_{\text{D}}^{22} = +19.37$ ($c = 0.51$ in CH_2Cl_2).

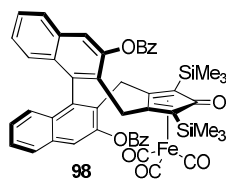
^1H NMR (400 MHz, CDCl_3): δ 7.90 (d, $^3J = 8.2$ Hz, 1H), 7.87 (d, $^3J = 8.2$ Hz, 1H), 7.80 (s, 1H), 7.73 (s, 1H), 7.52-7.43 (m, 2H), 7.25-7.17 (m, 2H), 6.99 (d, $^3J = 8.4$ Hz, 1H), 6.85 (d, $^3J = 8.4$ Hz, 1H), 4.00 (d, $^2J = 16.0$ Hz, 1H), 3.89 (d, $^2J = 14.3$ Hz, 1H), 3.36 (d, $^2J = 14.3$ Hz, 1H), 3.34 (d, $^2J = 16.0$ Hz, 1H), 2.45 (s, 3H), 2.39 (s, 3H), 0.45 (s, 9H), 0.32 (s, 9H).

^{13}C NMR (100 MHz, CDCl_3): δ 208.2, 181.0, 170.1, 169.8, 146.1, 138.8, 137.5, 133.0, 132.9, 130.2, 130.1, 128.7, 127.9, 127.8, 127.5, 127.0, 126.8, 126.7, 126.6, 121.6, 121.1, 112.0, 110.2, 74.9, 74.6, 27.5, 26.6, 22.3, 21.9, 0.9, 0.5.

IR (film): $\nu = 3062.4, 2953.9, 2923.6, 2903.3, 2852.7, 2062.5, 2007.5, 1989.7, 1768.4, 1624.25, 1189.4, 1155.6, 1087.7, 849.0$ cm^{-1} .

HRMS (ESI+): m/z 759.15207 [$\text{M} + \text{H}$] $^+$ (calcd. for $\text{C}_{50}\text{H}_{43}\text{O}_8\text{Si}_2\text{Fe}$: 759.15395).

6.5.3. Complex (R)-98



Benzoyl chloride (26 μL , 0.22 mmol, 3 eq) was slowly added to a stirred solution of (*R*)-**86** (50 mg, 0.07 mmol, 1 eq), Et_3N (41 μL , 0.3 mmol, 4 eq) and DMAP (0.8 mg, 0.007 mmol, 0.1 eq) in THF (1 mL), then the mixture was refluxed for 4 h. After this time, the mixture was diluted with CH_2Cl_2

and washed with 0.5 M HCl (2 × 5 mL), sat. aq. NaHCO₃ (5 mL) and brine (5 mL). The organic phase was then dried over Na₂SO₄. After concentration, the pure complex (*R*)-**98** - a pale yellow solid - was purified by flash column chromatography (95:5 to 9:1 hexane/EtOAc).

Yield 53 mg (81%); m.p. = 176 °C (dec.); [α]₄₃₆²⁷ = -108.6 (*c* = 0.25 in CH₂Cl₂).

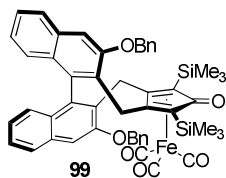
¹H NMR (400 MHz, CDCl₃): δ 8.26 (m, 1H), 8.24 (m, 1H), 8.21 (m, 1H), 8.19 (m, 1H), 7.92 (d, ³*J* = 4.7 Hz, 1H), 7.90 (d, ³*J* = 4.6 Hz, 1H), 7.83 (s, 1H), 7.82 (s, 1H), 7.72-7.64 (m, 2H), 7.59-7.46 (m, 6H), 7.31-7.26 (m, 2H), 7.01 (dd, ³*J* = 8.4, ⁴*J* = 0.6 Hz, 1H), 6.97 (dd, ³*J* = 8.5, ⁴*J* = 0.6 Hz, 1H), 4.01 (d, ²*J* = 14.5 Hz, 1H), 3.98 (d, ²*J* = 16.1 Hz, 1H), 3.58 (d, ²*J* = 14.6 Hz, 1H), 3.49 (d, ²*J* = 16.1 Hz, 1H), 0.10 (s, 9H), 0.03 (s, 9H).

¹³C NMR (100 MHz, CDCl₃): δ 208.1, 181.0, 167.0, 166.6, 147.3, 147.1, 139.0, 137.8, 134.2, 134.1, 133.3, 131.1, 130.7, 129.7, 129.7, 129.5, 129.2, 128.7, 127.8, 127.1, 126.9, 126.7, 121.1, 120.7, 113.2, 109.1, 75.7, 74.8, 27.7, 27.2, 0.7, 0.3.

IR (film): ν = 3062.9, 2953.9, 2897.5, 2062.0, 2007.5, 1990.2, 1740.4, 1624.7, 1266.0, 1246.3, 1090.1, 1022.1, 847.1, 711.1 cm⁻¹.

HRMS (ESI+): *m/z* 883.187411 [M + H]⁺ (calcd. for C₅₀H₄₃O₈Si₂Fe: 883.18537).

6.5.4. Complex (*R*)-**99**



Benzyl bromide (53 μ L, 0.45 mmol, 6 eq) was slowly added to a stirred solution of (*R*)-**86** (50 mg, 0.07 mmol, 1 eq) and K₂CO₃ (41 mg, 0.30 mmol, 4 eq) in DMF (0.37 mL) and stirred at 70 °C overnight. After this time, the reaction was cooled down to room temperature and diluted with Et₂O (8 mL). The mixture was washed with H₂O (3 × 5 mL) and the organic phase dried over Na₂SO₄. Complex (*R*)-**99** - a pale yellow solid - was purified by flash column chromatography (9:1 CH₂Cl₂/hexane).

Yield 42 mg (70%); m.p. = 155 °C (dec.); [α]_D³² = -20.6 (*c* = 0.92 in CH₂Cl₂).

¹H NMR (400 MHz, CDCl₃): δ 7.80 (d, ³*J* = 8.1 Hz, 1H), 7.71 (d, ³*J* = 8.1 Hz, 1H), 7.46-7.23 (m, 14H), 7.11-7.03 (m, 2H), 6.91-6.84 (m, 2H), 5.51 (d, ²*J* = 13.5 Hz, 1H), 5.46 (d, ²*J* = 13.5 Hz, 1H), 5.26 (d, ²*J*

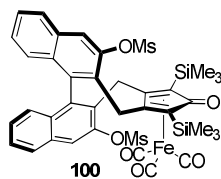
= 11.3 Hz, 1H), 5.17 (d, $^2J = 11.3$ Hz, 1H), 4.38 (d, $^2J = 15.6$ Hz, 1H), 4.29 (d, $^2J = 13.8$ Hz, 1H), 3.35 (d, $^2J = 13.8$ Hz, 1H), 3.15 (d, $^2J = 15.6$ Hz, 1H), 0.32 (s, 9H), 0.08 (s, 9H).

^{13}C NMR (100 MHz, CDCl_3): δ 208.6, 181.1, 154.1, 153.6, 139.0, 137.6, 136.7, 136.1, 133.8, 133.6, 129.1, 128.9, 128.7, 128.5, 128.1, 127.4, 127.4, 127.2, 127.1, 127.1, 127.0, 126.9, 126.9, 126.6, 126.4, 124.3, 124.3, 114.8, 108.7, 108.6, 107.3, 75.8, 75.1, 70.5, 70.1, 26.4, 26.2, 0.8, 0.2.

IR (film): $\nu = 3063.4, 3034.4, 2953.0, 2899.0, 2060.1, 2004.2, 1987.3, 1757.3, 1620.9, 1596.8, 1246.3, 1105.5, 850.5, 738.1$ cm^{-1} .

HRMS (ESI+): m/z 855.22583 $[\text{M} + \text{H}]^+$ (calcd. for $\text{C}_{50}\text{H}_{47}\text{O}_6\text{Si}_2\text{Fe}$: 855.22685).

6.5.5. Complex (R)-100



Methanesulfonyl chloride (17 μL , 0.22 mmol, 3 eq) was slowly added to a stirred solution of (R)-**86** (50 mg, 0.07 mmol, 1 eq), Et_3N (41 μL , 0.30 mmol, 4 eq) and DMAP (0.8 mg, 0.007 mmol, 0.1 eq) in THF (1 mL), then the mixture was refluxed for 5 h. After this time, the reaction was cooled down to room temperature, diluted with EtOAc (5 mL) and washed with 0.5 M HCl (2 \times 5 mL), sat. aq. NaHCO_3 (5 mL) and brine (5 mL). The organic phase was dried over Na_2SO_4 . After concentration, the pure complex (R)-**100** was obtained as a pale yellow solid.

Yield 40 mg (65%); m.p. = 172 $^\circ\text{C}$ (dec.); $[\alpha]_{\text{D}}^{27} = -6.8$ ($c = 1.4$ in CH_2Cl_2).

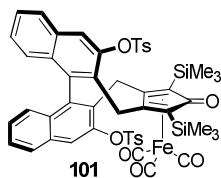
^1H NMR (400 MHz, CDCl_3): δ 8.12 (s, 1H), 8.09 (s, 1H), 7.99 (d, $^3J = 8.3$ Hz, 1H), 7.96 (d, $^3J = 8.3$ Hz, 1H), 7.56 (dd, $^3J = 8.3$ Hz, $^3J = 7.0$ Hz, 1H), 7.53 (dd, $^3J = 8.3$ Hz, $^3J = 6.9$ Hz, 1H), 7.33 (dd, $^3J = 8.4$ Hz, $^3J = 7.0$ Hz, 1H), 7.28 (dd, $^3J = 8.5$ Hz, $^3J = 6.9$ Hz, 1H), 6.99 (d, $^3J = 8.4$ Hz, 1H), 6.85 (d, $^3J = 8.5$ Hz, 1H), 4.25 (d, $^2J = 16.2$ Hz, 1H), 4.15 (d, $^2J = 14.4$ Hz, 1H), 3.35 (d, $^2J = 14.4$ Hz, 1H), 3.33 (d, $^2J = 16.2$ Hz, 1H), 3.31 (s, 3H), 3.29 (s, 3H), 0.45 (s, 9H), 0.33 (m, 9H).

^{13}C NMR (100 MHz, CDCl_3): δ 208.2, 181.4, 144.4, 143.5, 139.3, 138.0, 132.8, 132.7, 130.5, 130.5, 128.8, 128.5, 128.4, 128.2, 128.0, 127.8, 127.8, 127.7, 126.6, 126.3, 121.9, 121.4, 111.1, 110.1, 75.5, 75.1, 38.8, 38.6, 27.7, 26.7, 0.7, 0.5.

IR (film): $\nu = 3054.2, 2986.7, 2066.4, 2010.4, 1994.5, 1617.5, 1265.6, 739.1, 705.3$ cm^{-1} .

HRMS (ESI+): m/z 853.06820 $[\text{M} + \text{Na}]^+$ (calcd. for $\text{C}_{38}\text{H}_{38}\text{O}_{10}\text{S}_2\text{Si}_2\text{FeNa}$: 853.06985).

6.5.6. Complex (R)-101



p-Toluenesulfonyl chloride (43 mg, 0.22 mmol, 3 eq) was slowly added to a stirred solution of (R)-**86** (50 mg, 0.07 mmol, 1 eq), Et₃N (41 μ L, 0.03 mmol, 4 eq) and DMAP (0.8 mg, 0.007 mmol, 0.1 eq) in THF (1 mL), then the mixture was refluxed overnight. The reaction was cooled down to room temperature, diluted with EtOAc (5 mL) and washed with 0.5 M HCl (2 \times 5 mL), sat. aq. NaHCO₃ (5 mL) and brine (5 mL). The organic phase was dried over Na₂SO₄ and then concentrated. Complex (R)-**101** – a pale yellow solid – was purified by flash column chromatography (8:2 hexane/EtOAc). Yield 63 mg (96%); m.p. = 166-168 $^{\circ}$ C (dec.); $[\alpha]_D^{23} = +168.6$ ($c = 1.2$ in CH₂Cl₂).

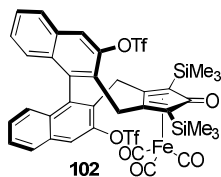
¹H NMR (400 MHz, CDCl₃): δ 7.92 (s, 1H), 7.85 (d, ³*J* = 8.3 Hz, 1H), 7.82 (d, ³*J* = 8.3 Hz, 1H), 7.79 (s, 1H), 7.70 (d, ³*J* = 8.0 Hz, 2H), 7.65 (d, ³*J* = 8.0 Hz, 2H), 7.51 (t, ³*J* = 7.5 Hz, 2H), 7.29-7.19 (m, 6H), 6.65 (d, ³*J* = 8.4 Hz, 1H), 6.54 (d, ³*J* = 8.5 Hz, 1H), 3.93 (d, ²*J* = 16.1 Hz, 1H), 3.92 (d, ²*J* = 14.3 Hz, 1H), 3.01 (d, ²*J* = 14.3 Hz, 1H), 2.86 (d, ²*J* = 16.1 Hz, 1H), 2.40 (s, 3H), 2.37 (s, 3H), 0.43 (s, 9H), 0.27 (s, 9H).

¹³C NMR (100 MHz, CDCl₃): δ 208.0, 181.3, 145.9, 145.9, 145.0, 145.0, 138.8, 137.3, 132.7, 132.5, 132.4, 130.2, 130.1, 130.0, 129.9, 129.3, 128.9, 128.8, 128.5, 128.4, 128.3, 127.4, 127.3, 127.3, 126.2, 126.1, 121.2, 121.2, 111.5, 108.6, 75.3, 74.9, 27.3, 26.4, 21.9, 21.9, 0.6, 0.6.

IR (film): $\nu = 3054.2, 2986.7, 2916.8, 2066.4, 2010.9, 1422.2, 1265.6, 895.8, 740.5, 705.3$ cm⁻¹.

HRMS (ESI+): m/z 983.14923 [M + H]⁺ (calcd. for C₅₀H₄₇O₁₀S₂Si₂Fe: 983.15069).

6.5.7. Complex (R)-102



N-(5-Chloro-2-pyridyl)bis(trifluoromethanesulfonimide) (1.2 g, 3.0 mmol, 3 eq) was added to a stirred solution of (R)-**86** (670 mg, 1.0 mmol, 1 eq), Et₃N (550 μ L, 4.0 mmol, 4 eq) and DMAP (12 mg, 0.1 mmol, 0.1 eq) in CH₂Cl₂ (30 mL) and stirred at room temperature overnight. The reaction

was diluted with CH₂Cl₂ (30 mL) and washed with 0.5 M HCl (2 × 50 mL), 0.5 M NaOH (2 × 50 mL) and brine (50 mL). The organic phase was then dried over Na₂SO₄. Complex (*R*)-**102** – a pale yellow solid – was purified by flash column chromatography (10:1 hexane/EtOAc).

Yield 882 mg (94%); m.p. = 142-143 °C (dec.); [α]_D²⁴ = +43.9 (c = 1.9 in CH₂Cl₂).

¹H NMR (400 MHz, CDCl₃): δ 8.14 (s, 1H), 8.12 (s, 1H), 8.03 (d, ³J = 8.5 Hz, 1H), 8.01 (d, ³J = 8.3 Hz, 1H), 7.62 (t, ³J = 7.5 Hz, 1H), 7.61 (t, ³J = 7.5 Hz, 1H), 7.40 (t, ³J = 8.2 Hz, 1H), 7.38 (t, ³J = 8.1 Hz, 1H), 6.90 (d, ³J = 8.5 Hz, 1H), 6.84 (d, ³J = 8.5 Hz, 1H), 4.18 (d, ²J = 16.2 Hz, 1H), 4.13 (d, ²J = 14.6 Hz, 1H), 3.40 (d, ²J = 14.7 Hz, 1H), 3.35 (d, ²J = 16.2 Hz, 1H), 0.41 (s, 9H), 0.31 (s, 9H).

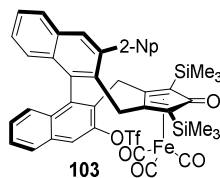
¹³C NMR (100 MHz, CDCl₃): δ 207.9, 181.3, 145.2, 144.9, 139.4, 137.9, 132.7, 132.6, 130.8, 130.7, 128.9, 128.8, 128.8, 128.7, 128.4, 128.3, 127.8, 127.1, 126.2, 126.0, 120.9, 120.8, 119.0 (q, ¹J_(C,F) = 324.5 Hz), 118.9 (q, ¹J_(C,F) = 324.5 Hz), 110.7, 108.7, 75.5, 75.5, 27.6, 26.8, 0.5, 0.4.

¹⁹F NMR (282 MHz, CDCl₃): δ -71.7, -72.7.

IR (film): ν = 3066.7, 2954.9, 2925.5, 2903.3, 2852.7, 2065.4, 2011.9, 1993.6, 1629.1, 1427.6, 1245.8, 1212.5, 1138.3, 915.5, 883.2, 844.7, 822.0 cm⁻¹.

HRMS (ESI+): *m/z* 961.01272 [M + Na]⁺ (calcd. for C₃₈H₃₂O₁₀F₆S₂Si₂FeNa: 961.01332).

6.5.8. Complex (*R*)-**103**



Complex (*R*)-**86** (100 mg, 0.1 mmol, 1 eq), Pd(OAc)₂ (4.5 mg, 0.02 mmol, 0.2 eq), PPh₃ (10.5 mg, 0.04 mmol, 0.4 eq), K₃PO₄ (63 mg, 0.3 mmol, 3 eq), KBr (26 mg, 0.22 mmol, 2.2 eq) and phenylboronic acid (30.5 mg, 0.25 mmol, 2.5 eq) were dissolved in dioxane (2.5 mL). The reaction was heated to 85 °C and stirred overnight. The mixture was diluted with CH₂Cl₂ (5 mL) and washed with 1 M NaOH (5 mL), H₂O (5 mL) and brine (5 mL), then dried over Na₂SO₄. Complex **103** – a yellow solid – was purified by flash column chromatography (7:3 CH₂Cl₂/hexane).

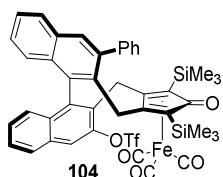
Yield 15 mg (17%).

¹H NMR (400 MHz, CDCl₃): δ 8.12 (s, 1H), 7.89-8.02 (m 6H), 7.81 (m, 2H), 7.62 (t, ³J(H,H) = 8.0, 1H), 7.54 (m, 3H), 7.41 (m 2H), 7.29 (t, ³J(H,H) = 8.0 Hz, 1H), 7.09 (m, 1H), 6.74 (d, ³J(H,H) = 8.0 Hz, 1H),

4.24 (d, $^2J(\text{H,H}) = 14.8$ Hz, 1H), 4.13 (d, $^2J(\text{H,H}) = 15.8$ Hz, 1H), 3.64 (d, $^2J(\text{H,H}) = 14.8$ Hz, 1H), 3.52 (d, $^2J(\text{H,H}) = 15.8$ Hz, 1H), 0.34 (s, 9H), -0.40 (s, 9H).

ESI-MS in CH_3CN : $[\text{M}+\text{H}]^{2+}$ m/z 917.2

6.5.9. Complex (R)-104



Complex (R)-**102** (100 mg, 0.1 mmol, 1 eq), $\text{Pd}(\text{OAc})_2$ (4.5 mg, 0.02 mmol, 0.2 eq), PPh_3 (10.5 mg, 0.04 mmol, 0.4 eq), K_3PO_4 (63 mg, 0.3 mmol, 3 eq), KBr (26 mg, 0.22 mmol, 2.2 eq) and phenylboronic acid (30.5 mg, 0.25 mmol, 2.5 eq) were dissolved in dioxane (2.5 mL). The reaction was heated to 85 °C and stirred overnight. The mixture was diluted with CH_2Cl_2 (5 mL) and washed with 1 M NaOH (5 mL), H_2O (5 mL) and brine (5 mL), then dried over Na_2SO_4 . Complex (R)-**103** – a yellow solid – was purified by flash column chromatography (6:4 to 8:2 CH_2Cl_2 /hexane).

Yield 69 mg (80%); m.p. = 157-158 °C (dec.); $[\alpha]_{\text{D}}^{21} = +88.3$ ($c = 0.6$ in CH_2Cl_2).

^1H NMR (400 MHz, CDCl_3): δ 8.10 (s, 1H), 8.01 (d, $^3J = 8.2$ Hz, 1H), 7.93 (d, $^3J = 8.2$ Hz, 1H), 7.90 (s, 1H), 7.63-7.31 (m, 8H), 7.26 (dd, $^3J = 8.5$ Hz, $^3J = 7.3$ Hz, 1H), 7.02 (d, $^3J = 8.5$ Hz, 1H), 6.70 (d, $^3J = 8.5$ Hz, 1H), 4.27 (d, $^2J = 14.8$ Hz, 1H), 4.11 (d, $^2J = 15.8$ Hz, 1H), 3.58 (d, $^2J = 14.8$ Hz, 1H), 3.50 (d, $^2J = 15.8$ Hz, 1H), 0.33 (s, 9H), -0.15 (s, 9H).

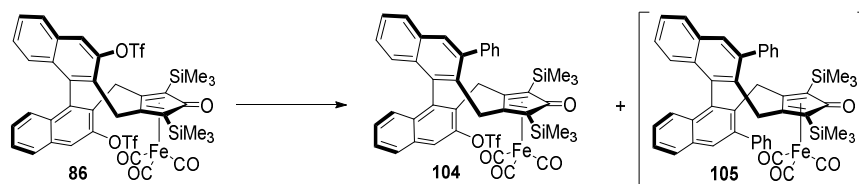
^{13}C NMR (100 MHz, CDCl_3): δ 208.1, 180.8, 144.9, 141.6, 141.3, 139.4, 136.1, 132.7, 132.5, 132.5, 132.1, 131.1, 130.9, 128.6, 128.3, 128.1, 127.9, 127.6, 127.4, 127.0, 126.4, 125.7, 120.0, 118.9 (q, $^1J_{\text{(C,F)}} = 321.3$ Hz), 111.8, 111.2, 75.9, 75.5, 29.5, 27.5, 0.5, 0.4.

^{19}F NMR (282 MHz, CDCl_3): δ -72.1.

IR (film): $\nu = 3054.7, 2987.2, 2065.4, 2009.5, 1639.7, 1421.8, 1265.6, 744.4, 705.3$ cm^{-1} .

HRMS (ESI+): m/z 889.10212 $[\text{M} + \text{Na}]^+$ (calcd. for $\text{C}_{43}\text{H}_{37}\text{O}_7\text{F}_3\text{S}_1\text{Si}_2\text{FeNa}$: 889.10049).

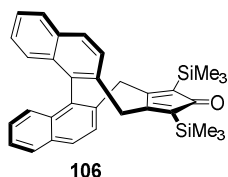
6.5.10. Conditions adopted for the attempted synthesis of complex 105



Entry	Catalyst	PhB(OH) ₂ [eq]	Base [eq]	Additive [eq]	T (°C)	Solvent	NMR ratio (%)		
							102	104	105
1 ^[151]	15% Pd(OAc) ₂ 18% PCy ₃	2.5	KF [3.3]		60	THF	97	3	-
2 ^[151]	15% Pd(OAc) ₂ 18% PCy ₃	2.5	KF [3.3]	KBr [2.2]	60	THF	97	3	-
3 ^[153]	25% Pd(OAc) ₂ 50% (S)-Phos	3	K ₃ PO ₄ [4]		85	toluene		100	-
4	20% Pd(OAc) ₂ 40% PPh ₃	2.5	K ₃ PO ₄ [3]		85	dioxane		80*	-
5	20% Pd(OAc) ₂ 40% PPh ₃	2.5	KBr [3]	KBr [2.2]	85	dioxane	2	80*	-
6 ^[150]	10% Pd(PPh ₃) ₄	2.5	K ₃ PO ₄ [3]	KBr [2.2]	85	dioxane	5	74*	-
7 ^[154]	[5%+5%] Pd(PPh ₃) ₄	2.5	K ₃ PO ₄ [3]	KBr [2.2]	85	dioxane		74*	-
8	10% Pd(PPh ₃) ₄	2.5	K ₃ PO ₄ [3]	KBr [2.2] H ₂ O [6]	85	dioxane		100	-
9	5% Pd(PPh ₃) ₄	2.5	K ₃ PO ₄ [3]	KBr [5.6]	110	dioxane		100	-
10	5% Pd(PPh ₃) ₄	2.5	K ₃ PO ₄ [5]		100	DMF	<i>degradation</i>		
11	5% Pd(PPh ₃) ₄	2.5	K ₃ PO ₄ [3]	TBAB [2.2]	85	dioxane	100		-
12	10% Pd(PPh ₃) ₄	5	K ₃ PO ₄ [6]	KBr [2.2]	85	dioxane/ H ₂ O	<i>degradation</i>		
13	10% Pd(PPh ₃) ₄	5	K ₃ PO ₄ [6]	KBr [2.2]	85	dioxane		100	-
14	5% Pd(PPh ₃) ₄	2.5	Ba(OH) ₂ · 8 H ₂ O [3]	KBr [2.2]	85	dioxane		100	-
15 ^[152]	10% Pd(PPh ₃) ₄	5	Ba(OH) ₂ · 8 H ₂ O [6]		85	DME/ H ₂ O	<i>degradation</i>		
16 ^[152]	10% Pd(PPh ₃) ₄	5	Ba(OH) ₂ · 8 H ₂ O [3]		85	DME/ H ₂ O	<i>degradation</i>		
17	10% Pd(PPh ₃) ₄	2.5	Ba(OH) ₂ [3]	KBr [2.2]	85	dioxane	65	35	-
18	5% Pd(PPh ₃) ₄	2.5	<i>t</i> BuOK [3]	KBr [2.2]	85	dioxane	<i>degradation</i>		
19 ^[155]	4% PEPPSI- <i>i</i> Pr	2.5	K ₂ CO ₃ [6]		60	dioxane	100		
20	5% PEPPSI- <i>i</i> Pr	2.5	K ₃ PO ₄ [3]		85	dioxane	100		
21	5% PEPPSI- <i>i</i> Pr	2.5	<i>t</i> BuOK [2.6]		60	<i>i</i> PrOH	<i>degradation</i>		
22 ^[156]	5% Pd(<i>i</i> Pr*) (cinnamyl)Cl	3	K ₂ CO ₃ [4]		40	EtOH	<i>degradation</i>		
23 ^[157]	5% NiCl ₂ (dppp)	4	K ₃ PO ₄ [8]		100	dioxane	<i>degradation</i>		
24	10% PdCl ₂ (dppp)	2.5	K ₃ PO ₄ [3]	KBr [2.2]	85	dioxane	50	50	-

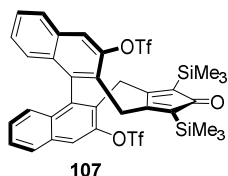
25	10% PdCl ₂ (dppp)	2.5	Ba(OH) ₂ · 8 H ₂ O [3]	KBr [2.2]	85	dioxane	50	50	-
-----------	---------------------------------	-----	---	-----------	----	---------	----	----	---

* Isolated yield

6.5.11. Free ligand 106

A solution of complex **58** (104 mg, 0.16 mmol, 1 eq), in THF (2.7 mL) and aqueous 1 M NaOH (1.3 mL) was stirred for 2.5 h under an argon atmosphere. Then 1-iodopentane was added (50 μ L, 0.38 mmol, 2.4 eq) and the yellow solution turned brown. After stirring the mixture for an additional 15 min under argon, H₃PO₄ (85%, 50 μ L) was added, the reaction stirred for 5 min and the organic layer separated. The aqueous layer was extracted with Et₂O (2 x 7 mL). The combined organic layers were dried over Na₂SO₄ and filtered through a short path of silica gel. After addition of Na₂S₂O₃·5 H₂O (105 mg) and Celite (65 mg) the filtrate was stirred slowly in the air for 16 h in the presence of daylight. Filtration through a short path of Celite, evaporation of the solvent, and flash chromatography (9:1 hexane/ CH₂Cl₂) of the residue on silica gel provided the free ligand **106**. Yield 79 mg (99%).

¹H NMR (400 MHz, CDCl₃): δ 7.95 (d, J = 8.4 Hz, 4H), 7.53 (d, J = 8.4 Hz, 2H), 7.51 – 7.46 (m, 2H), 7.30 (d, J = 3.6 Hz, 4H), 4.02 (d, J = 14.8 Hz, 2H), 3.22 (d, J = 14.8 Hz, 2H), 0.27 (s, 18H).

6.5.12. Free ligand 107

A solution of complex (*R*)-**102** (150 mg, 0.16 mmol, 1 eq), in THF (2.7 mL) and aqueous 1 M NaOH (1.3 mL) was stirred for 2.5 h under an argon atmosphere. Then 1-iodopentane was added (50 μ L, 0.38 mmol, 2.4 eq) and the yellow solution turned brown. After stirring the mixture for an additional 15 min under argon, H₃PO₄ (85%, 50 μ L) was added, the reaction stirred for 5 min and the organic layer separated. The aqueous layer was extracted with Et₂O (2 x 7 mL). The combined

organic layers were dried over Na₂SO₄ and filtered through a short path of silica gel. After addition of Na₂S₂O₃·5 H₂O (105 mg) and Celite (65 mg) the filtrate was stirred slowly in the air for 16 h in the presence of daylight. Filtration through a short path of Celite, evaporation of the solvent, and flash chromatography (9:1 hexane/CH₂Cl₂) of the residue on silica gel provided the free ligand **107**. Yield 35 mg (28%); m.p. = 204-207 °C; [α]_D²¹ = +112.4 (c = 0.6 in CH₂Cl₂).

¹H NMR (400 MHz, CDCl₃): δ 8.07 (s, 2H), 8.01 (d, ³J = 8.3 Hz, 2H), 7.62 (dd, ³J = 8.3, 6.4 Hz, 1H), 7.41 (dd, ³J = 8.4, 6.4 Hz, 1H), 7.20 (d, ³J = 8.5 Hz, 2H), 4.36 (d, ²J = 15.6 Hz, 2H), 3.06 (d, ²J = 15.6 Hz, 2H), 0.22 (s, 18H).

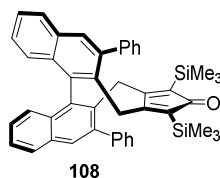
¹³C NMR (100 MHz, CDCl₃): δ 209.6, 164.7, 147.5, 138.9, 132.8, 132.1, 130.6, 129.1, 128.8, 128.3, 128.0, 126.7, 119.0, 118.9 (q, ¹J_(C,F) = 321.5 Hz), 30.1, 0.2.

¹⁹F NMR (282 MHz, CDCl₃): δ -72.75.

IR (film): ν = 2953.5, 2906.2, 1685.0, 1426.1, 1241.0, 1214.0, 1138.8, 847.1 cm⁻¹.

HRMS (ESI+): m/z 821.08966 [M + Na]⁺ (calcd. for C₃₅H₃₂O₇F₆S₂Si₂Na: 821.09244).

6.5.13. Free ligand **108**



(*R*)-5,16-Diphenyl-1,3-bis(trimethylsilyl)-4,17-dihydro-2*H*-cyclopenta[6,7]cycloocta[2,1-*a*:3,4-*a'*]dinaphthalen-2-one [**108**]

(*R*)-**107** (35 mg, 0.044 mmol, 1 eq), Pd(OAc)₂ (2 mg, 0.009 mmol, 0.2 eq), PPh₃ (4.6 mg, 0.018 mmol, 0.4 eq), K₃PO₄ (37 mg, 0.18 mmol, 3 eq), KBr (12 mg, 0.10 mmol, 2.2 eq) and phenylboronic acid (16 mg, 0.13 mmol, 3 eq) were dissolved in dioxane (1 mL). The reaction was stirred at 85 °C overnight. The mixture was diluted with CH₂Cl₂ (5 mL) and washed with 1 M NaOH (5 mL), H₂O (5 mL) and brine (5 mL), then dried over Na₂SO₄. Ligand (*R*)-**108** – a yellow solid – was purified by flash column chromatography (29:1 hexane/ CH₂Cl₂).

Yield 25 mg (86%); m.p. = 264-266 °C; [α]_D²⁰ = +150.5 (c = 0.5 in CH₂Cl₂).

¹H NMR (400 MHz, CDCl₃): δ 7.92 (d, ³J = 8.2 Hz, 2H), 7.79 (s, 2H), 7.51 (ddd, ³J = 8.1, 6.7 Hz, ⁴J = 1.2 Hz, 2H), 7.45-7.38 (m, 6H), 7.38-7.29 (m, 6H), 7.24 (d, ³J = 8.4 Hz, 2H), 4.00 (d, ²J = 15.4 Hz, 2H), 3.30 (d, ²J = 15.4 Hz, 2H), -0.20 (s, 18H).

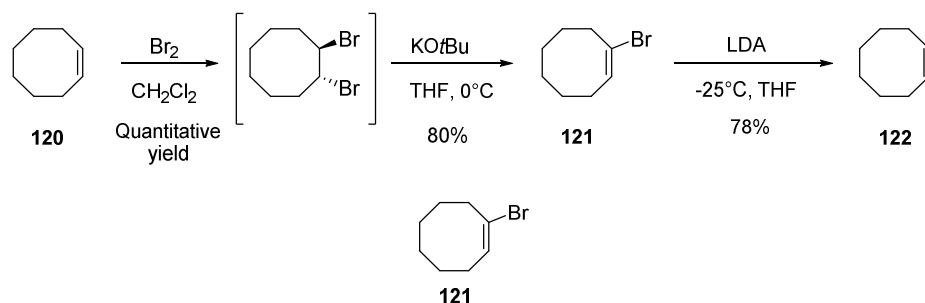
^{13}C NMR (100 MHz, CDCl_3): δ 210.8, 169.5, 142.1, 141.7, 137.7, 134.1, 132.3, 131.5, 129.9, 129.6, 128.6, 128.1, 127.5, 126.9, 126.5, 126.4, 33.8, 0.0.

IR (film): ν = 3058.6, 2958.8, 2896.1, 1679.7, 1542.3, 1245.3, 850.5, 748.2, 701.0 cm^{-1} .

HRMS (ESI+): m/z 655.28304 $[\text{M} + \text{H}]^+$ (calcd. for $\text{C}_{45}\text{H}_{43}\text{O}_1\text{Si}_2$: 655.28470).

6.6. Synthesis of (cyclopentadienone)iron tricarbonyl complexes using an intermolecular cyclative carbonylation/complexation

6.6.1. Cyclooctyne [122]



To a solution of cyclooctene (33.2 mL, 0.25 mol, 1 eq) in CH_2Cl_2 (100 mL) was added dropwise at -40°C a solution of Br_2 (0.25 mol) in CH_2Cl_2 (12 mL) until the yellow colour persisted. The reaction mixture was quenched with 10% $\text{Na}_2\text{S}_2\text{O}_3$ solution (50 mL) and extracted (2 x 100 mL) with CH_2Cl_2 . The organic layer was dried over Na_2SO_4 and concentrated *in vacuo* to give *trans*-1,2-dibromocyclooctane in quantitative yield, which was used in the following step without further purification.

^1H NMR (400 MHz, CDCl_3): δ 4.59–4.57 (m, 2H, CHBr), 2.46–2.37 (m, 2H), 2.15–2.05 (m, 2H), 1.88–1.81 (m, 2H), 1.70–1.56 (m, 4H), 1.54–1.46 (m, 2H).

^{13}C NMR (100 MHz, CDCl_3): 61.6, 33.3, 26.0, 25.5.

Trans-1,2-dibromocyclooctane (65.78 g, 244 mmol) was dissolved in THF (100 mL) and the resulting solution was added to a suspension of KOtBu (41.07 g, 370 mmol) in THF (40 mL) at 0°C . The reaction mixture was quenched with a saturated NH_4Cl -solution (100 mL), and THF was evaporated. The resulting crude was extracted with CH_2Cl_2 (2 x 100 mL). The organic layer was dried over Na_2SO_4 and concentrated *in vacuo*. The residue was purified by distillation (bp: $73\text{--}80^\circ\text{C}$ / 10 mbar) to obtain the 1-bromocyclooctene **121** as a colorless liquid.

Yield 36.8 g (80%).

^1H NMR (400 MHz, CDCl_3): δ 6.03 (t, $^3J = 8.5$ Hz, 1H), 2.58–2.64 (m, 2H), 2.08–2.19 (m, 2H), 1.51–1.62 (m, 8H).

^{13}C NMR (100 MHz, CDCl_3): 131.7, 35.2, 29.9, 28.6, 27.5, 26.4, 25.5.



122

1-Bromocyclooctene **121** (113.4 g, 0.60 mol) was added at once to a solution of lithium diisopropylamide, cooled at -25 °C. This solution was obtained by adding at -25 °C butyllithium (0.30 mol) in hexane (190 ml) to a mixture of dry diisopropylamine (32.3 g, 0.32 mol) and dry THF (125 mL). The temperature of the reaction mixture was allowed to rise gradually over a period of 45 min to 15 °C and was kept at this level for another 90 min. It was then poured into a cold solution of 3N hydrochloric acid. The solution was extract with pentane and the combined extracts were washed several times with water in order to remove the THF. The organic layer was dried over Na₂SO₄ and concentrated *in vacuo*. Careful distillation of the residue gave cyclooctyne (b.p. 50-55 °C / 20 torr).

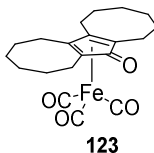
Yield 25.9 g (80%).

¹H NMR (400 MHz, CD₂Cl₂): δ 2.13 (m, 4H), 1.85 (m, 4H), 1.61 (m, 4H).

¹³C NMR (75 MHz, CD₂Cl₂): δ 94.90, 35.13, 30.32, 21.90.

IR (Nujol, selected band): ν = 2216 cm⁻¹ (C≡C stretch). Raman (Neat): 2217 cm⁻¹ (C≡C stretch).

6.6.2. [Bis(hexamethylene)cyclopentadienone]iron tricarbonyl complex **123**



123

Cyclooctyne **123** (230 μL, 1.85 mmol) and Fe(CO)₅ (1.2 mL, 9.25 mmol, 5 equiv) were dissolved in dry toluene (10 mL), under argon, and heated to 90 °C overnight in a sealed glass tube. After cooling down to room temperature, the reaction mixture was filtered through a pad of celite (rinsing with CH₂Cl₂). The filtrate was concentrated *in vacuo*, and the residue was purified by flash column chromatography (7:3 hexane/EtOAc) to obtain complex **123** as a yellow solid.

Yield 198 mg (56%); m.p. = 156 °C.

¹H NMR (400 MHz CDCl₃): δ 2.76-2.78 (m, 2H), 2.59-2.64 (m, 2H), 2.40-2.49 (m, 2H), 1.74-1.92 (m, 8H), 1.44-1.59 (m, 10H).

¹³C NMR (100 MHz CDCl₃): δ 209.35, 171.42, 102.42, 85.54, 31.29, 28.81, 26.24, 25.77, 23.70, 23.43.

FT-IR: $\nu = 2924.1, 2856.6, 2050.3, 1978.9, 1950.0, 1620.2, 1585.5, 1456.3, 1354.0, 1278.8, 1203.6, 1118.7, 1097.5, 1031.9, 987.5, 817.8, 736.8, 648.1, 621.1 \text{ cm}^{-1}$.

HRMS (ESI+): m/z 385.1098 $[M + H]^+$; 407.0919 $[M + Na]^+$ (calcd. for $C_{21}H_{25}O_4Fe$: 385,1102; $C_{20}H_{24}O_4FeNa$: 407.0922).

Table 18. X-Ray Crystal data and structure refinement of complex 123

Identification code	svf42	
Empirical formula	$C_{20}H_{24}FeO_4$	
Moiety formula	$C_{20}H_{24}FeO_4$	
Formula weight	384.24	
Temperature	100(2) K	
Wavelength	1.54178 Å	
Crystal system	Monoclinic	
Space group	$P2_1/n$	
Unit cell dimensions	$a = 9.7015(3) \text{ Å}$	$a = 90^\circ$
	$b = 16.0131(5) \text{ Å}$	$b = 102.5480(10)^\circ$
	$c = 11.9162(4) \text{ Å}$	$g = 90^\circ$
Volume	$1806.98(10) \text{ Å}^3$	
Z	4	
Density (calculated)	1.412 Mg/m^3	
Absorption coefficient	6.869 mm^{-1}	
F(000)	808	
Crystal size	$0.100 \times 0.100 \times 0.050 \text{ mm}^3$	
Theta range for data collection	4.699 to 72.289° .	
Index ranges	$-10 \leq h \leq 11, -19 \leq k \leq 19, -14 \leq l \leq 14$	
Reflections collected	18911	
Independent reflections	3539 $[R(\text{int}) = 0.0385]$	
Completeness to $\theta = 67.679^\circ$	99.5 %	
Absorption correction	Multiscan	
Max. and min. transmission	0.7536 and 0.5330	
Refinement method	Full-matrix least-squares on F^2	
Data / restraints / parameters	3539 / 0 / 244	
Goodness-of-fit on F^2	0.739	
Final R indices $[I > 2\sigma(I)]$	$R1 = 0.0315, wR2 = 0.0803$	
R indices (all data)	$R1 = 0.0347, wR2 = 0.0836$	
Extinction coefficient	n/a	
Largest diff. peak and hole	0.308 and -0.389 e.Å^{-3}	

Table 19. Selected bond lengths [Å] and angles [°] for complex 123

Fe(1)-C(3)	1.799(2)
Fe(1)-C(1)	1.8004(19)
Fe(1)-C(2)	1.801(2)
Fe(1)-C(7)	2.0718(17)
Fe(1)-C(6)	2.0789(17)
Fe(1)-C(8)	2.1140(17)
Fe(1)-C(5)	2.1246(18)
Fe(1)-C(4)	2.3968(18)
O(1)-C(1)	1.138(2)
O(2)-C(2)	1.142(3)
O(3)-C(3)	1.140(2)
O(4)-C(4)	1.241(2)
C(4)-C(8)	1.471(2)
C(4)-C(5)	1.478(2)
C(5)-C(6)	1.439(2)
C(6)-C(7)	1.429(3)
C(7)-C(8)	1.439(2)
C(8)-C(4)-C(5)	103.53(15)
C(6)-C(5)-C(4)	108.36(15)
C(7)-C(6)-C(5)	107.95(15)
C(6)-C(7)-C(8)	107.96(15)
C(7)-C(8)-C(4)	108.58(15)

Selected torsion angles [°]

C(4) C(5) C(6) C(7)	-11.83(19)
C(5) C(6) C(7) C(8)	0.03(19)
C(6) C(7) C(8) C(4)	11.84(18)
C(8) C(4) C(5) C(6)	18.37(18)
C(5) C(4) C(8) C(7)	-18.38(18)

C(7) C(6) C(15) C(16)	90.3(2)
C(6) C(5) C(20) C(19)	82.4(2)
C(8) C(7) C(14) C(13)	87.9(2)
C(7) C(8) C(9) C(10)	-79.7(2)

Planarity of 5-membered ring:

Distance from C(4) to lspl (C(5) C(6) C(7) C(8)) : 0.287(2)

see Listing

Least-Squares Planes - P*X+Q*Y+R*Z=S :: First Line Orthogonal(XO,YO,ZO), Second Line Fractional(X,Y,Z)

=====
Ring/Plan/Resd/Lspl N Indicates that the Ring/Plane/Residue Involves N Atoms

Sigref - R.M.S-Error of the Contributing Atoms

The Deviation D of an Atom with Sigpln - $\sqrt{\sum_{j=1:N}(D(j))^2/(N-3)}$

Chisq - Chi-Squared = $\sum_{j=1:N}(D(j))^2/\text{Sigref}^2$

Fractional Coordinates X,Y,Z may be Pl.Hyp. - Result of the Chi.Sq. Test for Planarity (See Stout & Jensen, p424)
Calculated via Substitution in

**** - Atoms Deviating by More Than 1.5 Angstrom and Hydrogen Atoms are NOT Listed

D = P*X + Q*Y + R*Z - S (2nd Line) Note - Weights : UNIT

**** - Maximum Metal Containing Ring Size: 6

- Maximum Number of Bonds to Ring Metal: 6

- Deviations from planes are in Ångström Units

- The Plane determining Atoms have been Marked #

- DISTANCES TO PLANES ROUNDED TO 3 DECIMALS

Nr 1 P Q R S Sigref 0.002 Sigpln 0.127 Chisq 10186.9 Pl.Hyp. P<5

Lspl 0.1670(9) 0.9829(2) 0.0781(9) 5.653(4) #C(4) 0.112(2) #C(5) -0.092(2) #C(6) 0.037(2)
#C(7) 0.036(2)

A 5 1.620(8) 15.739(3) 0.476(10) 5.653(4) #C(8) -0.092(2) O(4) 0.292(1) C(9) -0.086(2) C(10) 1.318(2)
C(14) 0.267(2) C(15) 0.219(2) C(19) 1.371(2) C(20) -0.060(2)

Nr 2 P Q R S Sigref 0.002 Sigpln 0.001 Chisq 0.2 Pl.Hyp.

Lspl 0.2121(10) 0.9643(3) 0.1586(11) 6.016(5) #C(5) 0.000(2) #C(6) 0.000(2) #C(7) 0.000(2)
#C(8) 0.000(2)

A 4 2.058(9) 15.441(5) 1.296(13) 6.016(5) O(4) 0.582(1) C(4) 0.287(2) C(9) 0.052(2) C(10) 1.461(2)
C(14) 0.121(2) C(15) 0.071(2) C(20) 0.076(2)

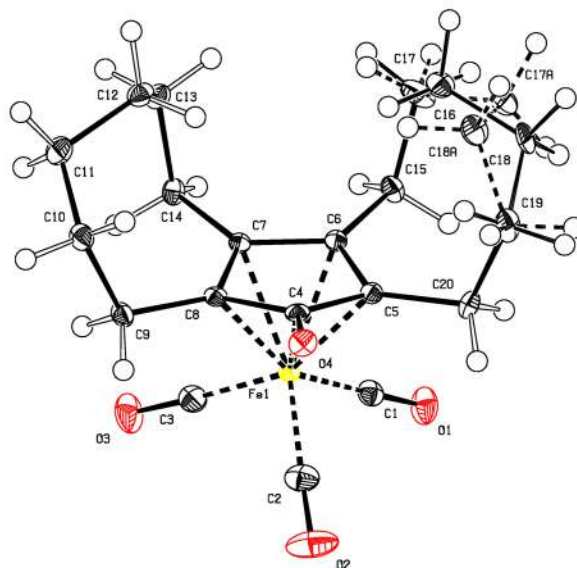
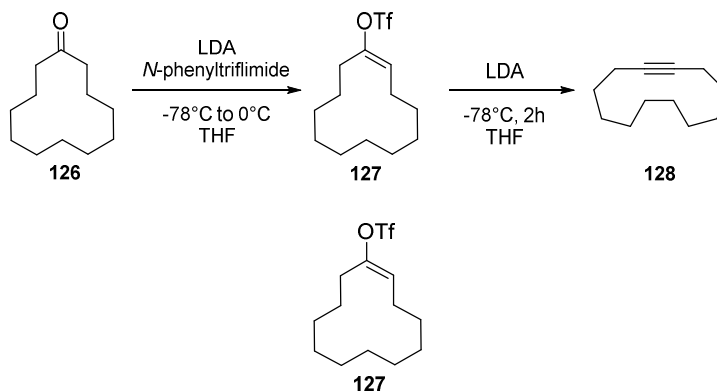


Figure 31. ORTEP diagram (CCDC 1511079) of the molecular structure of the [bis(hexamethylene)cyclopentadienone]iron complex 123

6.6.3. Cyclododecyne [128]



To a solution of cyclododecanone (1.0 g, 5.48 mmol) in 2 mL of THF was added lithium diisopropylamide (6.03 mL, 6.03 mmol, 1.1 eq) in 6 mL of THF at -78 °C. The resulting solution was stirred at -78 °C for 2 h at which time a solution of *N*-phenyltriflimide (2.09 g, 5.86 mmol, 1.07 eq) in 10 mL of THF was added and the reaction was allowed to warm to 0 °C. The reaction was maintained at this temperature until completion, as observed by TLC. The workup consisted of filtering the reaction solution through a plug of silica gel using ether as eluent. The solvent was removed under reduced pressure and the residue was purified by flash column chromatography (eluting with hexanes) furnishing an 85% yield of the corresponding vinyl triflate (1.47 g).

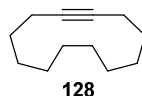
^1H NMR (400 MHz, CDCl_3): δ 5.37 (t, $J = 8.3$ Hz, 1H), 2.41 (t, $J = 6.3$ Hz, 2H), 2,25 (m, 2H), 1.55–1.25 (m, 16H).

^{13}C NMR (100 MHz, CDCl_3): δ 184.6, 123.8, 118.4 (q, $J = 319$ Hz), 33.2, 26.2, 25.7, 25.4, 25.3, 25.2, 24.5, 24.4, 24.2, 22.9.

IR (CHCl_3): $\nu = 1692, 1411, 1221, 1142$ cm^{-1} .

HRMS (ESI+): m/z 314.1160 $[\text{M} + \text{H}]^+$ (calcd. for $\text{C}_{13}\text{H}_{21}\text{F}_3\text{O}_3\text{S}$: 314.1163).

^1H NMR data of the contaminated *E*-isomer (8%): δ : 5.48 (t, $J = 8.3$ Hz, 1H), 2.45 (t, $J = 6.8$ Hz, 2H), 2.15 (dt, $J = 8.3, 6.8$ Hz, 2H), 1.70–1.25 (m, 16H).



To a solution of the vinyl triflate **127** (0.8 g, 2.54 mmol) in 1 mL of THF at -78 °C was added a solution of lithium diisopropylamide (5.08 mL, 5.08 mmol, 2 eq) in 1 mL of THF over 5 min. The reaction mixture was stirred at -78 °C for 2 h then poured into pentane/ H_2O . The aqueous phase

was extracted with pentane (3 x 10 mL) and the combined organic layers were washed with brine, dried over NaSO₄, filtered and concentrated *in vacuo*. Purification of the resulting oil by flash chromatography on silica gel (eluting with hexane) furnished cyclododecyne.

Yield 396 mg (95%).

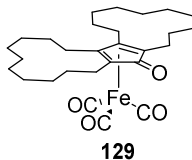
¹H NMR (400 MHz, CDCl₃): δ 2,20–2.17 (m, 4H), 1.58–1.51 (m, 8H), 1.47–1.40 (m, 8H).

¹³C NMR (100 MHz, CDCl₃): δ 81.6, 25.7, 25.5, 24.9, 24.6, 18.5.

IR (CHCl₃): ν = 1461, 1447, 1322 cm⁻¹.

HRMS (ESI+): *m/z* 164.1531 [M + H]⁺ (calcd. for C₁₂H₂₀: 164.1565).

6.6.4. [Bis(decamethylene)cyclopentadienone]iron tricarbonyl complex [129]



Cyclododecyne **128** (167 μL, 0.91 mmol) and Fe(CO)₅ (613 μL, 4.6 mmol, 5 eq) were dissolved in dry toluene (5 mL), under argon and heated to 110 °C overnight in a sealed glass tube. After cooling down to room temperature, the reaction mixture was filtered through a pad of celite (rinsing with CH₂Cl₂). The filtrate was concentrated *in vacuo*, and the residue was purified by flash column chromatography (6:4 hexane/EtOAc) to obtain complex **129** as a yellow solid.

Yield 12 mg (5%).

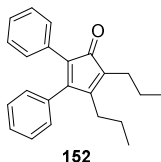
¹H NMR (400 MHz, CDCl₃): δ 2.37–2.35 (br, 4H), 2.10–2.08 (br, 2H), 1.94–1.97 (br, 2H), 1.78 (br, 2H), 1.56–1.30 (m, 27H), 1.21–1.19 (br, 3H).

¹³C NMR could not be registered

MS (ESI+): *m/z* 497.11 [M + H]⁺; 519.11 [M + Na]⁺ (calcd. for C₂₈H₄₁O₄Fe: 497.24; C₂₈H₄₀O₄FeNa: 519,22).

6.7. Towards a planar chirality

6.7.1. 2,3-diphenyl-4,5-dipropylcyclopenta-2,4-dien-1-one [152]



Diphenylcyclopropanone (400 mg, 1.94 mmol), 4-octyne (190 μ L, 1.3 mmol) and $[\text{RhCl}(\text{CO})_2]_2$ (5 mg, 1 mol%) were weighed out into a Schlenk with stirring bar under argon. To this was added toluene (600 μ L). The reaction was capped with a septum and heated at 80 $^{\circ}\text{C}$ for 7.5 h. The crude reaction mixture was then cooled to room temperature and purified by flash column chromatography pentane/ether (30:1) to yield compound **152** as an orange-red oil.

Yield 140 mg (34%).

^1H NMR (CDCl_3 , 400 MHz): 7.40-7.31 (m, 3H), 7.23 - 7.10 (m, 7H), 2.33 (t, $J = 8.0$ Hz, 2H), 2.23 (t, $J = 8.4$ Hz, 2H), 1.52 (m, 2H), 1.15 (m, 2H), 0.97 (t, $J = 7.6$ Hz, 3H), 0.78 (t, $J = 7.2$ Hz, 3H).

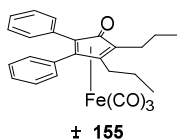
^{13}C NMR (CDCl_3 , 100 MHz) δ : 202.6, 156.4, 154.1, 134.6, 131.0, 129.7, 128.6, 128.2, 128.1, 127.8, 126.9, 126.5, 124.7, 28.5, 25.9, 22.9, 21.6, 14.3, 14.1.

FTIR (thin film): $\nu = 3396, 3056, 2960, 2931, 2870, 1949, 1881, 1805, 1707, 1600, 1573, 1498, 1463, 1443, 1357, 1339, 1307, 1090, 1071, 1027, 970, 914, 756, 691$ cm^{-1} .

HRMS (ESI+): m/z 339.1725 $[\text{M} + \text{Na}]^+$ (calcd. for $\text{C}_{23}\text{H}_{24}\text{NaO}$: 339.1731).

Elemental analysis (%): C 87.34, H 7.49 (calcd. for $\text{C}_{23}\text{H}_{24}\text{O}$: C 87.30, H 7.64).

6.7.2. Complex 155



(2,3-diphenyl-4,5-dipropylcyclopenta-2,4-dien-1-one)iron tricarbonyl complex [155]

Compound **152** (70 mg, 0.22 mmol) and $\text{Fe}(\text{CO})_5$ (207 μ L, 1.54 mmol, 7 eq) were dissolved in dry toluene (2 mL) in a glass tube autoclave, under argon and heated to 90 $^{\circ}\text{C}$ overnight. After cooling down to room temperature, the reaction mixture was filtered through a pad of celite (rinsing with CH_2Cl_2). The filtrate was concentrated *in vacuo*, and the residue was purified by flash column chromatography (9:1 cyclohexane/ Et_2O) to obtain complex **155** as an orange oil.

Yield 86 mg (80%).

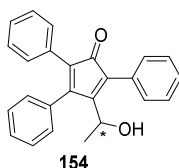
^1H NMR (400 MHz, CDCl_3): δ 7.70-7.67 (dd, $^3J = 7.8$, $^4J = 1.8$, 2H), 7.36-7.34 (m, 3H), 7.27-7.24 (dd, $^3J = 7.8$, $^4J = 1.8$, 2H), 7.18-7.14 (m, 3H), 2.57-2.47 (m, 1H), 2.36-2.33 (m, 1H), 2.23-2.16 (m, 2H), 1.88-1.80 (m, 1H), 1.69-1.59 (m, 1H), 1.35-1.27 (m, 1H), 1.09 (t, $^3J = 7.3$ Hz, 1H), 0.72 (t, $^3J = 7.3$ Hz, 1H).

^{13}C NMR (CDCl_3 , 100 MHz): δ 208.9, 171.7, 131.8, 131.2, 130.5, 129.2, 128.7, 128.5, 127.8, 127.4, 103.4, 102.4, 85.4, 80.9, 27.4, 26.7, 24.6, 22.8, 15.0, 14.3.

FTIR (thin film): $\nu = 2960.73$, 2931.8, 2872.01, 2058.05, 2000.18, 1980.89, 1710.86, 1637.56, 1600.92, 1577.77, 1498.69, 1463.97, 1446.61, 1411.89, 1379.1, 1336.67, 1313.52, 1276.88, 1261.45, 1188.15, 1157.29, 1122.57, 1087.85, 1074.35, 1051.2, 1028.06, 1001.06, 983.7, 970.19, 852.54, 802.39, 767.67, 744.52, 729.09, 694.37, 669.3, 613.36 cm^{-1} .

HRMS (ESI+): m/z 479.0908 [$\text{M} + \text{Na}$] $^+$ (calcd. for $\text{C}_{23}\text{H}_{24}\text{O}_4\text{FeNa}$: 479.0922).

6.7.3. 2,3,5-triphenyl-4-(1-hydroxy-1ethyl)-cyclopenta-2,4-dien-1-one [154]



Diphenylcyclopropanone (186 mg, 903 μmol) and 4-phenyl-but-3-yn-2-ol (88 mg, 602 μmol) were weighed out into a Schlenk with stir bar under nitrogen. To this was added dry toluene (2.0 mL) and $[\text{RhCl}(\text{CO})_2]_2$ (2.4 mg, 6.0 μmol). The tube was then capped with a septum and then heated at 110 $^\circ\text{C}$ overnight under nitrogen. The crude reaction mixture was then cooled to room temperature and purified by flash column chromatography (6:1 pentane/EtOAc). Product-containing fractions were collected and concentrated under reduced pressure to give a red solid. Yield 135 mg (64%); m. p. 59-61 $^\circ\text{C}$.

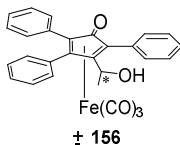
^1H NMR (CDCl_3 , 400 MHz): δ 7.46-7.34 (m, 10H), 7.20-7.13 (m, 5H), 4.93 (dq, $J_{\text{quart}} = 6.6$ Hz, $J_{\text{double}} = 6.5$ Hz, 1H), 1.60 (d, $J = 6.4$ Hz, 1H), 1.26 (d, $J = 6.7$ Hz, 3H).

^{13}C NMR (CDCl_3 , 100 MHz): δ 200.6, 157.4, 154.6, 134.7, 130.7, 130.4, 130.1 (2C), 129.8 (2C), 128.8 (2C), 128.7 (2C), 128.6, 128.3 (2C), 128.1, 127.9 (2C), 127.4, 126.4, 125.5, 65.3, 22.7.

FTIR (thin film): $\nu = 3523$, 3054, 2929, 2360, 2341, 1710, 1596, 1491, 1443, 1347, 1263, 1158, 1090, 1072, 1029, 1015, 910, 796, 740, 697 cm^{-1} .

HRMS (ESI+): m/z 352.1460 [M + Na]⁺ (calcd. for C₂₅H₂₀O₂: 352.1463).

6.7.4. Complex 156



(2,3,5-triphenyl-4-(1-hydroxy-1-ethyl)-cyclopenta-2,4-dien-1-one)iron tricarbonyl complex [**156**]

Compound **154** (80 mg, 0.23 mmol) and Fe(CO)₅ (153 μL, 1.13 mmol, 5 eq) were dissolved in dry toluene (2 mL) in a glass tube autoclave, under argon and heated to 90 °C overnight. After cooling down to room temperature, the reaction mixture was filtered through a pad of celite (rinsing with CH₂Cl₂). The filtrate was concentrated *in vacuo*, and the residue was purified by flash column chromatography (6:1 hexane/EtOAc) to obtain complex **156** as an orange oil.

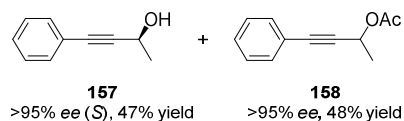
Yield 86 mg (80%).

¹H NMR (400 MHz, CDCl₃): δ 7.74-7.42 (br, 10 H), 7.28-7.10 (br, 5H), 4.53 (br, 1H), 1.53-1.12 (br, 3H), 0.79 (br, 1H).

¹³C NMR could not be registered

HRMS (ESI+): m/z 479.0908 [M + Na]⁺ (calcd. for C₂₃H₂₄O₄FeNa: 479.0922).

6.7.5. Racemic resolution of 4-phenyl-but-3-yn-2-ol



To a hazy yellow solution of 0.3 g of racemic alcohol **153** in 20 mL of dry hexane and activated 4Å molecular sieves, at room temperature and under Argon, 0.69 g of vinyl acetate were added giving a clear solution. To this solution 0.15 g (0.5 mass equiv) of the Amano Lipase AK were added and the resulting brown suspension was stirred vigorously. The solution was stirred at 25 °C and the course of the reaction was followed by ¹H NMR. After 7 h, ¹H NMR indicated 52% conversion. The solution was filtered through a medium-fritted funnel, saving the recovered enzyme and volatiles were removed by reduced pressure giving a crude yellow oil. The crude product was chromatographed, eluting 20:1 hexane:EtOAc to afford the acetate and the alcohol.

(*R*)-acetate, **158**: 29.5 g (50%) as a light yellow oil, [α]_D = + 173 (c 0.42, MeOH), 98% *ee*.

The column was then eluted with 1:1 hexane:EtOAc to elute the alcohol:

(*S*)-4-phenyl-but-3-yn-2-ol, **156**: 24.7 g (49.5%) as a light yellow oil. $[\alpha]_D = -31$ (c 0.77, MeOH), 96% *ee*.

^1H NMR (400 MHz, CDCl_3): 7.42 (m, 2H), 7.27 (m, 3H), 4.75 (q, $J = 6.6$ Hz, 1H), 2.81 (br s, 1H), 1.54 (d, $J = 6.6$ Hz, 3H).

^{13}C NMR (100 MHz, CDCl_3): 131.6, 128.3, 128.2, 125.5, 90.9, 83.9, 58.7, 24.3.

6.8. General procedure for hydrogenation

6.8.1. General procedure for hydrogenation reactions with Me₃NO as activator

Hydrogenations were run in a 450 mL Parr autoclave equipped with a removable aluminum block that can accommodate up to fifteen magnetically stirred 7 mL glass vials. The pre-catalyst [0.01 mmol (2 mol%) or 0.005 mmol (1 mol%)] was weighed in glass vials, which were accommodated in the aluminum block after adding magnetic stir bars in each of them. The block was placed in a Schlenk tube, where it was subjected to three vacuum/nitrogen cycles. *i*PrOH (0.25 mL) was added to each vial, and stirring was started. Me₃NO [2 eq respect to the catalyst, 0.02 mmol (4 mol%) or 0.01 mmol (2 mol%)] was added to each vial as an H₂O solution (0.1 mL). After stirring at room temperature under nitrogen for 10 min, the substrate (0.5 mmol) was added to the mixture. Each vial was capped with a Teflon septum pierced by a needle, the block was transferred into the autoclave, and stirring was started. After purging four times with hydrogen at the selected pressure, heating was started. The reactions were stirred under hydrogen pressure overnight and then filtered through a pad of celite and analyzed for determining the conversion. Conversions were determined by ¹H-NMR, ¹⁹F-NMR or by GC for conversion and *ee* determination.

6.8.2. General procedure for photolytically induced hydrogenation

Hydrogenation experiments were carried out in a custom-made glass autoclave equipped with a thick-walled glass reaction vessel (total capacity 20 mL, maximum pressure 25 bar), a single inlet valve, a manometer, and safety relieve valve. UV irradiation experiments were carried out in a Rayonet RPR-100 (Southern New England UV Company, USA). The UV lamps used have the specification F8T5BLB, 8 W, 352 nm (Sanyo Denki, Japan).

Acetophenone (5.50 μL, 47.1 μmol, 1 equiv) and dodecane (8.0 μL, 44.0 μmol) were dissolved in toluene (1.0 mL) in a glass autoclave (20 mL capacity) under a stream of argon. A 0.0236 mM toluene stock solution of the iron pre-catalyst (0.1 mL, 2.36 μmol, 0.05 equiv) was added. The autoclave was sealed and filled with and then carefully discharged from argon (14 to 1 bar) and it was purged for three times with hydrogen (14 bar). After the last fill/vent cycle, the autoclave was loaded with hydrogen (14 bar) and discharged to the desired reaction pressure (10 bar). The vessel was placed in a Rayonet RPR-100 (Southern New England UV Company) and irradiated (λ_{max} = 350 nm). The reaction mixture was stirred under hydrogen pressure and 40 °C as indicated by the total reaction time. Conversions were determined by GC using dodecane as internal standard.

6.8.3. General procedure for the transfer hydrogenation

A 10 mL Schlenk was charged with a stir bar and the iron complex (0.01 mmol, 0.02 eq) in *i*PrOH (1 mL), followed by addition of a stock solution of Me₃NO (1.5 mg, 0.02 mmol, 0.04 eq) in H₂O (0.4 mL). After stirring for 5 min, acetophenone (117 μ L, 120.2 mg, 1.0 mmol, 1 eq) was added, and the obtained mixture was heated at 70 °C and stirred for 16 h. Conversions were determined by GC using dodecane as internal standard.

6.8.4. Conditions for conversion and *ee* determination by GC for products in Table 9

Products' absolute configurations (Table 9, paragraph 4.3.4) were assigned by comparison of the sign of optical rotation with literature data (see the references cited for each compound).

(S)-1-Phenylethanol (GC): capillary column: MEGADEX DACTBS β , diacetyl-*tert*-butylsilyl- β -cyclodextrin, 0.25 μ m; diameter = 0.25 mm; length = 25 m; carrier: hydrogen; inlet pressure: 1 bar; oven temperature: 95 °C for 20 min: $t_{\text{substrate}}$ = 6.0 min; $t_{\text{product}(R)}$ = 13.2 min; $t_{\text{product}(S)}$ = 15.1 min.^[193]

(S)-1-(4-(Trifluoromethyl)phenyl)ethanol (GC): capillary column: MEGADEX DACTBS β , diacetyl-*tert*-butylsilyl- β -cyclodextrin, 0.25 μ m; diameter = 0.25 mm; length = 25 m; carrier: hydrogen; inlet pressure: 1 bar; oven temperature: 110 °C for 20 min: $t_{\text{substrate}}$ = 6.4 min; $t_{\text{product}(R)}$ = 14.3 min; $t_{\text{product}(S)}$ = 15.4 min.^[194]

(S)-1-(4-Methoxyphenyl)ethanol (GC): capillary column: MEGADEX DACTBS β , diacetyl-*tert*-butylsilyl- β -cyclodextrin, 0.25 μ m; diameter = 0.25 mm; length = 25 m; carrier: hydrogen; inlet pressure: 1 bar; oven temperature: 110 °C for 10 min; 30 °C/min gradient; 120 °C for 10 min; 30 °C/min gradient; 130 °C: $t_{\text{substrate}}$ = 20.1 min; $t_{\text{product}(R)}$ = 21.1 min; $t_{\text{product}(S)}$ = 22.6 min.^[195]

(S)-1-(4-Chlorophenyl)ethanol (GC): capillary column: MEGADEX DACTBS β , diacetyl-*tert*-butylsilyl- β -cyclodextrin, 0.25 μ m; diameter = 0.25 mm; length = 25 m; carrier: hydrogen; inlet pressure: 1 bar; oven temperature: 110 °C for 10 min; 30 °C/min gradient; 120 °C for 10 min; 30 °C/min gradient; 130 °C: $t_{\text{substrate}}$ = 12.8 min; $t_{\text{product}(R)}$ = 23.4 min; $t_{\text{product}(S)}$ = 24.3 min.^[195]

(S)-1-(Naphthalen-2-yl)ethanol (GC): capillary column: MEGADEX DACTBS β , diacetyl-*tert*-butylsilyl- β -cyclodextrin, 0.25 μ m; diameter = 0.25 mm; length = 25 m; carrier: hydrogen; inlet pressure: 1 bar; oven temperature: 150 °C for 20 min: $t_{\text{substrate}}$ = 10.6 min; $t_{\text{product}(R)}$ = 16.9 min; $t_{\text{product}(S)}$ = 17.9 min.^[195]

(S)-1-Phenylpropan-1-ol (GC): capillary column: MEGADEX DACTBS β , diacetyl-*tert*-butylsilyl- β -cyclodextrin, 0.25 μ m; diameter = 0.25 mm; length = 25 m; carrier: hydrogen; inlet pressure: 1 bar; oven temperature: 95 °C for 20 min: $t_{\text{substrate}}$ = 9.4 min; $t_{\text{product}(R)}$ = 16.6 min; $t_{\text{product}(S)}$ = 18.5 min.^[196]

(S)-1-Cyclohexylethanol (GC): capillary column: MEGADEX DACTBS β , diacetyl-*tert*-butylsilyl- β -cyclodextrin, 0.25 μ m; diameter = 0.25 mm; length = 25 m; carrier: hydrogen; inlet pressure: 1 bar; oven temperature: 120 °C for 20 min: $t_{\text{substrate}}$ = 4.9 min; $t_{\text{product(S)}}$ = 6.2 min; $t_{\text{product(R)}}$ = 7.6 min.^[197]

(S)-1,2,3,4-Tetrahydronaphthalen-1-ol (GC): capillary column: MEGADEX DACTBS β , diacetyl-*tert*-butylsilyl- β -cyclodextrin, 0.25 μ m; diameter = 0.25 mm; length = 25 m; carrier: hydrogen; inlet pressure: 1 bar; oven temperature: 120 °C for 20 min: $t_{\text{substrate}}$ = 9.5 min; $t_{\text{product(R)}}$ = 11.0 min; $t_{\text{product(S)}}$ = 12.2 min.^[198]

(R)-2,3-Dihydro-1H-inden-1-ol (GC): capillary column: MEGADEX DACTBS β , diacetyl-*tert*-butylsilyl- β -cyclodextrin, 0.25 μ m; diameter = 0.25 mm; length = 25 m; carrier: hydrogen; inlet pressure: 1 bar; oven temperature: 110 °C for 20 min: $t_{\text{substrate}}$ = 12.9 min; $t_{\text{product(S)}}$ = 11.8 min; $t_{\text{product(R)}}$ = 14.2 min.^[199]

rac-4-Methylpentan-2-ol (GC): capillary column: MEGADEX DACTBS β , diacetyl-*tert*-butylsilyl- β -cyclodextrin, 0.25 μ m; diameter = 0.25 mm; length = 25 m; carrier: hydrogen; inlet pressure: 1 bar; oven temperature: 120 °C for 20 min): $t_{\text{substrate}}$ = 10.6 min; $t_{\text{en.1}}$ = 11.6 min; $t_{\text{en.2}}$ = 13.5 min.

(S)-1-(Naphthalen-1-yl)ethanol (GC and HPLC): GC conditions for conversion determination: capillary column: MEGADEX DACTBS β , diacetyl-*tert*-butylsilyl- β -cyclodextrin, 0.25 μ m; diameter = 0.25 mm; length = 25 m; carrier: hydrogen; inlet pressure: 1 bar; oven temperature: 150 °C for 15 min): $t_{\text{substrate}}$ = 8.0 min; $t_{\text{product(R+S)}}$ = 10.4 min. HPLC conditions of *ee* determination: column: Daicel Chiralcel OD-H; eluent: 9:1 *n*-hexane/*i*PrOH; flow: 1 mL/min; λ = 210 nm; $t_{\text{substrate}}$ = 7.1 min; $t_{\text{product(S)}}$ = 9.3 min; $t_{\text{product(R)}}$ = 13.3 min.^[195]

(S)-1-(Pyridin-3-yl)ethanol (GC and HPLC): GC conditions for conversion determination: capillary column: MEGADEX DACTBS β , diacetyl-*tert*-butylsilyl- β -cyclodextrin, 0.25 μ m; diameter = 0.25 mm; length = 25 m; carrier: hydrogen; inlet pressure: 1 bar; oven temperature: 130 °C for 15 min: $t_{\text{substrate}}$ = 3.4 min; $t_{\text{product(R+S)}}$ = 12.0 min. HPLC conditions of *ee* determination: column: Daicel Chiralcel OB-H; eluent: 9:1 *n*-hexane/*i*PrOH; flow: 0.8 mL/min; λ = 210 nm; $t_{\text{product(S)}}$ = 10.6 min; $t_{\text{product(R)}}$ = 17.4 min; $t_{\text{substrate}}$ = 20.1 min.^[170]

(S)-3,3-Dimethylbutan-2-ol (GC): capillary column: CP-Chirasil-Dex CB, 0.25 μ m; diameter = 0.25 mm; length = 25 m; carrier: hydrogen; inlet pressure: 1.89 bar; oven temperature: 60 °C for 11 min: $t_{\text{substrate}}$ = 3.3 min; $t_{\text{product(S)}}$ = 10.1 min; $t_{\text{product(R)}}$ = 10.6 min.^[200]

(R)-1,2,3,4-Tetrahydronaphthalen-2-ol (GC): the product was derivatized as acetate before injection. Capillary column: MEGADEX DACTBS β , diacetyl-*tert*-butylsilyl- β -cyclodextrin, 0.25 μ m; diameter = 0.25 mm; length = 25 m; carrier: hydrogen; inlet pressure: 1 bar; oven temperature: 110 °C for 40 min: $t_{\text{product(R)}}$ = 29.3 min; $t_{\text{product(S)}}$ = 30.3 min; $t_{\text{substrate}}$ = 35.1 min.^[201]

6.8.5. NMR conversion and conditions for conversion by GC for products in Table 12

NMR conversions (Table 12, paragraph 4.4.1) were calculated from the signal integrals (all the substrates and reduction products are known compounds, and the spectra are superimposable to those reported in the literature). The NMR spectra were measured taking $d_1 = 20$ s.

1-Phenylethanol: Capillary column: MEGADEX DACTBS β , diacetyl-tert-butylsilyl- β -cyclodextrin, 0.25 μ m; diameter = 0.25 mm; length = 25 m; carrier: hydrogen; inlet pressure: 1 bar; oven temperature: 95 °C for 20 min: $t_{\text{substrate}} = 6.0$ min; $t_{\text{product(R)}} = 13.2$ min; $t_{\text{product(S)}} = 15.1$ min. After the hydrogenation, the volatiles were evaporated and the residue was purified by flash column chromatography (eluent: 9:1 hexane/AcOEt). The product was isolated as a colorless oil. Yield: 239 mg (98%). Its physical and spectroscopic data are superimposable with those reported in the literature. $^1\text{H-NMR}$ (300 MHz, CDCl_3): δ 7.43-7.34 (m, 4H), 7.33-7.28 (m, 1H), 4.92 (q, $J = 6.5$ Hz, 1H), 1.91 (s, 1H), 1.53 (d, $J = 6.5$ Hz, 3H).^[202]

1-(3-Nitrophenyl)ethanol: $^1\text{H-NMR}$ (300 MHz, CDCl_3): δ 8.22 (s, 1H), 8.09 (d, $J = 6.8$ Hz, 1H), 7.70 (d, $J = 6.8$ Hz, 1H), 7.49 (t, $J = 6.0$ Hz, 1H), 5.01 (q, $J = 6.0$ Hz, 1H), 2.73 (br s, 1H), 1.52 (d, $J = 6.0$ Hz, 3H).^[202]

1-(4-Methoxyphenyl)ethanol: After the hydrogenation, the volatiles were evaporated and the residue was purified by flash column chromatography (eluent: 9:1 hexane/AcOEt). The product was isolated as a colorless oil. Yield: 298 mg (98%). Its physical and spectroscopic data are superimposable with those reported in the literature. $^1\text{H-NMR}$ (300 MHz, CDCl_3): δ 7.32 (d, $J = 8.7$ Hz, 2H), 6.91 (d, $J = 8.7$ Hz, 2H), 4.88 (q, $J = 6.4$ Hz, 1H), 3.83 (s, 3H), 1.82 (br s, 1H), 1.50 (d, $J = 6.4$ Hz, 3H).^[202]

4-Bromophenyl)ethanol: After the hydrogenation, the volatiles were evaporated and the residue was purified by flash column chromatography (eluent: 9:1 hexane/AcOEt). The product was isolated as a white solid. Yield: 390 mg (97%). Its physical and spectroscopic data are superimposable with those reported in the literature. $^1\text{H-NMR}$ (300 MHz, CDCl_3): δ 7.49 (d, $J = 8.4$ Hz, 2H), 7.27 (d, $J = 8.4$ Hz, 2H), 4.89 (q, $J = 6.5$ Hz, 1H), 1.85 (s, 1H), 1.49 (d, $J = 6.5$ Hz, 3H).^[203]

1-(2-Methoxyphenyl)ethanol: $^1\text{H-NMR}$ (300 MHz, CDCl_3): δ 7.33 (d, $J = 7.6$ Hz, 1H), 7.24 (dt, $J = 7.6, 1.6$ Hz, 1H), 6.95 (t, $J = 7.6$ Hz, 1H), 6.87 (d, $J = 7.6$ Hz, 1H), 5.09 (q, $J = 6.4$ Hz, 1H), 3.84 (s, 3H), 2.74 (br s, 1H), 1.49 (d, $J = 6.4$ Hz, 3H).^[203]

1-(2-Chlorophenyl)ethanol: $^1\text{H-NMR}$ (300 MHz, CDCl_3): δ 7.56 (d, $J = 7.6$ Hz, 1H), 7.29 (m, 2H), 7.18 (d, $J = 7.6$ Hz, 1H), 5.26 (d, $J = 6.4$ Hz, 1H), 2.45 (br s, 1H), 1.45 (d, $J = 6.4$ Hz, 3H).^[203]

1-(Pyridin-2-yl)ethanol: $^1\text{H-NMR}$ (300 MHz, CDCl_3): δ 8.52 (d, $J = 7.7$ Hz, 1H), 7.69 (t, $J = 7.9$ Hz, 1H), 7.30 (d, $J = 7.9$ Hz, 1H), 7.19 (t, $J = 7.9$ Hz, 1H), 4.90 (d, $J = 6.5$ Hz, 1H), 4.46 (br s, 1H), 1.50 (d, $J = 6.5$ Hz, 3H).^[202]

1,2,3,4-Tetrahydronaphthalen-1-ol: Hydrogenated product (conv. = 80%): $^1\text{H-NMR}$ (300 MHz, CDCl_3): δ 7.44 (m, 1H), 7.24-7.19 (m, 2H), 7.13-7.10 (m, 1H), 4.76 (s, 1H), 2.87-2.70 (m, 2H), 2.01-1.76 (m, 5H).

Residual starting material (20%): $^1\text{H-NMR}$ (300 MHz, CDCl_3): δ 8.03 (d, $J = 8.0$ Hz, 1H), 7.46 (t, $J = 7.6$ Hz, 1H), 7.30 (t, $J = 7.6$ Hz, 1H), 7.25 (d, $J = 7.6$ Hz, 1H), 2.96 (t, $J = 6.0$ Hz, 2H), 2.65 (t, $J = 6.4$ Hz, 2H), 2.17-2.10 (m, 2H).^[203]

Octan-3-ol: $^1\text{H-NMR}$ (300 MHz, CDCl_3): δ 3.53 (br s, 1H), 1.25-1.56 (m, 11H), 0.86-0.97 (m, 6H).^[204]

1-Cyclopropylethanol: $^1\text{H-NMR}$ (300 MHz, CDCl_3): δ 3.05 (dq, $J = 8.3, 6.2$ Hz, 1H), 1.85 (s, 1H), 1.25 (d, $J = 6.2$ Hz, 3H), 0.91-0.84 (m, 1H), 0.48-0.46 (m, 2H), 0.26-0.23 (m, 1H), 0.17-0.15 (m, 1H).^[205]

4-Phenylbut-3-en-2-ol: $^1\text{H-NMR}$ (300 MHz, CDCl_3): δ 7.18-7.39 (5H, m), 6.53-6.58 (1H, m), 6.22-6.29 (1H, m), 4.46-4.50 (1H, m), 1.36 (d, $J = 6.0$ Hz, 3H).^[206]

4-Phenylbutan-2-ol: $^1\text{H-NMR}$ (300 MHz, CDCl_3): δ 7.18-7.39 (m, 5H), 3.78-3.85 (m, 1H), 2.63-2.75 (m, 2H), 3.78-3.85 (m, 1H), 1.78 (br s, 1H), 1.75-1.77 (m, 2H), 1.22 (d, $J = 6.0$ Hz, 3H).^[207]

3,5,5-Trimethylcyclohex-2-enol: Hydrogenated product (conv. = 15%): $^1\text{H-NMR}$ (300 MHz, CDCl_3): δ 5.89 (s, 1H), 2.20 (2H, s), 2.17 (s, 2H), 1.94 (s, 3H), 1.04 (s, 6H).

Residual starting material (85%): $^1\text{H-NMR}$ (300 MHz, CDCl_3): δ 5.43 (m, 1H), 4.25 (m, 1H), 1.87-1.74 (m, 10H), 1.68 (s, 3H), 1.96-2.10 (m, 1H).^[206]

2-Methylcyclopentan-1-ol (mixture of *trans* and *cis* isomer): *Trans* isomer: $^1\text{H-NMR}$ (300 MHz, CDCl_3): δ 3.73 (q, $J = 6.0$ Hz, 1H), 1.31-1.89 (m, 8H), 1.20 (d, $J = 7.0$ Hz, 3H).

Cis isomer: $^1\text{H-NMR}$ (300 MHz, CDCl_3): δ 4.06 (m, 1H), 1.31-1.89 (m, 5H), 1.16 (m, 1H), 0.96 (d, $J = 7.0$ Hz, 3H). No attempts were made to separate the two isomers.^[208]

Benzyl alcohol: Capillary column: MEGADEX DACTBS β , diacetyl-*tert*-butylsilyl- β -cyclodextrin, 0.25 μm ; diameter = 0.25 mm; length = 25 m; carrier: hydrogen; inlet pressure: 1 bar; oven temperature: 95 $^\circ\text{C}$ for 20 min: $t_{\text{substrate}} = 3.54$ min; $t_{\text{product}} = 11$ min.

After the hydrogenation, the volatiles were evaporated and the residue was purified by flash column chromatography (eluent: 9:1 hexane/AcOEt). The product was isolated as a colorless liquid. Yield: 203 mg (94%). Its physical and spectroscopic data are superimposable with those reported in the literature. $^1\text{H-NMR}$ (300 MHz, CDCl_3): δ 7.30-7.42 (m, 5H), 4.73 (s, 2H), 1.66 (s, 1H).^[202]

Cyclohexylmethanol: Capillary column: MEGADEX DACTBS β , diacetyl-*tert*-butylsilyl- β -cyclodextrin, 0.25 μm ; diameter = 0.25 mm; length = 25 m; carrier: hydrogen; inlet pressure: 1 bar; oven temperature: 95 $^\circ\text{C}$ for 20 min: $t_{\text{substrate}} = 2.98$ min; $t_{\text{product}} = 18.9$ min.

After the hydrogenation, the reaction mixture was diluted with water and extracted with Et_2O (3 x 10 mL). The combined organic extracts were dried over Na_2SO_4 and then the solvent was

removed by rotary evaporator (temperature, pressure and time of evaporation had to be carefully controlled, as the product is quite volatile). The residue was purified by flash column chromatography (eluent: CD_2Cl_2), giving a colorless liquid. Yield: 196 mg (86%). Its physical and spectroscopic data are superimposable with those reported in the literature. $^1\text{H-NMR}$ (300 MHz, CDCl_3): δ 3.47 (d, $J = 6.4$ Hz, 2H), 1.83-1.66, (m, 5H), 1.56-1.39 (m, 2H), 1.35-1.12 (m, 3H), 0.97 (m, 2H).^[209]

Dodecan-1-ol: Capillary column: MEGADEX DACTBS β , diacetyl-*tert*-butylsilyl- β -cyclodextrin, 0.25 μm ; diameter = 0.25 mm; length = 25 m; carrier: hydrogen; inlet pressure: 1 bar; oven temperature: 95 °C for 17 min, then 30 °C/min ramp to 200 °C: $t_{\text{substrate}} = 19.5$ min; $t_{\text{product}} = 20.1$ min. $^1\text{H-NMR}$ (300 MHz, CDCl_3): δ 3.39 (t, $J = 6.6$ Hz, 2H), 1.61-1.68 (m, 2H), 1.57-1.59 (m, 2H), 1.24-1.34 (m, 16H), 0.88 (t, $J = 6.81$ Hz, 3H).^[210]

3-Phenylprop-2-en-1-ol: Capillary column: MEGADEX DACTBS β , diacetyl-*tert*-butylsilyl- β -cyclodextrin, 0.25 μm ; diameter = 0.25 mm; length = 25 m; carrier: hydrogen; inlet pressure: 1 bar; oven temperature: 95 °C for 20 min: $t_{\text{substrate}} = 19.6$ min; $t_{\text{product(a)}} = 19.2$ min; $t_{\text{product(b)}} = 20.1$ min.

$^1\text{H NMR}$ (300 MHz, CDCl_3): δ 4.36 (d, $J = 5.7$, 2H), 6.37-6.43 (m, 1H), 6.65 (d, $J = 15.9$ Hz, 1H), 7.22-7.43 (m, 5H).^[211]

3-Phenyl-1-propanol: Capillary column: MEGADEX DACTBS β , diacetyl-*tert*-butylsilyl- β -cyclodextrin, 0.25 μm ; diameter = 0.25 mm; length = 25 m; carrier: hydrogen; inlet pressure: 1 bar; oven temperature: 95 °C for 20 min: $t_{\text{substrate}} = 19.6$ min; $t_{\text{product(b)}} = 19.2$ min; $t_{\text{product(a)}} = 20.1$ min.

$^1\text{H NMR}$ (300 MHz, CDCl_3): δ 7.22-7.31 (m, 5H), 3.71 (t, $J = 6.4$ Hz, 2H), 2.74 (t, $J = 7.2$ Hz, 2H), 1.93 (m, 2H).^[212]

Benzyl alcohol and 2,2,2-trifluoroethanol: For benzyl alcohol, see above. 2,2,2-Trifluoroethanol (conv. = 99%): $^1\text{H-NMR}$ (300 MHz, CDCl_3): δ 3.92 (q, $J = 8.4$ Hz, 2H), 3.40 (br s, 1H). $^{19}\text{F NMR}$ (300 MHz, CDCl_3): δ -76.93 (s, 3F).

Residual of starting material (1%): $^1\text{H-NMR}$ (300 MHz, CDCl_3): δ 7.40 (s, 5H), 5.36 (s, 2H). $^{19}\text{F NMR}$ (282 MHz, CDCl_3): δ -75.96 (s, 3F).^[213]

6.8.6. Determination of the hydrogenation kinetics of acetophenone

Abbreviations used: $R_{\text{sub},t}$ = fraction of unreacted substrate ($R_{\text{sub},0} = 1$); c_{cat} = catalyst concentration; $c_{0,\text{sub}}$ = initial substrate concentration.

Experimental parameters: $T = 243.15$ K; $c_{0,\text{sub}} = 0.501$ M; $c_{\text{cat}} = 5$ mM; solvent: 5:2 *i*PrOH/ H_2O ; $P_{\text{hydrogen}} = 30$ bar.

General procedure. The kinetic experiments were carried out using a computer-controlled Parr multireactor. Each reaction was set up as follows: the pre-catalyst **46** or **123** (0.03508 mmol, 0.01 equiv) was weighted in a glass vessel and, after purging with argon for 2 minutes, it was dissolved in dry *i*PrOH (5 mL), and then a solution of Me₃NO (5.3 mg, 0.07016 mmol, 0.02 equiv) in H₂O (2 mL) was added. The resulting solution was stirred for 10 minutes, and then the vessel was placed into the autoclave, evacuated and filled with hydrogen ($P = 30$ bar). Mechanical stirring (300 rpm) was immediately started together with heating (70 °C), and the reaction was run overnight measuring the hydrogen uptake, from which conversion values were calculated. The final conversion was confirmed by GC analysis of the crude reaction mixture.

Note: time = 0 was marked when the reactor was filled with hydrogen. Pseudo-first order rate constants k_{app} and corresponding half-lives $t_{1/2}$ were determined from the slope of a linear least squares fit to the graph of $\ln(R_{sub.,t}) = -kt$. Second order constants k were calculated dividing k_{app} by c_{cat} (assumed to be constant).

Figure 32. Kinetics of the hydrogenation of acetophenone promoted by pre-catalyst **123** activated with Me₃NO.

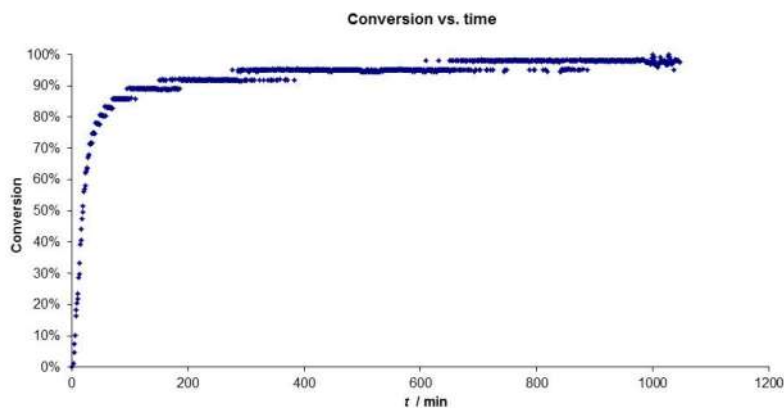


Table 20. Kinetic parameters of the hydrogenation of acetophenone promoted by pre-catalyst **123** activated with Me₃NO.

Regression interval = 12-24 min		
Linear regression	Slope	Intercept
	-0,0360	0,0000
Standard error =	0,0010	#N/D
R ² =	0,9899	0,0695
F index =	1174,7910	12,0000
	5,6825	0,0580
k_{app} (min ⁻¹) =	0,036	
$t_{1/2}$ (min) = $\ln(2) / k$ =	19,27	
k (L mol ⁻¹ min ⁻¹) =	7,19	

Figure 33. Kinetics of the hydrogenation of acetophenone promoted by pre-catalyst 46 activated with Me_3NO .

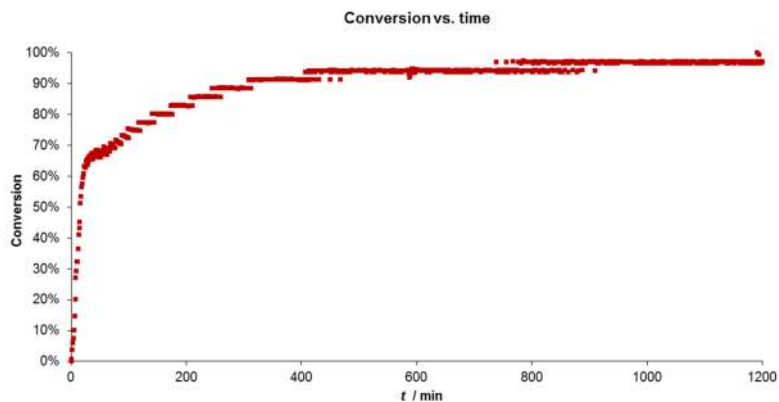


Table 21. Kinetic parameters of the hydrogenation of acetophenone promoted by pre-catalyst 46 activated with Me_3NO .

Regression interval = 6 - 16 min		
Linear regression	Slope	Intercept
	-0,0396	0,0000
Standard error =	0,0012	#N/D
$R^2 =$	0,9916	0,0439
F index =	1174,5795	10,0000
	2,2630	0,0193
$k_{\text{app}} (\text{min}^{-1}) =$	0,040	
$t_{1/2} (\text{min}) = \ln(2) / k =$	17,49	
$k (\text{L mol}^{-1} \text{min}^{-1}) =$	7,93	

7. Literature

- [1] Prices obtained on <http://www.infomine.com/investment/metal-prices/> as for 1.12.2015
- [2] CRC Handbook of Chemistry and Physics, 77th Edition
- [3] R. M. Bullock, *Catalysis without Precious Metals*, Wiley-VCH, **2010**
- [4] (a) M. Darwish, M. Wills, *Catal. Sci. Technol.* **2012**, *2*, 243 – 255; (b) specifically on Fe-catalysed reduction methodologies: R. H. Morris, *Chem. Soc. Rev.* **2009**, *38*, 2282 – 2291; (c) K. Gopalalaha, *Chem. Rev.* **2013**, *113*, 3248–3296; (d) I. Bauer, H. J. Knolker, *Chem. Rev.* **2015**, *115*, 3170 – 3387; (e) D. S. Mérela, M. Loan Tran Doa, S. Gaillarda, P. Dupaud, J. L. Renauda, *Coord. Chem. Rev.* **2015**, *288*, 50 – 68; (f) A. Pinaka, G.C. Vougioukalakis, *Coord. Chem. Rev.* **2015**, *288*, 69 – 97; (g) L. C. Misal Castro, H. Li, J. B. Sortais, C. Darcel, *Green Chem.* **2015**, *17*, 2283 – 2303.
- [5] S. J. Lippard, J. M. Berg, *Principles of Bioinorganic Chemistry*, University Science Books, Mill Valley, **1994**.
- [6] F. Naud, F. Spindler, C. J. Rueggeberg, A. T. Schmidt, H. U. Blaser, *Org. Process Res. Dev.*, **2007**, *11*, 519 – 523.
- [7] S. Enthaler, K. Junge, M. Beller, *Angew. Chem. Int. Ed.* **2008**, *47*, *18*, 3317 – 3321.
- [8] Carsten Bolm, *Nature Chemistry* **2009**, *1*, 420.
- [9] (a) B. Plietker, A. Dieskau, *Eur. J. Org. Chem.* **2009**, 775 – 787; (b) O. G. Manchegno, *Angew. Chem. Int. Ed.* **2011**, *50*, 2216 – 2218; (c) I. Bauer, H.-J. Knolker, *Chem. Rev.* **2015**, *115*, 3170 – 3387.
- [10] B. Plietker, *Iron Catalysis in Organic Chemistry*, Wiley-VCH Verlag, Weinheim, **2008**.
- [11] (a) R. G. Pearson, *J. Am. Chem. Soc.* **1963**, *85*, *22*, 3533 – 3539; (b) R. G. Pearson, *J. Chem. Educ.* **1968**, *45*, 581 – 586; (c) R. G. Pearson, *J. Chem. Educ.* **1968**, *45*, 643 – 648.
- [12] R. G. Parr, R. G. Pearson, *J. Am. Chem. Soc.* **1983**, *105*, *26*, 7512 – 7516.
- [13] P. J. Chirik, *J. Am. Chem. Soc.* **2009**, *131*, 3788 – 3789.
- [14] B. L. Booth, H. Goldwhite, R. N. Haszeldine, *J. Chem. Soc.*, **1966**, 1447 – 1449.
- [15] H.-J. Knölker, H. Goesmann, R. Klaus, *Angew. Chem.* **1999**, *111*, 727 – 731; *Angew. Chem. Int. Ed.* **1999**, *38*, 702 – 705.
- [16] P. J. Chirik, K. Wieghardt, *Science* **2010**, *327*, 794 – 795.
- [17] S. Blanchard, E. Derat, M. Desage-El Murr, L. Fensterbank, M. Malacria, V. Mouriès-Mansuy, *Eur. J. Inorg. Chem.* **2012**, 376 – 389.
- [18] H. U. Blaser, C. Malan, B. Pugin, F. Spindler, H. Steiner, M. Studer, *Adv. Synth. Catal.*, **2003**, *345*, 103 – 151.
- [19] B. de Bruin, *Eur. J. Inorg. Chem.* **2012**, 340 – 342.
- [20] K. Jørgensen, *Coord. Chem. Rev.* **1966**, *1*, 164 – 178.
- [21] (a) H. Grützmacher, *Angew. Chem. Int. Ed.* **2008**, *47*, 1814 – 1818; (b) J. I. van der Vlugt, J. N. H. Reek, *Angew. Chem. Int. Ed.* **2009**, *48*, 8832 – 8846.
- [22] M. Calvin, *J. Am. Chem. Soc.* **1939**, *61*, 2230 – 2234.
- [23] J. A. Osborn, F. H. Jardine, J. F. Young, G. Wilkinson, *J. Chem. Soc.* **1966**, *12*, 1711 – 1732.
- [24] (a) R. Noyori, *Angew. Chem. Int. Ed.* **2002**, *41*, 2008 – 2022. (b) W. S. Knowles, *Angew. Chem. Int. Ed.* **2002**, *41*, 1998 – 2007
- [25] (a) A. Gillon, K. Heslop, D. J. Hyett, A. Martorell, A. G. Orpen, P. G. Pringle, C. Claver, E. Fernandez, *Chem. Commun.* **2000**, 961 – 962; (b) M. T. Reetz, G. Mehler, *Angew. Chem. Int. Ed.* **2000**, *39*, 3889 – 3890; (c) F. Guillen, J.-C. Fiaud, *Tetrahedron Lett.* **1999**, *40*, 2939 – 2942; (d) M. van den Berg, A. J. Minnaard, E. P. Schudde, J. van Esch, A. H. M. de Vries, J. G. de Vries, B. L. Feringa, *J. Am. Chem. Soc.* **2000**, *122*, 11539 – 11540; (e) A. Börner, *Phosphorus Ligands in Asymmetric Catalysis: Synthesis and Applications*, Wiley-VCH, **2008**.

- [26] (a) R. Noyori, *Angew. Chem. Int. Ed.* **2002**, *41*, 2008 – 2022; (b) W. S. Knowles, *Angew. Chem. Int. Ed.* **2002**, *41*, 1998 – 2007; (c) K. B. Sharpless, *Angew. Chem. Int. Ed.* **2002**, *41*, 2024 – 2032.
- [27] <http://www.fda.gov/Drugs/GuidanceComplianceRegulatoryInformation/Guidances/>
- [28] S. Gladiali, E. Alberico, *Chem. Soc. Rev.* **2006**, *35*, 226 – 236.
- [29] M.A. Esteruelas, L.A. Oro, *Chem. Rev.* **1998**, *98*, 577 – 588.
- [30] (a) W. Hieber, F. Leutert, *Naturwissenschaften*, **1931**, *19*, 360 – 361; (b) T. Weichselfelder, B. Thiede *Justus Liebigs Ann Chem.* **1926**, *447*, 64 – 77.
- [31] L.F. Dahl, J.F. Blount, *Inorg. Chem.* **1965**, *4*, 1373.
- [32] L. Manojlovic-Muir, K.W. Muir, J.A. Ibers, *Inorg. Chem.* **1970**, *9*, 447 – 452.
- [33] L.J. Guggenberger, D.D. Titus, M.T. Flood, R.E. Marsh, A.A. Orio, H.B. Gray, *J. Am. Chem. Soc.* **1972**, *94*, 1135 – 1143.
- [34] S. Samson, G. R. Stephenson, *Pentacarbonyliron 2004*, Paquette, L. Encyclopedia of Reagents for Organic Synthesis. New York, J. Wiley & Sons.
- [35] J. R. Partington, *A History of Chemistry*, MacMillan & Co, New York, **1964**.
- [36] L. Mond, F. Quinke, *J. Chem. Soc.* **1891**, *59*, 604 – 607.
- [37] For early studies using iron salts activated by aluminum compounds see: Y. Takegami, T. Ueno, T. Fujii, *Bull. Chem. Soc. Jpn.* **1969**, *42*, 1663 – 1667.
- [38] E. N. Frankel, E. A. Emken, H. M. Peters, V. K. Davison, R. O. Butterfield, *J. Org. Chem.* **1964**, *29*, 3292 – 3297.
- [39] R. Noyori, I. Umeda, T. Ishigami, *J. Org. Chem.* **1972**, *37*, 1542 – 1545.
- [40] M. A. Schroeder, M. S. Wrighton, *J. Am. Chem. Soc.* **1976**, *98*, 551 – 558.
- [41] (a) B. H. Weiller, M. E. Miller, E. R. Grant, *J. Am. Chem. Soc.* **1987**, *109*, 352 – 361; (b) B. H. Weiller, E. R. Grant, *J. Am. Chem. Soc.* **1987**, *109*, 1051 – 1055; (c) M. E. Miller, E. R. Grant, *J. Am. Chem. Soc.*, **1987**, *109*, 7951.
- [42] (a) R. B. King, *Organometallic Syntheses*, Volume 1, Transition-Metal Compounds, Academic Press: New York, **1965**; (b) E. H. Braye, W. Hübel, *Diiron Enneacarbonyl*, *Inorg. Synth.* **1966**, *8*, 178.
- [43] K. Kano, M. Takeuchi, S. Hashimoto, Z. I. Yoshida, *Chem. Commun.* **1991**, 1728 – 1729.
- [44] (a) S. Sakaki, T. Sagura, T. Arai, T. Kojima, T. Ogata, K. Ohkubo, *J. Mol. Catal.* **1992**, *75*, L33 – L37; (b) S. Sakaki, T. I. Kojima, T. Arai, *J. Chem. Soc., Dalton Trans.* **1994**, 7 – 11.
- [45] (a) J. W. Peters, W. N. Lanzilotta, B. J. Lemon, L. C. Seefeldt, *Science*, **1998**, *282*, 1853 – 1858; (b) Y. Nicolet, A. L. de Lacey, X. Vernede, V. M. Fernandez, E. C. Hatchikian, J. C. Fontecilla-Camps, *J. Am. Chem. Soc.* **2001**, *123*, 1596 – 1601; (c) Y. Nicolet, C. Piras, P. Legrand, C. E. Hatchikian, J. C. Fontecilla-Camps, *Structure* **1999**, *7*, 13 – 23; (d) J. W. Peters, W. N. Lanzilotta, B. J. Lemon, L. C. Seefeldt, *Science* **1998**, *282*, 1853 – 1858; (e) Y. Nicolet, A. L. de Lacey, X. Vernede, V. M. Fernandez, E. C. Hatchikian, J. C. Fontecilla-Camps, *J. Am. Chem. Soc.* **2001**, *123*, 1596 – 1601; (f) M. Frey, *Chembiochem* **2002**, *3*, 153 – 160.
- [46] (a) A. Volbeda, E. Garcin, C. Piras, A. L. de Lacey, V. M. Fernandez, E. C. Hatchikian, M. Frey, J. C. Fontecilla-Camps, *J. Am. Chem. Soc.* **1996**, *118*, 12989 – 12996; (b) A. Volbeda, M-H Charon, C. Piras, E. C. Hatchikian, M. Frey, J. C. Fontecilla-Camps, *Nature* **1995**, *373*, 580 – 587; (c) A. Volbeda, L. Martin, C. Cavazza, M. Matho, B. W. Faber, W. Roseboom, S. P. J. Albracht, E. Garcin, M. Rousset, J. C. Fontecilla-Camps, *J. Biol. Inorg. Chem.* **2005**, *10*, 239 – 249.
- [47] (a) H. Inoue, M. Sato, *Chem. Commun.* **1983**, 983–984; (b) H. Inoue, M. Suzuki, *Chem. Commun.* **1980**, 817 – 818.
- [48] C. Bianchini, A. Meli, M. Peruzzini, P. Frediani, C. Bohanna, M. A. Esteruelas, L. A. Oro, *Organometallics* **1992**, *11*, 138 – 152.

- [49] C. Blanchini, A. Meli, M. Peruzzini, F. Vizza, F. Zanobini, *Organometallics* **1989**, *8*, 2080 – 2082.
- [50] E. J. Daida, J. C. Peters, *Inorg. Chem.* **2004**, *43*, 7474 – 7485.
- [51] H. Fong, M. Moret, Y. Lee, J. C. Peters, *Organometallics*, **2013**, *32*, 3053 – 3062.
- [52] G. Wienhofer, F. Westerhaus, R. V. Jagadeesh, K. Junge, H. Junge, M. Beller, *Chem. Commun.* **2012**, *48*, 4827 – 4829.
- [53] D. Srimani, Y. Diskin-Posner, Y. Ben-David, D. Milstein, *Angew. Chem. Int. Ed.* **2013**, *52*, 14131 – 14134.
- [54] D. J. Frank, L. Guet, A. Kaslin, E. Murphy, S. P. Thomas, *RSC Adv.* **2013**, *3*, 25698 – 25701.
- [55] M. Kamitani, Y. Nishiguchi, R. Tada, M. Itazaki, H. Nakazawa, *Organometallics* **2014**, *33*, 1532 – 1535.
- [56] S. C. Bart, E. Lobkovsky, P. J. Chirik, *J. Am. Chem. Soc.* **2004**, *126*, 13794 – 1380.
- [57] (a) G. J. P. Britovsek, V. C. Gibson, B. S. Kimberley, P. J. Maddox, S. J. McTavish, G. A. Solan, A. J. P. White, D. J. Williams *Chem. Commun.* **1998**, *59*, 849 – 850; (b) B. L. Small, M. Brookhart, A. M. A. Bennett, *J. Am. Chem. Soc.* **1998**, *120*, 4049 – 4050.
- [58] V. C. Gibson, C. Redshaw, G. A. Solan, *Chem. Rev.* **2007**, *107*, 1745 – 1776.
- [59] S. C. Bart, K. Chlopek, E. Bill, M. W. Bouwkamp, E. Lobkovsky, F. Nesse, K. Weighardt, P. J. Chirik, *J. Am. Chem. Soc.* **2006**, *42*, 128, 13901 – 13912.
- [60] Studies on the non-innocent nature of the bis(imino)pyridine ligand: (a) S. Stieber, E. Chantal, C. Milsman, J. M. Hoyt, Z. R. Turner, K. D. Finkelstein, K. Wiegardt, S. DeBeer, J. P. Chirik, *Inorg. Chem.* **2012**, *51*, 3770 – 3785; (b) A. M. Tondreau, S. Stieber, E. Chantal, C. Milsman, E. Lobkovsky, T. Weyhermuller, S. Semproni, J. P. Chirik, *Inorg. Chem.* **2013**, *52*, 635 – 646.
- [61] R. J. Trovitch, E. Lobkovsky, P. J. Chirik, *Inorg. Chem.* **2006**, *45*, 7252 – 7260.
- [62] S. C. Bart, E. J. Hawrelak, E. Lobkovsky, *Organometallics* **2005**, *24*, 5518 – 5527.
- [63] P. Phua, L. Lefort, J. A. F. Boogers, M. Tristany, J. G. de Vries, *Chem. Commun.* **2009**, 3747 – 3749.
- [64] R. Bedford, M. Betham, D. Bruce, S. Davis, R. Frost and M. Hird, *Chem. Commun.* **2006**, 1398 – 1400.
- [65] M. Stein, J. Wieland, P. Steurer, F. Teolle, R. Moulhaupt, B. Breit, *Adv. Synth. Catal.* **2011**, *353*, 523 – 527.
- [66] A. Welther, M. Bauer, M. Mayer, A. J. von Wangelin, *Chem. Cat. Chem.* **2012**, *4*, 1088 – 1093.
- [67] T. N. Gieshoff, A. Welther, M. T. Kessler, M. H. G. Pechtl, A. von Wangelin, *J. Chem. Commun.* **2014**, *50*, 2261 – 2264.
- [68] V. Kelsen, B. Wendt, S. Werkmeister, K. Junge, M. Beller, B. Chaudret, *Chem. Commun.* **2013**, *49*, 3416 – 3418.
- [69] I. Bauer, H.-J. Knölker, *Chem. Rev.* **2015**, *115*, 3170 – 3387.
- [70] (a) L. Markó, M. A. Radhi *J. Organomet. Chem.* **1981**, *218*, 369 – 376; (b) L. Markó, J. Pala, *Transition Met. Chem.* **1983**, *8*, 207 – 209.
- [71] J.-S. Chen, L.-L. Chen, Y. Xing, G. Chen, W.-Y. Shen, Z.-R. Dong, Y.-Y. Li, J.-X. Gao *Acta Chim. Sin.* **2004**, *62*, 1745 – 1750.
- [72] S. Enthaler, B. Hagemann, G. Erre, K. Junge, M. Beller, *Chem. Asian J.* **2006**, *1*, 598 – 604.
- [73] G. Wienhofer, F. A. Westerhaus, K. Junge, R. Ludwig, M. Beller, *Chem. Eur. J.* **2013**, *19*, 7701 – 7707.
- [74] L.-Q. Lu, Y. Li, K. Junge, M. Beller, *Angew. Chem. Int. Ed.* **2013**, *52*, 8382 – 8386.
- [75] S. Enthaler, G. Erre, M. K. Tse, K. Junge, M. Beller, *Tetrahedron Lett.* **2006**, *47*, 8095 – 8099.

- [76] S. Enthaler, B. Spilker, G. Erre, K. Junge, M. K. Tse, M. Beller, *Tetrahedron* **2008**, *64*, 3867 – 3876.
- [77] S. L. Yu, W. Y. Shen, Y. Y. Li, Z. R. Dong, Y. Q. Xu, Q. Li., J. N. Zhang, J. X. Gao *Adv. Synth. Catal.* **2012**, *354*, 818 – 822.
- [78] Y.-Y. Li, S.-L. Yu, W.-Y. Shen, J.-X. Gao, *Acc. Chem. Res.* **2015**, *48*, 2587 – 2598.
- [79] Y. Y. Li, S. L. Yu, X. F. Wu, J. L. Xiao, W. Y. Shen, Z. Dong, J. X. Gao, *J. Am. Chem. Soc.* **2014**, *136*, 4031 – 4039.
- [80] C. Sui-Seng, F. Freutel, A. Lough, R. H. Morris, *Angew. Chem. Int. Ed.* **2008**, *47*, 940 – 943.
- [81] D. E. Prokopchuk, J. F. Sonnenberg, N. Meyer, I. M. Zimmer-De, A. J. Lough, R. H. Morris, *Organometallics* **2012**, *31*, 3056 – 3064.
- [82] (a) N. Meyer, A. J. Lough, R. H. Morris, *Chem. Eur. J.* **2009**, *15*, 5605 – 56010; (b) C. Sui-Seng, F. N. Haque, A. Hadzovic, A.-M. Pütz, V. Reuss, N. Meyer, A. J. Lough, M. Zimmer-De Iulii, R. H. Morris, *Inorg. Chem.* **2009**, *48*, 735 – 743.
- [83] J. F. Sonnenberg, R. H. Morris, *ACS Catal.* **2013**, *3*, 1092 – 1102; (b) J. F. Sonnenberg, N. Coombs, P. A. Dube, R. H. Morris, *J. Am. Chem. Soc.* **2012**, *134*, 5893 – 5899.
- [84] (a) A. A. Mikhailine, E. Kim, C. Dingels, A. J. Lough, R. H. Morris, *Inorg. Chem.* **2008**, *47*, 6587 – 6589; (b) A. A. Mikhailine, A. J. Lough, R. H. Morris, *J. Am. Chem. Soc.* **2009**, *131*, 1394 – 1395; (c) P. O. Lagaditis, A. A. Mikhailine, A. J. Lough, R. H. Morris, *Inorg. Chem.* **2010**, *49*, 1094 – 1102.
- [85] (a) P. O. Lagaditis, A. J. Lough, R. H. Morris, *Inorg. Chem.* **2010**, *49*, 10057 – 10066; (b) A. A. Mikhailine, R. H. Morris, *Inorg. Chem.* **2010**, *49*, 11039 – 11044; (c) P. O. Lagaditis, A. J. Lough, R. H. Morris, *J. Am. Chem. Soc.* **2011**, *133*, 9662 – 9665.
- [86] P. E. Sues, A. J. Lough, R. H. Morris, *Organometallics* **2011**, *30*, 4418 – 4431.
- [87] (a) A. A. Mikhailine, M. I. Maishan, A. J. Lough, R. H. Morris, *J. Am. Chem. Soc.* **2012**, *134*, 12266 – 12280; (b) D. E. Prokopchuk, R. H. Morris, *Organometallics* **2012**, *31*, 7375 – 7385.
- [88] (a) W. Zuo, Y. Li, A. J. Lough, R. H. Morris, *Science* **2013**, *342*, 1080 – 1083; (b) W. Zuo, S. Tauer, D. E. Prokopchuk, R. H. Morris, *Organometallics* **2014**, *33*, 5791 – 5801; (c) S. A. M. Smith, R. H. Morris, *Synthesis* **2015**, *47*, 1775 – 1779.
- [89] (a) C. A. Sandoval, T. Ohkuma, K. Muniz, R. Noyori, *J. Am. Chem. Soc.* **2003**, *125*, 13490 – 13503; (b) R. Noyori, M. Kitamura, T. Ohkuma, *Proc. Natl. Ac. Sci.* **2004**, *101*, 5356 – 5362.
- [90] P. O. Lagaditis, P. E. Sues, J. F. Sonnenberg, K. Y. Wan, A. J. Lough, R. H. Morris, *J. Am. Chem. Soc.* **2014**, *136*, 1367 – 1380.
- [91] M. Ranocchiari, A. Mezzetti, *Organometallics* **2009**, *28*, 1286 – 1288.
- [92] R. Bigler, E. Otth, A. Mezzetti, *Organometallics* **2014**, *33*, 4086 – 4099.
- [93] R. Bigler, A. Mezzetti, *Org. Lett.* **2014**, *16*, 6460 – 6463.
- [94] R. Bigler, R. Huber, A. Mezzetti, *Angew. Chem. Int. Ed.* **2015**, *54*, 5171 – 5174.
- [95] (a) R. Langer, G. Leitius, Y. Ben-David, D. Milstein, *Angew. Chem. Int. Ed.* **2011**, *50*, 2120 – 2124; (b) R. Langer, M. A. Iron, L. Kostantinovski, Y. Diskin-Posner, G. Leitius, Y. Ben-David, D. Milstein, *Chem. Eur. J.* **2012**, *18*, 7196 – 7209.
- [96] R. Langer, M. A. Iron, L. Konstantinovski, Y. Diskin-Posner, G. Leitius, Y. Ben-David, D. Milstein *Chem. Eur. J.* **2012**, *18*, 7196 – 7209.
- [97] T. Zell, Y. Ben-David, D. Milstein, *Angew. Chem. Int. Ed.* **2014**, *53*, 4685 – 4689.
- [98] (a) E. Alberico, P. Sponholz, C. Cordes, M. Nielsen, H.-J. Drexler, W. Baumann, H. Junge, M. Beller, *Angew. Chem. Int. Ed.* **2013**, *52*, 14162 – 14166; (b) S. Werkmeister, K. Junge, B. Wendt, E. Alberico, H. Jiao, W. Baumann, H. Junge, F. Gallou, M. Beller, *Angew. Chem. Int. Ed.* **2014**, *53*, 8722 – 8726; (c) I. Koehne, T. J. Schmeier, E. A. Bielinski, C. J. Pan, P. O. Lagaditis, W. H. Bernskoetter, M. K. Takase, C. Würtele, N. Hazari, S. Schneider, *Inorg. Chem.* **2014**, *53*, 2133 – 2143.

- [99] S. Chakraborty, H. Dai, P. Bhattacharya, N. T. Fairweather, M. S. Gibson, J. A. Krause, H. Guan, *J. Am. Chem. Soc.* **2014**, *136*, 7869 – 7872.
- [100] (a) D. Spasyuk, D. G. Gusev, *Organometallics* **2012**, *31*, 5239 – 5242; (b) A. Acosta-Ramirez, M. Bertoli, D. G. Gusev, M. Schlaf, *Green Chem.* **2012**, *14*, 1178 – 1188.
- [101] C. Bornschein, S. Werkmeister, B. Wendt, H. Jiao, E. Alberico, W. Baumann, H. Junge, K. Junge, M. Beller, *Nat. Commun.* **2014**, *5*, 4111 – 4122.
- [102] A. Naik, T. Maji, O. Reiser, *Chem. Commun.* **2010**, *46*, 4475 – 4477.
- [103] W. Reppe, H. Vetter, *Liebigs Ann. Chem.* **1953**, *582*, 133 – 163.
- [104] (a) H.-J. Knolker, J. Heber, C. H. Mahler, *Synlett* **1992**, 1002 – 1004; (b) H.-J. Knolker, J. Heber, *Synlett* **1993**, 924 – 926; (c) H.-J. Knolker, E. Baum, R. Klauss, *Tetrahedron Lett.* **1995**, *36*, 7647 – 7650.
- [105] (a) A. J. Pearson, R. A. Dubbert *J. Chem. Soc. Chem. Commun.* **1991**, 202 – 203; (b) A. J. Pearson, R. J. Shively, R. A. Dubbert, *Organometallics* **1992**, *11*, 4096 – 4104; (c) A. J. Pearson, R. J. Shively, Jr., *Organometallics* **1994**, *13*, 578 – 584; (d) A. J. Pearson, A. Perosa, *Organometallics* **1995**, *14*, 5178 – 5183; (e) A. J. Pearson, X. Yao, *Synlett* **1997**, 1281 – 1282.
- [106] (a) H.-J. Knölker, E. Baum, H. Goesmann, R. Klauss, *Angew. Chem.* **1999**, *111*, 2196 – 2199; *Angew. Chem. Int. Ed.* **1999**, *38*, 2064 – 2066.
- [107] (a) C. P. Casey, H. Guan, *J. Am. Chem. Soc.* **2007**, *129*, 5816 – 5817; For an highlight on this discovery: (b) R. M. Bullock, *Angew. Chem.* **2007**, *119*, 7504 – 7507; *Angew. Chem. Int. Ed.* **2007**, *46*, 7360 – 7363.
- [108] For the first preparation of Shvo complex: (a) Y. Blum, D. Czarkie, Y. Rahamim, Y. Shvo, *Organometallics* **1985**, *4*, 1459 – 1461; (b) Y. Shvo, D. Czierkie, Y. Rahamin, D. F. Ghodosh, *J. Am. Chem. Soc.* **1986**, *108*, 7400 – 7402; For reviews on the Shvo catalyst: (c) R. Prabhakaran, *Synlett* **2004**, 2048 – 2049; (d) R. Karvembu, R. Prabhakaran, K. Natarajan, *Coord. Chem. Rev.* **2005**, *249*, 911 – 918; (e) B. L. Conley, M. K. Pennington-Boggio, E. Boz, T. J. Williams, *Chem. Rev.* **2010**, *110*, 2294 – 2312.
- [109] B. Schneider, I. Goldberg, D. Reshef, Z. Stein, Y. Shvo, *J. Organomet. Chem.* **1999**, *588*, 92 – 98.
- [110] (a) J.S.M. Samec, J.-E. Bäckvall, P.G. Andersson, P. Brandt, *Chem. Soc. Rev.* **2006**, *35*, 237 – 248; (b) J.S.M. Samec, J.-E. Bäckvall, *Chem. Eur. J.* **2002**, *13*, 2955 – 2961; (c) J. S. M. Samec, L. Mony, J.-E. Bäckvall, *Can. J. Chem.* **2005**, *83*, 909 – 916; (d) Y. Shvo, I. Goldberg, D. Czierkie, D. Reshef, Z. Stein, *Organometallics* **1997**, *16*, 133 – 138; (e) C.P. Casey, S. W. Singer, D. R. Powell, R. K. Hayashi, M. Kavana, *Journal of the American Chemical Society* **2001**, 123 – 126.
- [111] (a) S. Gaillard, J.-L. Renaud, *ChemSusChem* **2008**, *1*, 505 – 507; (b) G. Bauer, K. A. Kirchner, *Angew. Chem., Int. Ed.* **2011**, *50*, 5798 – 5800.
- [112] X. Lu, R. Cheng, N. Turner, Q. Liu, M. Zhang, X. Sun *J. Org. Chem.* **2014**, *79*, 9355 – 9364.
- [113] (a) S. Moulin, H. Dentel, A. Pagnoux-Ozherelyeva, S. Gaillard, A. Poater, L. Cavallo, J.-F. Lohier, J.-L. Renaud, *Chem. Eur. J.* **2013**, *19*, 17881 – 17890; (b) D. S. Mérel, M. Elie, J.-F. Lohier, S. Gaillard, J.-L. Renaud, *ChemCatChem* **2013**, *5*, 2939 – 2945; (c) A. Pagnoux-Ozherelyeva, N. Pannetier, M. D. Mbaye, S. Gaillard, J.-L. Renaud, *Angew. Chem.* **2012**, *124*, 5060 – 5064; *Angew. Chem. Int. Ed.* **2012**, *51*, 4976 – 4980; (d) T.-T. Thai, D. S. Mérel, A. Poater, S. Gaillard, J.-L. Renaud, *Chem. Eur. J.* **2015**, *21*, 7066 – 7070; (e) H.-J. Knölker, E. Baum, J. Heber, *Tetrahedron Lett.* **1995**, *36*, 42, 7647 – 7650; (f) A. J. Pearson, Y. Kwak, *Tetrahedron Lett.* **2005**, *46*, 5417 – 5419; (f) B. Dasgupta, W. A. Donaldson, *Tetrahedron Lett.* **1998**, *39*, 343 – 346; (g) T.-Y. Luh, *Coordination Chemistry Reviews*, **1984**, *60*, 255 – 276; (h) A. J. Pearson, R. J. Shively, *Organometallics* **1994**, *13*, 578 – 584.
- [114] S. Fleischer, S. Zhou, K. Junge, M. Beller, *Angew. Chem.* **2013**, *125*, 5224 – 5228; *Angew. Chem. Int. Ed.* **2013**, *52*, 5120 – 5124.

- [115] A. Tlili, J. Schranck, H. Neumann, M. Beller, *Chem. Eur. J.* **2012**, *18*, 15935 – 15939.
- [116] For a recent review on (cyclopentadienone)iron complexes, see: A. Quintard, J. Rodriguez, *Angew. Chem.* **2014**, *126*, 4124 – 4136; *Angew. Chem. Int. Ed.* **2014**, *53*, 4044 – 4055.
- [117] (a) A. Berkessel, S. Reichau, A. von der Höh, N. Leconte, J.-M. Neudörfl, *Organometallics* **2011**, *30*, 3880 – 3887; (b) A. Berkessel and A. Van der Höh, *ChemCatChem*, **2011**, *3*, 861 – 867.
- [118] J. P. Hopewell, J. E. D. Martins, T. C. Johnson, J. Godfrey, M. Wills, *Org. Biomol. Chem.* **2012**, *10*, 134 – 145.
- [119] (a) Plank, T. N.; Drake, J. L.; Kim, D. K.; Funk, T. W. *Adv. Synth. Catal.* **2012**, *354*, 597 – 601. (b) T. N. Plank, J. L. Drake, D. K. Kim, T. W. Funk, *Adv. Synth. Catal.* **2012**, *354*, 1175 – 1179.
- [120] S. Zhou, S. Fleischer, K. Junge, M. Beller, *Angew. Chem. Int. Ed.* **2011**, *50*, 5120 – 5124.
- [121] S. Fleischer, S. Zhou, S. Werkmeister, K. Junge, M. Beller, *Chem. Eur. J.* **2013**, *19*, 4997 – 5003.
- [122] S. Fleischer, S. Werkmeister, S. Zhou, K. Junge, M. Beller, *Chem. Eur. J.* **2012**, *18*, 9005 – 9010.
- [123] S. Zhou, S. Fleischer, H. Jiao, K. Junge, M. Beller, *Adv. Synth. Catal.* **2014**, *356*, 3451 – 3455.
- [124] F. Zhu, L. Zhu-Ge, G. Yang, S. Zhou, *ChemSusChem* **2015**, *8*, 609 – 612.
- [125] A. Pagnoux-Ozherelyeva, N. Pannetier, M. D. Mbaye, S. Gaillard, J.-L. Renaud, *Angew. Chem. Int. Ed.* **2012**, *51*, 4976 – 4980.
- [126] T.-T. Thai, D. S. Merel, A. Poater, S. Gaillard, J. -L. Renaud, *Chem. Eur. J.* **2015**, *21*, 7066 – 7070.
- [127] T. Yan, B. L. Feringa, K. Barta, *Nat. Commun.* **2014** *5*, 5602 doi: 10.1038/ncomms6602.
- [128] H.-J. Pan, T. Wei Ng, Y. Zhao, *Chem. Commun.* **2015**, *51*, 11907 – 11910.
- [129] C. Federsel, A. Boddien, R. Jackstell, R. Jennerjahn, P. Dyson, R. Scopelliti, G. Laurencyzy, M. Beller, *Angew. Chem. Int. Ed.* **2010**, *49*, 9777 – 9780. For a review on hydrogenation of sodium carbonate and carbon dioxide see: T. Zell, R. Langer, *Recycl. Catal.* **2015**; *2*, 87 – 109.
- [130] C. Ziebart, C. Federsel, P. Anbarasan, R. Jackstell, W. Baumann, A. Spannenberg, M. Beller, *J. Am. Chem. Soc.* **2012**, *134*, 20701 – 20704.
- [131] R. Langer, Y. Diskin-Posner, G. Leitus, L. J. W. Shimon, Y. Ben-David, D. Milstein, *Angew. Chem. Int. Ed.* **2011**, *50*, 9948 – 9952.
- [132] F. Bertini, I. Mellone, A. Ienco, M. Peruzzini, L. Gonsalvi *ACS Catal.* **2015**, *5*, 1254 – 1265.
- [133] F. Zhu, L. Zhu-Ge, G. Yang, S. Zhou, *ChemSusChem* **2015**, *8*, 609 – 612.
- [134] T.-T. Thai, D. S. Merel, A. Poater, S. Gaillard, J. -L. Renaud, *Chem. Eur. J.* **2015**, *21*, 7066 – 7070.
- [135] C. P. Casey, H. Guan, *J. Am. Chem. Soc.* **2009**, *131*, 2499 – 2507.
- [136] S. Elangovan, S. Quintero-Duque, V. Dorcet, T. Roisnel, L. Norel, C. Darcel, J. B. Sortais, *Organometallics* **2015**, *34*, 4521 – 4528
- [137] P. Gajewski, M. Renom-Carrasco, S. Vailati Facchini, L. Pignataro, L. Lefort, J. G. de Vries, R. Ferraccioli, A. Forni, U. Piarelli and C. Gennari, *EurJOC*, **2015**, *9*, 1887 – 1893.
- [138] P. Gajewski, M. Renom-Carrasco, S. Vailati Facchini, L. Pignataro, L. Lefort, J. G. de Vries, R. Ferraccioli, U. Piarelli and C. Gennari, *EurJOC*, **2015**, *25*, 5526 – 5536.
- [139] (a) B. Ye, N. Cramer, *Angew. Chem.* **2014**, *126*, 8030-8033; *Angew. Chem. Int. Ed.* **2014**, *53*, 7896-7899; (b) B. Ye, N. Cramer, *J. Am. Chem. Soc.* **2013**, *135*, 636 – 639.
- [140] Estimated price per gram upon purchase of 1 kg of (*R*)-BINOL from Reuter Chemischer Apparatebau KG.
- [141] (a) D. Kampen, C. Reisinger, B. List, *Top. Curr. Chem.* **2009**, *291*, 1 – 37.

- [142] M. Terada, *Chem. Commun.* **2008**, 4097 – 4112.
- [143] T. Ooi, M. Kameda, K. Maruoka, *J. Am. Chem. Soc.* **2003**, *125*, 5139 – 5151.
- [144] M. Ikunaka, K. Maruoka, Y. Okuda, T. Ooi, *Org. Process Res. Dev.* **2003**, *7*, 644 – 648.
- [145] B. L. Feringa, J. F. Teichert, *Angew. Chem. Int. Ed.* **2010**, *49*, 2486 – 2528.
- [146] C. Vollhardt, C. A. Parnell, K. Peter, *Tetrahedron* **1985**, *41*, 5791 – 5796.
- [147] R. Patchett, I. Magpantay, L. Saudan, C. Schotes, A. Mezzetti, F. Santoro, *Angew. Chem. Int. Ed.* **2013**, *52*, 10352 – 10355.
- [148] (a) G. A. Olah, S. C. Narang, L. D. Field, R. Karpeles, *J. Org. Chem.* **1981**, *46*, 2408 – 2410; (b) P. R. Brooks, M. C. Wirtz, M. G. Vetelino, D. M. Rescek, G. F. Woodworth, B. P. Morgan, J. W. Coe, *J. Org. Chem.* **1999**, *64*, 9719 – 9721.
- [149] D. L. Comins, A. Dehghani, *Tetrahedron Letters* **1992**, *33*, 6299 – 6302.
- [150] T. Ohe, N. Miyaura, A. Suzuki, *J. Org. Chem.* **1993**, *58*, 2201 – 2208.
- [151] A. F. Littke, C. Dai, G. C. Fu, *J. Am. Chem. Soc.* **2000**, *122*, 4020-4028.
- [152] T. Watanabe, N. Miyaura, A. Suzuki, *Synlett* **1992**, 207 – 210.
- [153] R. A. Altman, S. Buchwald, *Nat. Protoc.* **2007**, *2*, 3115 – 3121.
- [154] T. Ohe, N. Miyaura, A. Suzuki, *J. Org. Chem.* **1993**, *58*, 2201 – 2208.
- [155] C. J. O'Brien, E. A. B. Kantchev, C. Valente, N. Hadei, G. A. Chass, A. Lough, A. C. Hopkinson, M. G. Organ, *Chem. Eur. J.* **2006**, *12*, 4743 – 4748.
- [156] D. P. Hruszkewycz, D. Balcells, L. M. Guard, N. Hazari, M. Tilset, *J. Am. Chem. Soc.* **2014**, *136*, 7300 – 7316.
- [157] T.-L. Zhao, Y. Li, S.-M. Li, Y.-G. Zhou, F.-Y. Sun, L.-X. Gao, F.-S. Hana, *Adv. Synth. Catal.* **2011**, *353*, 1543 – 1550.
- [158] M. Boiani, A. Baschieri, C. Cesari, R. Mazzoni, S. Stagni, S. Zacchini, L. Sambri, *New J. Chem.* **2012**, *36*, 1469 – 1478.
- [159] For discussion on a possible decomposition pathway of the Knölker-Casey catalyst, see: M. G. Coleman, A. N. Brown, B. A. Bolton, H. Guan, *Adv. Synth. Catal.* **2010**, *352*, 967 – 970.
- [160] a) X. Lu, Y. Zhang, P. Yun, M. Zhang, T. Li, *Org. Biomol. Chem.* **2013**, *11*, 5264 – 5277.
- [161] a) D. Fornals, M. A. Pericas, F. Serratosa, J. Vinaixa, M. Font-Altaba, X. Solans, *J. Chem. Soc., Perkin Trans. 1* **1987**, 2749 – 2752; b) C. G. Krespan, *J. Org. Chem.* **1975**, *40*, 261 – 262; c) J. L. Boston, D. W. A. Sharp, G. Wilkinson, *J. Chem. Soc.* **1962**, 3488 – 3494.
- [162] a) G. N. Schrauzer, *Chem. Ind.* **1958**, 1403; b) G. N. Schrauzer, *Chem. Ind.* **1958**, 1404; c) W. Hübel, E. H. Braye, *J. Inorg. Nucl. Chem.* **1959**, *10*, 250-268.
- [163] L. Brandsma, H. D. Verkuijsse, *Synthesis* **1978**, 290
- [164] H. Kolshorn, H. Meier und Eu. Miiller, *Tetrahedron Letters*, **1971**, *19*, 1469 – 1472. Potochemie von Acetylenen in Gegenwart von Metallocarbonylen. Die thermische und photochemische Reaktion von Cyclooctin mit Eisenpentacarbonyl (13% of the compound)
- [165] M. A. Bennett, I. W. Boyd, G. B. Robertson, W. A. Wickramasinghe, *Journal of Organometallic Chemistry*, **1985**, *290*, 181 – 197.
- [166] G. Wittig, P. Fritze, *Liebigs Ann. Chem.* **1968**, *712*, 79 – 83.
- [167] (a) E. Weiss, W. Hubel, *J. Inorg. Nucl. Chem.* **1959**, *11*, 42; (b) E. Weiss, R. Merenyi, W. Hubel, *Chem. Ind. (London)* **1960**, 407; (c) E. Weiss, R. Merenyi, W. Hubel, *Chem. Ber.* **1962**, *95*, 1170.
- [168] (a) P. L. Pauson, *Tetrahedron* **1985**, *41*, 5855 – 5860; (b) J. Blanco-Urgoiti, L. Añorbe, L. Pérez-Serrano, G. Domínguez, J. Pérez-Castells, *Chem. Soc. Rev.* **2004**, *33*, 32 – 42.
- [169] A. J. Pearson, R. A. Dubbert, *J. Chem. Soc., Chem. Commun.* **1991**, 202 – 203.
- [170] Prepared from cyclododecanone according to a known procedure, see: K. M. Brummond, K. D. Gesenberg, J. L. Kent, A. D. Kerekes, *Tetrahedron Lett.* **1998**, *39*, 8613 – 8616.

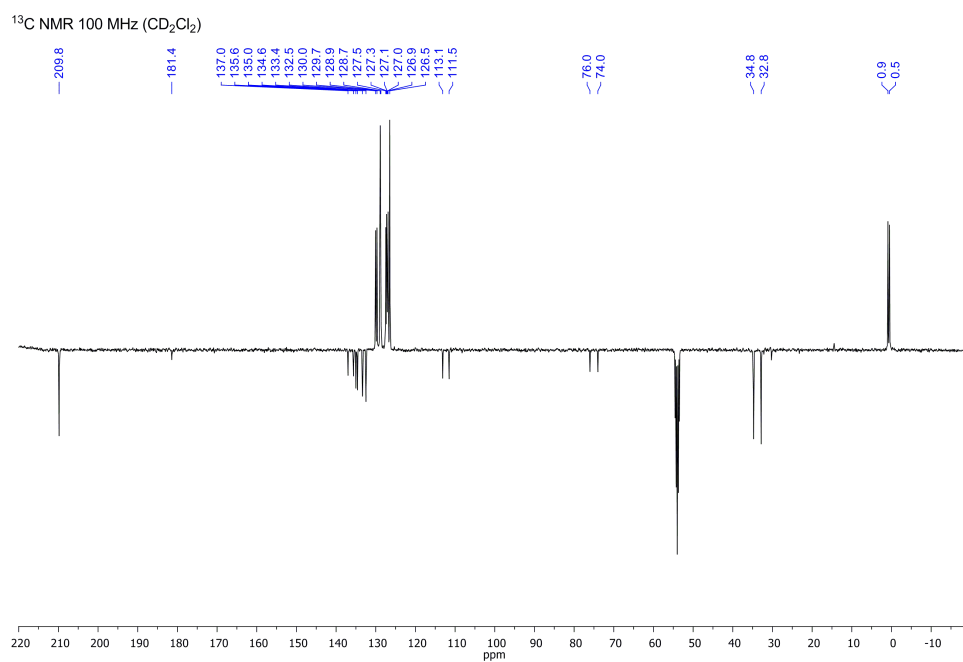
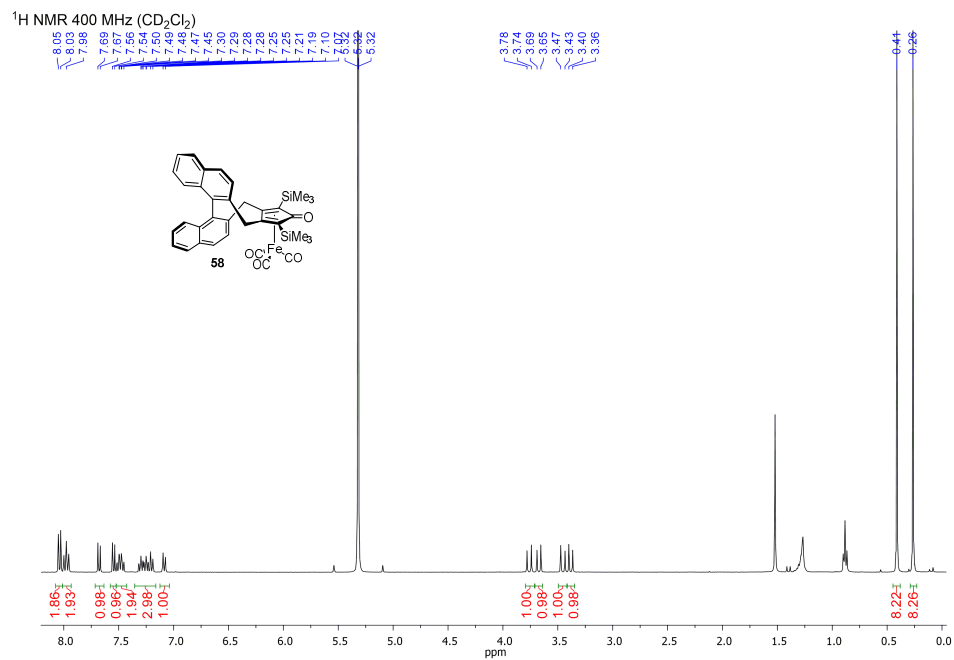
- [171] T. Zell, D. Milstein, *Acc. Chem. Res.* **2015**, *48*, 1979 – 1994.
- [172] X. Zhang, J-B Han, P-F Li, X. Ji, Z. Zhang, *Synthetic Communications*, **2009**, *39*, 3804 – 3815.
- [173] K. C. Miles, C. “Chip” Le, J. P. Stambuli, *Chem. Eur. J.* **2014**, *20*, 11336 – 11339.
- [174] (a) S. Zheng, H. Tan, X. Zhang, C. Yu, Z. Shen, *Tetrahedron Letters*, **2014**, *55*, 975 – 978; (b) J. Cossy, D. Belotti, A. Maguer, *Synlett*, **2003**, *10*, 1515 – 1517.
- [175] A. Tutar, O. Cakmak, M. Balci, *Tetrahedron*, **2001**, *57*, 9759 – 9763.
- [176] (a) M. Hussain, N.T. Hung, R. A. Khera, A. Villinger, P. Langer, *Tetrahedron Letters*, **2011**, *52*, 184 – 187; (b) R. A. Khera, M. Hussain, N. T. Hung, N. Eleya, H. Feist, A. Villinger, P. Langer, *Helvetica Chimica Acta*, **2012**, *95*, 469 – 482.
- [177] M. A. Ogliaruso, M. O. Romanelli, E. I. Becker, *Chem. Rev.*, **1965**, *65*, 261 – 367.
- [178] C. Cesari, L. Sambri, S. Zacchini, V. Zanotti, R. Mazzoni, *Organometallics*, **2014**, *33*, 2814 – 2819.
- [179] C. Chen, C. Xi, Y. Jiang, X. Hong, *J. Am. Chem. Soc.* **2005**, *127*, 8024 – 8025.
- [180] Y. Xu, J. Zhao, H. Chen, W. Wu, H. Jiang, *Chem. Commun.*, **2014**, *50*, 2488 – 2490.
- [181] P. A. Wender, T. J. Paxton, T. J. Williams, *J. Am. Chem. Soc.* **2006**, *128*, 14814 – 14815.
- [182] S. Seyfi, F. Rostami-Charati, Z. Hossaini, M. R. Zardoost, *Letters in Organic Chemistry*, **2014**, *11*, 409 – 412.
- [183] (a) K. Burgess, L. D. Jennings, *J. Am. Chem. Soc.* **1991**, *113*, 6129 – 6139; (b) C. A. Busacca, B. Qu, E. Farber, N. Haddad, N. Grët, A. K. Saha, M. C. Eriksson, J.-P. Wu, K. R. Fandrick, S. Han, N. Grinberg, S. Ma, H. Lee, Z. Li, M. Spinelli, A. Gold, G. Wang, P. Wipf, C. H. Senanayake, *Org. Lett.* **2013**, *15*, 1132 – 1135.
- [184] W. C. Still, M. Kahn, A. Mitra, *J. Org. Chem.* **1978**, *43*, 2923 – 2925.
- [185] T. Ooi, M. Kameda, K. Maruoka, *J. Am. Chem. Soc.* **2003**, *17*, 5104 – 5111.
- [186] M. Vondenhof, J. Mattay, *Tetrahedron Lett.* **1990**, *31*, 985 – 988.
- [187] S. Sengupta, M. Leite, D. S. Raslan, C. Quesnelle, V. Snieckus, *J. Org. Chem.* **1992**, *57*, 4066 – 4068.
- [188] N. Maignot, J.P. Mazeleyrat, *Synthesis* **1985**, 317 – 319.
- [189] Bruker, SMART, SAINT and SADABS, Bruker AXS Inc., Madison, Wisconsin, USA, **1997**.
- [190] G. M. Sheldrick, *Acta Crystallogr. Sect. A* **2008**, *64*, 112 – 122.
- [191] M. N. Burnett, C. K. Johnson, ORTEP-III: Oak Ridge Thermal Ellipsoid Plot Program for Crystal Structure Illustrations, Oak Ridge National Laboratory Report ORNL-6895, **1996**.
- [192] L. Xu, M. R. Muller, X. Yu, B-Q Zhu, *Syn. Comm.* **2009**, *39*, 1611 – 1618.
- [193] R. Patchett, I. Magpantay, L. Saudan, C. Schotes, A. Mezzetti, F. Santoro, *Angew. Chem. Int. Ed.* **2013**, *52*, 10352-10355
- [194] H. Yue, H. Huang, G. Bian, H. Zong, F. Li, L. Song, *Tetrahedron Asymmetry* **2014**, *25*, 170 – 180.
- [195] Y. Li, S. Yu, X. Wu, J. Xiao, W. Shen, Z. Dong, J. Gao, *J. Am. Chem. Soc.* **2014**, *136*, 4031 – 4039.
- [196] Y.-S. Shih, R. Boobalan, C. Chen, G.-H. Lee, *Tetrahedron: Asymmetry* **2014**, *25*, 327 – 333.
- [197] J. Li, Y. Tang, Q. Wang, X. Li, L. Cun, X. Zhang, J. Zhu, L. Li, J. Deng, *J. Am. Chem. Soc.* **2012**, *134*, 18522 – 18525.
- [198] R. Soni, J.-M. Collinson, G. C. Clarkson, M. Wills, *Org. Lett.* **2011**, *13*, 4304 – 4307.
- [199] H. Mizoguchi, T. Uchida, T. Katsuki, *Angew. Chem.* **2014**, *126*, 3242-3246; *Angew. Chem. Int. Ed.* **2014**, *53*, 3178 – 3182.

- [200] A. Z. Gonzalez, J. G. Román, E. Gonzalez, J. Martinez, J. R. Medina, K. Matos, J. A. Soderquist, *J. Am. Chem. Soc.* **2008**, *130*, 9218 – 9219.
- [201] K. Matsumura, N. Arai, K. Hori, T. Saito, N. Sayo, T. Ohkuma, *J. Am. Chem. Soc.* **2011**, *133*, 10696 – 10699.
- [202] K. Revunova, G. I. Nikonov, *Chem. Eur. J.* **2014**, *20*, 839 – 845.
- [203] F. Jiang, K. Yuan, M. Achard, C. Bruneau, *Chem. Eur. J.* **2013**, *19*, 10343 – 10352.
- [204] M. L. Kantam, R. Kishore, J. Yadav, M. Sudhakar, A. Venugopal, *Adv. Synth. Catal.* **2012**, *354*, 663 – 669.
- [205] D. Xu, S. Wang, Z. Shen, C. Xia, W. Sun, *Org. Biomol. Chem.* **2012**, *10*, 2730 – 2732.
- [206] M. Nardi, G. Sindona, P. Costanzo, M. Oliverio, A. Procopio, *Tetrahedron* **2015**, *71*, 1132 – 1135.
- [207] I. P. Query, P. A. Squier, E. M. Larson, N. A. Isley, T. B. Clark, *J. Org. Chem.* **2011**, *76*, 6452 – 6456.
- [208] P. Canonne, M. Bernatchez, *J. Org. Chem.* **1987**, *52*, 4025 – 4031.
- [209] G. Hamasaka, H. Tsuji, Y. Uozumi, *Synlett* 2015, *26*, 2037 – 2041.
- [210] W. Kuriyama, T. Matsumoto, O. Ogata, Y. Ino, K. Aoki, S. Tanaka, K. Ishida, T. Kobayashi, N. Sayo, T. Saito, *Org. Process Res. Dev.* **2012**, *16*, 166 – 171.
- [211] R. Tomita, K. Mantani, A. Hamasaki, T. Ishida, M. Tokunaga, *Chem. Eur. J.* **2014**, *20*, 9914 – 9917.
- [212] E. Brenna, F. Cannavale, M. Crotti, F. Parmeggiani, A. Romagnolo, F. Spina, G. C. Varese, *J. Mol. Catal. B: Enzym.* **2015**, *116*, 83 – 88.
- [213] T. Otsuka, A. Ishii, P. A. Dub, T. Ikariya, *J. Am. Chem. Soc.* **2013**, *26*, 135, 9600 – 9603.

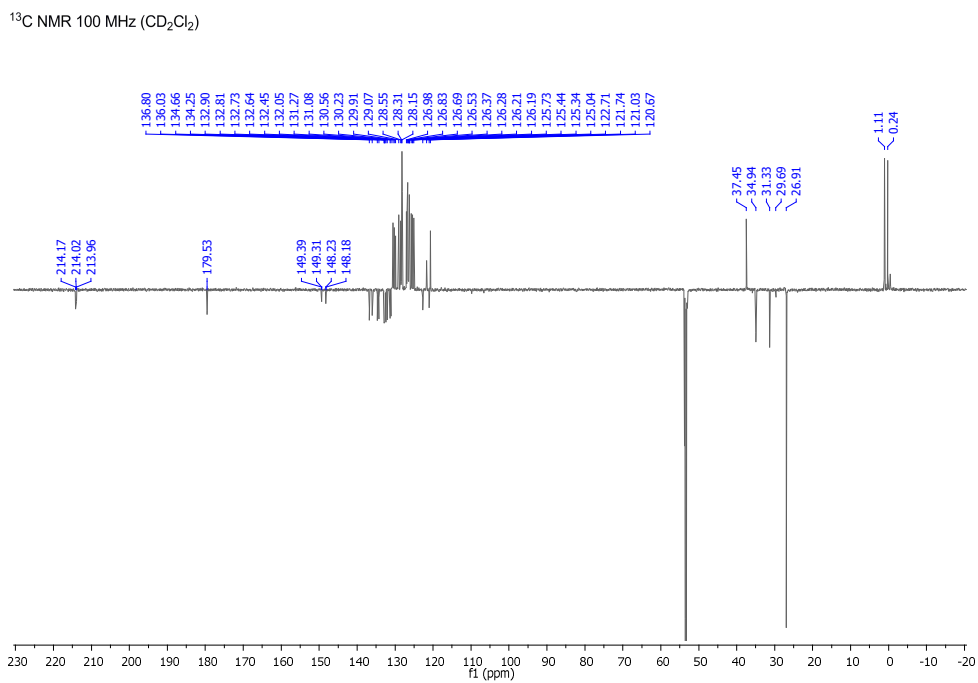
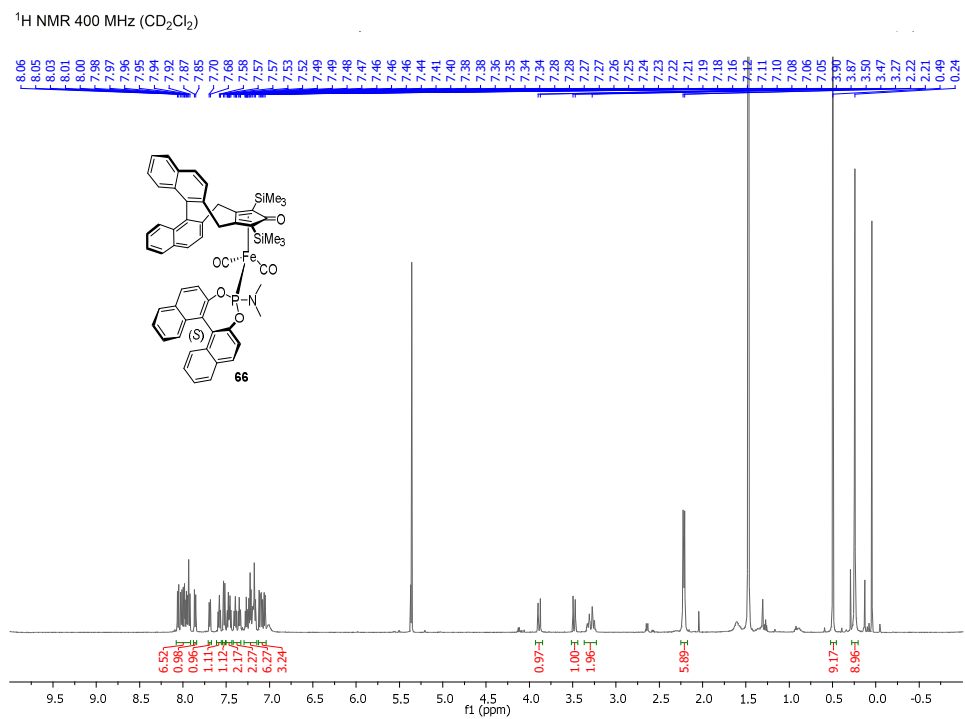
Appendix

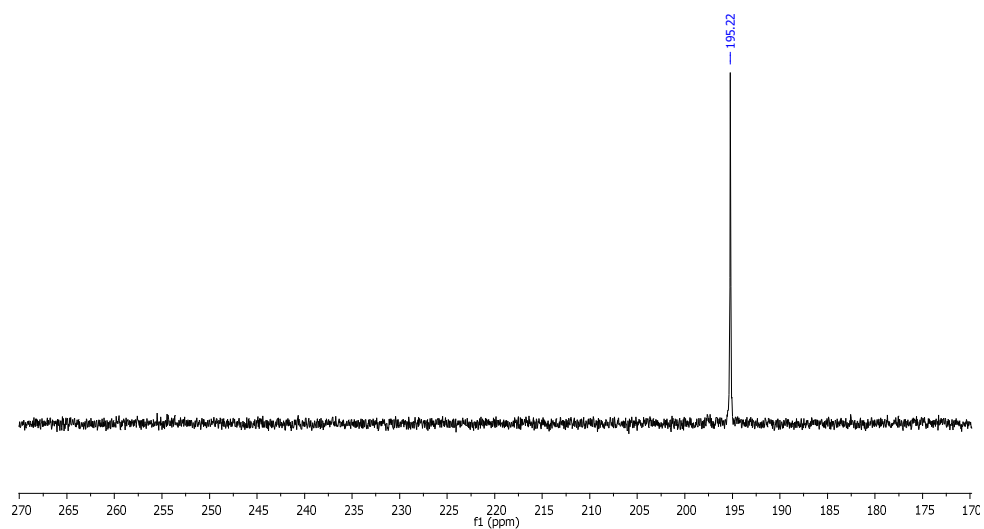
7.1. NMR Spectra

7.1.1. Complex (R)-58

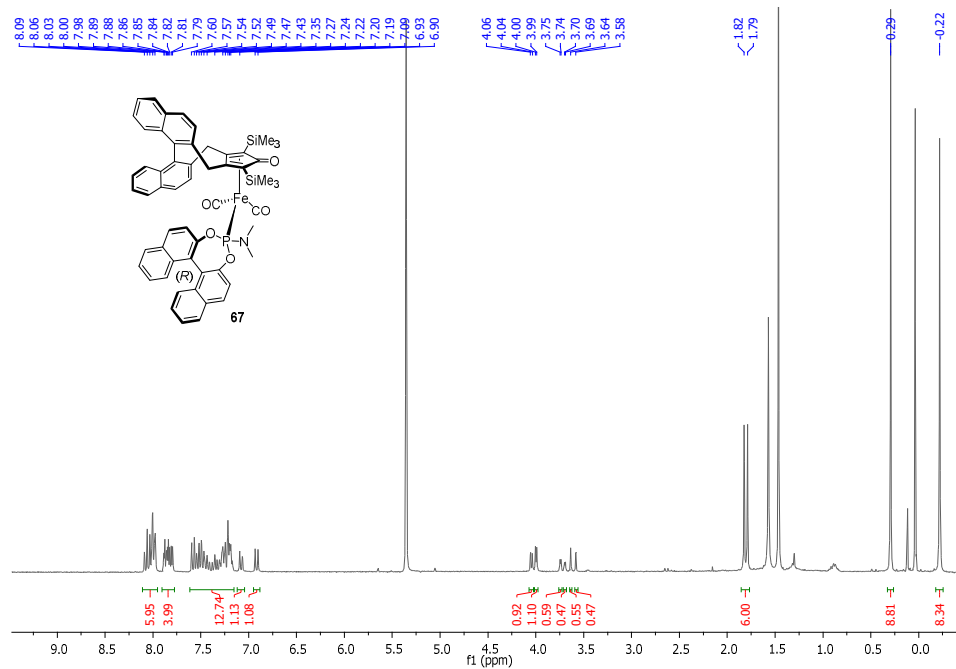


7.1.2. Complex 66

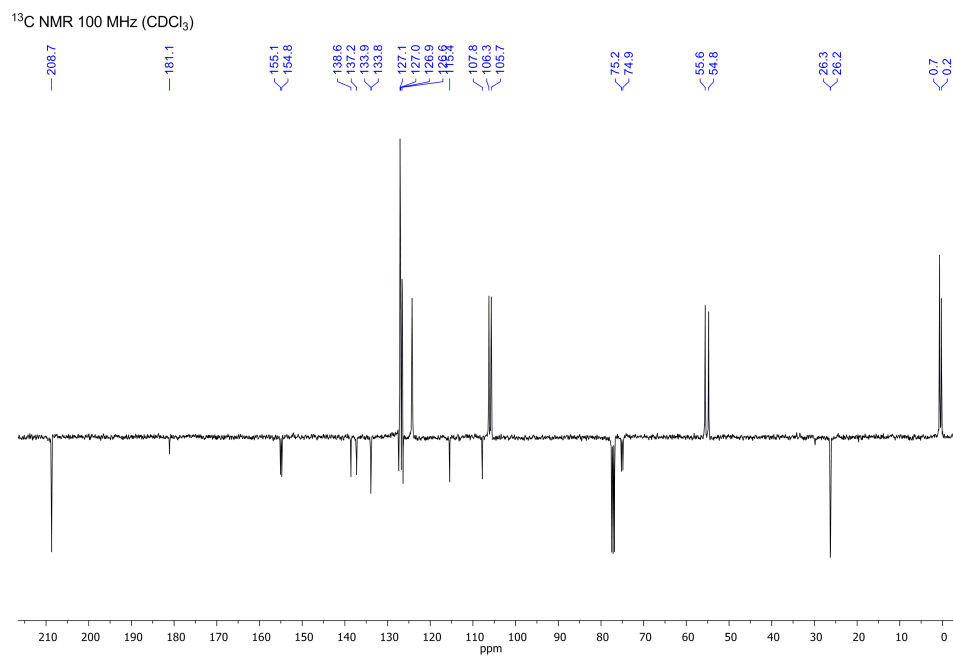
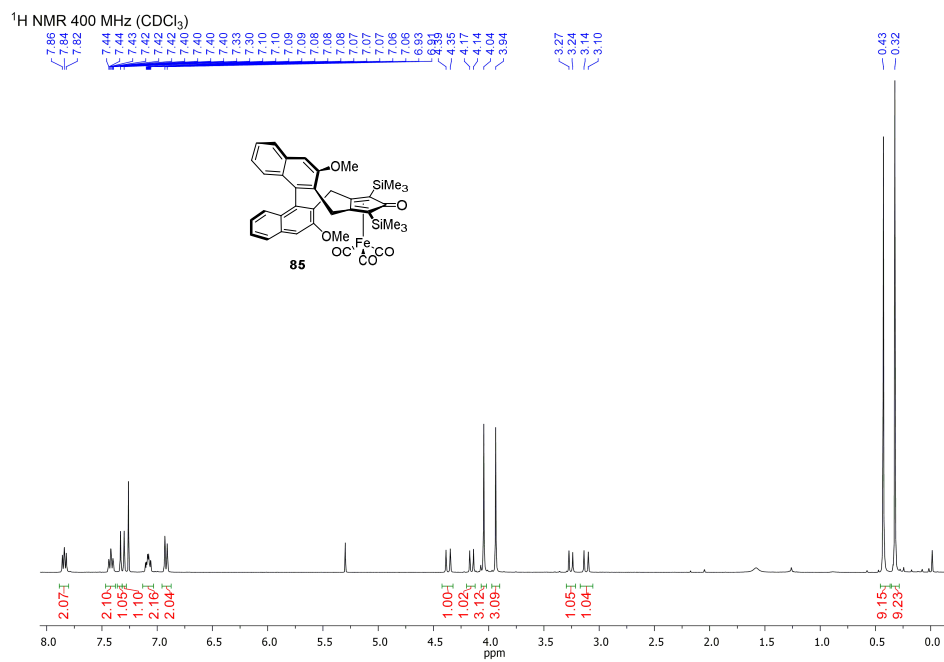


^{31}P NMR 161.9 MHz (CD_2Cl_2)

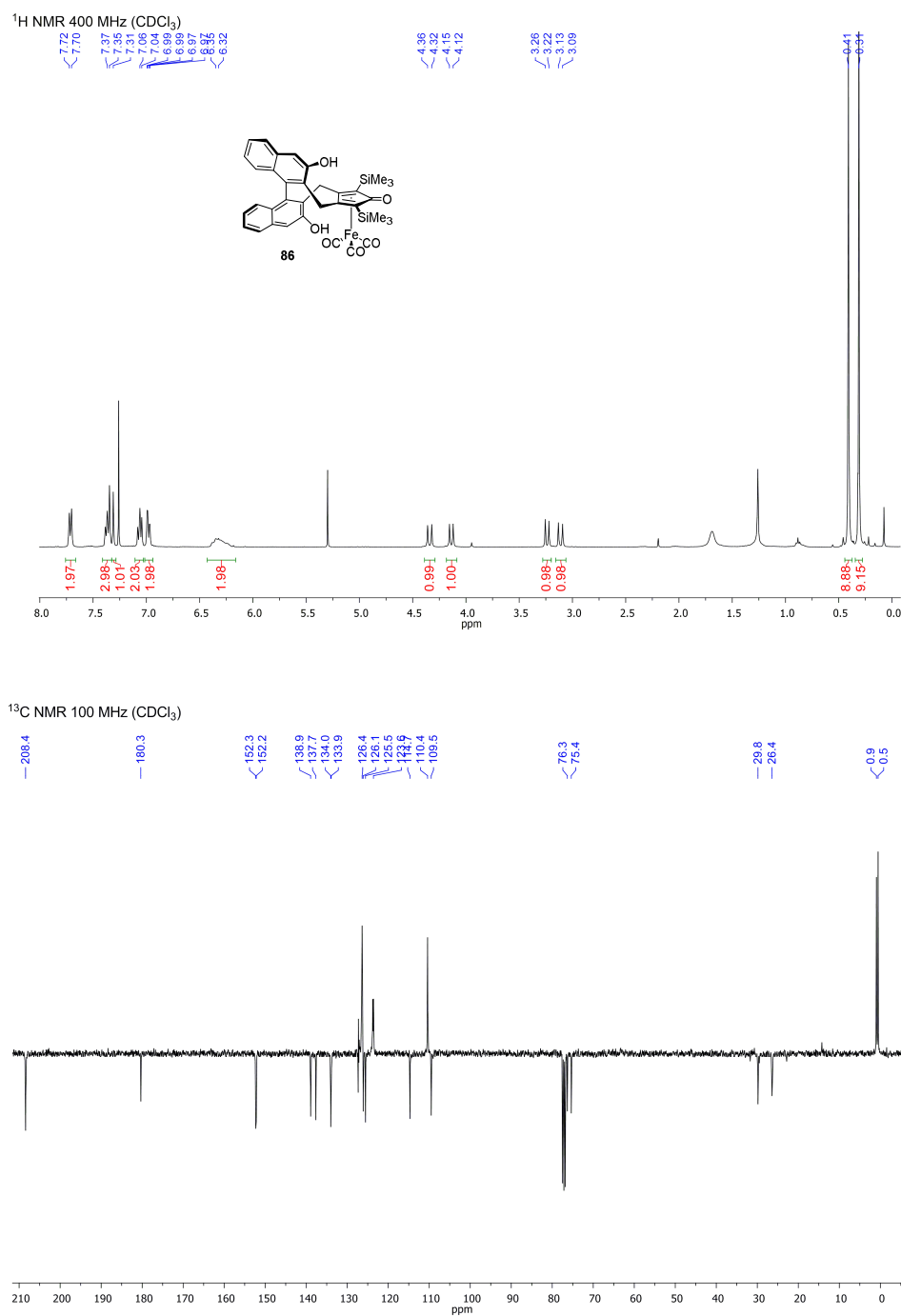
7.1.3. Complex 67

 ^1H NMR 400 MHz (CD_2Cl_2)

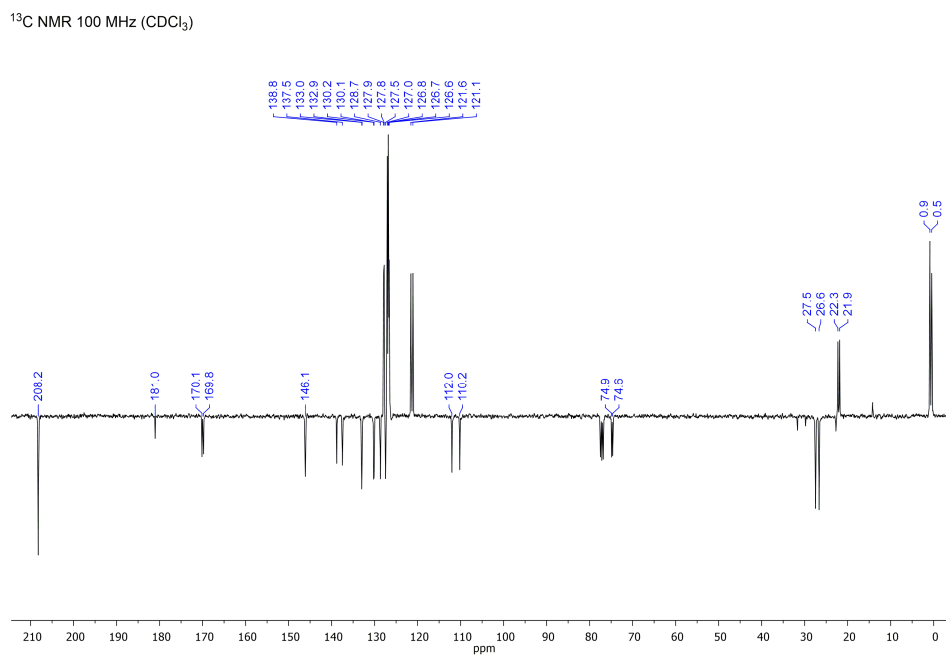
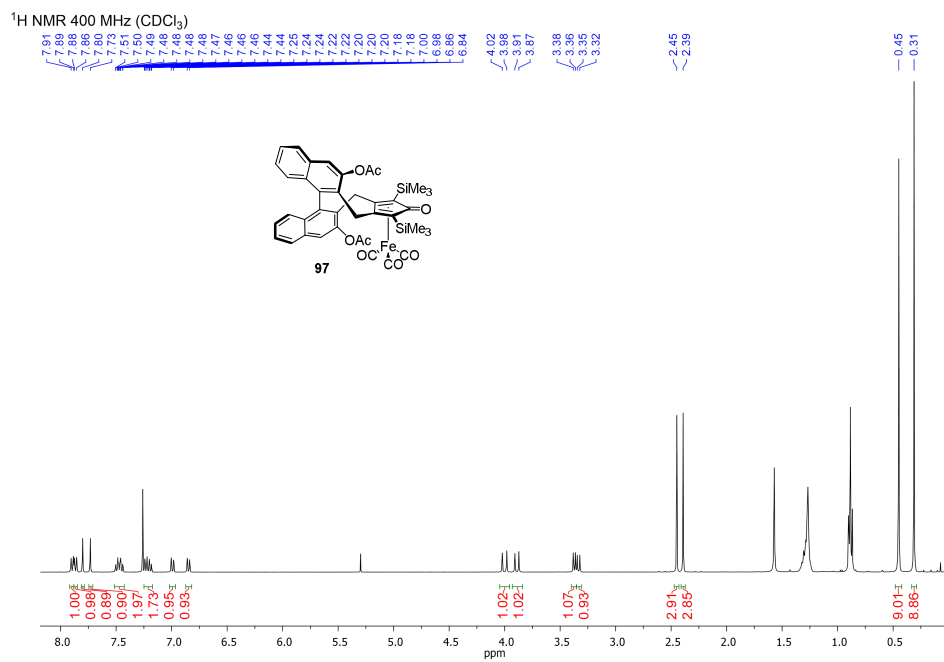
7.1.4. Complex (R)-85



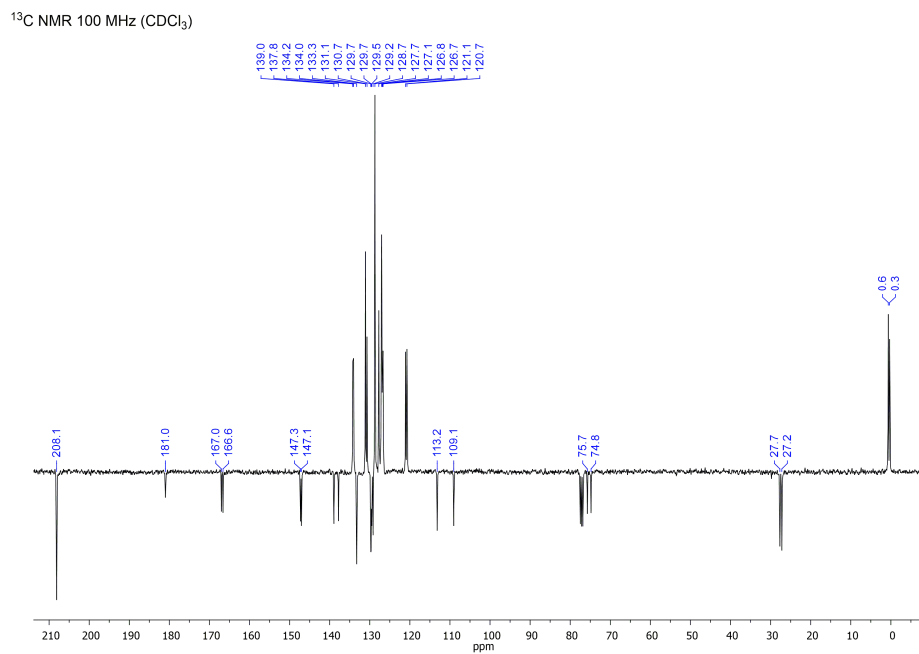
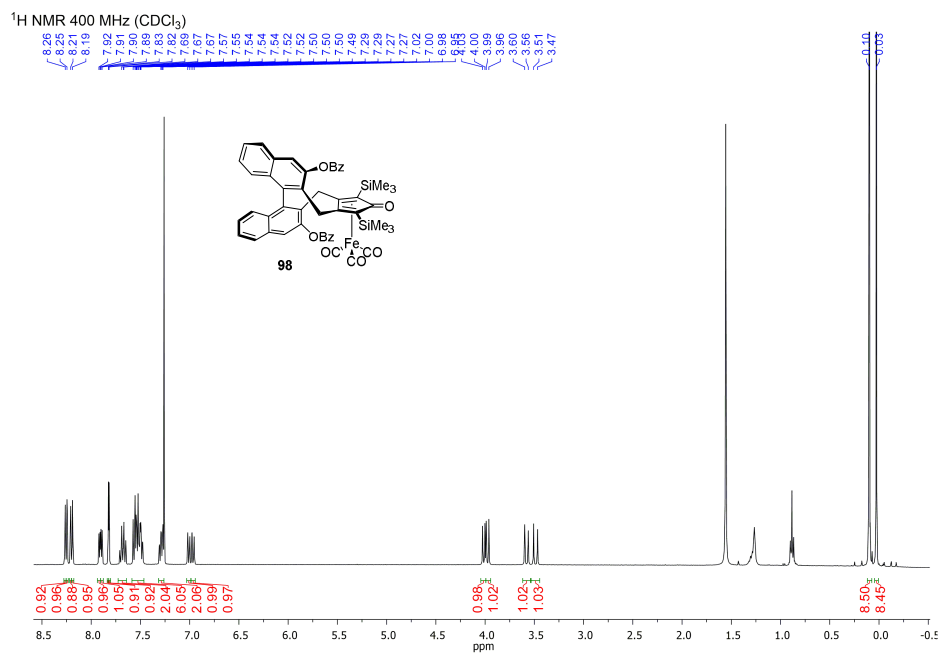
7.1.5. Complex (R)-86



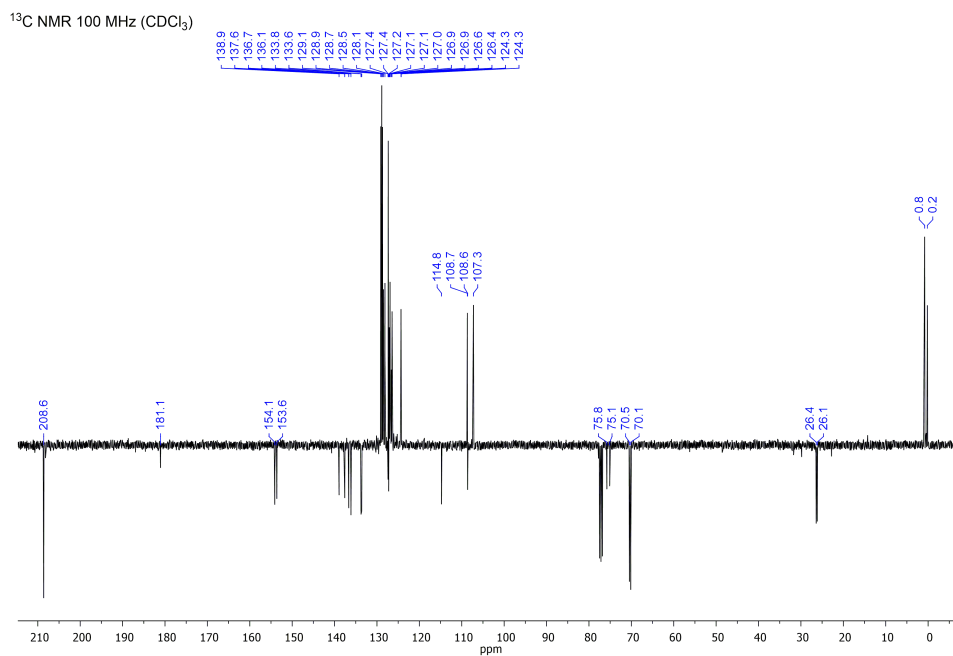
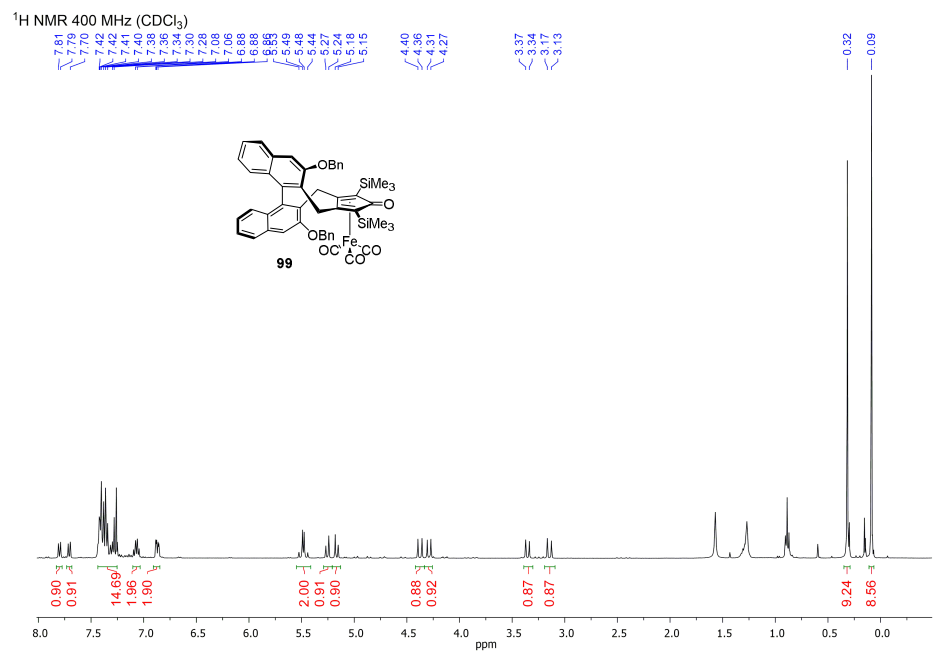
7.1.6. Complex (R)-97



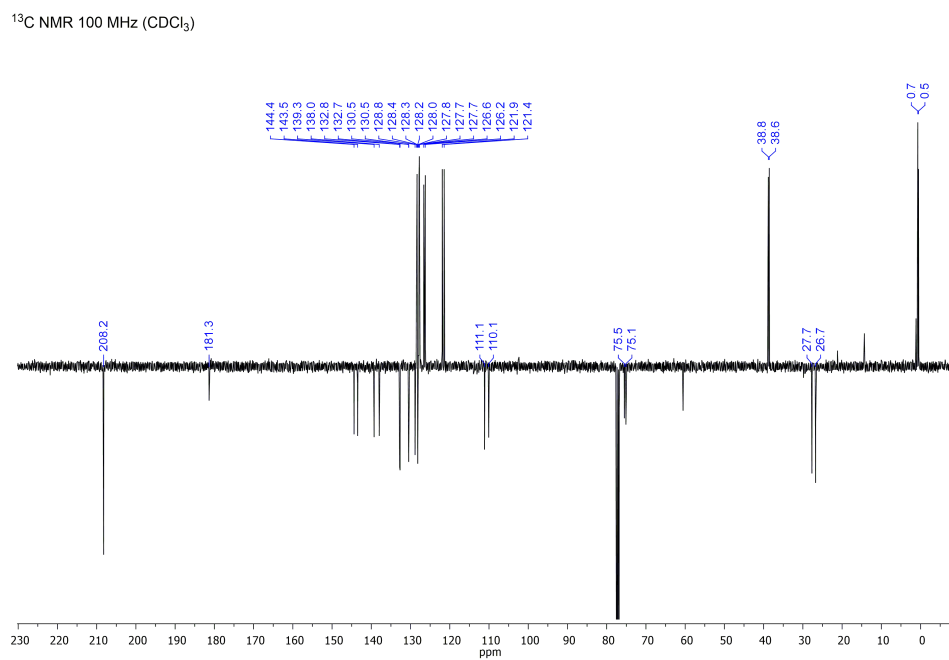
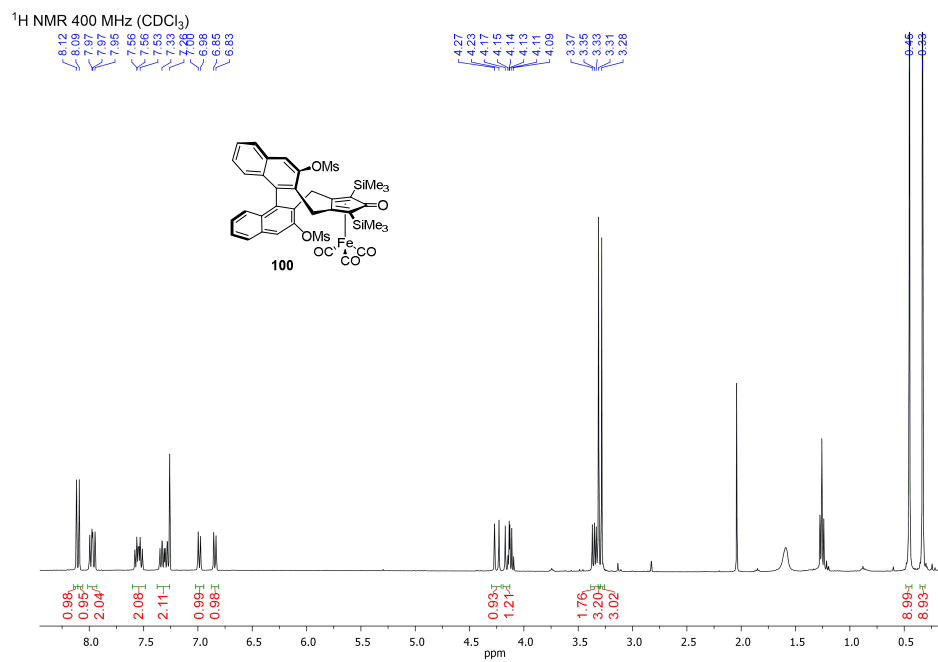
7.1.7. Complex (R)-98



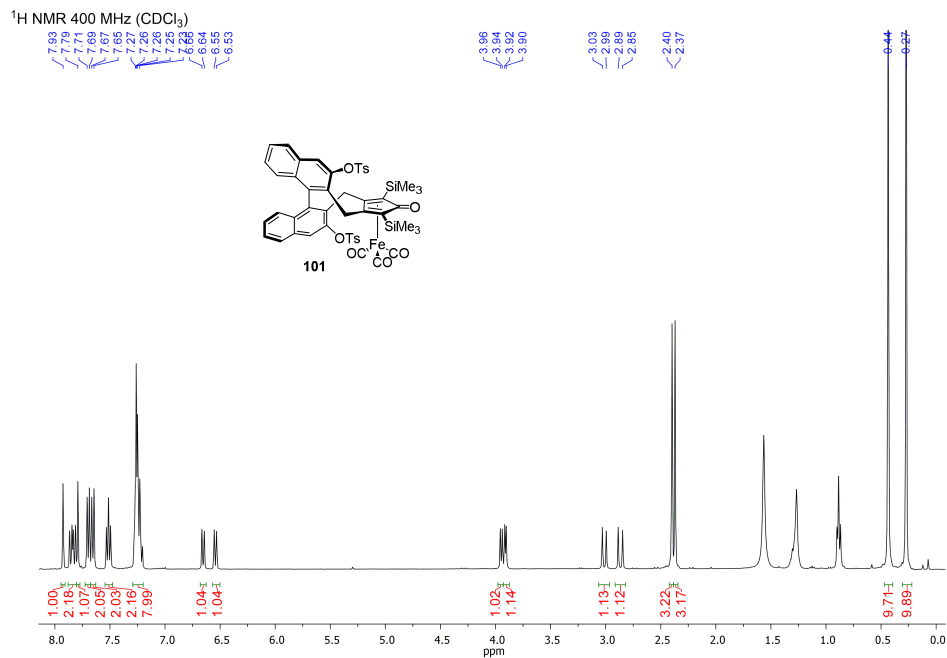
7.1.8. Complex (R)-99



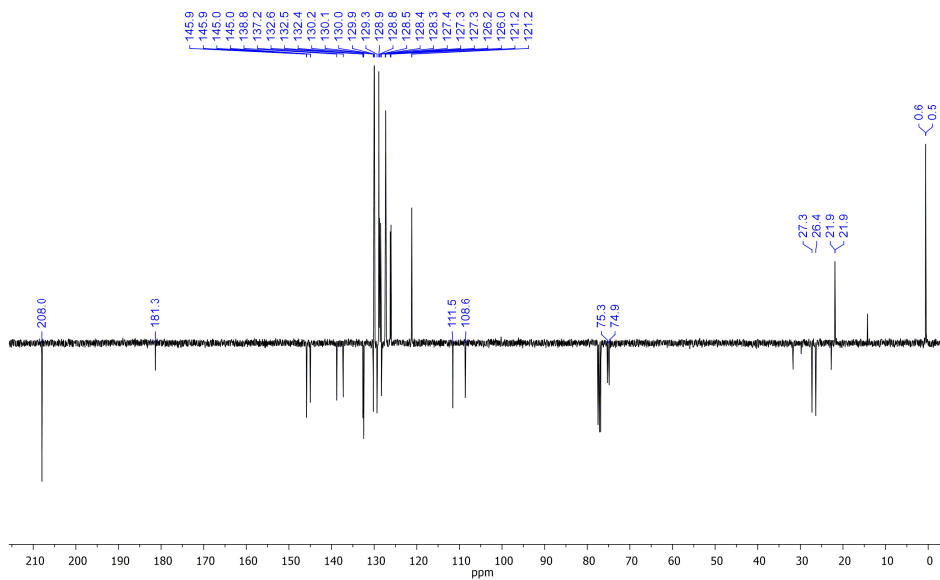
7.1.9. Complex (R)-100



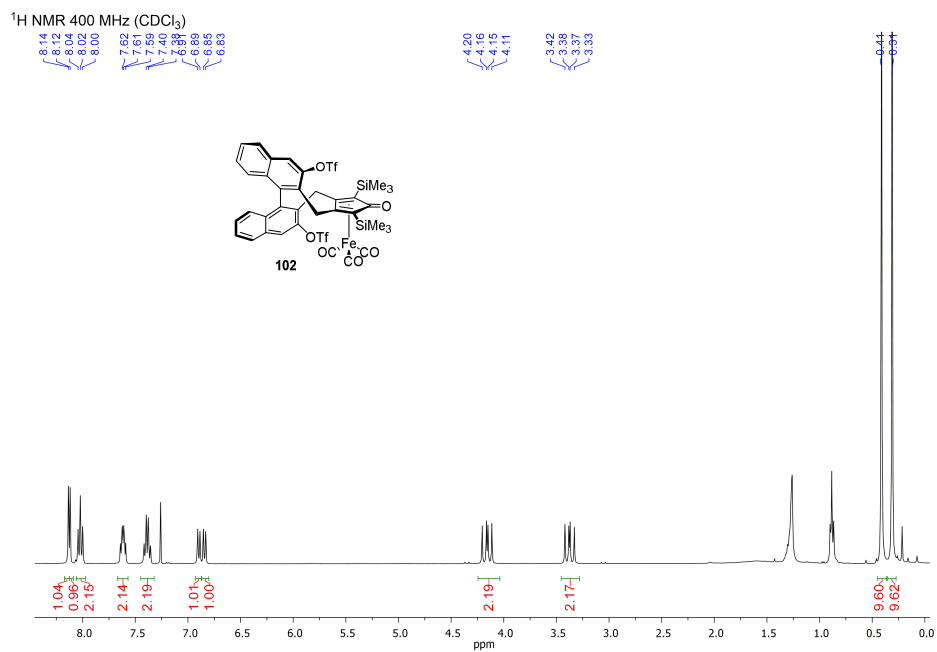
7.1.10. Complex (R)-101



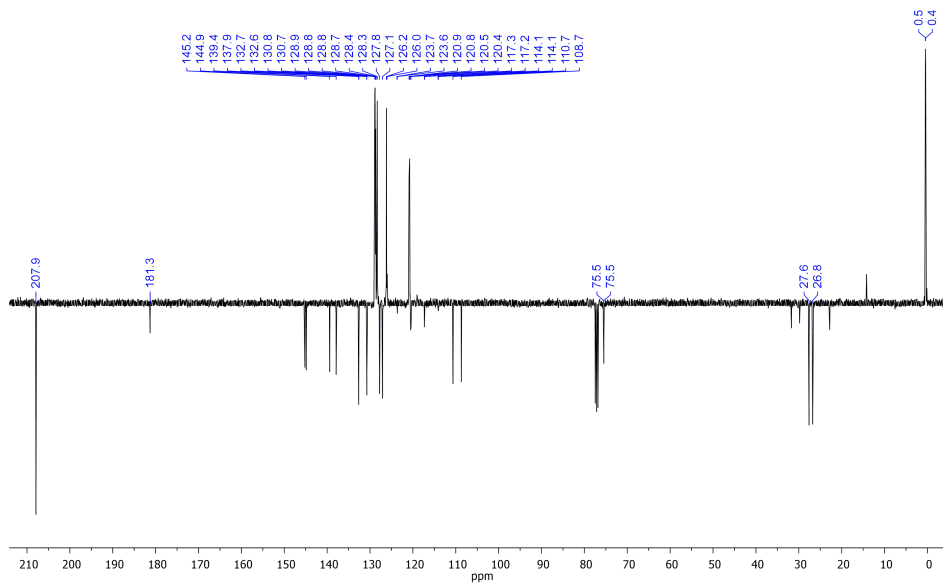
¹³C NMR 100 MHz (CDCl₃)

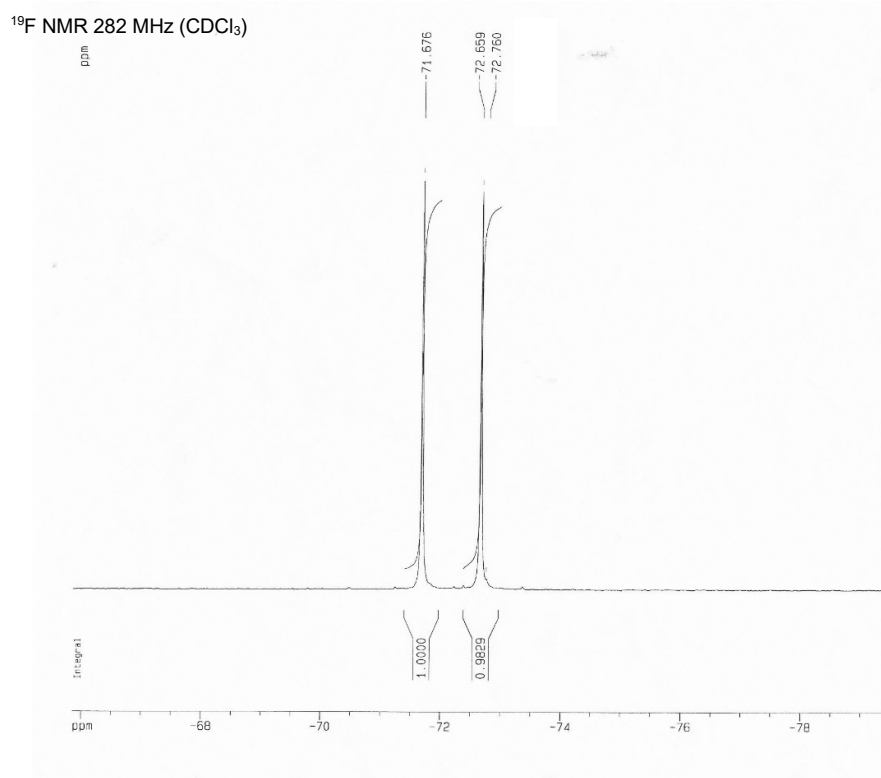


7.1.11. Complex (R)-102

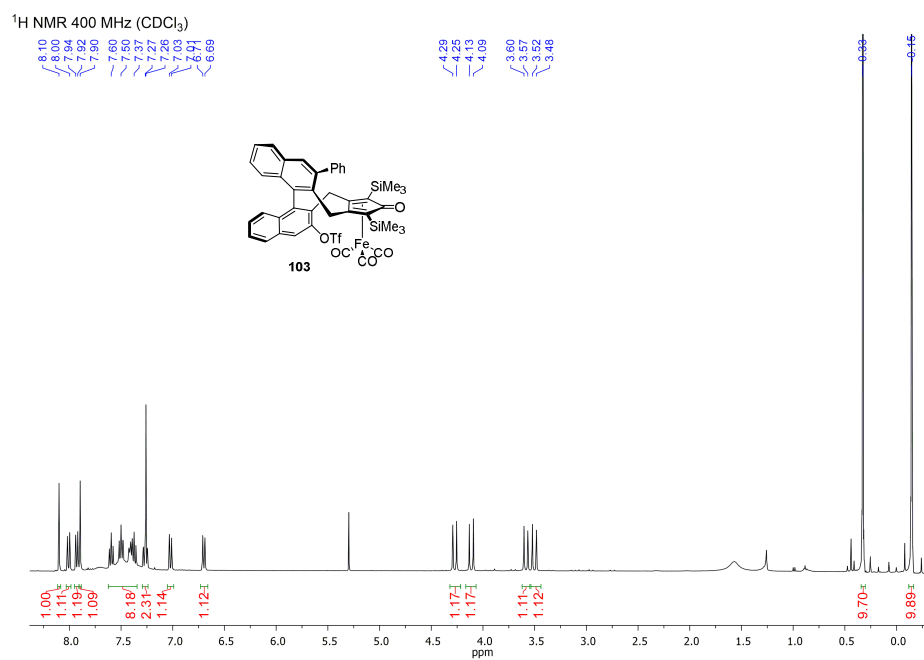


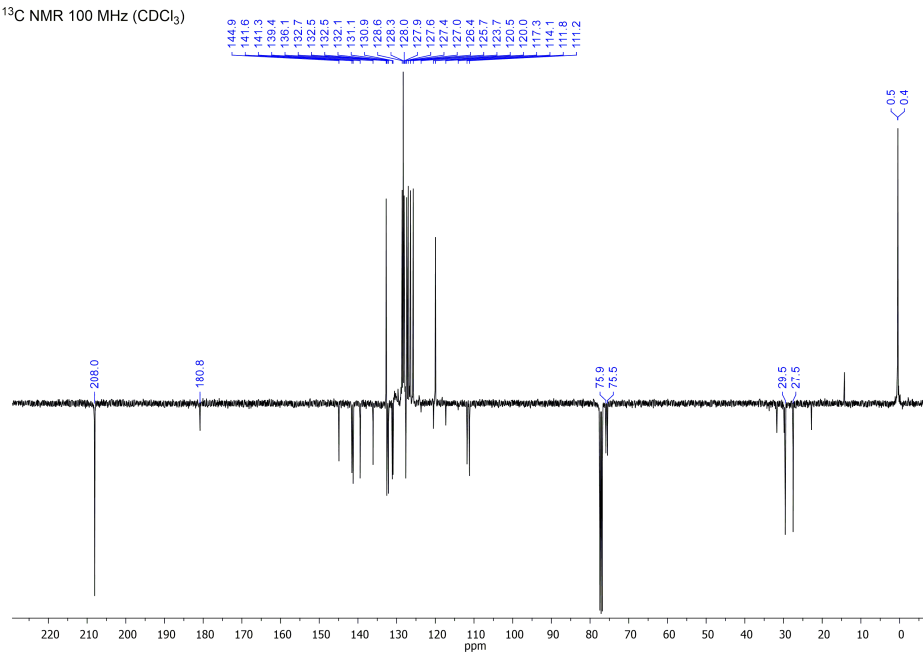
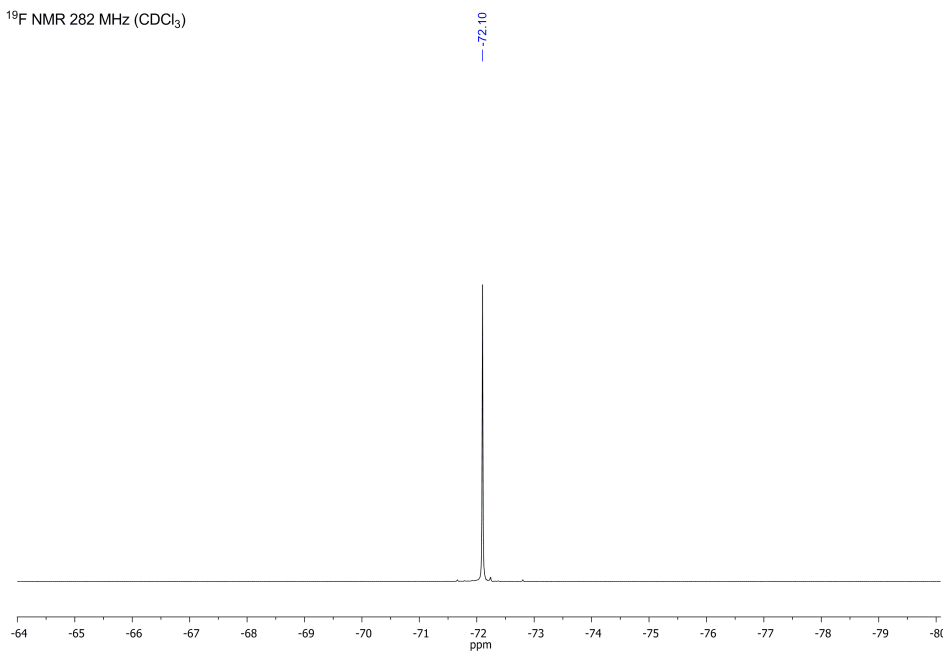
^{13}C NMR 100 MHz (CDCl_3)



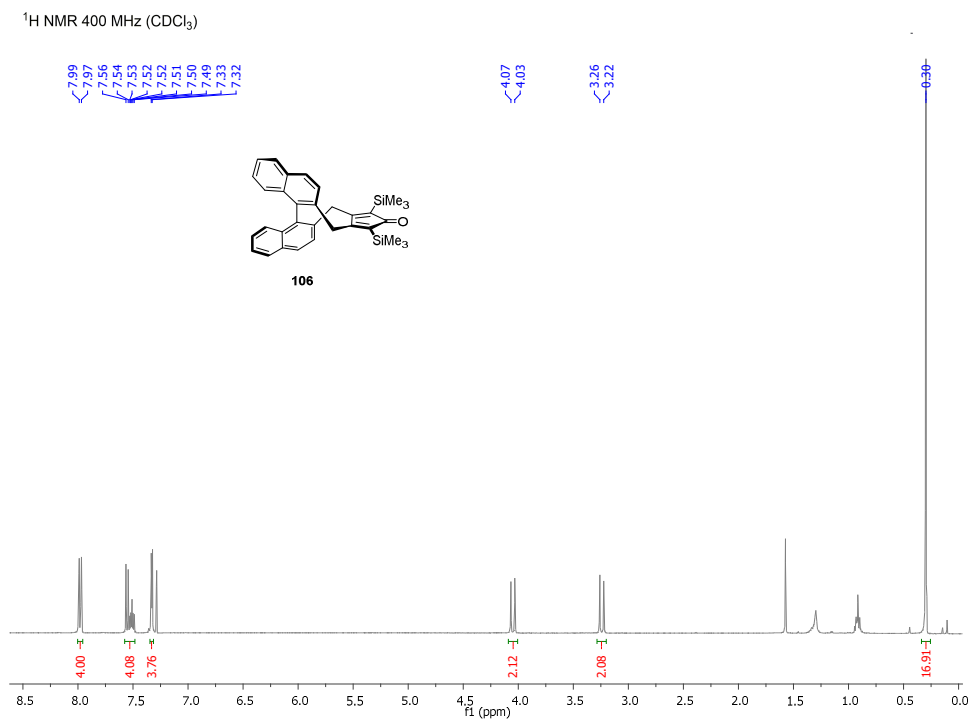


7.1.12. Complex (R)-103

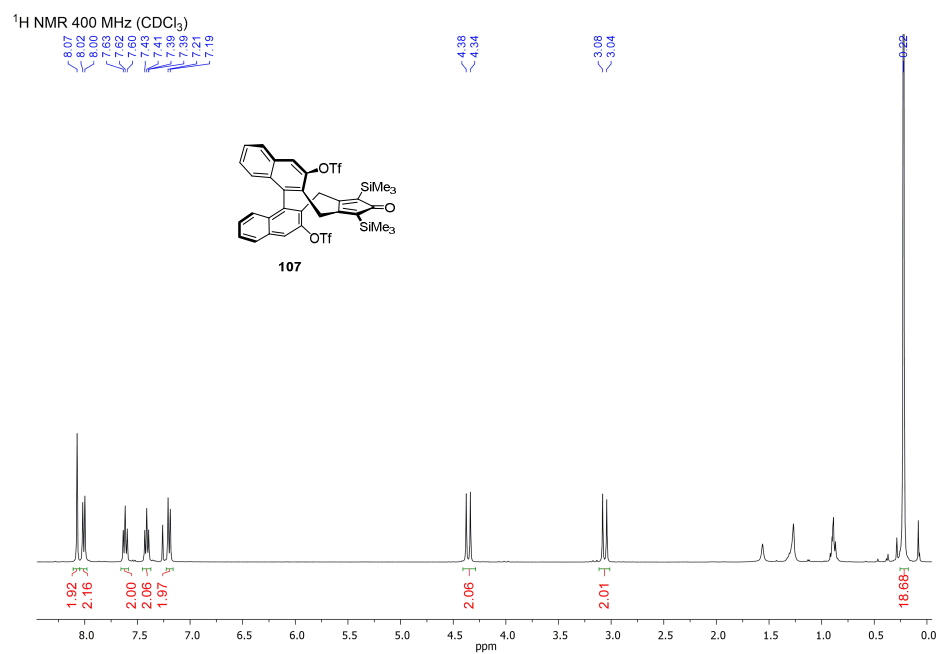


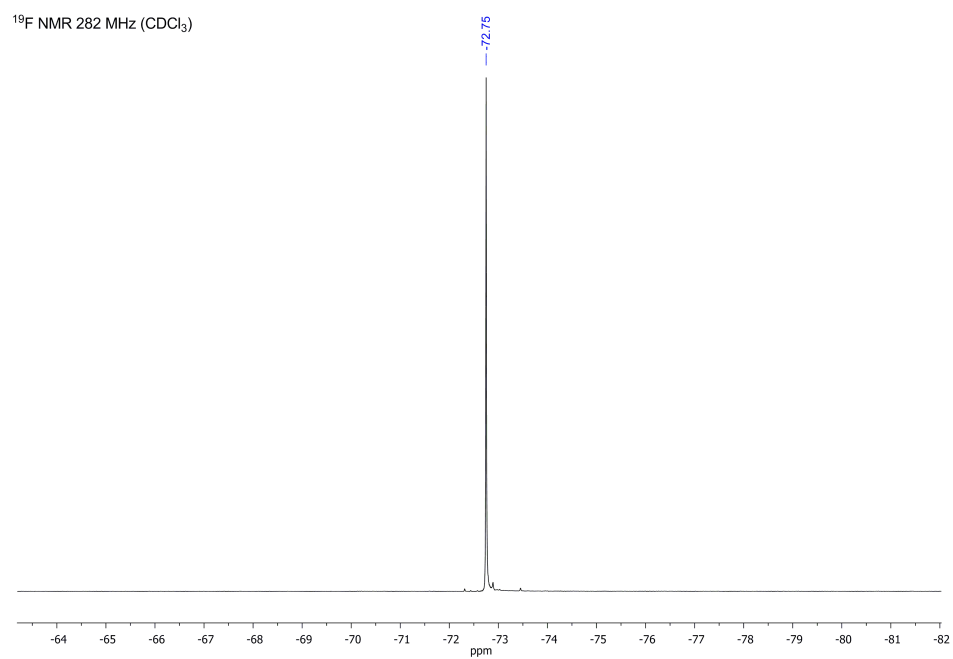
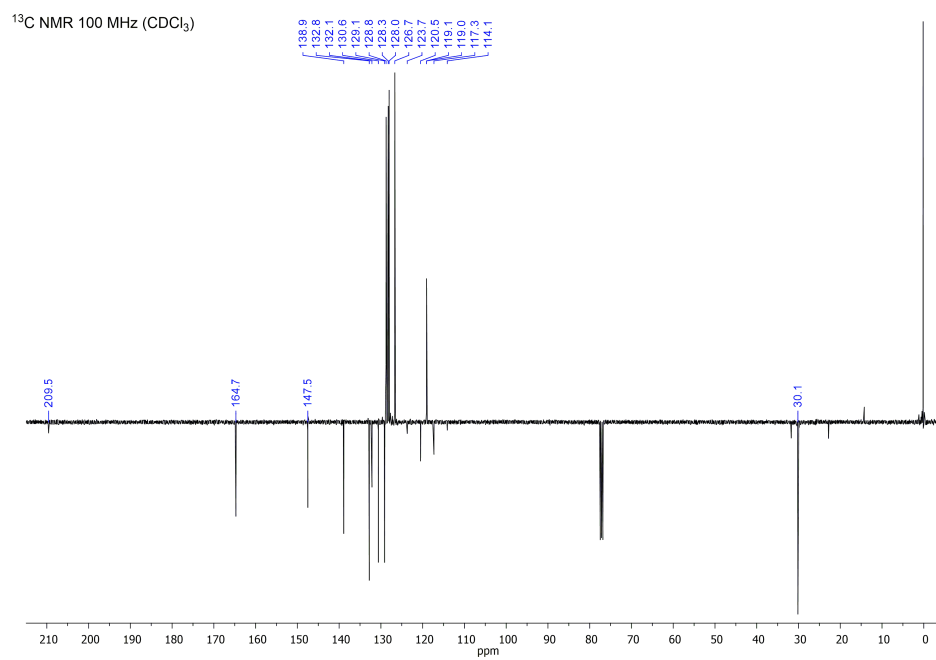
^{13}C NMR 100 MHz (CDCl_3) ^{19}F NMR 282 MHz (CDCl_3)

7.1.13. Free ligand 106

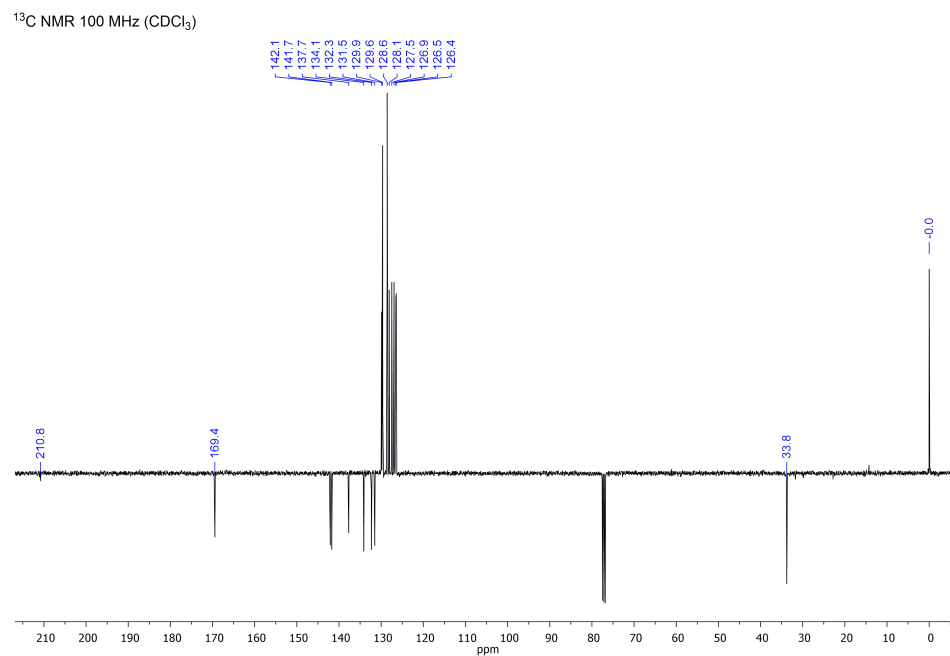
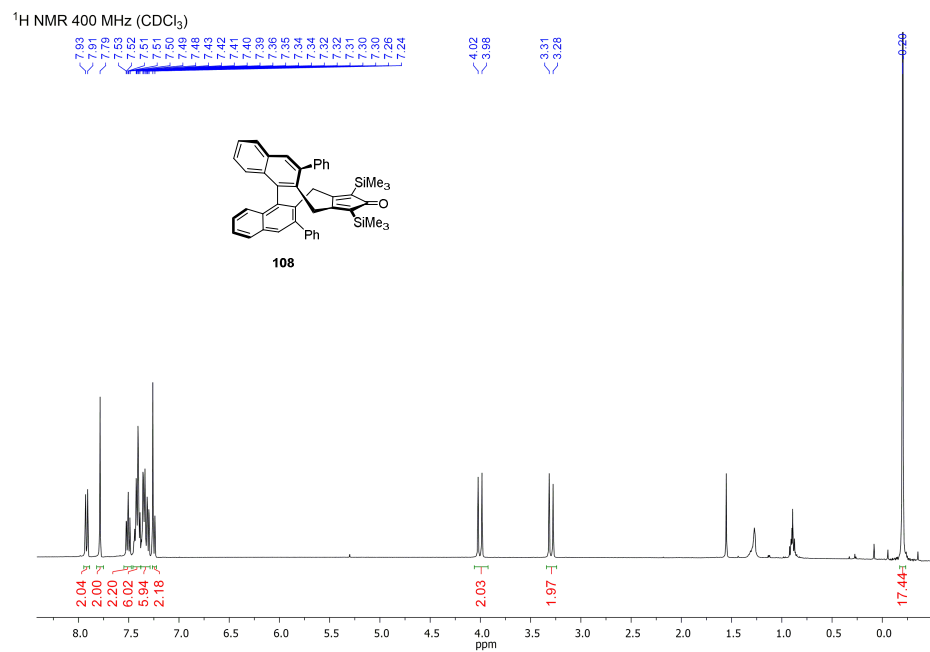


7.1.14. Free ligand 107

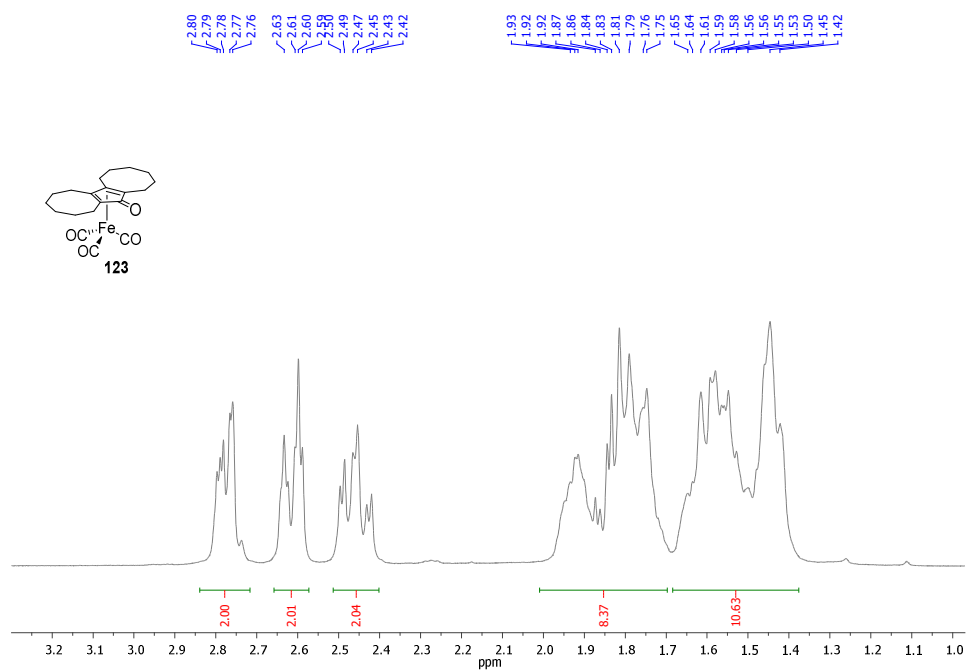
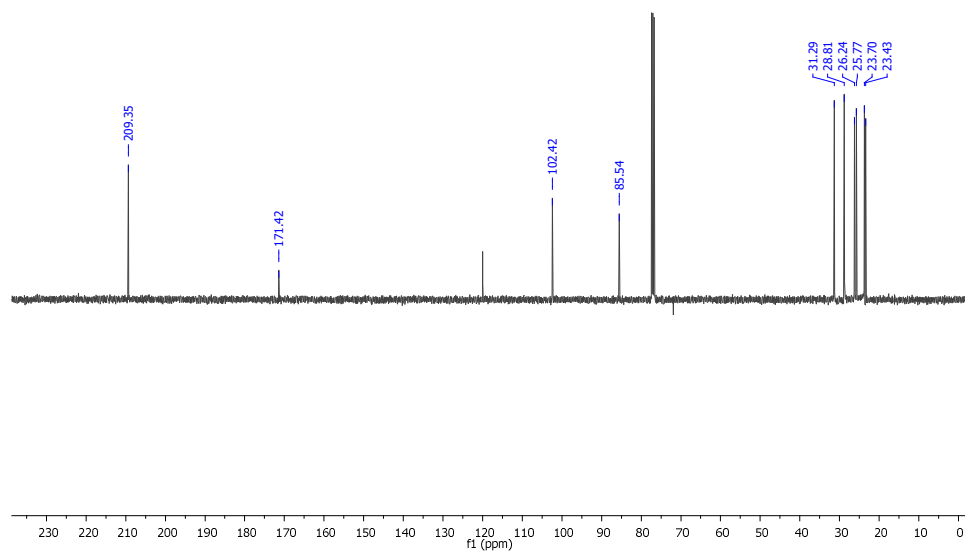




7.1.15. Free ligand 108



7.1.16. Complex 123

 ^1H NMR 400 MHz (CDCl_3) ^{13}C NMR 100 MHz (CDCl_3)

7.1.17. Complex 155

